Marrow fat and perfusion in osteoporosis

GRIFFITH James Francis

A Thesis Submitted in Fulfillment

of Requirements for Degree of

DOCTOR OF MEDICINE

© The Chinese University of Hong Kong

June 2009

TABLE OF CONTENTS

PREFACE AND DECLARATION

The series of studies presented in this thesis was based on 4 years of prospective data collection in the Department of Diagnostic Radiology and Organ Imaging, Prince of Wales Hospital.

I was responsible for the research protocol design, literature review, study implementation, supervision, data analysis and manuscript preparation of the studies described in sections 4 to 7. Ethical approval for all studies was obtained from the Ethics Committee of our institution. The work of the thesis includes a total of eight original studies, which have resulted in 18 immediately related peer-reviewed publications, 17 ancillary peer-reviewed publications and 19 presentations in international and local scientific conferences.

This thesis has not previously been submitted to another university or institute for a higher degree or diploma.

<u>DEDICATION</u>

This thesis is dedicated to my most wonderful loving parents Mum and Dad, my wife

Clara and daughters Isobel and Olivia.

ACKNOWLEDGEMENT

PRECIS

Title: Marrow fat and perfusion in osteoporosis

MR allows non-invasive means of evaluating the non-mineralized components of bone, particularly the bone marrow. This thesis focuses on potential changes occurring in bone marrow perfusion and marrow fat in osteoporosis, - changes which may improve our understanding of osteoporosis pathophysiology. We know from histology studies that as osteoporosis develops and bone tissue is lost, it is replaced by fat filling the vacated marrow space. MR allows non-invasive quantification of this fat component. Although fat content may be increasing, it is not known whether any change in fat composition occurs with osteoporosis i.e. does the type of fat within bone change. Epidemiological studies have indicated a link between arterial disease and osteoporosis. It is not known, however, whether any changes occur in bone perfusion in osteoporosis and how these may be related to increasing fat within the marrow.

The hypothesis to be tested is that: " Advanced magnetic resonance (MR) techniques can be applied to investigate the non-mineralised components of bone tissue in osteoporosis thereby providing more information on bone physiology both in health and disease"

This thesis is based on a series of eight studies designed to study the relationship between bone marrow perfusion, bone marrow fat content, bone marrow fat composition and bone mineral density. These studies showed that as bone mineral density decreased, bone marrow perfusion decreased. A strong reciprocal relationship was found between decreasing bone marrow perfusion and increasing

marrow fat. The reduction in perfusion occurred only with bone and did not affect the extra-osseous tissues alongside bone with the same arterial supply. This indicates that the reduction in bone perfusion is not simply a reflection of a more generalized circulatory impairment in subjects with osteoporosis. This same effect is seen in both males and females and in the proximal femora as well as the spine.

In animal-based studies, we found that reduction in bone perfusion was apparent as little as two weeks after orchidectomy or oorphorectomy and closely paralleled features of impaired endothelial function as well as decreased bone mineral density and a hitherto unrecognized reduction in red marrow fraction within the medullary canal. Nitric oxide synthase, produced by the endothelium, is a potent stimulator of angiogenesis and osteoblastic activity. Mesenchymal stem cell differentiation may switch from osteoblastogenesis to adipocytogenesis under hypoxic conditions, while haematopoetic stem cells also supply endothelial stem cells. Potentially endothelial dysfunction, mesenchymal stem cell differentiation and haematopoetic stem cell maturation may be implemented in the development of osteoporosis.

In normal subjects, blood perfusion was markedly reduced in the femoral head compared to the femoral neck. In osteoporotic subjects, a further reduction in blood perfusion occurred in both areas. Overall perfusion indices reduced relatively more in the femoral neck than the femoral head region. These changes in bone perfusion help explain why subjects with osteoporosis have impaired healing of femoral neck fractures though do not seem to be at increased risk of avascular necrosis. At a micro-architectural level, reduced bone perfusion may also help explain the impaired healing of microfractures seen in subjects with osteoporosis, a feature likely to

contribute to reduce bone strength, microfracture accumulation and eventually clinical insufficiency fracture.

Marrow fat was increased in subjects with osteoporosis. Our studies showed that percentage marrow fat content increased even allowing for the quantitative effect increased marrow fat has on the bone densitometry measurements. This effect was shown to be of negligible clinical significance. We found a strong reciprocal relationship between increasing fat and decreasing bone perfusion in both the proximal femur and vertebral body. Although fat content increased, very little difference in marrow fat composition was apparent between normal subjects and those with osteoporosis. We found no difference was apparent in either the N3/N6 marrow fat ratio or the spectrum of individual fatty acids in the marrow of subjects with either normal bone mineral density or osteoporosis. This suggests that alternation of marrow fat composition is not likely to be a direct contributory factor in osteoporosis. Also marrow fat increase was shown to be due to an increase in number rather than size of marrow fat cells. This suggests that marrow fat increases as a result of a switch in mesenchymal cell maturation to adipocytes rather than osteoblasts.

Below average perfusion indices in the acetabulum and adductor muscle is predictive of more pronounced bone loss at the femoral neck over the ensuing four years. Perfusion indices can also predict between fast and slow losers with a high sensitivity

To summarise, in the eight studies presented, it was shown that osteoporosis is associated with a significant reduction in bone perfusion and a reciprocal increase in marrow fat content though no change in marrow fat composition. Reduction in bone perfusion is most likely due to an accompanying reduction in functioning marrow fraction. Marrow fat increase is most likely the result of a switch in mesenchymal cell maturation to adipocytes rather than osteoblasts. The studies present in this thesis confirmed the initial hypothesis that "Advanced magnetic resonance techniques can be applied to investigate the non-mineralised components of bone tissue in osteoporosis thereby providing more information on bone physiology both in health and disease".

PUBLICATIONS & PRESENTATIONS OF STUDIES RELATED TO THIS THESIS:

(A). PUBLICATIONS:

1. Griffith JF, Yeung DK, Ma HT, Leung JC, Kwok TC, Leung PC. Bone marrow fat content in the elderly: A reversal of sex difference seen in younger subjects. **J Magn Reson Imaging**. 2012:36(1):225-230.

2. Griffith JF, Yeung DK, Leung JC, Kwok TC, Leung PC. Prediction of bone loss in elderly female subjects by MR perfusion imaging and spectroscopy. **Eur Radiol**.2011;21:1160-9.

3. Ma HT, Griffith JF, Yeung DK, Leung PC. Modified brix model analysis of bone perfusion in subjects of varying bone mineral density. **J Magn Reson Imaging**. 2010;31:1169-75.

4. Griffith JF, Wang YX, Zhou H, Kwong WH, Wong WT, Sun YL, Huang Y, Yeung DK, Qin L, Ahuja AT. Reduced bone perfusion in osteoporosis: likely causes in an ovariectomy rat model. **Radiology**. 2010;254(3):739-46.

5. Wang YX, Griffith JF, Kwok AW, Leung JC, Yeung DK, Ahuja AT, Leung PC. Reduced bone perfusion in proximal femur of subjects with decreased bone mineral density preferentially affects the femoral neck. **Bone**. 2009;45:711-5

6.   Zhang YF, Wang YX, Griffith JF, Kwong WK, Ma HT, Qin L, Kwok TC. Proximal femur bone marrow blood perfusion indices are reduced in hypertensive rats: a dynamic contrast-enhanced MRI study. **J Magn Reson Imaging**. 2009;30:1139-44.

7. Griffith JF, Yeung DK, Chow SK, Leung JC, Leung PC. Reproducibility of MR perfusion imaging and (1)H spectroscopy of bone marrow. **J Magn Reson Imaging** 2009;29:1438-1442.

8. Wang YX, Zhou H, Griffith JF, Zhang YF, Yeung DK, Ahuja AT. An in vivo magnetic resonance imaging technique for measurement of rat lumbar vertebral body blood perfusion. **Lab Anim**. 2009;43:261-5.

9. Griffith JF, Yeung DK, Ahuja AT, Choy CW, Mei WY, Lam SS, Lam TP, Chen ZY, Leung PC. A study of bone marrow and subcutaneous fatty acid composition in subjects of varying bone mineral density. **Bone** 2009;44:1092-6.

10. Blake GM, Griffith JF, Yeung DK, Leung PC, Fogelman I. Effect of increasing vertebral marrow fat content on BMD measurement, T-Score status and fracture risk prediction by DXA. **Bone** 2009;44(3):495-501.

11. Wang YX, Griffith JF, Zhou H, Choi KC, Hung VW, Yeung DK, Qin L, Ahuja AT. Rat lumbar vertebrae bone densitometry using multidetector CT. **Eur Radiol** 2009;19(4):882-90.

12. Wang YX, Zhang YF, Griffith JF, Zhou H, Yeung DK, Kwok TC, Qin L, Ahuja AT. Vertebral blood perfusion reduction associated with vertebral bone mineral density reduction: a dynamic contrast-enhanced MRI study in a rat orchiectomy model. **J Magn Reson Imaging** 2008;28(6):1515-8.

13. Griffith JF, Yeung DK, Tsang PH, Choi KC, Kwok TC, Ahuja AT, Leung KS, Leung PC. Compromised bone marrow perfusion in osteoporosis. **J Bone Miner Res** 2008;23(7):1068-75.

14. Yeung DK, Lam SL, Griffith JF, Chan AB, Chen Z, Tsang PH, Leung PC. Analysis of bone marrow fatty acid composition using high-resolution proton NMR spectroscopy. **Chem Phys Lipids** 2008;151(2):103-9.

15. Griffith JF, Yeung DK, Antonio GE, Wong SY, Kwok TC, Woo J, Leung PC. Vertebral marrow fat content and diffusion and perfusion indexes in women with varying bone density: MR evaluation. **Radiology** 2006;241(3):831-8.

16. Yeung DK, Griffith JF, Antonio GE, Lee FK, Woo J, Leung PC. Osteoporosis is associated with increased marrow fat content and decreased marrow fat unsaturation: a proton MR spectroscopy study. **J Magn Reson Imaging** 2005;22(2):279-85.

17. Griffith JF, Yeung DK, Antonio GE, Lee FK, Hong AW, Wong SY, Lau EM, Leung PC. Vertebral bone mineral density, marrow perfusion, and fat content in healthy men and men with osteoporosis: dynamic contrast-enhanced MR imaging and MR spectroscopy. **Radiology** 2005;236(3):945-51.

18. Yeung DK, Wong SY, Griffith JF, Lau EM. Bone marrow diffusion in osteoporosis: evaluation with quantitative MR diffusion imaging. **J Magn Reson Imaging** 2004;19(2):222-8.

(B) <u>ANCILLARY STUDIES AND REVIEWS</u>:

1. Griffith JF, Genant HK. New advances in imaging osteoporosis and its complications. **Endocrine**. 2012 May 23. [Epub ahead of print]

2. Deng M, Griffith JF, Zhu XM, Poon WS, Ahuja AT, Wang YX. Effect of ovariectomy on contrast agent diffusion into lumbar intervertebral disc: a dynamic contrast-enhanced MRI study in female rats. **Magn Reson Imaging**. 2012;30(5):683-8.

3. Wang YX, Griffith JF, Deng M, T H, Zhang YF, Yan SX, Ahuja AT. Compromised perfusion in femoral head in normal rats: distinctive perfusion MRI evidence of contrast washout delay. **Br J Radiol**. 2011 Dec 13. [Epub ahead of print]

4. Griffith JF, Genant HK. New imaging modalities in bone. **Curr Rheumatol Rep**. 2011;13(3):241-50

5. Wang YX, Kwok AW, Griffith JF, Leung JC, Ma HT, Ahuja AT, Leung PC. Relationship between hip bone mineral density and lumbar disc degeneration: a

study in elderly subjects using an eight-level MRI-based disc degeneration grading system. **J Magn Reson Imaging**. 2011;33:916-20.

6. Wang YX, Griffith JF. Menopause causes vertebral endplate degeneration and decrease in nutrient diffusion to the intervertebral discs. **Med Hypotheses** 2011 ;77(1):18-20.

7. Griffith JF, Kumta SM, Huang Y. Hard arteries, weak bones. **Skeletal Radiol**. 2011;40(5):517-21..

8. Wang YX, Griffith JF, Ma HT, Kwok AW, Leung JC, Yeung DK, Ahuja AT, Leung PC. Relationship between gender, bone mineral density, and disc degeneration in thelumbar spine: a study in elderly subjects using an eight-level MRI-based disc degeneration grading system. **Osteoporos Int**. 2011;22:91-6.

9. Griffith JF, Engelke K, Genant HK. Looking beyond bone mineral density: Imaging assessment of bone quality. **Ann N Y Acad Sci**. 2010;1192:45-56.

10. Wang YX, Griffith JF. Effect of menopause on lumbar disk degeneration: potential etiology. **Radiology**. 2010;257(2):318-20.

11. Ma HT, Griffith JF, Yang Z, Kwok AW, Leung PC, Lee RY. Kinematics of the lumbar spine in elderly subjects with decreased bone mineral density. **Med Biol Eng Comput.** 2009;47:783-789.

12. Yang Z, Griffith JF, Leung PC, Lee R. Effect of osteoporosis on morphology and mobility of the lumbar spine. **Spine** 2009;34(3):E115-21.

13. Yang Z, Griffith JF, Leung PC, Lee R. Effect of osteoporosis on morphology and mobility of the lumbar spine. **Spine** (Phila Pa 1976). 2009 Feb 1;34(3):E115-21.

14. Ma HT, Griffith JF, Yang Z, Wai Leung Kwok A, Leung PC, Lee RY. Effect of vertebral morphology on lumbar kinematics in elderly subjects with decreased bone mineral density. **Conf Proc IEEE Eng Med BiolSoc**. 2008;883-6.

15. Griffith JF, Genant HK. Bone mass and architecture determination: state of the art. **Best Pract Res Clin Endocrinol Metab.** 2008;22(5):737-64.

16. Ma HT, Yang Z, Griffith J, Leung PC and Lee RYW (2008). A new method for determining lumbar spine motion using Bayesian Belief Network. **Med Biol Eng Comput.** 2008:46(4):333-340

17. Griffith JF, Wang YX, Antonio GE, Choi KC, Yu A, Ahuja AT, Leung PC. Modified Pfirrmann grading system for lumbar intervertebral disc degeneration. **Spine** 2007; 32(24):E708-12.

(C). CONFERENCE PRESENTATIONS:

1. Anthony WL Kwok, James F. Griffith, Heather Ting Ma, Yixiang Wang, Ping Chung Leung, Jason Leung, David KW Yeung (2008). Estimated volume of both vertebral body and disc decreases as BMD decreases though this effect is seen more in the vertebral body than the disc. International Conference on Osteoporosis and Bone Research 2008, Beijing, China.

2. Heather Ting Ma, James F. Griffith, Yixiang Wang, Anthony WL Kwok, Ping Chung Leung, Jason Leung, David KW Yeung (2008). Is there any relationship between lumbar endplate changes (Modic changes, Schmorl nodes) and bone mineral density?. International Conference on Osteoporosis and Bone Research 2008, Beijing, China.

3. Yi-Xiang Wang, James F. Griffith, Heather Ting Ma, Anthony WL Kwok, Ping Chung Leung, Jason Leung, David KW Yeung (2008). Is decreased BMD associated with less severe lumbar disc degeneration?. International Conference on Osteoporosis and Bone Research 2008, Beijing, China.

4. Heather T. Ma, James F. Griffith, P.C. Leung (2008). As bone mass decreases, paravertebral muscle mass also decreases though not to the same degree

thereby decreasing the functional muscle-bone unit. International Conference on Osteoporosis and Bone Research 2008, Beijing, China.

5. Anthony Kwok, James F. Griffith, Heather T. Ma, Y.X. Wang, P.C. Leung, Jason Leung, David KW Yeung (2008). Lumbar vertebral body and disc summated height and volume estimation in elderly subjects. ESMRMB (European Society for Magnetic Resonance in Medicine and Biology) Congress 2008, The 25th Annual Meeting, Valencia/ES.

6. Heather T. Ma, James F. Griffith, Y.X. Wang, Anthony Kwok, P.C. Leung, Jason Leung, David KW Yeung (2008). Relationship between lumbar endplate changes (Modic changes, Schmorl nodes), bone mineral density, and disc degeneration. ESMRMB (European Society for Magnetic Resonance in Medicine and Biology) Congress 2008, The 25th Annual Meeting, Valencia/ES.

7. Y.X. Wang, James F Griffith, Heather T. Ma, Anthony Kwok P.C. Leung, Jason Leung, David KW Yeung (2008). Reduced lumbar vertebral bone mineral density is associated with less severe disc degeneration. ESMRMB (European Society for Magnetic Resonance in Medicine and Biology) Congress 2008, The 25th Annual Meeting, Valencia/ES.

8. Heather T. Ma, James F. Griffith, P.C. Leung (2008). Lumbar "Functional Muscle-Bone Unit" in normal and osteoporotic subjects. ESMRMB (European Society for Magnetic Resonance in Medicine and Biology) Congress 2008, The 25th Annual Meeting, Valencia/ES.

9. Wang YX, Griffith JF, Yeung DK, Zhou H, Zhang YF, Qin L. Decease of vertebra bone mineral density is associated with decease of vertebra blood perfusion: dynamic contrast enhanced MRI study in rat ovariectomy model. 54th Annual Meeting of the Orthopaedic Research Society, San Francisco, CA, 2008 Mar 2-5

10. Heather Ting Ma, James F. Griffith, Zhengyi Yang, Anthony Wai Leung Kwok, Ping Chung Leung, and Raymond Y.W. Lee (2008). Effect of Vertebral

Morphology on Lumbar Kinematics in Elderly Subjects with Decreased Bone Mineral Density. The 30th Annual International Conference of the IEEE EMBS (Engineering in Medicine and Biology Society), Vancouver, Canada.

11. Heather Ting Ma, James F.Griffith, Zhengyi Yang, Anthony Wai Leung Kwok, Ping Chung Leung, and Raymond Y.W. Lee (2008). Study on the kinematic pattern of lumbar spine in subjects with varied bone mineral density. In: Proceedings of the 5th International Conference on Information Technology and Applications in Biomedicine (in conjunction with) 2nd International Symposium & Summer School on Biomedical and Health Engineering, Shenzhen, China, P62.

12. Ma H, Yang Z, Griffith JF and Lee RYW (2007). Measurement of intervertebral motions of the lumbar spine using Bayesian Belief Network. In: Proceedings of the 2007 Annual Meeting of the Spine Society of Europe, Brussels, Belgium, p106.

13. Ma HT, Yang ZY, Griffith JF, Leung PC, and Lee RYW (2007). Modelling of lumbar spine motion using Bayesian Belief Network. XXI Congress of the International Society of Biomechanics, Taiwan. J Biomech 40 (Supp 2), p S599.

14. Yang ZY, Sun LW, Lu W, Luk KDK and Lee RYW (2007). Errors in the measurement of lumbar spine motions using skin mounted sensors. XXI Congress of the International Society of Biomechanics, Taiwan. J Biomech 40 (Supp 2), p S600.

15. Yang ZY, Griffith J, Leung PC, Pope M, Lee RYW. (2006) Effects of osteoporosis on the morphology and mobility of the lumbar spine. In: Proceedings of the 33rd Annual Meeting of the International Society for the Study of the Lumbar Spine, Bergen, Norway, p83.

16. Yang Z, Griffith JF, Leung PC, Pope M, Sun LW, Lee RYW (2005). The accuracy of surface measurement for motion analysis of osteoporotic thoracolumbar spine. In: Proceedings of the 27th Annual International

Conference of the IEEE Engineering in Medicine and Biology Society, Shanghai, China, p278.

17. Yang ZY, Griffith J, Leung P, Pope M and Lee RYW (2005). An inverse kinematic model of the osteoporotic spine. In: Proceedings of the 13th Nordic Baltic Conference in Biomedical Engineering and Medical Physics, Umea, Sweden, p257-8.

18. Yang ZY, Sun LW, Griffith JF, Leung PC and Lee RYW (2005). The accuracy of surface measurement for osteoporotic spine motion analysis. In: Proceedings of the XXth Congress of the International Society of Biomechanics and the 29th Annual Meeting of the American Society of Biomechanics, Cleveland, USA, p793.

19. G.M. Blake[1], J.F. Griffith[2], D.K.W. Yeung[2], P.C. Leung[2], I. Fogelman[1]. [1]King's College London Medical School, London, UK, [2]Chinese University of Hong Kong, Prince of Wales Hospital, Shatin, Hong Kong. The Effect of Vertebral Marrow Fat Content on the Diagnosis of Osteoporosis. Poster presentation American Society of Bone and Mineral Research 2008.

Marrow fat and perfusion in osteoporosis

INTRODUCTION

This introduction provides background information to help understand the studies presented in this thesis. The bone disorder osteoporosis is explained as are some of the currently associated problems associated with osteoporosis diagnosis and management. The rationale for performing the studies undertaken in this thesis is outlined. The necessary information on bone, bone marrow, bone blood supply and methods of assessment to help understand the studies presented in this thesis is then provided. Only that information immediately pertinent to the studies undertaken in this thesis is presented.

OUTLINE

1.1   Osteoporosis

1.2   Some current dilemmas with osteoporosis.

1.3   Rationale for doing studies presented in this thesis

1.1.   OSTEOPOROSIS

The World Health Organization (WHO) defines osteoporosis as a disease characterized by reduced bone mass and micro-architectural deterioration of bone leading to increased susceptibility to fracture (Figure 1). Osteoporosis is characterized by a reduction in trabecular number and thickness and cortical bone thinning (Figure 2) .

Osteoporosis is associated with increased fracture risk. This fracture risk increases with advancing age, especially in women and particularly affects those bones that depend more on trabecular bone for there strength such as the vertebral body, proximal humerus, distal radius, and to a lesser extent, the proximal humerus and calcanei. The sacrum and pubic bones, although not possessing a particularly large amount of trabecular bone, are also affected a stress is concentrated in these areas during weightbearing. As osteoporosis, in the absence of fracture, has no recognized adverse effect on general health, one can reasonably argue that the sole purpose of

osteoporosis screening, identification and treatment is to prevent fracture (Figure 1).
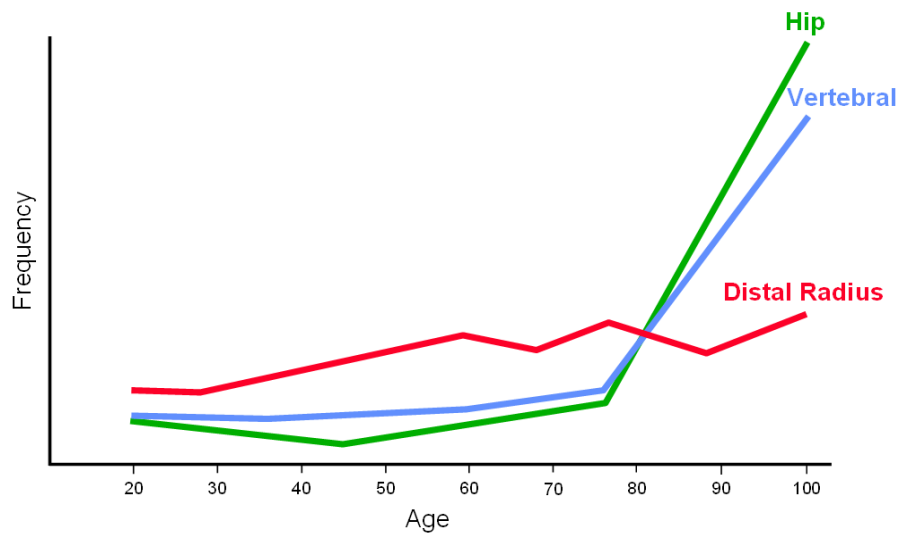
Figure 1. Increased susceptibility to hip and vertebral fractures and, to a lesser degree, distal radial fractures, in the elderly and mostly consequent upon osteoporosis. Proximal femoral and vertebral fractures are uncommon in the young or middle-aged. (adapted from Copper and Melton 1992)

Osteoporosis is a very common disease affecting 1:4 females and 1.8 males over the age of 65 years. While most American women under the age of 50 years of age have normal bone mineral density (BMD), 27% are osteopenic and 70% osteoporotic by the age of 80 years (Cooper et al. 1999). Osteoporotic fractures lead to severe morbidity and mortality as well as high economic cost. Osteoporotic fracture alone costs the USA about $18 billion/ year and the UK about £1.7 billion/year (Cooper C et al. 1999).
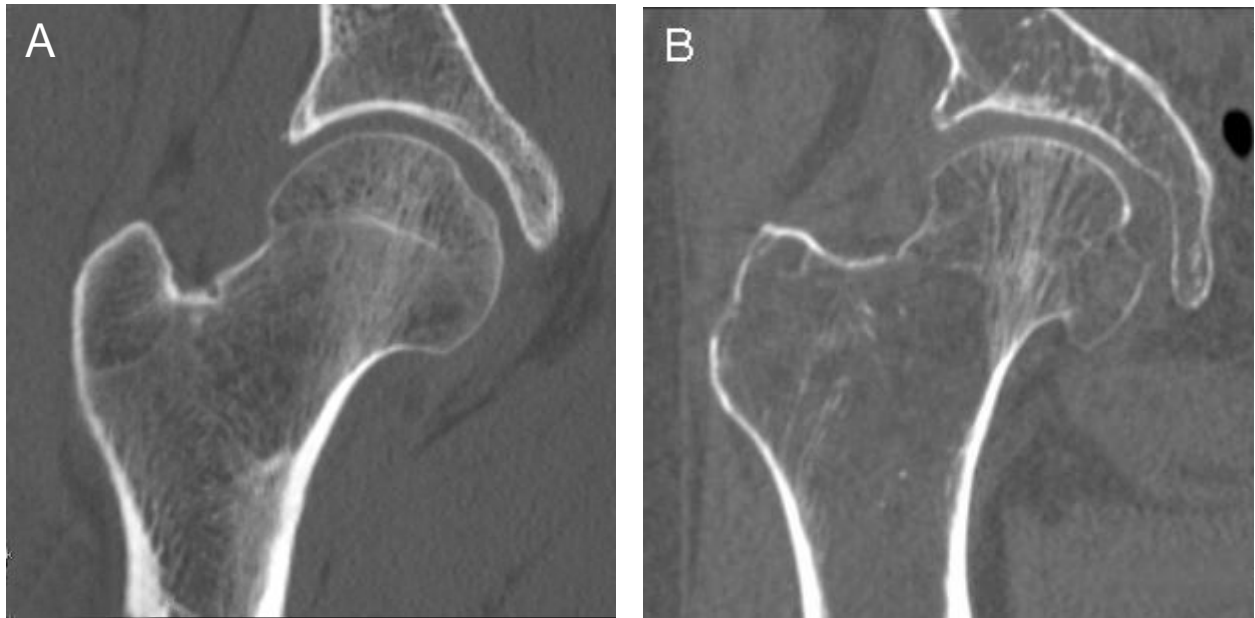
Figure 2. CT image of A) normal hip in 48-year-old man and B) severely osteoporotic hip in 74-year-old female. In the normal hip (A), note how the cortex in the proximal femur is normally relatively thin compared to the shaft with a good trabecular network. In the osteoporotic hip (B), there is almost complete absence of (tensile) trabeculae in the femoral neck and proximal shaft region. It is easily comprehended how patients with osteoporosis are prone to insufficiency fracture.

After peak bone mass is reached during the third decade of life, there is a progressive physiological decline in bone mass of about 0.5% per year (Tenenhouse A et al. 2000). Around the time of the menopause, accelerated bone loss occurs of about 2-3% per year. This accelerated bone loss, which is particularly prevalent in females, though also seen in men, settles down over the next five to ten years to a slower decline of about 1.0% per annum. Osteoporosis is more specifically a disease of reduced bone strength rather than reduced bone density. As evidenced by the WHO definition of osteoporosis, reduced bone density is an important feature of osteoporosis rather than the sole defining hallmark of this disease. However, bone mineral density is the most readily available surrogate marker of bone strength currently and, though densitometry testing, bone mineral density measurements and T-scores are widely applied to diagnose and monitor osteoporosis.

Although decreasing BMD is strongly associated with increased fracture risk and the most applicable surrogate marker of fracture risk, in reality, most fractures occur in subjects who are osteopenic (low bone mass) rather than osteoporotic. This ambiguity can be attributed to many more people being osteopenic than osteoporotic and bone density being but one facet of bone strength. For example, one large study showed that 48% of post-menopausal women with non-traumatic or mildly traumatic fracture over a 9-year follow-up period had a baseline bone density in the osteopenic range while 8% had a normal baseline bone density (Sornay-Rendu E et al. 2005). In other words, 56% of patients in this study with fracture did not have osteoporosis as defined by T-score. In another similar study, 44% of all non-vertebral fractures occurred in women with a T score above -2.5 (Schuit SC et al. 2004).

It is not clear why some people develop osteopososis and others of comparable age gender and lifestyle do not. Many risk factors for osteoporosis have been identified such as increasing age, thin build, female gender, family history, smoking, alcohol, arterial calcification, steroid medication, thiazide diuretics though a common linking pathway has not been found. This main theme of the studies presented in this thesis is to further explore the physiology behind osteoporosis particularly looking primarily at the non-osteoid components of bone (marrow and perfusion). MR imaging has provided us a means of studying these bone components which have not been studied in detail previously in respect to osteoporosis.

1.2 SOME CURRENT DILEMMAS WITH OSTEOPOROSIS:

A. *Osteoporosis is being diagnosed too late.* Current methods of diagnosing osteoporosis rely on bone being lost. Bone needs to be lost before densitometry can detect reduced bone mass or high resolution imaging

techniques can detect structural changes in bone architecture. Osteoporosis results in progressive cortical thinning, trabecular thinning and loss of trabeculae (Figure 5). Once trabeculae have been lost, many do not seem to recover. The increase in bone density which occurs with treatment seems to occur as a result of thickening of residual trabeculae and cortices rather than regeneration of previously reabsorbed trabeculae.
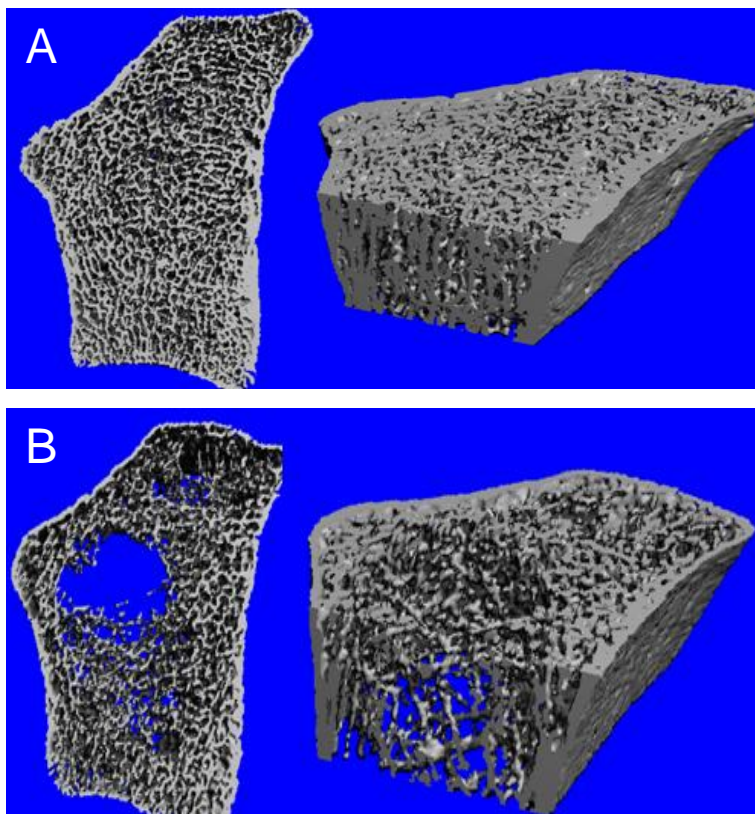
Figure 5. High resolution Xtreme CT images of distal radius showing A) normal and B) osteoporotic bone. Cortices and trabeculae are thinned and trabeculae reduced in number in osteoporotic bone. There are large areas in osteoporotic bone devoid of trabeculae. With osteoporotic treatment, these holes in the trabecular network do not seem to re-fill. (Courtesy of Prof Qin Lin)

In other words, once holes appear in the trabecular bone network, they do not necessarily re-fill with improvement in BMD. As a result treated osteoporotic bone will remain structurally inferior to normal bone. Currently, we have no means of diagnosing osteoporosis before significant bone loss occurs. Could changes in marrow fat or perfusion predate loss of bone mass such that one can intervene with treatment before bone loss occurs?

B. *The pathogenesis of osteoporosis remains unknown*. Many risks factors for osteoporosis have been identified (female gender, increasing age, family history, smoking, alcohol, drugs) though no universal common pathway has been identified. At a metabolic level, many links between osteoporosis, vascularity and fat have been inentified including, for example, the inflammatory cytokine IL-6 which can give rise to bone loss and atherosclerosis and is secreted by adipocytes (McLean RR 2009). Not knowing the true cause of osteoporosis limits the development of effective therapy. Do vascular or marrow elements hold the key to the pathogenesis of osteoporosis?

C. *Monitoring treatment effect is slow.* Effect of treatment can only be realized 12-18 months minimum after initiation as bone metabolizes slowly and it takes time before any true effect on bone density can be recognized. To see whether this effect is maintained and to show fracture reduction usually takes at least five years such that whole programme moves along at a slow pace. Do changes in vascularity or marrow composition predate change in bone mass thereby allowing one to determine the efficacy or otherwise or treatment at a much earlier stage?

1.2. HYPOTHESIS TO BE TESTED AND RATIONALE FOR DOING STUDIES PRESENED IN THIS THESIS

The <u>hypothesis</u> to be tested is that: " Advanced magnetic resonance (MR) techniques can be applied to investigate the non-mineralised components of bone tissue in osteoporosis thereby providing more information on bone physiology both in health and disease"

With this aim in mind there were two main reasons for undertaking the studies presented in this thesis.

First, little is known about what happens to the bone marrow in osteoporosis. For example, in 2002, the year we started these studies, not a single abstract dealt with bone marrow, perfusion or marrow fat out of over 2000 abstracts presented at the Bone and Mineral Research Annual meeting. Yet per unit volume, bone is composed mainly not of mineralized tissue but of soft tissue as in marrow tissue. Second, MR imaging provided a means of non-invasively evaluating the bone marrow. Understandably, the vast majority of research on the pathogenesis of osteoporosis has focused on studying the mineralized elements of bone particularly bone formation and resorption pathways. At the outset of our studies, we had no idea as to the relationship between bone mass and marrow perfusion and in fact our initial thoughts were the osteoporosis may even be associated with increased rather than decreased bone perfusion as the relationship between hyperaemia and increased osteoclastic activity is well recognized. We were also interested in marrow fat as osteoblasts and marrow fat share a common pre-cursor cell and bone marrow in the adult is comprised mainly of fat. Fat surrounds cortical bone and, more importantly, surrounds biologically active trabecular bone within the bone marrow.

1.4 BONE – MINERALISED COMPONENT

Bone is a specialized type of connective tissue which provides structural support, protection and plays a major role in the regulation of haematostais and calcium balance. The organic matrix of bone is osteoid. Osteoid is primarily (95%) composed of Type I collagen fibers while the remaining 5% comprises chondroitin sulfate proteoglycans and a variety of other non-collagenous proteins (Marks SC et al.

2002). This largely collagenous matrix is hardened through mineralization where calcium hydroxyapatite crystals $[Ca_5(PO_4)_3(OH)]$ are deposited into the organic matrix. Mineralization increases resistance to compression. Mature mineralized bone is therefore composed of Type I collagen fibers (40% by volume) interspersed with calcium hydroxyapatite crystals $[Ca_5(PO_4)_3(OH)]$ (45% by volume) and water (15% by volume) bound to collagen or free (Hadjidakis DJ et al . 2006).

Cortical or compact bone forms the compact outer shell of bone. It accounts of 80% of mineralised bone mass, is composed of tightly packed collagen fibrils organized around central nutrient canals, has a slow turnover rate and high resistance to bending and torsion. Trabecular or cancellous bone consists of a honeycomb of bone struts irregularly criss-crossing the marrow cavity. Cortical bone measures 1-8mm in thickness being thickest on the anterior shaft of the tibia. Trabecular bone is much thinner at between 200-400µm (i.e. 0.2 -0.5mm). Trabecular bone is the dynamic component of bone by virtue of its large surface area and thin architecture. Although trabecular bone represents 20% of mineralised bone mass, it includes 80% of the overall bone surface area (Hadjidakis DJ et al. 2006) and is 10-20 times more metabolically more active than cortical bone.

Although longitudinal bone growth largely ceases at the end of adolescence, human bone is continually remodeled throughout adulthood with about 10% of adult bone being remodeled each year (Theill L et al. 2002). Bone remodeling serves to repair microdamage and adapt bone structure to mechanical strains and functional requirements. Bone remodeling is a highly regulated process that is orchestrated by three cell types: osteocytes, osteoblasts, and osteoclasts.

Osteocytes. Osteoblasts trapped within osteoid are called osteocytes. They have long cell processes which help to form a network of thin calaliculi permeating the

entire bone matrix (Hadjidakis DJ et al. 2006). The exact function of osteocytes is not clear though it is likely they respond to bone strain and enhance bone remodeling by recruiting osteoclasts to sites where bone resorption is required (Hadjidakis DJ et al. 2006). (Figure 6).
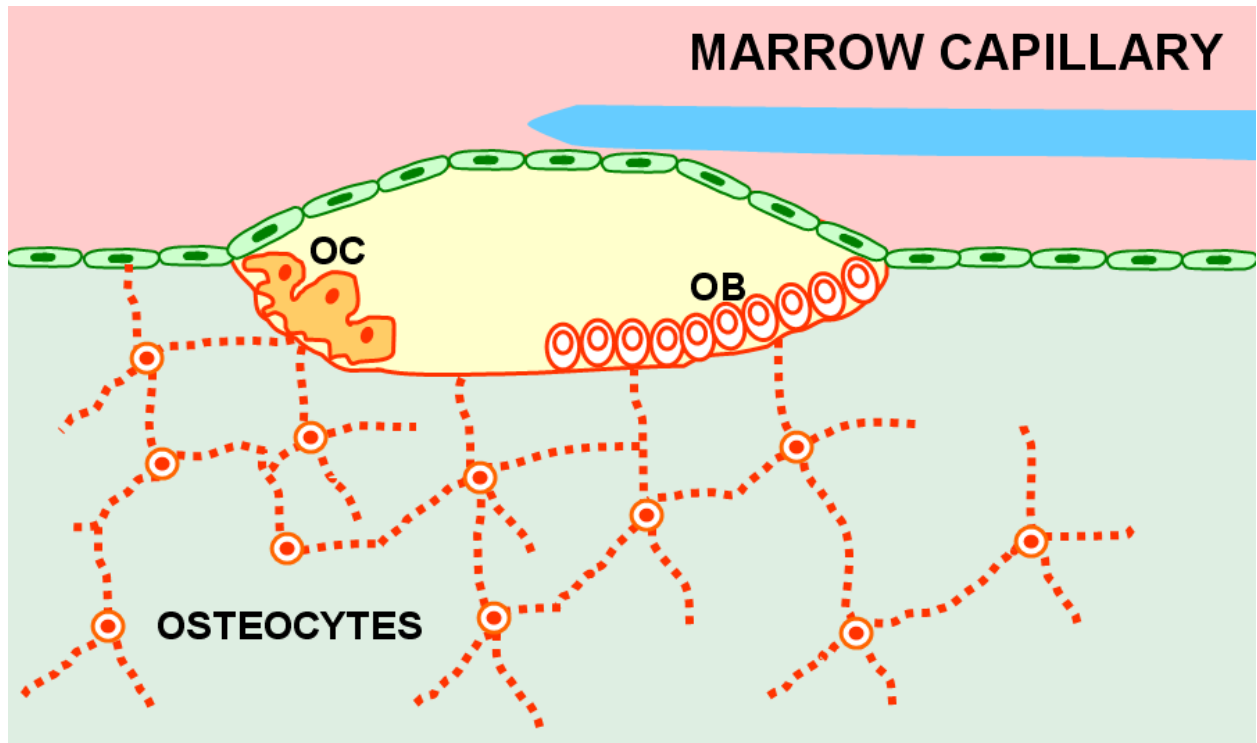
Figure 6. Connections between osteocytes and bone remodeling compartment containing osteocystes (OC) and osteoblasts OB). The BMC is lined by specialized cells outside of which lie the capillaries or venous sinuses. (Modified from Martin TJ, Seeman E 2008)

Osteoblasts. An osteoblast is a mononuclear cell that produces osteoid matrix and facilitates mineralization of this osteoid. Osteoblasts arise from mesenchymal stem cells located in the bone marrow and periosteum. These multipotent mesenchymal stem cells in the marrow can also differentiate into adipocytes, chondrocytes, fibroblasts, or myoblasts. Osteoblasts do not function individually but they are found in clusters along the surface of the bone they are producing (Hadjidakis DJ et al. 2006). (Figure 6).

Osteoclasts. Bone resorption is carried out by osteoclasts. Unlike osteoblasts, osteoclasts do not derive from the mesenchymal cell line but instead derive from the haemopoetic stem cell line (which also gives rise to erythroblasts, megakaryoblasts, myeloblasts and monoblasts) (Hadjidakis DJ et al. 2006). They are usually found on the bone surface alongside osteoblasts (Figure 6).

Bone remodeling compartments. Bone remodeling takes place in specialized vascular structures on the bone surface known as bone remodeling compartments (BMC's) (Hauge EM et al. 2001) (Figure 6). The inner lining of the BMC is made up of the bone surface lined with either osteoclast or osteoblast cells depending on the state of the remodeling cycle. There is a thin layer of specialized cells showing positive immunoreactivity to a whole array of markers. The venous sinusoid lies outside this cell layer. It is unclear whether osteoblast or osteoclast precursors enter the BMC from the adjacent marrow space or whether they arise in the BMC de novo. Much still remains to be discovered about the physiology of the BMC (Eriksen EF et al. 2007)

The importance of the RANKL/OPG system for the regulation of osteoclast activity is well established. Osteoclastogenesis is mainly controlled by a triad of proteins consisting of a receptor RANK (receptor-activated nuclear-kappa), a ligand (receptor-activated nuclear-kappa B ligand, RANK-L), and a decoy receptor osteoprotegerin (Hadjidakis DJ et al. 2006). RANK is a protein found on the membranes of osteoclast precursors and mature osteoclasts. RANK-L is produced by a range of cells including osteoblasts and activated T-cells. Osteoprotegerin is also secreted by a range of cells including osteoblasts. Binding of RANK-L to RANK promotes osteoclastogenesis and inhibits osteoclast apoptosis. Binding of RANK-L to osteoprotegerin prevents osteoclastogenesis and promotes osteoclast apoptosis.

Osteoclast number and activity is therefore largely controlled by the balance between RANK, RANK-L and osteoprotegerin (Hadjidakis DJ et al. 2006).

There are a large number of growth factors regulating controlling osteoblast differentiation and maturation (such as parathyroid hormone, growth hormone, thyroid hormone, insulin, prolactin as well as the sex hormones) while an even larger number of growth factors are produced by osteoblasts which may serve with self-regulation (such as bone morphogenetic protein, canonical Wnt, core binding factor-1, fibroblast growth factor, platelet-derived growth factor, transforming growth factor-beta, Osterix, Col1, alkaline phosphatase, osteocalcin, osteopontin, and osteonectin) (Nakashima K et al. 2003, Hadjidakis DJ et al. 2006).

Bone shape: Longitudinal bone growth largely ceases in humans at the time of skeletal maturity which for the main long bones of the lower limbs is about 17 years in females and 18 years in males. Although longitudinal bone growth stops, bone, nevertheless, continues to be remodeled throughout life. Overall bone cross-sectional area and cortical thickness is maintained by a balance between bony apposition and deposition on the endosteal and periosteal margins of the cortex. The general tendency is for bone to widen with aging. Slight increases in bone cross-sectional area allows one to maintain bone strength with the same bone mass (Seeman et al. 2007). Increase in bone cross-sectional area results from a predominance of periosteal bone deposition and endosteal bone apposition (Seeman et al. 2007). This adaptive response is mainly seen in the weightbearing bones and varies with age and gender (Seeman et al. 2007).

In the shafts of long bones, the cortex is thick, the marrow cavity relatively small and the number of trabeculae in the marrow cavity relatively sparse. This thick cortex

affords rigidity to the bone. At the ends of long bones, and in other bones such as the vertebral bodies or calcanei, the cortex is relatively thin and the marrow cavity wide. A large marrow cavity allows the bone to expand while still maintaining a reasonable weight. Large bones and expanded ends of long bones are there to maintain body size, maintain stability and support joints. When the marrow cavity is large, the cortex is relatively thin. To main the overall strength of the bone, the relatively thinned cortex of the expanded bone is supported by a well-developed trabecular network crisscrossing the medullary canal. In general, wherever the cortex is thin, the trabecular network is well-developed and visa versa.

1.5 BONE MASS, BONE DENSITY, AND METHODS OF ASSESSMENT

Mass is the weight of an object. Density is mass per unit volume (mass /volume). Common tissue densities are shown in Table 1 (Weiss LP et al 1987, Goodsitt MM et al 1994) as well as peak bone mineral densities as measured by DXA (Lynn HS et al 2008) and the composition of fat, cortical bone and lean muscle (White DR et al 1965).

Bone mass equates to bone mineral content (BMC) and is the amount of bone mineral present in a structure measured in grams. Bone mineral density (BMD) is the amount of bone per unit volume and is measured in grams/cm^3. Densitometry devices do not measure true bone mineral density since this should be 'mass of bone per unit volume of bone' i.e. exclusive of marrow or other non-osseous tissue. Since densitometry techniques such as DXA or QCT measure a combination of bone and bone marrow, the value obtained is termed 'apparent bone mineral density' though this has become synonymous with bone mineral density (BMD) (Faulkner K 2005).

Densitometry results are reported as T and Z scores, both of which rely on the standard deviation (s.d.) of the measurement. In a normally distributed population, approximately 68% people will fall within ± 1 s.d. of the mean, 95% within ± 2 s.d's and 99.7% within ± 3 s.d's of the mean. An Z score is the number of s.d's difference that a patient's BMD is above or between the mean BMD of age-matched controls. Therefore, a Z score of 0 indicates a BMD equal to a person of the same age while a Z score of > -2.0 indicates a BMD > 2 s.d's below the mean for subjects of the same age or a BMD less than the BMD of 97% of subjects of the same age. An T score is the number of s.d's difference that a patient's BMD is above or between the mean BMD of a control group of healty young adults. A T score of 0 indicates a BMD equal to the young adult mean while a T score of >-1.0 indicates a BMD <1 s.d than the young adult mean or in other words a BMD < 68% of the BMD young adult population.

TABLE !: Density and Chemical Composition of common tissues

TISSUE	DENSITY	COMPOSITION (element fraction by weight)									
		H	C	N	O	Na	Mg	P	S	K	Ca
Red marrow	1.02g/cm^3	___	___	___	___	___	___	___	___	___	___
Blood	1.05g/cm^3	10.2	11.0	3.3	74.5	0.1	0.0	0.1	0.2	0.0	0.0
Fatty Marrow	0.95 g/cm^3	___	___	___	___	___	___	___	___	___	___
Adipose tissue	0.92 g/cm^3	11.4	59.8	0.7	27.8	0.1	0.0	0.0	0.1	0.0	0.0
Lean Muscle	1.00g/cm^3	10.2	12.3	3.50	72.9	0.08	0.02	0.2	0.5	0.5	0.01
Cortical bone	1.85g/cm^3	3.4	15.5	4.0	44.1	0.06	0.21	10.2	0.31	0.0	22.2
Trabecular bone	1.70g/cm^3	___	___	___	___	___	___	___	___	___	___
ANATOMINAL AREA											
Lumbar spine	0.99 ± 0.10g/cm^2										
Total hip	0.89 ± 0.11g/cm^2										
Femoral neck	0.75 ± 0.09g/cm^2										

Table 1: Densities and chemical composition of common tissues (from Hubbell JH et al. 2009) as well as peak BMD of lumbar spine and hip region (as measured by DXA). The density of water is 1.0g/cm^3. Measurements from DXA are in g/cm^2 rather than g/cm^3 as DXA measures areal rather than volumetric density.

There are several methods of measuring bone densitometry including radiography, quantitative ultrasound, dual x-ray absorptiometry, and quantitative computed tomography. As dual x-ray absorptiometry (DXA) and quantitative computed tomography (QCT) were the methods used in the studies presented in the thesis, only these two methods will be described.

Dual x-ray absorptiometry.

In all clinical studies in this thesis, bone density was assessed by DXA. Dual x-ray absorptiometry (DXA), as the name implies, measures the relative tissue absorption of a dual energy x-ray spectrum (Figure 7). The dual energy spectrum is produced in one of two ways. Either a cerium filter is applied to absorb the mid-energy spectrum waves of an x-ray beam yielding effective energies of 40 and 70keV or a dual energy x-ray source is utilized rapidly switching between low (~ 70kVp) and high (~ 140kVp) tube potentials (Damilakis J 2007). DXA is a projectional imaging technique which measures areal density as g/cm^2. Area BMD is measured by dividing bone mineral content (BMC) by the projected area of the scan. Since its introduction into clinical practice in 1987, DXA has become the most widely accepted means of measuring BMD. DXA measures 'integral' bone mineral density since it is unable to distinguish between cortical and trabecular bone. Most centers measure anteroposterior lumbar spine (L1-L4) and hip BMD.

Figure 7A. DXA machine during examination of the hips. Lower limbs are internally rotated to align femoral necks more parallel to the table top.
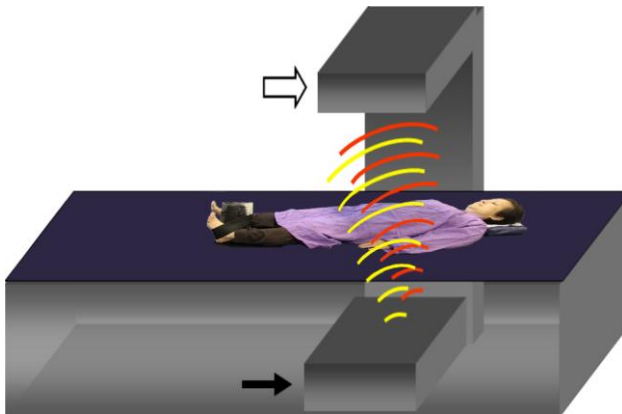
Figure 7B. Schematic representation of open DXA machine. The x-ray tube (arrow) produces dual energy x-ray beam which after transmission is detected by the detectors (open arrow)

Figure 7C. Position during examination of AP lumbar spine. Hips are flexed to smooth our lumbar lordosis.

Bone mineral density as measured by DXA is an important predictor of osteoporotic fracture risk (Johnell O et al. 2005). In a 14 year prospective study of over 1,500 patients aged more than 60 years, the risk of hip fracture was increased 3.6-fold in women and 3.4-fold in men for each s.d. reduction in femoral neck baseline BMD measurement (Nguyen ND et al. 2005).

In pre- and peri-menopausal women, the lumbar spine is the optimal site for serial

monitoring of changes in BMD due to its greater rate of bone mineral density change while the hip is the best site for predicting proximal femoral fracture (Sahota O et al. 2000, Marshall D et al. 1996) (Figure 8). However, in post-menopausal women, serial measurement of lumbar spine BMD is less reliable since it is heavily influenced by new bone formation related to spinal degenerative disease. Hence lumbar spine BMD measurement by DXA will often be see to increase over time rather than decrease in elderly subjects. In elderly subjects, therefore, hip BMD is the better reflection of true BMD change on serial examinations rather than lumbar spine BMD (Figure 9).
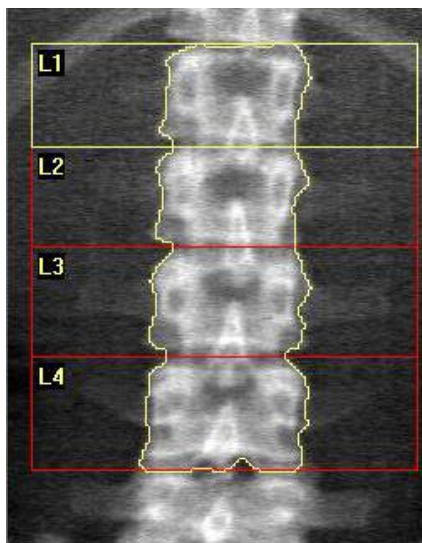
Figure 8. AP DXA lumbar spine. L1-L4 vertebrae are analyzed.
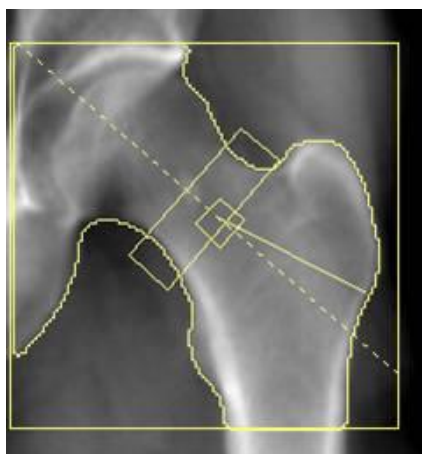
Figure 9. DXA hip. Either the femoral neck BMD or total hip BMD are commonly used for analysis. One measure does not have any particular advantage over the other.

Reduction in BMD can occur either as a result of an decease in BMC or an increase

in bone area. For example, between 30-50 years of age, BMD decreases by 0.4% per annum due to an annual decline in BMC of 0.2% per annum and an annual increase in bone cross-sectional area of 02% per annum (Hui SL et al. 2002, Looker AC et al. 1998).

BMD estimation by DXA is influenced by precision and accuracy errors. Precision errors are mainly equipment and positioning related and are measured by analyzing reproducibility (coefficient of variation) of repeated measurements in the same subject group. Accuracy errors are more subtle and less easily detected then precision errors, being the result of calibration and geometric assumptions, and variable distribution of muscle, fat and bone tissue among different subjects. For example, overestimation of BMD measurements can occur in subjects with spinal degenerative disease, scoliosis, vertebral collapse or aortic calcification. Similarly, it has recently been recognized that underestimation of BMD measurement by DXA may occur if there is accumulation of marrow fat. Phantom DXA studies have suggested a BMD correction of 0.003 g/cm^2 per 1% marrow fat content (Bolotin H et al. 2003). For example, if vertebral marrow increases from 25% to 75% fat fraction, measured BMD by DXA should be decreased by 50 x 0.003g/cms^2 = 0.15g/cm^2. In Study 3 of this thesis we re-evaluate this correction factor and show that correction factor for every % increase in marrow fat should be less than that proposed by Bolotin.

Quantitative computed tomography (QCT).

Computed tomography methods used to assess bone mass and architecture include standard QCT, volumetric QCT, peripheral QCT (pQCT), high resolution pQCT and

microCT (Figures 8 and 9). QCT was used in Study 7 to measure the density of rat vertebrae. We have shown in a further study (not presented in this thesis) that QCT using a clinical CT scanner has several distinct advantages over pQCT when measuring density in experimental animals (Wang YX et al 2008)

Figure 10: Quantitative CT examination of the L2 vertebral body. The graded calibration phantoms which are examined at the same time are shown (arrow).

Peripheral QCT (Figure 11) uses a specialized peripheral QCT system (pQCT) and is used in humans to measure the size and bone mineral density of peripheral bones (the distal radius and distal tibia). PQCT offers isotropic spatial resolution of approximately 500μm. This resolution is sufficient to allow cortical and trabecular bone mineral density to be analyzed separately. In small animals, pQCT can also be used to assess bone mineral density of the spine. However, since rat vertebrae are considerably smaller than the distal radius or tibia in humans, the resolution of pQCT is not sufficient to allow cortical and trabecular bone to be analyzed separately in small animals. pQCT measures volumetric density and measurements are reported in mg/cm^3 as opposed to the areal (g/cm^2) density measurements of DXA.
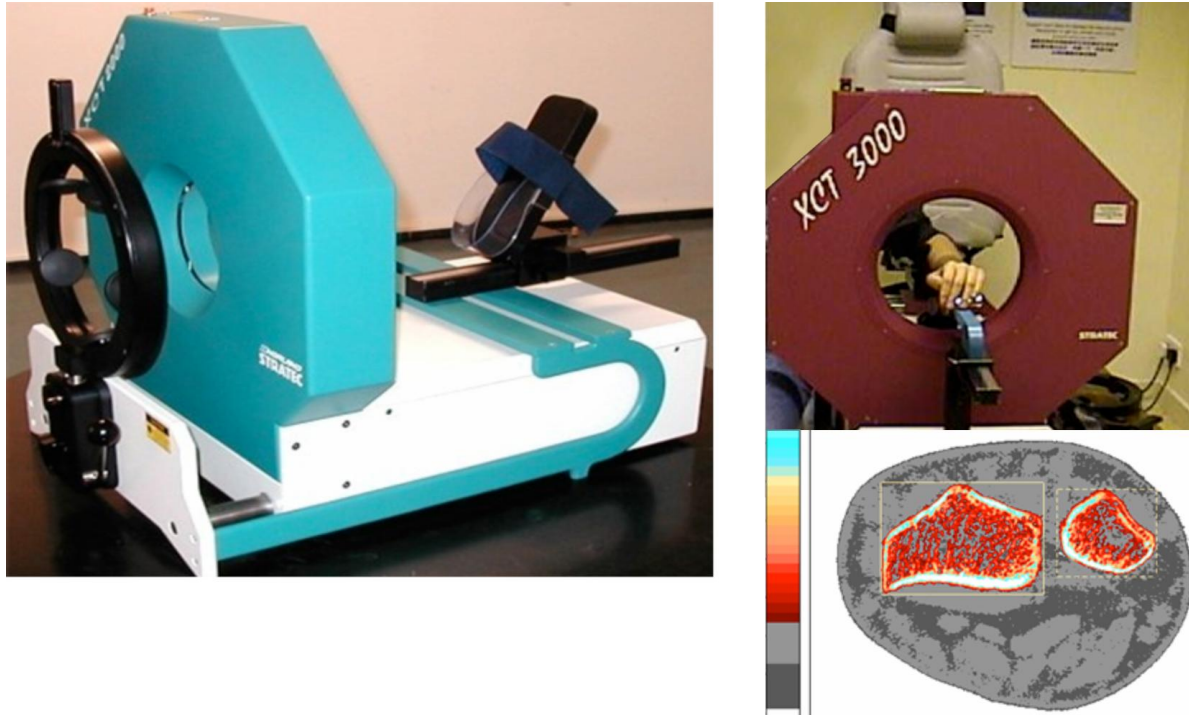
Figure 11: Slide and front views of two different pQCT machines. Wrist image quality is shown.

BONE REMODELLING

We have not studied bone remodeling per se in this thesis though it will be briefly

discussed here as it is an important facet of bone metabolism related to bone density

and an independent predictor of fracture risk. Currently, the gold standard for bone

remodeling is dynamic quantification by tetracycline labeling followed by bone biopsy

at the iliac crest. This method of is not ideal as it is invasive and assessment of any

treatment response involves multiple biopsies. Also, it is more or less limited to the

iliac crest and this site is not necessarily representative of other skeletal sites and is

also subject to large measurement error [Compston JE et al 1991]. A alternative

method is to use urinary and serum markers of bone turnover and these are helpful

in the in the early detection of treatment response [Garnero et al 1999]. However,

they too are subject to wide variability and are limited in providing a measure of total skeletal metabolism and as such may not reflect what is happening at specific sites such as the spine and hip.

It is apparent that a non-invasive method which could measure bone metabolism at a specific site would be very helpful. PET imaging has shown promise in this area. Using ^{18}F-fluoride, PET imaging does allow a non-invasive quantitative assessment of bone metabolism at specific skeletal sites of the skeleton [Cook GJR et al 2000, Frost ML et al 2003] with significant correlation been shown between PET-derived regional skeletal kinetic parameters and bone formation or mineral apposition rate assessed on bone histomorphometry [Messa C et al 1993, Piert M et al 2001]. Whether MR imaging has this potential has not been addressed in this thesis.

1.6 BONE MARROW

The bone marrow is found in the central cavity of bones interspersed and supported by the bony trabeculae and a fibrous tissue retinaculum. The bone marrow is a large organ accounting for about 4% body weight in humans (Travlos GS et al. 2006) such that in a 70kg man, the bone marrow would weigh 2.8kg making it one of the heaviest organs behind the bony skeleton, the skin, and subcutaneous fat (Hwang S et al. 2007).

The bone marrow cavity is made up of trabecular bone, marrow fat, non-fatty cellular elements, water and vascular channels though the actual composition does vary considerably with age, anatomical location and physiological state (Hwang S et al. 2007). The non-fatty cellular elements comprise stem cells, haemopoetic cells

(erythrocytes, granulocytes, lymphocytes, monocytes and platelets) and their precursors. Erythropoesis takes place in distinct anatomical units ('erythroblastic islands'); granulopoesis takes place in less distinct foci and platelet production (megakaryocytosis) occurs adjacent to the sinus epithelium (Travlos GS 2006). Upon maturation haemopoetic cells transverse the wall of the venous sinuses to enter the bloodstream while platelets enter the bloodstream by cytoplastic processes from megakaryocytes penetrating the sinus wall into the sinus lumen (Travlos GS 2006).

At birth, the bone marrow is nearly entirely haemopoetic expect for the epiphysis and apophyses which contain predominantly fat. With maturation, the marrow converts to a predominantly fatty marrow in a symmetrical centripetal fashion (Hwang S et al. 2007). Red marrow converts to fatty marrow from the periphery to the central skeleton. Superimposed on this centripedal pattern, red marrow converts to fatty marrow in the tubular bones proceeding from diaphysis to metaphysis (Hwang S et al. 2007, Hartsock RJ et al. 1965) (Figure 12). By about 10 years of age, marrow conversion of red to fatty marrow has begun in the diaphyses and spread to the metaphyses particularly in the distal diaphyses (Hwang S et al. 2007) (Figure 12). By 20 years, nearly all of the long bone marrow is completely fatty except for the proximal metaphyses (Hwang S et al. 2007) (Figure 12). By thirty years, some red marrow remains only in the proximal metaphyses, and the axial skeletal (pelvis, spine, scapulae, clavicles, sternum and skull). In the event of an increased functional demand for haematopoesis, this sequence of events can reconvert with fatty marrow reconverting to red marrow in a reverse, symmetrical centrifugal manner (Poulton TB et al. 1993).
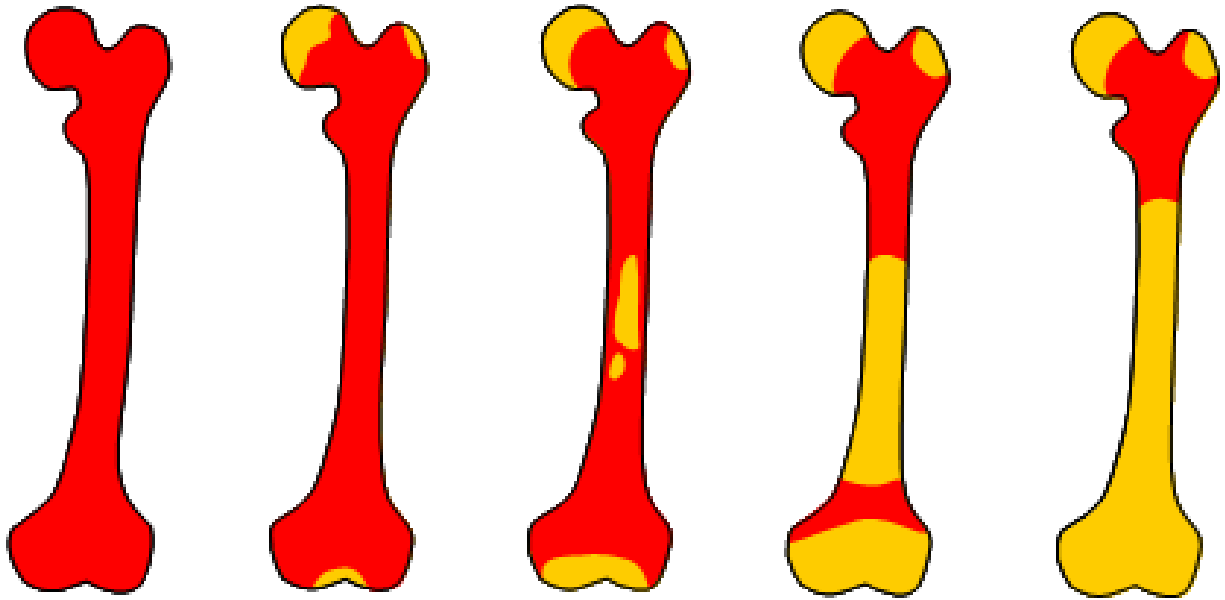
Figure 12: From birth, red marrow converts to fatty marrow from the periphery to the central skeleton. Superimposed on this centripedal pattern, red marrow converts to fatty marrow in the tubular bones proceeding from diaphysis to metaphysis until by the age of 20 years only the proximal metaphysic contains appreciable red marrow. (Adapted from Moore SG et al, 1990).

Bone marrow temperature is slightly lower (1.6-4.8^{0}C) than normal body temperature. The propensity of red marrow to remain in the warmer more central parts of the skeleton may be related to temperature. It has been noted that the armadillos markedly increases its marrow fat during the winter months which is then replaced by red marrow during the warmer summer months (Weiss LP et al. 1956). The composition of reindeer marrow fat has been shown to change with under-nutrition during the winter months changing back to a different composition during the summer months (Soppela P et al. 2001).

Although red and fatty marrow are of course a continuum, what is generally termed 'red' marrow contains about 60% haematopoetic cells and about 40% fat cells (Figure 13 and 14). 'Fatty' marrow, on the other hand, contains about 5% haematopoetic cells and about 95% adipocytes (Steiner RM et al. 1993, Hwang S et al. 2007). In other words, neither red marrow or fatty marrow are 100%

haematopoetic or fatty marrow with fatty marrow being more 'pure' then red marrow

(Figure 13 and 14).
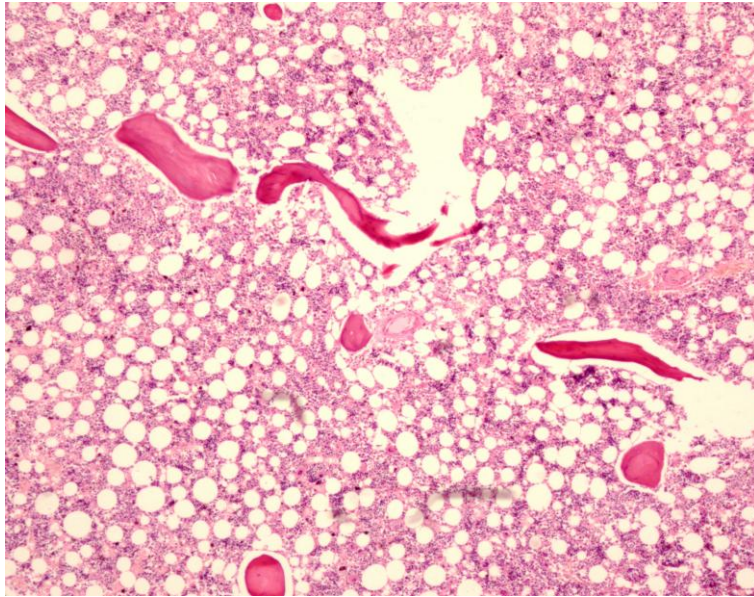
Figure 13. Histology of predominantly red marrow. There is still quite an abundance of fat cells present.
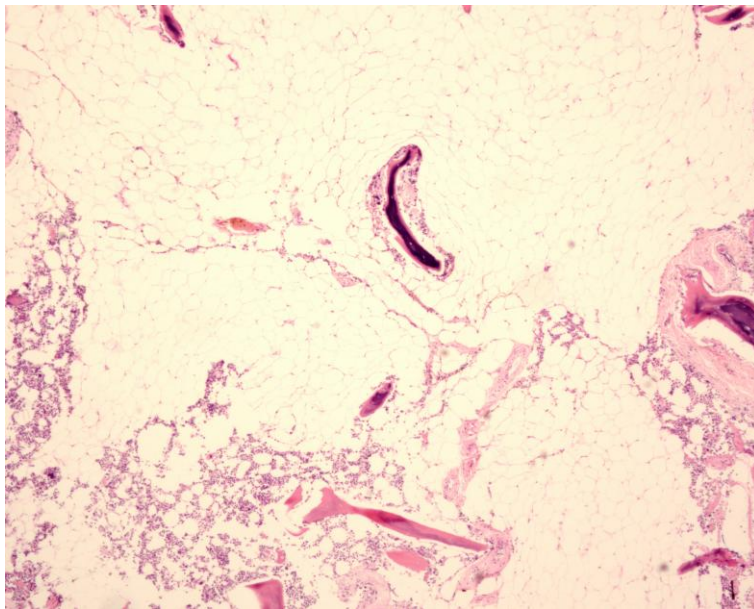
Figure 14. Histology of predominantly fatty marrow. Much fewer red cells are present.
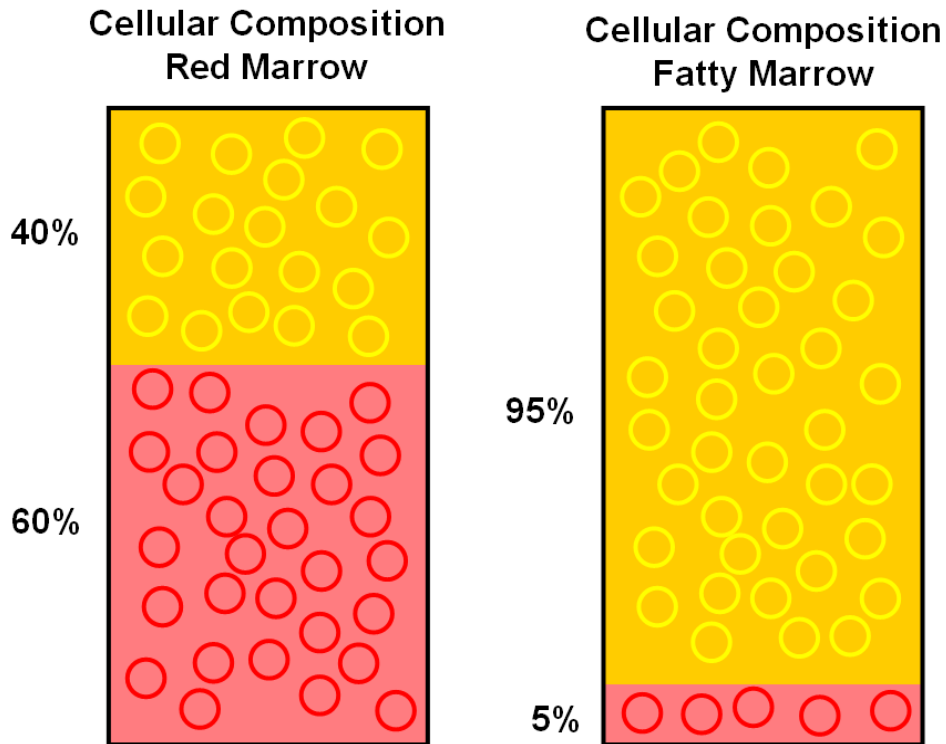
Figure 15: Cellular composition of red marrow and fatty marrow. O = red marrow; o = yellow marrow. Red and yellow marrow are, of course, a continuum though what is termed 'yellow' marrow is more pure than 'red' marrow which still contains quite a lot of fat. (Modified from Hwang S et al 2007).

The broad chemical composition of red marrow is about 50% lipid, 35% water and 15% protein (Steiner RM et al. 1993, Hwang S et al. 2007) (Figure 15). Adipocytes understandably contain more fat than haematopoetic cells while haematopoetic cells contain slightly more water and protein than adipocytes. The broad chemical composition of fatty marrow is therefore about 80% lipid, 15% water and 5% protein (Steiner RM et al. 1993, Hwang S et al. 2007) (Figure 15). This is important since MR spectroscopy uses the fat;water ratio to determine the fat fraction in tissues. The amount of water actually present is assumed to be constant though this may not necessary be the case.
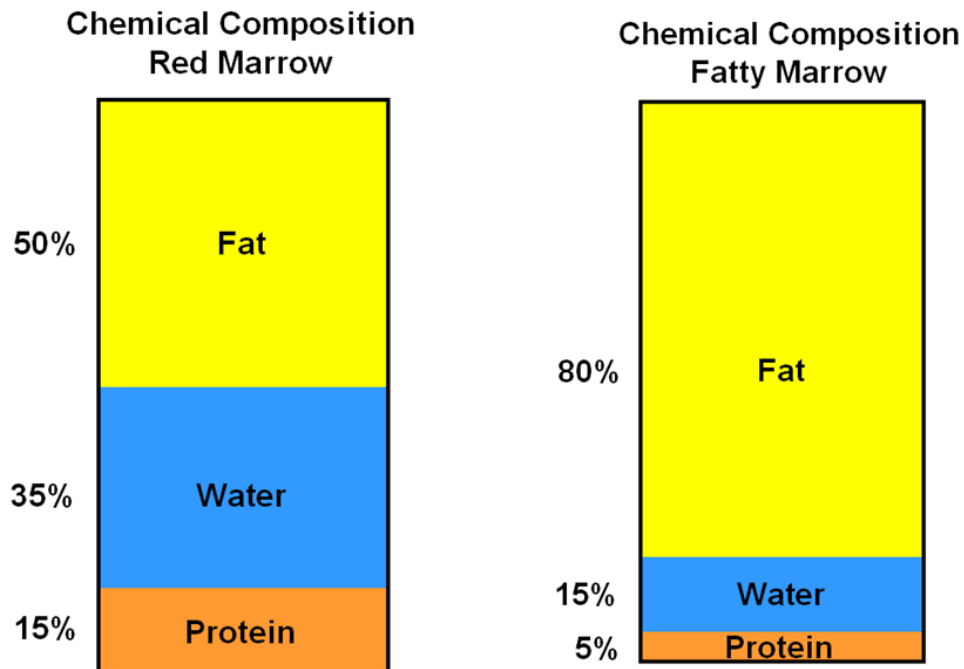
Figure 16: Chemical composition of red marrow and fatty marrow. Haematopoetic marrow contains more water than fatty marrow. (Modified from Hwang S 2007).

The viscosity of the bone marrow in the proximal aspects of the bones such as the proximal femur is several times greater (123-400cP) than the distal bones such as the distal radius or calcaneus (37.5 – 44cP) (Gurkan UA et al. 2008). These figures can be compared to the viscosity of water which is 1cP.

1.7 BONE MARROW FAT

Adult trabecular bone, the most metabolically active component of bone, is bathed in fat i.e. fat forms the main microenvironment of trabecular bone. The endosteal and, to a lesser degree, the cortical margins of bone cortex are also in contact with fat. Bone metabolism may well react to changes in its microenvironment and potentially may react to changes in fat composition. We undertook Study 6 in this thesis to explore this possibility. To comprehend Study 6, some background information on fat and bone marrow fat is necessary. All fats are composed of carbon, hydrogen and

oxygen. Carbon has four bonds available, oxygen has two and hydrogen one (Figure 17).
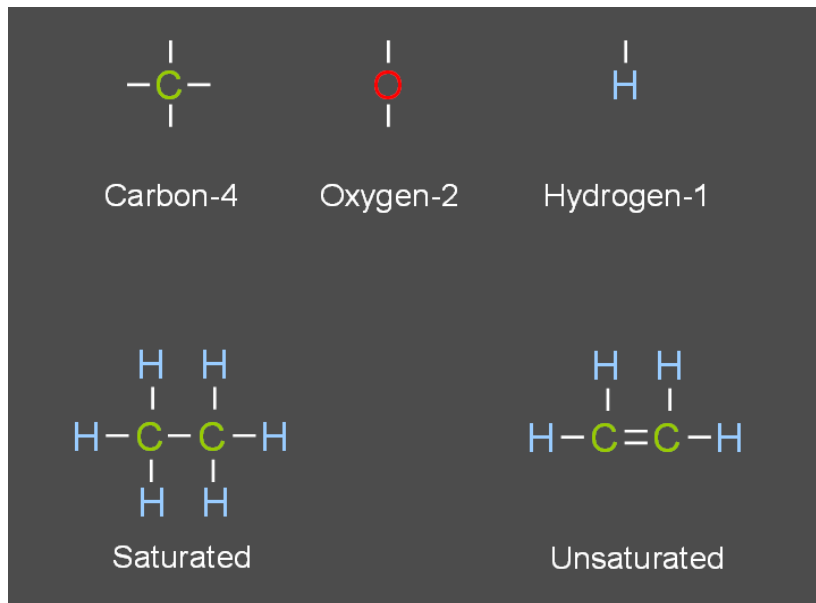
Figure 17. Basic structure of carbon, oxygen and hydrogen with saturated and unsaturated molecule.

Two carbon atoms next to each other can share either a single or double bond. Carbons atoms held together by a single bond are 'saturated' because they are saturated with hydrogen. Two carbons connected by a double bond are 'unsaturated' because each carbon atom can also potentially attach to one more hydrogen atom.

Fatty tissue is made up of fat (~80%), water (~15%) and protein (~5%). The main constituent of fat is fatty acids. There are at least 80 identified fatty acids but only about 30 common fatty acids. Fatty acids are chains of carbon atoms with hydrogen atoms attached to each carbon and an acid (carboxyl, -OH) group at one end. The two important determining factors as to the type of fatty acid are the number of carbon atoms in the fatty acid chain and whether single or double bonds exist between the carbons.

Fatty acids with less than four carbons are known as short-chain fatty acids, fatty acids with between 6-18 carbon atoms are known as medium-chain fatty acids while

fatty acids with 18–28 carbon atoms are known as long chain fatty acids. Fatty acids with no double bones in the chain are called saturated while those with one double bond are called monounsaturated fatty acids (MUFA) and those with two or more double bonds are called polyunsaturated fatty acids (PUFA) (Figure 18).
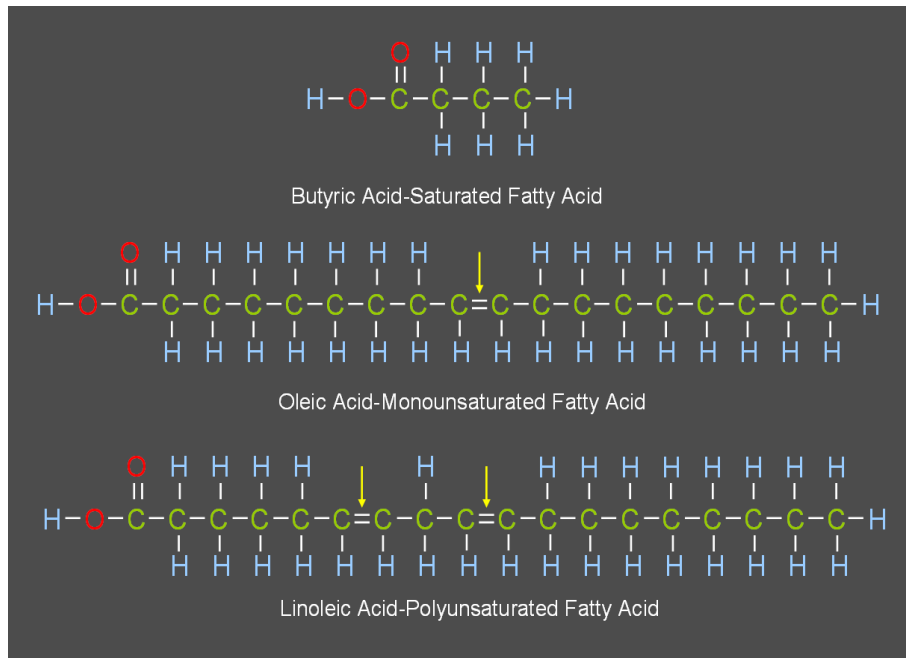
Figure 18: Schematic representation of short chain saturated and long chain monounsaturated and polyunsaturated fatty acids.

Saturated fatty acids and unsaturated fatty acids have different characteristics. Saturated fats, as expected, have limited opportunity for interaction with other atoms and tend to be stable and more inert. As bending occurs at double bonds, saturated fatty acids tend to be straighter unsaturated fatty acids (Figure 19). Straight chains fit together tightly and hence saturated fats like butter and lard are solid at room temperature.
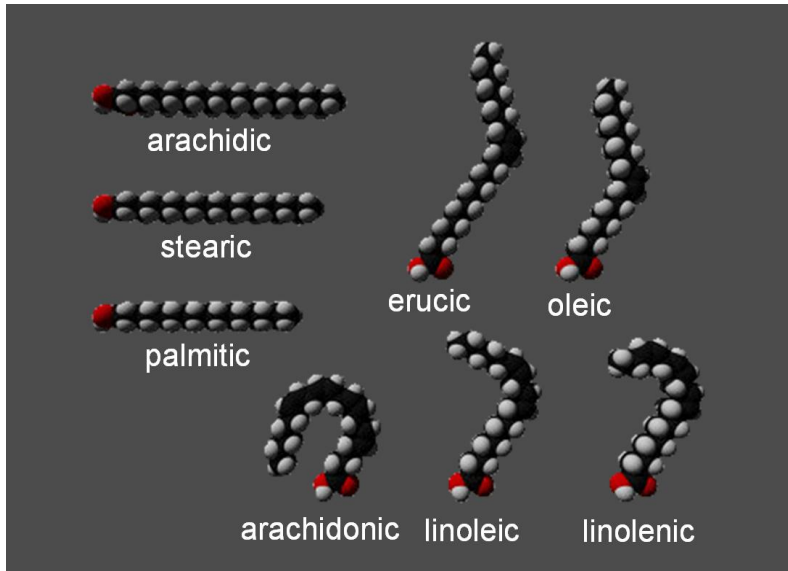
Figure 19: Schematic representation showing how saturated fatty acids form straight chains, monounsaturated fatty acids are slightly curved while polyunsaturated fatty acids are very curved.

Since bending occurs at double bonds, monounsaturated or polyunsaturated fatty acids do not to form straight chains and don't fit snugly together (Figure 19 and 20). As a result, they tend to be liquid at room temperature like vegetable oil. Because of the double bond, they are also less stable. The more double bonds present, the more likely a fatty acid is going to be liquid at room temperature and the more unstable that fatty acid is likely to be (Figure 20). For these and other reasons, polyunsaturated fatty acids tend to be the most metabolically active fatty acids and are the group of fatty acids we will discuss in most detail.
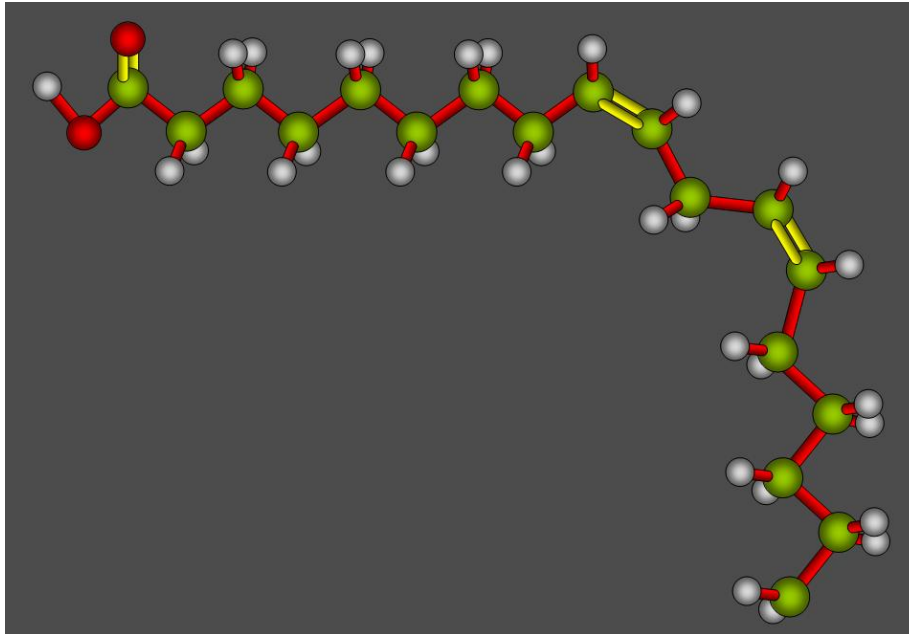
Figure 20;
Schematic representation of linoleic acid (18:2, n=6) which has 2 double bonds the first of which is located at carbon 6 position from the methyl (-CH$_3$) group
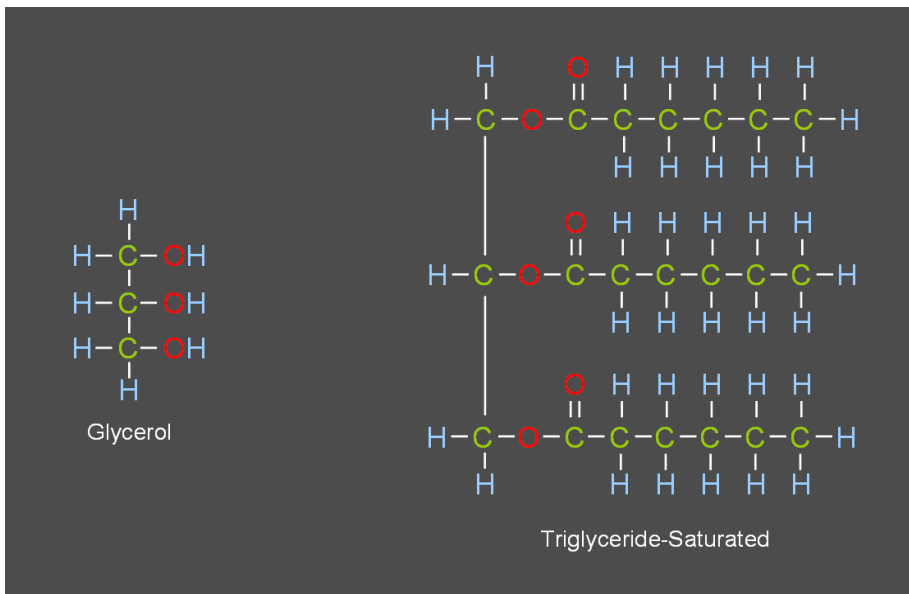
Figure 21:
Schematic representation of glycerol and triglyceride molecule.

Most fats in the body and in food are in the form of triglyceride molecules.

Triglyceride molecules comprise one glycerol molecule (or glycerin, a sugar alcohol) with three fatty acids attached (Figure 21).
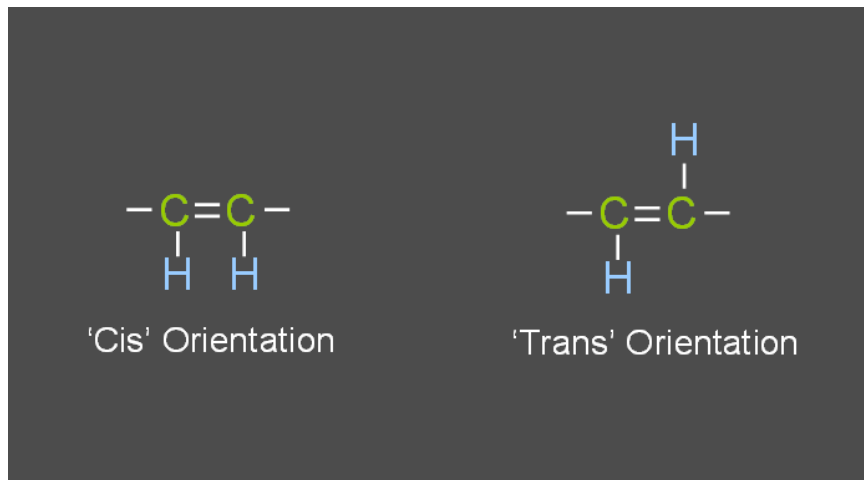
Cis and trans fatty acids. Unsaturated fats with the same composition can have a different configuration according to which side of the double bond the hydrogen atoms align. This concept is important because the shape of the whole triglyceride molecule, and its properties and characteristics, is affected by what happens at each double bond. In a 'cis' formation, the hydrogen atoms align on the same side while in a 'trans' formation; the hydrogen atoms align on opposite sides of the double bond (Figure 22).

Most naturally occurring unsaturated fatty acids contain cis bonds. Most fatty acids with a trans configuration ('trans fats') are the result of human processing. The double bonds in trans fatty acids are easily broken, allowing the formation of free radicals - highly reactive molecules with an unpaired electron (Figure 23). In the studies presented, we have not assessed the relationship between 'cis' and 'trans' marrow fats and osteoporosis.
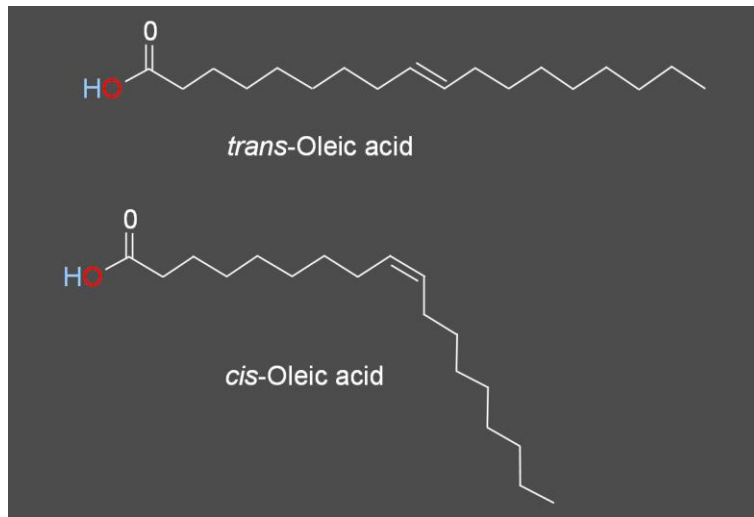
Figure 23: Schematic representation showing how *cis-* or *trans-* orientation can dramatically alter the shape of a fatty acid although the chemical composition remains the same.

Nomenclature of fatty acids. Fatty acids vary in chain length as well as the position and number of double bonds along the chain (Leonard AE et al. 2004). The number of carbon atoms in the chain varies from 4 (butyric acid) to 80 (though most have been 8 and 28 carbons atoms). Fatty acid nomenclature allows one to appreciate fatty acid structure. To describe the structure of a fatty acid molecule, one must give the length of the carbon chain (number of carbon atoms), the number of double bonds and also the position of these double bonds (which will define the biological reactivity of the fatty acid molecule).

The briefest description is to include only the number of carbon atoms and number of double bonds (e.g., C18:0). C18:0 (or 18:0 for short) indicates that the carbon chain of the fatty acid contains 18 carbon atoms with no double bonds. C18:1 would indicate an 18 carbon chain with one double bond while C18:3 indicates an 18 carbon chain with three double bonds. More detailed description also indicates the location of the first double bond. For example, α-linolenic acid (18:3, n=6) indicates an 18 chain fatty acid with three double bonds, the first of which is located at carbon 6 position from the methyl (-CH$_3$) group. Linoleic acid (18:2, n=6) indicates an 18

chain fatty acid with two double bonds, the first of which is located at carbon 6 position from the methyl (-CH$_3$) group.

One can appreciate how the same basic fatty acid can have many different expressions. For example, not all C:18 fatty acids are identical. It may have one or more double bonds in the fatty acid, making it mono- or polyunsaturated rather than saturated. Also each double bond can have a cis or trans confirmation significantly changing the physical properties and reactivity of the fatty acid (Figure 23).

Essential fatty acids. All but two of the fatty acids can be produced endogenously. Two fatty acids can only be obtained from the diet. These are α-linolenic acid (18:3, n=3) and linoleic acid (18:2, n=6). They are called 'essential' fatty acids as they are only obtainable from diet since humans do not possess the ability to synthesize a double bond prior to carbon 9 in the fatty acid chain (Poulsen RC, 2007).

The first of the essential fatty acids is α-linolenic acid (18:3, n=3). This, as the name shows, has an 18-carbon backbone and three carbon-carbon bonds, the first of which is located at carbon-3 when counting from the methyl (-CH3) terminus. This is the parent compound for the n-3 (or omega 3, ω3). polyunsaturated fatty acid series. The other essential fatty acid is linoleic acid (18:2, n=6) (Figure 20). This has an 18-carbon backbone and two carbon-carbon bonds, the first of which is located at carbon-6 when counting from the methyl terminus. This is the parent compound for the n-6 (or omega 6, ω6) polyunsaturated fatty acid series. Most of the long chain polyunsaturated fatty acids have their first double bond located at either carbon-3 (i.e. n-3) or carbon-6 (i.e. n-6) while a few long chain polyunsaturated fatty acids are n-9.

In general, n-3 polyunsaturated fatty acids are protective to health while n-6 polyunsaturated fatty acids adversely affect health.

n-3/n-6 ratio. The fatty acid profile in your body in many respects mirrors the fatty acid composition of your diet over the proceeding months to years. As noted, the two essential fatty acids (α-linolenic acid and linoleic acid), which form the parent compunds of the n-3 and n-6 fatty acid series, cannot be synthesized endogenously. The best dietary source of α-linolenic acid is fish oil as well as fresh green vegetables. Linoleic acid, on the other hand, is present in edible plant oils, such as corn oil and soybean oil, and in the seeds of most plants except coconut, cocoa and palm. Conola oil (derived from rapeseed) contains relatively more n-6 than n-3 fatty acids. Desaturation enzymes synthesize the other longer chain fatty acids from these two parent fatty acids, though these longer chain fatty acids can also be obtained from the diet. The n-3 and n-6 fatty acids chain complete with each other for the limited pool of desaturation enzymes. Hence the n-3/n-6 ratio is in a state of flux very much dependent on dietary intake. The typical western diet nowadays contains much less of the parent compound for n-3 fatty acids (α-linolenic acid) than the parent compound for n-6 fatty acids (linoleic acid). The n-3/n-6 ratio is considered to be of importance to health with, as mentioned, a high n-3/n-6 ratio being advantageous to health while a low n-3/n-6 ratio being disadvantageous to health.

Fatty acids and their metabolites are closely involved in a range of biological activity such as prostaglandin production, inflammatory mediator production, haemostasis, neurotransmitter production, regulation of vascular reactivity and tone as well as cell membrane production. Long chain polyunsaturated fatty acids, in particular, are the

most unstable and hence the most metabolized fatty acids. They are the precursors of a variety of biological products including prostaglandins, leukotrienes, thromboxanes, lipoxins, resolvins and protectins (Poulsen RC et al 2008). One can now appreciate how the concentration of fatty acids as well as the configuration of these fatty acids can potentially influence many biological activities.

1.8. NON-INVASIVE ASSESSMENT OF BONE MARROW FAT

Little information about bone marrow composition can be obtained from radiographs. Computed tomography (CT) provides much more detail in this respect though is still limited in assessment. Nowadays, the main imaging methods by which bone marrow is structurally and functionally assessed in vivo are magnetic resonance spectroscopy (MRS) and nuclear medicine studies including positron emission tomography (PET). In our experiments we used MR spectroscopy to quantify the amount of marrow fat. PET imaging was not used in these experiments but will nevertheless be briefly discussed since PET imaging can provide a measure of marrow metabolism.

MR spectroscopy is the most widely used method to quantitatively assess marrow fat. MR spectroscopy (MRS) is fundamentally similar to magnetic resonance imaging (MRI). Basically, conventional MR imaging measures signals emitted by nuclei within small pixels selected though phase and frequency encoding along magnetic field gradients. This high resolution spatial mapping enables the signal to be transferred into high detail structural images. The signal emitted from each pixel is a product of the water, fat and other chemicals, typically amino acids, contained within that pixel within a frequency scale between fat and water.

MRS uses the same basic principles as MRI but rather than generating an image, focuses on analyzing the frequencies of the signals emitted from the area of interest. In this way, MRS can extract information about the chemicals that reside within a particular frequency scale in both a qualitative and quantitative manner. Because you are analyzing particular frequencies, rather than a range of frequencies, the area examined with MRS is larger than individual pixels as analyzed by MRI. In other words, MRI provides very high structural information about a small area by studying a range of frequencies. MRS, on the other hand, analyses individual frequencies within an area much larger than that of an individual pixel.

MR spectroscopy can be used to measure a large number of nuclei (such as hydrogen, phosphorus and carbon) through, in the bone marrow, we focus on hydrogen nuclei, since hydrogen is these are by far the most abundant nucleus and also emits the most intense radiofrequency signal within an external magnetic field. MRS of hydrogen nuclei is known as proton MRS or ^{1}H-MRS. The size of a typical pixel used from standard MRI imaging is 1-2mm^2 while that of a voxel used in MR spectroscopy is 1.5ml.

There are two methods of proton magnetic resonance spectroscopy: single voxel and multivoxel, with or without spectroscopic imaging. Single voxel proton magnetic resonance spectroscopy provides a rapid biochemical profile of a localized volume within a region of interest. Spectroscopic imaging provides biochemical information about multiple, small and contiguous volumes focalized on a particular region of interest that may allow the mapping of metabolic tissue distribution. By using this method, the data obtained may be superimposed on a standard MR image, thereby

allowing correlation of between the structural changes and the distribution of metabolites within that area. Multivoxel MRS is also known as chemical shift imaging (CSI). In the studies presented in this thesis, single voxel MRS was used.

MR spectroscopy, rather than analyzing frequencies per se, in effect concentrates more on the differences in frequencies between nuclei. Depending on their microenvironment, different nuclei will resonate at slightly different frequencies. MRS readout utilizes a "parts per million or "ppm" scale to describe the "position" of the resonance frequencies on the x-axis. The ppm is calculated by dividing the difference in frequency (in Hertz) of two peaks (with one peak being the reference) by the operating frequency of the MR scanner (in Hertz). This makes comparison of a peak location found on the spectrum of a 1.5T scanner comparable to that found at that location on a 7.0T MR scanner. In other words, the same metabolite will appear at the same location on the ppm scale irrespective of whether the MR unit used was 1.0 T, 1.5T, 3T or 7T strength. The signal intensity (amplitude on the y-axis) and line width provide an area under the peak which can be used to quantify the amount of observed chemical.

The two sequences commonly used in clinical proton magnetic resonance spectroscopy to localize the volume or interest are PRESS (point-resolved spectroscopy) and STEAM (stimulated echo acquisition mode). Both sequences stimulate protons within the volume of interest with minimal signal contamination from outside the region of interest. The STEAM technique generates a cubic or rectangular voxel by using three orthogonal slice selective 90-degree pulses and is useful when a short T1 is required. The PRESS technique also generates a cubic or rectangular voxel using three orthogonal slice selective pulses, although these differ

in that a 90-degree pulse is followed by two 180-degree pulses. Although the voxel generated by PRESS is not as precisely defined as that of STEAM, the signal to noise ratio of PRESS is twice that of STEAM. In the bone marrow, PRESS is therefore preferable to STREAM since precise definition of the volume of interest is not an overriding issue. For MRS performed in other areas such as the brain, the water signal is suppressed allowing other metabolites to be measured and longer echo times (> 135 milliseconds) used. This leads to smaller numbers of metabolites being detected and with better definition of peaks. This high definition of peaks is not necessary in the bone marrow since the two main components present are water and fat.

Other non-spectroscopic yet precise methods of quantifying fat fraction have recently been introduced such as the three-point IDEAL (**I**terative **D**ecomposition of water and fat with **E**cho **A**symmetry and **L**east-squares estimation) or the 2-point Dixon method which involves sequential suppression or fat and water. There is good correlation between all methods with regard quantification of fat in sample.
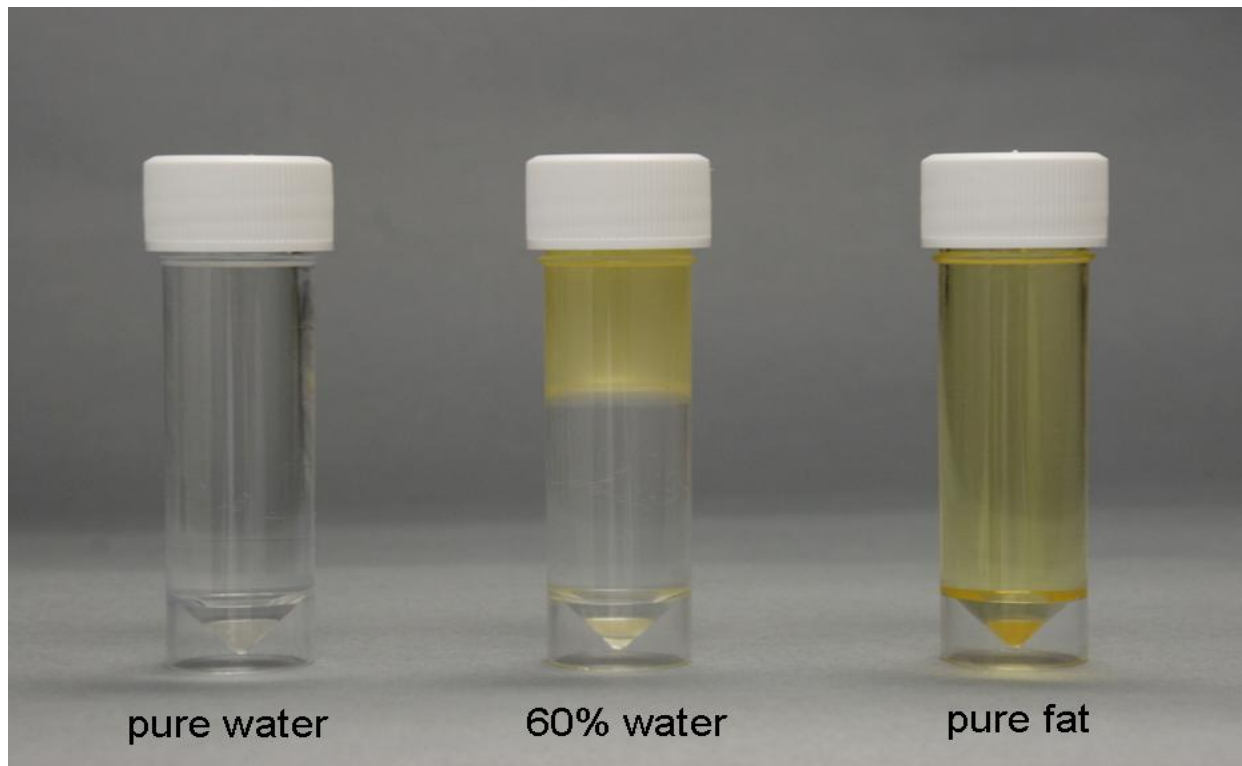
Figure 24. Bernard et al used MRS to quantify the amount of fat in eleven different samples (only three of which are represented for illustration) with varying amounts of fat ranging from pure water to pure fat. The fact that oil and water do not mix does not influence the result as MR fat quantification methods determine the amount of fat and water in the sample as a whole.

The accuracy of MRI spectroscopic and non-spectroscopic methods in detecting the relative amount of water and fat in a sample has been tested against 11 different emulsions of increasing fat content. These test bottles contained increasing amounts of fat from zero (pure water) to pure fat (soya oil) (Figure 24). This study confirmed a high correlation ($r^2 > 0.92$) between MR methods of fat quantification and the % fat volume fraction within test bottles (Bernard C et al. 2008).

MR methods of quantifying fat in tissue use the water;fat ratio. This produces accurate results in vitro as shown above when tested against tissue samples (Bernard C et al. 2008). The limitation, however, is that the amount of water present is assumed to be constant. This in reality may not be the case. MR methods of

quantifying fat have not been quantified in vivo and we have specifically assessed this in our studies to date.

In our studies, we used MR spectroscopy rather than non-spectroscopic methods to quantify marrow fat fraction largely because proton MR spectroscopy is more widely available and online post-processing tools exist which enable ready quantification of fat fraction.

In our experiments, we undertook MR spectroscopy first of the vertebral body (Study 1 and 2) and later of the proximal femur (Study 4). For the vertebral body, the width (w), depth (d) and height (h) of the L3 vertebral body were measured on MR images to define a volume of interest (VOI). A VOI with dimensions w/2 × d/2 × h/2 cm^3 was located centrally in the vertebral body. After local shimming and gradient adjustments, data was acquired at a spectral bandwidth of 1,000 Hz with 512 data points and 64 non-water suppressed signals were obtained using a point resolved spectroscopic sequence (TR/TE, 3000/25 msec). For the proximal femur, three separate standardized volumes of interest (VOI) were placed in the femoral head (1·5 × 1·5 × 1·5 cm^3), femoral neck (1·0 × 1·5 × 1·5 cm^3), and sub-trochanteric region of the femoral shaft (1·0 × 1·0 × 3·0 cm^3). After local shimming and gradient adjustments, data was acquired at a spectral bandwidth of 1,000 Hz with 512 data points and 64 non-water suppressed signals obtained using a point resolved spectroscopic sequence (TR/TE, 3000/25 msec).

One of the main advantages that nuclear medicine and PET imaging has is to assess bone marrow metabolism using 18F-fluorodeoxyglucose positron emission tomography (FDG-PET) imaging. Basu et al has combined segmented volumetric

data from magnetic resonance imaging and quantitative metabolic information from positron emission tomography (PET) and shown how a combined structure function approach can be achieved by combining structural information from MRI with function PET information (Basu S et al. 2007). Vertebral body volume at L1, L3, and L5 was calculated. The red and fat marrow areas were then segmented within these vertebrae using specialized software and respective red and yellow volume calculated in addition to bone volume. Mean of maximum standardized uptake values (mean SUVmax) for bone marrow were calculated in L1, L3 and L5 and then my relating this to the amount of marrow overall as well as the red and fatty marrow components, the activity of red and fatty marrow could be calculated. The mean volume of the lumbar vertebral body was 15.6±1.4 cm^3 of which about 50% was red marrow and 50% fatty marrow. The mean SUV max of bone marrow, fatty marrow and haematopoetic marrow was 1.5 ± 0.3, 0.38 ± 0.1 and 2.6 ± 0.6 respectively. Metabolic volumetric product (MVP) of bone marrow was also calculated by multiplying bone marrow volume by bone marrow SUV. The MVP for lumbar vertebrae, fatty marrow and haematopoetic marrow was 23.4 ± 5.9, 2.9 ± 0.9 and 20.5± 5.9 respectively.

1.9. BONE BLOOD FLOW AND PERFUSION

Although the terms blood flow and perfusion are often used interchangeably, they refer to different physiological processes (Figure 25). Blood flow is flow within vessels i.e. intravascular flow. Perfusion, on the other hand, is a measure of blood flow together with capillary permeability and interstitial diffusion. Perfusion therefore is also dependent on a host of other variables such as capillary surface area, capillary exchange, interstitial space, interstitial pressure, interstitial diffusion, and

venous flow.
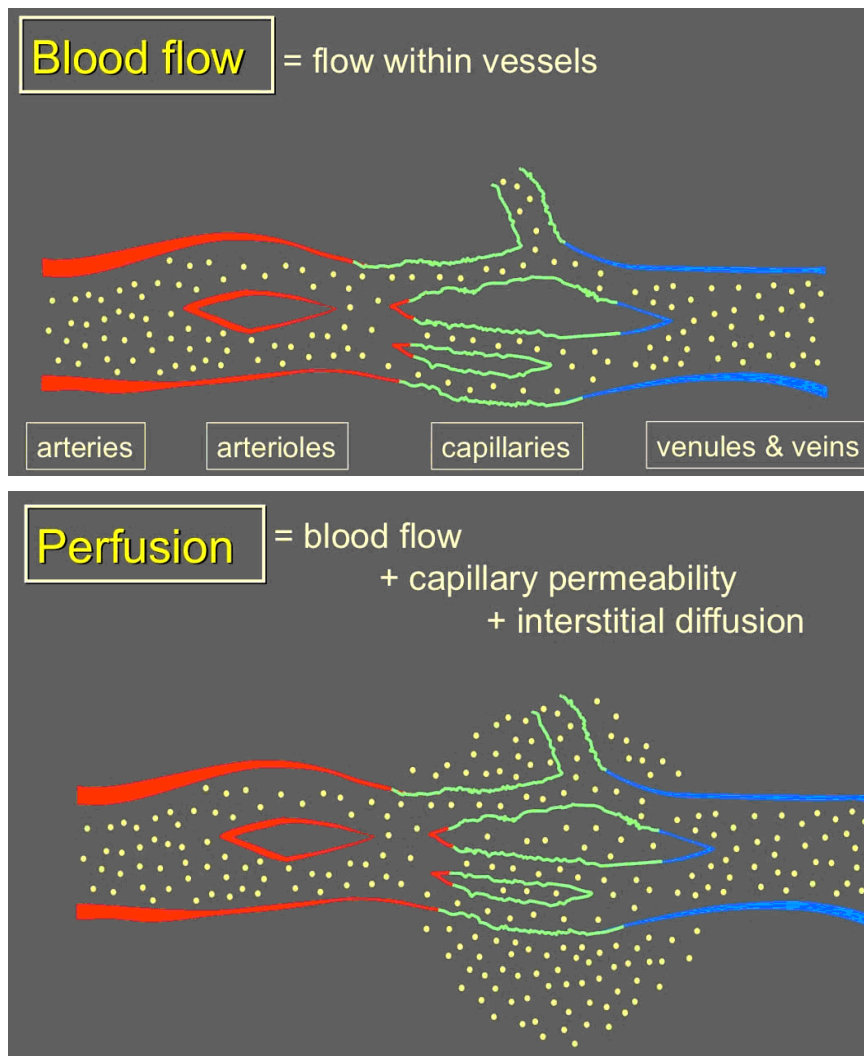
Figure 25. Schematic representation of blood flow and perfusion. Perfusion is a more encompassing term than blood flow.

Since the marrow is encased in bone, arteries and veins must transverse compact bone to enter and exit the marrow compartment. The number of vessels supplying bone varying considerably. The arteries supplying the marrow originate from two systems which anastomose within the marrow. The smaller periosteal arteries supply the cortex and penetrate towards the marrow. The larger nutrient arteries pass through the cortical bone entering the marrow cavity (Travlos GS, 2006) (Figure 26). After entry in the marrow cavity, the artery splits into ascending and descending branches which run parallel along the central part of the marrow cavity (Travlos GS, 2006). The artery branches to give rise to a multitude of small thin-walled arterioles that extend outwardly towards the cortex. The arterioles open up and anastomose

with a plexus of venous sinuses which are more akin to small lakes rather than channels. The venous sinuses are thin-walled and composed of flat endothelial cells with a discontinuous basement membrane (Travlos GS, 2006, Lichtman MA, 1981). This endothelial lining is highly permeable to many solutes but restricts the endothelial movement of cells. The venous sinuses drain via collecting venules back to the nutrient or emissary veins (Figure 26). Thus there is a circular flow pattern to blood flow within the marrow cavity i.e. in towards the centre, out to the periphery and then back to the centre again. This structural arrangement leads to a higher number of vessels and sinuses in the periphery and also slower flow at the periphery of the marrow cavity.

Cortical bone receives the majority (approximately two-thirds) of its blood supply from the medulla and the remainder from the periosteal arteries (Knothe Tate ML 1998). The flat bones possess more numerous nutrient channels through which pass both small and large nutrient vessels (Travlos GS, 2006).

The bone marrow does not have a lymphatic drainage. The bone marrow is innervated with myelinated and non-myelinated cells entering through the nutrient foramina and following the course of the arteries and arterioles. Nerves bundles supply the arteriole smooth muscle with some branches terminating in haemopoetic cells (Travlos GS, 2006).
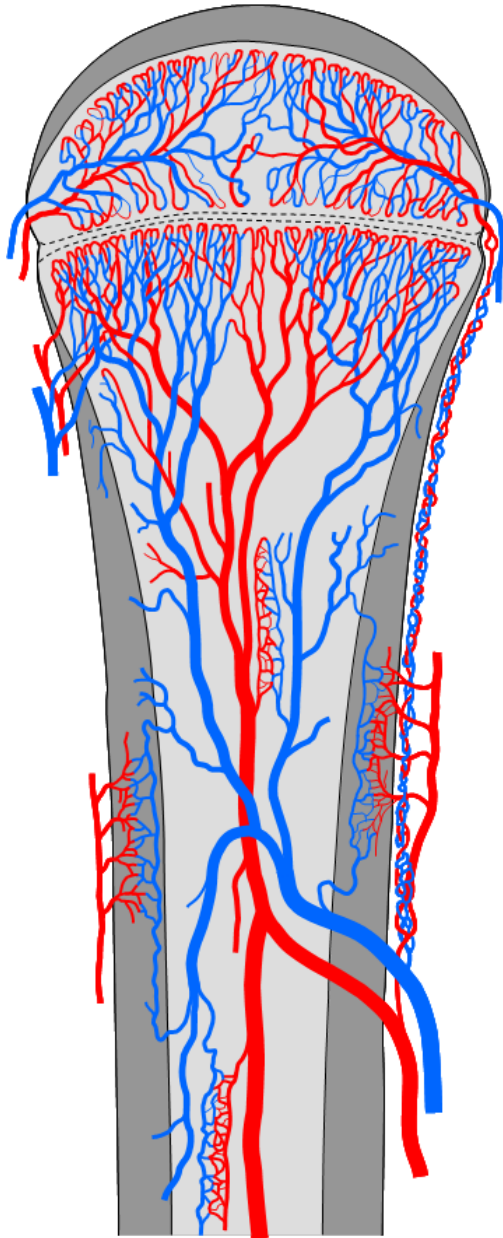
Figure 26: Schematic representation of bone blood supply. Two anastomosing systems are present – the periosteal and nutrient arterial systems. Nutrient arteries branch into arterioles which drain to a network of capillary sinusoids (not shown). Sinusoids are akin to venous lakes. Sinusoids drain to venules which coalesce to form emissary veins exiting via the same nutrient foramina.

The medullary canal is wholly supplied by the nutrient arteries. Approximately, the inner two-thirds of the cortex is supplied by nutrient arteries while the outer one-third is supplied by the periosteal arteries (modified from Diagnogis of Bone and Joint Disorders, 4th Edition, Ed Resnick D. WB Sauders Volume 3, page 2381).

The intramedullary pressure is normally about one-fourth systolic pressure. (Shaw NE 1963). For example if the systolic blood pressue in 120mmHg, one would expect to find the marrow pressure to be 30mmHg. Notwithstanding this, there does also seems to be some regulatory mechanism, probably maintained by the innervated marrow cavity arteries, that maintains a fairly constant marrow pressure within the physiological blood pressure range. Marrow pressure will only drop significantly after systolic pressure falls below 80mmHg (Gurkan UA et al, 2008).

Vertebral body blood supply:

In Study 1 marrow perfusion of the L3 vertebral body was measured using MR perfusion imaging while in Study 2 marrow perfusion of the L3 vertebral body and paraspinal musculature was measured using MR perfusion imaging. The vertebral bodies and the erector spinae muscles are both supplied by the paired segmental lumbar arteries. Each lumbar artery courses around the waist of the vertebral body and passes backwards as a single trunk to cross its respective intervertebral foramen. Each lumbar artery gives off two sets of branches to the vertebral body. The first of these are the short centrum branches which penetrate vascular foramina at regular intervals. The second are the long ascending and descending branches which form dense networks around the vertebral bodies and giving rise to the metaphyseal branches close to the endplates (Figure 27). At the level of the exit foramen, the lumbar artery divides sending branches to the spinal canal, the paraspinal muscles, the posterior spinal elements and the vertebral body (Figure 27) (Crock HV et al. 1976, Ratcliffe JF 1980, Williams A et al. 2005, Kato H et al. 1999). The erector spinae muscle complex lies in the space between the transverse and spinous processes of the vertebrae. In the upper lumbar region it is composed to three columns which are, from medial to lateral, spinalis, longissimus and iliocostalis (Williams A et al. 2005) (Figure 27)
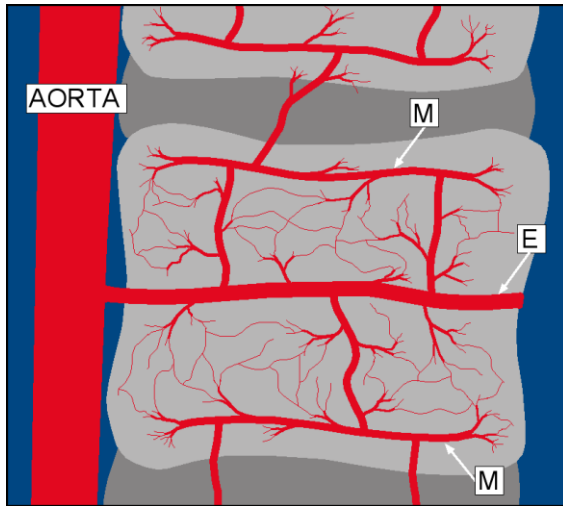
Figure 27A. Schematic representation of vertebral arterial supply. The short centrum branches and the longer ascending and descending branches arising from the lumbar arteries are shown. E = Epiphyseal or lumbar artery; M = metaphyseal artery.
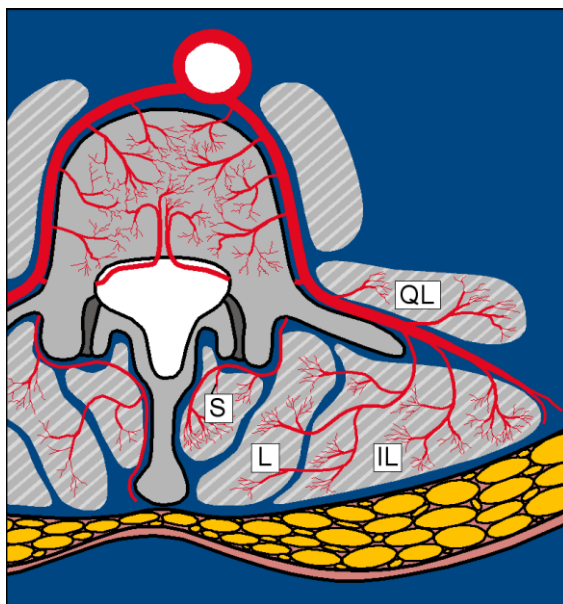
Figure 27B: Schematic representation of vertebral arterial supply. Each lumbar artery divides to send a nutrient artery to the posterior aspect of the vertebral body and additional arteries to supply the paravertebral muscles. L = lumbar artery. QL = quadratus lumborum, S = spinalis, L= longissimus, IL = iliocostalis.

Proximal femur blood supply: In Study 4, the blood supply of the proximal femur, acetabulum and adductor musculature was measuring using MR perfusion imaging. Both the proximal femur and the adductor thigh musculature are both supplied by the profunda femoris artery. The proximal femur is supplied primarily via the medial femoral circumflex artery, the first branch of the profunda femoris artery (Gautier E et al. 2000) (Figure 28) while the adductor thigh musculature is supplied by perforating muscular branches which arise from the profunda femoris artery just distal to the medial femoral circumflex artery (Angrigiani C et al. 2001). The lateral circumflex femoral artery also arises from the profunda femoris artery just distal to the medial

circumflex femoral artery. The two circumflex arteries form an extracapsular arterial ring at the base of the femoral neck (Figure 28). From here, ascending cervical branches penetrate the capsule of the hip joint to form the retinacular arteries just deep to the synovial membrane covering the neck of femur. As the retinacular arteries ascend along the femoral neck, they give off metaphyseal branches that penetrate the femoral neck. They also provide the lateral epiphyseal arteries which continues roughly along the line of the fused epiphyseal plate to the fovea and many smaller lateral epiphyseal braches which supply the femoral head around the margin of the articular cartilage. Some medial epiphyseal branches arise from the artery of the ligamentum teres (a continuation (or branch) of either the obturator artery or less commonly the medial femoral circumflex artery) supplying a small portion of the head than the lateral epiphyseal arteries (Weathersby HT 1959) (Figure 28). The acetabulum is supplied the internal iliac artery via the superior gluteal, inferior gluteal and obturator arteries (Beck M et al. 2003).
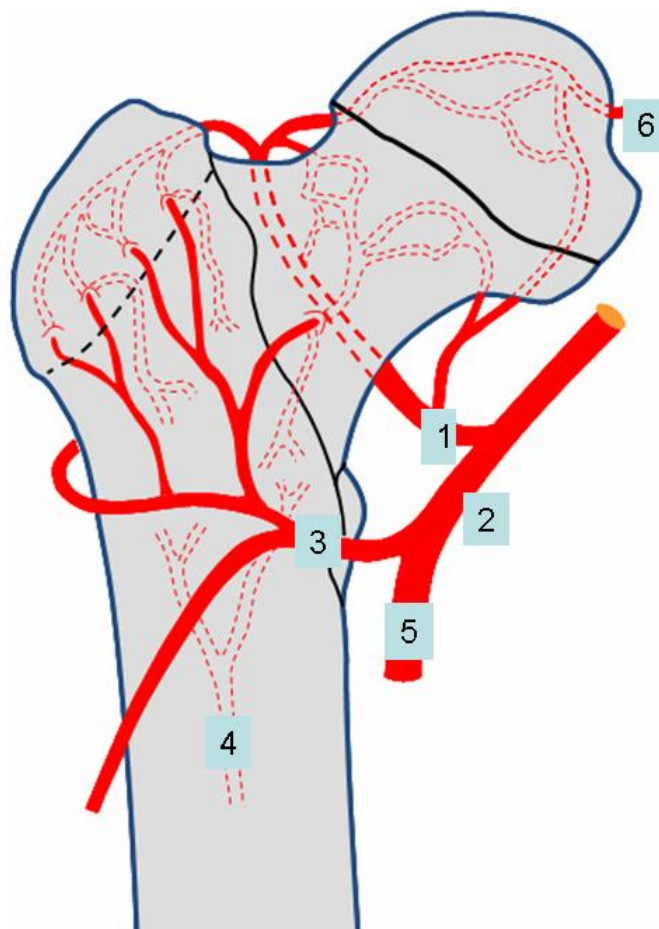
Figure 28: Schematic diagram of proximal femoral perfusion. The proximal femur is primarily supplied by the medial and lateral circumflex femoral arteries – the first and second branches of the profunda femoris artery.

1. Medial circumflex femoris a.
2. Profunda femoris a.
3. Lateral circumflex femoris a.
4. Ascending nutrient a. branch.
5. Muscular br. profunda fem. a.
6. Artery of ligamentum teres

(Modified from Gautier E et al 2000)

1.10 NON-INVASIVE ASSESSMENT OF BONE BLOOD FLOW AND PERFUSION

Only recently did non-invasive methods of measuring bone blood flow become available, namely MR perfusion imaging and nuclear medicine studies including PET imaging. Two reasons mainly contributed to bone marrow blood flow being difficult to measure. First, the present of a bone cortex ensures that the implantation of any intraosseous instrument will by its very nature alter intramedullary status, flow and pressure. Second, each bone is served by a multitude of arterial and venous channels Early researchers tried venous sampling (Cumming JD et al. 1960), thermocouple devices (Shaw NE et al. 1963), plethysmography (Edholm DG et al. 1945) and intravenous dye. In the 1950's and 1960's, the availability of

radiopharmaceuticals lead to radioactive tracers ([86]Stronium, [45]Calcium, [43]Potassium, [86]Rubium, [18]Fluoride, [24]Sodium, [86]Sulphur) being used to assess blood flow by a large number of researchers (Edholm DG et al. 1953 , Frederickson JM et al. 1955, Cumming JD et al. 1960, Holling HE et al. 1961, Weinmann DT et al. 1963, Copp DH et al. 1965, Van Dyke et al. 1965, Shim SS et al. 1967). Other researches have used xenon (Lahtinen T et al. 1981) while more lately PET imaging with various tracers such as radioactive oxygen ([15]0) labelled to carbon dioxide (Martiat P et al. 1987) or water (Piert M et al. 1998) and radioactive ^{18}F labeled to fluoride (Piert M et al. 1998, Blake GM et al. 2001) have been used to assess bone blood flow or perfusion. Microspheres are the gold substance used to assess blood flow in animal models (Gross PM et al. 1979, Chen LT et al. 1986, Schoutens A et al. 1990, Iversen O et al. 1992). From the injection site in the left ventricle microspheres are distributed homogenously in arterial blood and are dispersed to the peripheral vascular systems where, due to their large size, they become lodged in either arterioles or capillaries. Because of their homogenous distribution, the number of spheres lodged in an organ is directly proportional to the blood flow of the organ. Blood flow is calculated as number of spheres in an organ compared to an arterial reference sample. The number of spheres is calculated either by their radioactivity, colour or fluorescence (Anetzberger H et al 2004). Microspheres are only used in preclinical studies and cannot be used in humans since they occlude vascular beds. Also as microspheres do not diffuse into the interstitial space they provide a measure of tissue blood flow rather than perfusion.

Whatever the method used, it is clear that bone blood flow or perfusion measurement is very much dependent on the physical and pharmokinetic

characteristics of the tracer being used. When deciding on a use of a tracer to measure blood flow or tissue perfusion, one should take into account the tracer distribution to the tissue (which should be proportional to arterial input), capillary permeability, lack of any binding capacity, absence of metabolism and washout (which should be proportional to the venous return. The ideal tracer should also not enhance or diminish blood flow or perfusion of the tissue under investigation.

Bone perfusion assessed by MR imaging

MRI is the most widely used method of assessing tissue perfusion. Dynamic contrast-enhanced magnetic resonance imaging (DCE-MRI) (or MR perfusion imaging) involves the rapid acquisition of serial MRI images before, during, and after the administration of an MR contrast agent. The contrast agent used in these studies was Gd-DOTA (DOTAREM).

Gadolinium is an ionic macrocyclic thermodynamically stable molecule (Port M et al. 2008) (Figure 29). These properties make it safer than open chain non-ionic gadolinium contrast agents with respect to the development of nephrogenic sclerosing fibrosing (NSF). NSF always develops in patients with chronic or acute renal disease (Knopp EA et al. 2008). Of those with chronic kidney disease, an estimated glomerular filtration rate (eGFR) of 30 ml/min/1.73 m^2 or less seems to be a prerequisite for developing NSF (Knopp EA et al. 2008). The plasma elimination half life of gadolinium compounds is about 1.5 hours but is dramatically increased (up to and beyond thirty hours) in subjects with severe renal failure. Persistence of a high concentration of Gd^{3+} chelate in the body increases the likelihood of dissociation of Gd^{3+} from its chelate though this is more common in non-ionic open chain molecules rather than in the in cyclic arrangement of DOTAREM where the

Gd^{3+} is more shielded from its chemical microenvironment (Figure 26). Subjects undergoing perfusion MR imaging are at likely to be at greater risk of NSF since a double or treble dose of contrast medium is often employed to improve signal:noise ratio when assessing areas with relatively poor perfusion. In the clinical studies presented in this thesis, which were performed only on healthy subjects, we ensured that there was no history of renal disease and only performed perfusion MR imaging provided renal function was normal serologically within twelve months of the MR examination.
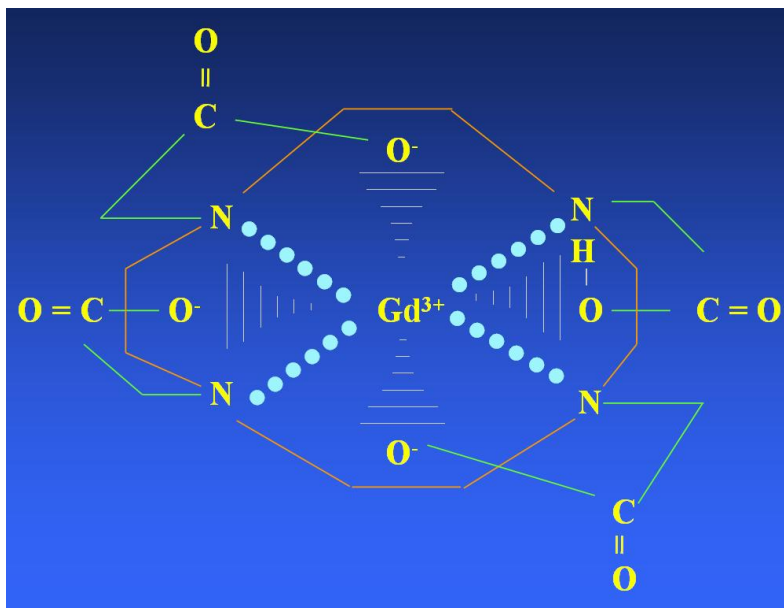
Figure 29: Macrocyclic molecular structure of Gd-DOTA (DOTAREM). Note how the Gd3+ ion is effectively isolated within the chelate complex so that it cannot react normally with other elements or ions.
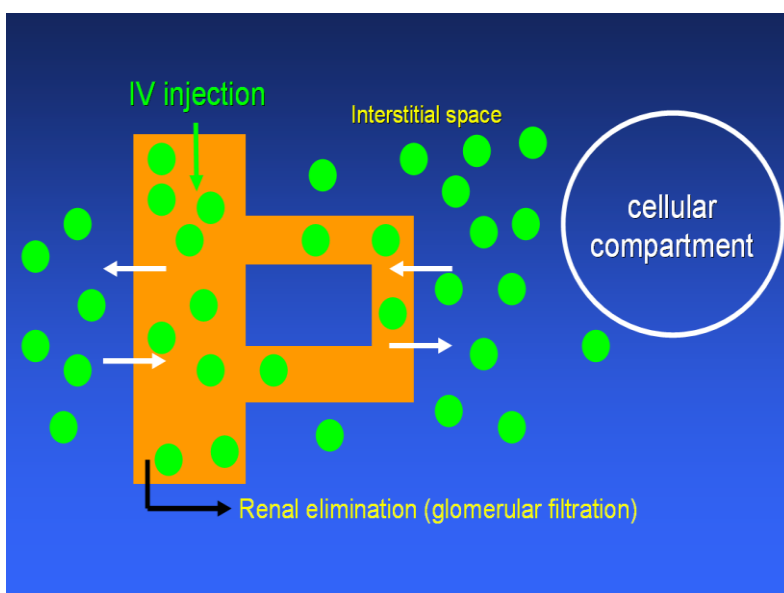
Figure 30: Bicompartmental model of Gd-DOTA (DOTAREM). Following injection it is either in the intervascular space or the interstitial space. It does not enter the intracellular space.

DOTAREM is a small hydrophilic complex with a pharmacokinetic profile quite similar to water-soluble iodinated contrast agent i.e. it conforms to a two compartmental model (intravascular space and interstitial space) without metabolism and is excreted by passive renal glomerular filtration (Figure 30). It does not pass through the cell membrane and therefore is not subject to enzymatic activity and does not bind to proteins in the intervascular or interstitial spaces.

Quantification of contrast agent concentration in tissues necessitates the acquisition of a T1-value of the target tissues before DCE MRI, i.e. the native T1 value of each pixel within the imaged area, or T1 value within a region of interest (ROI) if the signal to noise ratio does not allow pixel-by-pixel analysis. Gadolinium chelate contrast agents (such as DOTAREM) rapidly diffuse into the extravascular interstitial space (also called the 'leakage space'), at a rate determined by blood flow, capillary permeability, capillary surface area and interstitial pressure, interstitial space and interstitial flow. Gadolinium exerts a paramagnetic effect on nearby water protons, causing them to relax more rapidly on T_1-weighted imaging. As a result, T1 signal intensity increases proportionate to the concentration of gadolinium chelate. Pharmacokinetic modeling ideally requires a nearly linear relationship between gadolinium chelate concentration and signal intensity. Exact linearity is never achieved and can only be approximated with low doses of gadolinium chelate (Donahue MJ et al. 2006). Linearity, while desirable, is not an absolute necessity as many physiological phenomena can be observed with slightly non-linear gadolinium concentration-signal intensity pharmokinetics.

Unlike conventional enhanced MRI, which simply provides a snapshot of enhancement at a single time point, DCE-MRI permits a depiction of the wash-in and wash-out contrast kinetics within the tissue under investigation. DCE-MRI or

perfusion imaging is a very robust imaging technique which can be applied to almost any tissue. Empirical measures such as maximal signal intensity enhancement and enhancement slope can be readily obtained. This data is also amenable to two-compartment pharmacokinetic modeling from which parameters based on the rates of exchange between both compartments can be generated. DCE MRI has been used to evaluate the pathophysiological status of many diseases where circulatory disturbances occur such as tumours, inflammation, and osteonecrosis (Galbraith SM et al. 2002).

For DCE MRI studies, many variables should be standardized such as the dose of contrast agent, method of contrast administration, speed and duration of image acquisition, spatial resolution and coverage, and data analysis. Spatial sampling (single or multiple slices, in-plane spatial resolution, and slice thickness) and temporal sampling (the rate at which the time-varying signal intensity curve is sampled) are interrelated variables that are limited by the signal-to-noise ratio and the inherent contrast of the target tissue. The purpose of DCE MRI is not to provide ultimate spatial resolution. Greater spatial resolution requires longer sampling times and therefore slower temporal sampling rates. Faster temporal sampling, as in the case of blood volume mapping, is usually restricted to one or two slices. Faster imaging rates and smaller voxel sizes decrease SNR and counterbalance the sensitivity and reliability of dynamic contrast enhanced MRI.

It is in these respects that DCE MRI differs significantly from conventional post-contrast MRI examinations in that particular care must be exercised to ensure uniformity of positioning and examination technique, contrast agent injection rate, dosage and timing of image acquisition. The protocol should be precise and detailed, and the examination and analysis carried out by experienced, personnel familiar with

the examination protocol. Failure to obtain uniformity in DCE MRI examination and analysis will confound the results of cross-sectional and longitudinal studies.

In the studies presented in this thesis, we evaluated bone marrow perfusion rather than bone perfusion per se. Bone marrow perfusion is likely to be akin to the perfusion of bone trabeculae as the bone trabeculae are so thin, do not have their own inherent blood supply and are nourished via the surrounding marrow. The blood supply of cortical bone is different to that of bone marrow and in the bones examined (vertebrae and proximal femur) is different to measures as in these bones the cortex is relatively thin with a greater reliance on the trabecular network for bone strength at thee locations. It may be possible to measure bone blood supply of the thick anterior cortex of the tibia.

Perfusion indices used in dynamic-contrast enhanced MRI. Empirical (semi-quantitative) measures describe tissue enhancement using a number of parameters derived from a time-signal intensity enhancement curve following contrast agent injection (Figure 31). Parameters that can be used are (1) onset time (time from contrast agent injection to the first increase in tissue signal enhancement), (2) mean gradient of the enhancement curve upsweep (E^{slope}), (3) maximum signal intensity (E^{max}), (4) washout gradient as well as (5) the initial area under the time-intensity curve (AUC). Of these five parameters, the two most robust and commonly applied parameters are enhancement slope (known as ES or E^{slope}) and enhancement max (known as ME or E^{max}). (Figure 31)
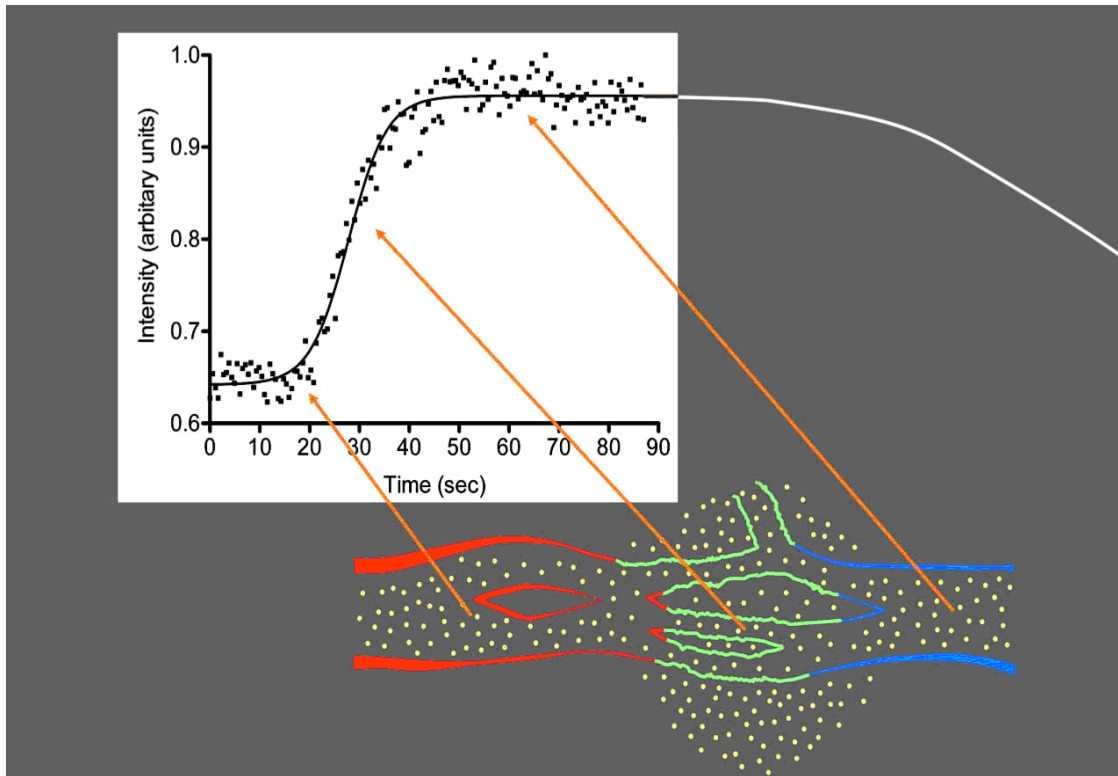
Figure 31: Time-intensity curve. Baseline represents time between injection and contrast arriving in tissues. Slope represents contrast in arterioles and capillaries of tissues and diffusing into interstitial space. Plateau represents contrast equilibrium in tissues. This occurs within the first 60 sec after injection (X-axis). Washout-phase occurs over the ensuing five minutes.

Enhancement slope is defined as the rate of enhancement between 10% and 90% of maximum signal intensity post enhancement (I_{max}) and baseline prior to enhancement (I_{base}) (Figure 29). Maximal enhancement (E^{max}) and enhancement slope (E^{slope}) are calculated according to Equation 1,2 .

$E^{max} = [(I_{max} - I_{base})/ I_{base}] \times 100$ Equation 1

$E^{slope} = \{[(I_{max} - I_{base}) \times 0.8]/[I_{base} \times (t_{90\%} - t_{10\%})]\} \times 100$ Equation 2

Where $t_{10\%}$ and $t_{90\%}$ represent the time interval for the signal intensity following enhancement to reach 10% and 90% of the maximum signal intensity difference between I_{base} and I_{max}.
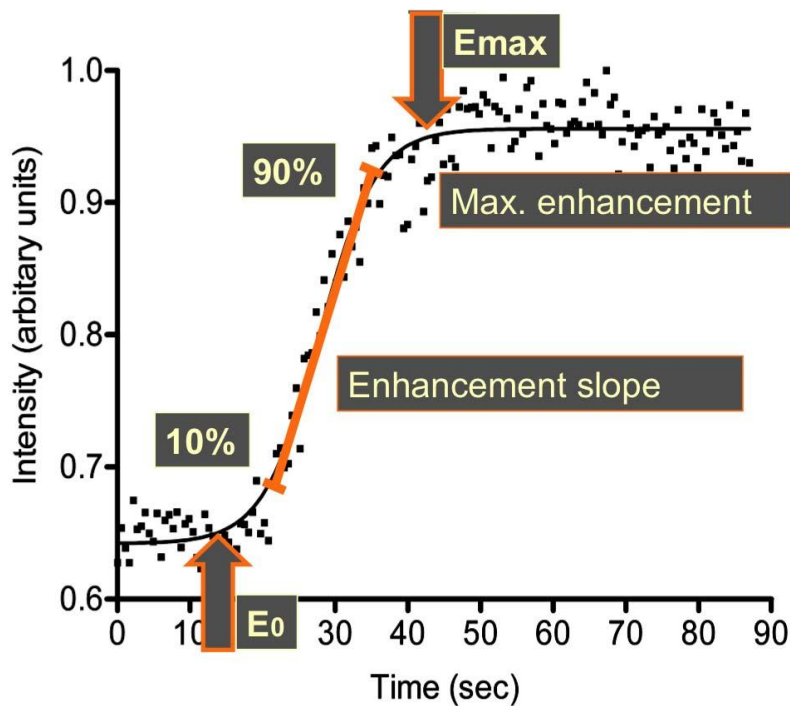
Figure 32: Time-intensity curve with E^{max} and E^{slope}. E^{max} represents maximum enhancement while E^{slope} represents the slope of the rapidly up-rising part of the curve.

E^{slope} and E^{max} are derived from the first-pass phase of signal intensity enhancement and are considered to represent arrival of contrast material into the arteries and capillaries and its diffusion into the extracellular space (Figure 32). E^{slope} and E^{max} are advantageous parameters in being relatively straightforward to analyse, but do have limitations. Maximum enhancement and enhancement slope time-signal intensity curve indexes are dependent on many factors, including amount and speed of administration of contrast material, blood volume, tissue permeability, and available leakage space with elevated interstitial fluid pressure being a likely physiological barrier to contrast agent exchange. In other words, E^{slope} and E^{max} represent indices of perfusion, they are not in themselves a direct measure of perfusion. Nevertheless, they have been shown to be strongly predictive of tissue vascularity, microvessel density and tissue necrosis (Choyke PL et al. 2003, Knopp MV et al. 2001).

More detailed pharmokinetic modeling methods for MR perfusion imaging.

E^{slope} and E^{max} represent the simplest methods of analyzing perfusion data using time-intensity curves. Largely the same perfusion data acquired from dynamic contrast-enhanced MR imaging is also amenable to two-compartment pharmacokinetic modeling which can provide a measure of the rates of exchange between both compartments. Two such models have been used in perfusion studies of brain and breast tissue, namely the Tufts model and the Brix model. Data acquisition is very similar to that acquired in our studies although acquisition should go on for several minutes instead of the 90-120 sec used in our studies.

The Tufts model (Figure 33) analyses the concentration of contrast in the tissues using a combination of arterial input function (AIF), and rate constants K^{trans}, K^{ex} and K^{el}. Arterial input function is a measure of the amount of contrast in the feeding artery. Ideally, at the time of image acquisition all the contrast should still be a bolus. However, in reality, as it takes time to inject contrast which then mixes with blood, the true input function is more like a bell curve. The arterial input function can be assessed by knowing the caliber of the main supplying artery and its first pass intensity profile. K^{trans} refers to the transport constant and is influenced primarily by blood flow. K^{ex} refers to capillary exchange and is influenced by capillary space, permeability, interstitial pressure and extracellular space. K^{el} refers to elimination or wash-out and is influenced by venous flow and venous return to the heart.
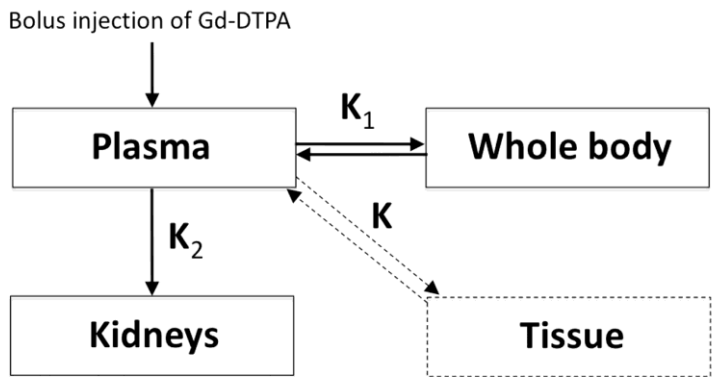
Figure 33: Schematic representation of Tofts model

The Brix model (Figure 34) is in many respects a simpler model than the Tofts model. It does not rely on arterial input function (AIF) or K^{trans} but still considers K^{ex} and K^{el}. It instead assumes a linear relationship between MR signal enhancement and tissue contrast concentration. In other words, it assumes that tissue contrast concentration is a direct measure of perfusion.
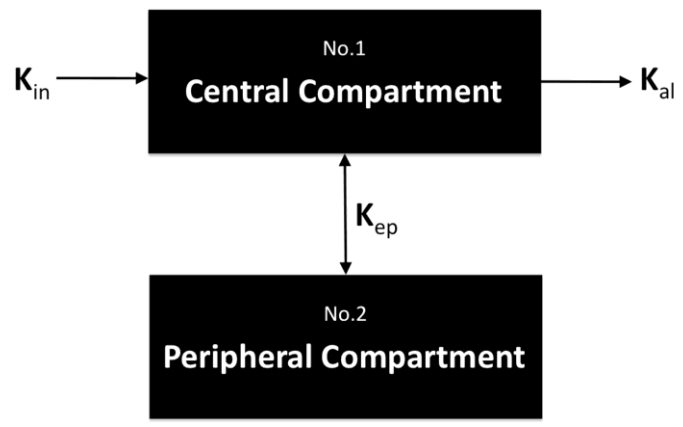
Figure 34: Schematic representation of Brix model

There are other methods of measuring tissue perfusion using MR imaging that not been used in this study. These are $T2^*$-weighed imaging (also known as blood oxygenation level dependent or BOLD imaging) and arterial spin labeling. These methods have been used to assess musculoskeletal sarcoma, synovitis and muscle perfusion (Lang P et al. 1995, Reddick WE et al. 1999, Reece RJ et al. 2002) though

have not been used to evaluate bone marrow perfusion.

Bone perfusion assessed by PET imaging

PET CT assessment of perfusion is usually undertaken using ^{18}F-fluoride which has a half-life of 112 minutes. As this tracer is metabolized by bone, PET imaging using ^{18}F-fluoride is a combined measure of both bone perfusion and bone metabolism as compared to MR perfusion imaging which measures bone perfusion in isolation. Pure bone perfusion can be evaluated by PET using the freely diffusible tracer [15]OH_2O. However, these studies are not readily available since [15]OH_2O has a half life of only 122 seconds and thus requires an on-site cyclotron. Nevertheless, a highly significant correlation between blood perfusion measured using ^{18}F-fluoride and true bone perfusion using [15]OH_2O has been reported [Piert M et al. 2002].

A standard PET technique using ^{18}F-fluoride to assess bone perfusion comprises a preliminary 15-minute scan of [68]Ge/^{68}Ga rods for attenuation correction purposes. After injection with ^{18}F-fluoride, a 60-minute emission scan is obtained during which up to 300 images acquisitions are obtained. At the same time, venous (or arterial) blood samples are taken at regular intervals to measure plasma ^{18}F-fluoride concentration for assessment of arterial input function.

Skeletal ^{18}F-fluoride kinetic parameters are estimated using a three compartmental tracer kinetic model, comprising a vascular compartment, an extravascular bone compartment and a bone mineral compartment [Hawkins RA et al. 1992] (Figure 35). Rate constant K1 describes clearance of fluoride from plasma to bone, K2 describes the reverse transport of fluoride from bone extravascular compartment to plasma,

and K3 and K4 represent the incorporation and release from the bone mineral compartment. A fifth constant Ki can be added to represent fluoride metabolism by bone.

Figure 35: Schematic representation of three compartmental PET imaging bone kinetic model described by Hawkins et al. showing rate constants K1-K4. Fifth constant Ki is not shown.

One can appreciate that PET perfusion imaging takes a lot longer than MR imaging to perform and is more labor intensive. PET also has a notably poorer spatial resolution then MRI (>5mms for PET compared to <1mm for MRI) limiting separate analysis of smaller areas such as trabecular bone and cortical bone. Also muscle cannot be evaluated in the absence of additional CT imaging. Overall, in the assessment of skeletal tissue perfusion, PET imaging seems to have many more disadvantages rather than advantages compared to MR imaging

Following sections. In the following sections, eight studies we have undertaken to determine the relationship between marrow and muscle perfusion, bone marrow fat and osteoporosis will be described.

STUDY 1:

What is the relationship between bone perfusion, marrow fat and bone mineral density?

Aim: To study whether marrow perfusion is altered in subjects with reduced bone mineral density and to see how this relates to marrow fat content

Rationale for doing this study:

Over the last two decades, increasing indirect evidence has suggested a link between osteoporosis and vascular disease. Epidemiological and clinical studies have shown how aortic calcification is an independent predictor of hip osteoporosis (Bagger YZ et al. 2006); how atherosclerosis is more common in women with osteoporosis than those with osteopenia or normal BMD (Ness J et al. 2006) and how low BMD independently predicts coronary artery disease in women undergoing coronary angiography better than traditional risk factors such as age, hypertension, diabetes, smoking, family history, or dyslipidemia (Marcovitz PA et al. 2005). Other clinical studies have shown that increased serum-angiotensin converting enzyme activity and impaired endothelial function are features of osteoporosis (Sanada M et al. 2004, Samuels A et al. 2001). Histological studies have shown how progressive occlusion of intraosseous arteries, arterioles or arterial capillaries occurs in patients with increasing age (Bridgeman G et al. 1996) and in patients with proximal femoral osteoporosis (Laroche M et al. 1995).

Recent MR-based studies have shown that changes in bone marrow fat content and bone marrow perfusion occur with aging. Dynamic contrast-enhanced MR imaging studies have shown that vertebral marrow perfusion is reduced in older subjects

(Chen WT et al. 2001, Montazel JL et al. 2003, Baur A et al. 1997). Proton (^{1}H) MR spectroscopic studies have shown an age-dependent linear increase in vertebral marrow fat content (Schellinger D et al. 2001, Kugel H et al. 2001). These studies examined the relationship between aging, perfusion and fat content though did not specifically examine whether this relationship was related to bone mineral density (BMD). Thus the aim of our first study was to use ^{1}H MR spectroscopy and dynamic contrast-enhanced MR imaging to measure vertebral body marrow fat content and bone marrow perfusion of older male subjects with varying BMD as documented by dual energy x-ray absorptiometry (DXA). Male, rather than femles patients were investigated as they were attending the hospital as part of a an on-going study (MrOS study) investigating the prevalence of osteoporosis and osteoporotic fracture in elderly males in Hong Kong

STUDY OUTLINE:

```
┌─────────────────────────────────────────────────────────────┐
│                          STUDY 1                            │
└─────────────────────────────────────────────────────────────┘
                              ↓
┌─────────────────────────────────────────────────────────────┐
│ What is the relationship between bone perfusion, marrow fat │
│                 and bone mineral density?                   │
└─────────────────────────────────────────────────────────────┘
                              ↓
┌─────────────────────────────────────────────────────────────┐
│                   90 elderly male subjects                  │
│                                                             │
│  • Lateral radiograph thoracic and lumbar spines            │
│  • DEXA lumbar spine and right hip                          │
│  • MR perfusion imaging lumbar spine - mid-sagittal plane   │
│  • Proton MR spectroscopy of L3 vertebral body              │
└─────────────────────────────────────────────────────────────┘
                              ↓
┌─────────────────────────────────────────────────────────────┐
│                       MAIN FINDINGS                         │
│                                                             │
│  • Osteoporotic bone has significantly ↓ perfusion compared │
│    to osteopenic bone which in turn has significantly ↓      │
│    perfusion compared to bone of normal BMD                 │
│                                                             │
│  • Osteoporotic bone contains significantly ↑ fat compared  │
│    to osteopenic or normal density bone.                    │
└─────────────────────────────────────────────────────────────┘
```

ABSTRACT

Purpose: To prospectively use (proton) ^1H magnetic resonance (MR) spectroscopy and dynamic contrast-enhanced (DCE) MR imaging to measure the vertebral body marrow fat content and bone marrow perfusion of older male subjects with varying bone mineral density as documented by dual energy x-ray absorptiometry (DXA).

Materials and Methods: Our Institutional Review Board approved the study and all participants provided signed informed consent. Radiography, DXA, ^1H MR spectroscopy and DCE MR imaging of the lumbar spine were performed on 90 male

subjects (mean age 73 years, range 67-101 years). Vertebral marrow fat content and perfusion (maximum enhancement and enhancement slope) were compared for subject groups of differing bone density (normal, osteopenia, and osteoporosis). *t*-test comparison between groups and Pearson test for correlation between marrow fat content and perfusion indices were applied.

Results: Eight subjects were excluded yielding a final cohort of 82 subjects (mean age, 73 years; range, 67-101 years) comprising 42 normal bone density subjects (mean T score, 0.8 $\pm$ 1.1(SD)), 23 osteopenic subjects (-1.6 $\pm$ 0.4) and 17 osteoporotic subjects (-3.2 $\pm$ 0.5). Vertebral marrow fat content was significantly increased in osteoporotic subjects (mean, 58.23 $\pm$ 7.83%) (P = 0.002) and osteopenic subjects (55.68 $\pm$ 10.2%) (P = 0.034) compared to those with normal bone density (50.45 $\pm$ 8.73%). Perfusion indices were significantly decreased in osteoporotic subjects (enhancement slope, 0.78 $\pm$ 0.33 %/sec) compared to osteopenic subjects (1.15 $\pm$ 0.59 %/sec) (P = 0.007) or those with normal bone density (1.48 $\pm$ 0.73 %/sec) (P < 0.0001).

Conclusion: Osteoporotic subjects have decreased vertebral marrow perfusion and increased marrow fat compared to osteopenic subjects. Similarly, osteopenic subjects have decreased vertebral marrow perfusion and increased marrow fat compared to subjects with normal bone density.

STUDY DETAILS:

MATERIALS AND METHODS

Subject Selection. Between January and June 2004, 90 male subjects above the age of 65 years (mean age 73 years, range 67-101 years) were recruited into this prospective study. These male patients were part of an on-going larger non-interventional study in male subjects (MrOS study) investigating the prevalence of osteoporosis and osteoporotic fracture in elderly males in Hong Kong. The Institutional Clinical Research Ethics Committee approved the study (Appendix) and all participants provided signed informed consent. Following clinical assessment, all subjects underwent lateral radiographic examination of the thoracic and lumbar spines, dual X-ray absorptiometry (DXA) examination of the lumbar spine, ^{1}H MR spectroscopy and DCE MR imaging of the lumbar spine. Subjects were either not recruited or excluded from further analysis if (a) there was clinical or imaging evidence of metabolic bone disease or metastases; (b) a history of lumbar spinal surgery or irradiation; (c) MR imaging evidence of large intravertebral disc herniation, haemangioma or fatty rest; (d) a contraindication to MR imaging examination; or (e) an incomplete MR examination.

Radiographic and DXA Examination. Lateral radiographic examination of the thoracic and lumbar spines was performed on all subjects within one month prior to MR examination. Radiographs were obtained to assess the presence of vertebral fracture and aid detection of any other bony abnormality that could affect DXA or MR measurements. Radiographs were reviewed by a single radiologist with a vertebral fracture being diagnosed if vertebral height was decreased by 20% or greater (Genant HK et al. 1993). DXA examination of the lumbar region (L1-L4) was

performed on all subjects (Hologic QDR-4500W, Hologic, Inc., Waltham, MA) within one month prior to MR examination. The in-vitro short and long term CV of DXA lumbar spine used in this study was 0.65% while the in-vitro long term CV was 0.398. Based on DXA results, subjects were grouped into three categories according to their T-score results and World Health Organization criteria (WHO Study Group, 1994). Normal bone mineral density was defined as a T-score greater than -1.0, osteopenia as a T-score between -1.0 and -2.5, and osteoporosis as a T-score less than -2.5.

MR Examination. MR examinations were performed on a 1.5-T whole-body MR imaging system (Intera NT, Philips, Best, Netherlands) with a 30 mT/m maximum gradient capability. A 20-cm diameter circular surface coil, centered at the third lumbar vertebra (L3), was used to optimize the sensitivity of both ^{1}H MR spectroscopy and DCE MR imaging examination. L3 was chosen as optimal coil positioning was facilitated by surface landmarks (iliac crests). For ^{1}H MR spectroscopy (Figure 1), VOI size ranged from 8 to 17 cm^3 depending on vertebral body size. After local shimming and gradient adjustments, data were acquired at a spectral bandwidth of 1,000 Hz and 64 non-water suppressed signals were obtained using a point resolved spectroscopic sequence (TR/TE, 3000/25).

Figure 1.

74-year-old man with osteoporosis (T score -3.5). ^{1}H MR spectroscopy examination of the L3 lumbar spine. (a) Sagittal T2-weighted MR image (3500/120) of the lumbar spine showing positioning of the VOI for spectroscopy within the L3 marrow cavity.

Dynamic contrast-enhanced MR imaging was acquired on completion of spectroscopy examination at which time the subject would have laid still within the scanner gantry for a period of at least fifteen minutes. Dynamic images were acquired in the sagittal plane using a short T1-weighted gradient-echo sequence (TR/TE, 2.9/1.1; pre-pulse inversion time, 400 msec; flip angle, 15°; section thickness, 10 mm; number of slices, one; field of view, 250 mm; acquisition matrix, 256 × 256; one signal acquired). A total of 160 dynamic images were obtained from the mid-sagittal plane of the vertebral body with a temporal resolution of 540 msec. A bolus of gadoteric acid (Dotarem; Guerbet, France) at a concentration of 0.15 mmol per kilogram of body weight was injected manually at an injection rate of approximately 2.0 mL/sec through a 21-gauge intravenous catheter previously inserted in the right antecubital vein. The injection was immediately followed by a 20-mL saline flush at the same injection rate. Dynamic MR imaging started as soon as the injection of contrast medium commenced (time zero). Dynamic contrast-

enhanced MR images acquired during the first-pass phase of signal enhancement were analyzed. On the mid-sagittal T1-weighted image, a region of interest (ROI) (Figure 2) encompassing the L3 vertebral body, was drawn manually by a single observer using a radiology workstation (Viewforum, Philips Medical System, Best, The Netherlands).
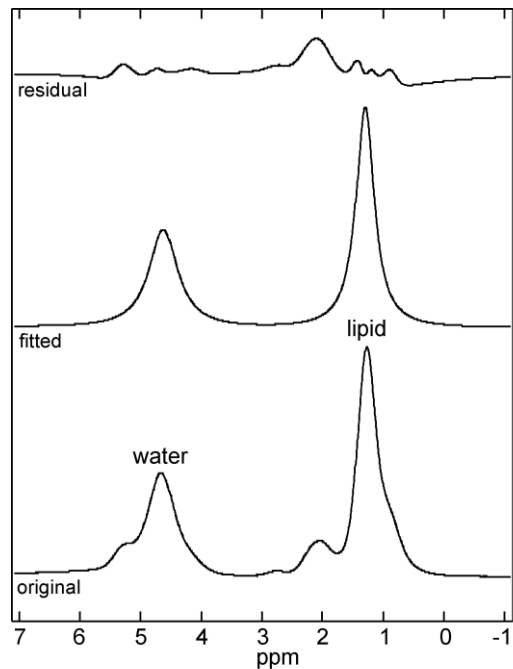
Figure 2.

[1]H spectrum acquired from this VOI showing a relatively intense lipid peak (1.3 ppm) compared to the water peak (4.65 ppm) indicating increased marrow fat content within the vertebral body. Bottom trace is the original spectrum while the middle shows the fitted spectrum from which peak intensity values were derived and top trace is the residual spectrum.

Data Analysis. (a) Spectroscopy data. Spectroscopic data were analyzed as per Appendix 1. Specifically, vertebral body fat content, defined as the relative fat signal amplitude in percentage of total signal amplitude (water and fat), was calculated according to the equation (Schellinger et al, 2001):

$$\text{Fat content} = \left(I_{fat}/\left(I_{fat} + I_{water}\right)\right) \times 100 \, [\%]$$

where I_{fat} and I_{water} are the peak amplitudes of fat and water, respectively.
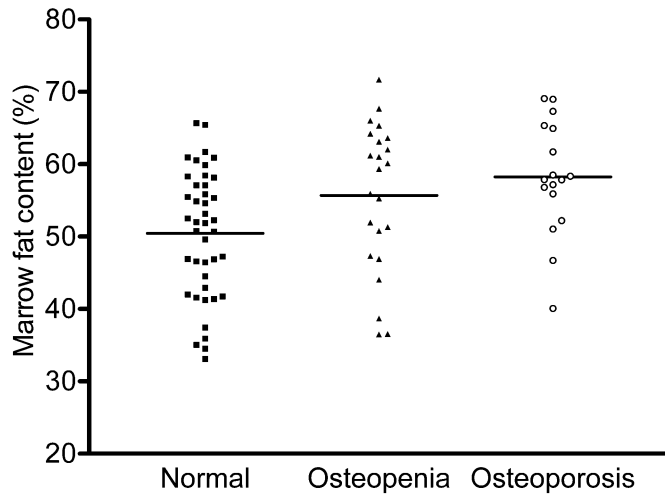
Figure 3.

Marrow fat content distribution among subject groups (normal bone density, osteopenia and osteoporosis). Mean value for each group is represented by the horizontal bar.

(b) Perfusion Data. Perfusion data was analysed as explained in Appendix 1. Two perfusion parameters were measured namely: maximum enhancement and enhancement slope. Maximum enhancement is defined as the maximum percentage increase ($I_{max} - I_{base}$) in signal intensity from baseline (I_{base}).

$$\text{Maximum enhancement} = \frac{(I_{max} - I_{base})}{I_{base}} \times 100\%$$

Enhancement slope is defined as the rate of enhancement between 10% and 90% of maximum signal intensity difference between I_{max} and I_{base}.

$$\text{Enhancement slope} = \frac{(I_{max} - I_{base}) \times 0.8}{I_{base} \times (t_{90\%} - t_{10\%})} \times 100\%$$

where $t_{10\%}$ and $t_{90\%}$ are the time intervals when the rise in signal intensity reaches 10% and 90% of the maximum signal intensity difference between I_{base} and I_{max}, respectively

Both parameters were derived from the first-pass phase of signal enhancement or rapidly rising part of the time-intensity curve and are considered to represent arrival of the contrast material into the arteries and capillaries of the vertebral marrow and its diffusion into the extracellular space (Cova M et al. 1991).

Statistical Analysis. Overall mean values for vertebral marrow fat content, maximum enhancement and enhancement slope were obtained in additional to the mean values for each of the three bone density groups (normal bone density, osteopenia and osteoporosis). Student t test comparison between mean age of each group was performed. Pearson correlation test was used to assess correlation between marrow fat content, maximum enhancement and enhancement slope and bone density (T-score) for the three bone density groups. Analyses were performed using SPSS for Windows (Release 11.0, SPSS Inc., Chicago, Illinois). P values of < 0.05 were considered to indicate statistically significant differences.

RESULTS

Subjects. Eight subjects were excluded from the 90 male subjects initially recruited, due to failed injection in three and motion artifact in five subjects, leaving a final cohort of 82 subjects (mean age, 73 years; age range, 67-101 years), all of whom successfully completed both ^{1}H MR spectroscopy and DCE MR imaging. No subject in the study cohort had a thoracic or lumbar vertebral fracture on radiography. Bone mineral density was normal in 42 subjects (T score, 0.8 ± 1.1(SD)), osteopenic in 23 subjects (T score, -1.6 ± 0.4) and osteoporotic in 17 subjects (T score, -3.2 ± 0.5). The mean age for normal bone density group was 72 years (range, 67-82 years), for osteopenic group 74 years (range, 67-101 years) and for osteoporotic group 74 years (range, 68-84 years). Age differences between the three groups were not statistically significant (osteoporosis vs normal, $p = 0.096$; osteoporosis vs osteopenia, $p = 0.958$; osteopenia vs normal, $p = 0.194$).

Vertebral Marrow Fat Content. When analyzed according to bone density, osteoporotic subjects (58.23 ± 7.8%) had the highest mean vertebral marrow fat content followed by osteopenic subjects (55.68 ± 10.2%) and subjects with normal bone density (50.45 ± 8.7%) (Figure 4). The observed difference between osteoporotic subjects and those with normal bone density was significant (p = 0.002) as was the observed difference between osteopenic subjects and those with normal bone density (P = 0.034) subjects (Figure 4). The observed increase in marrow fat content in osteoporotic subjects compared to osteopenic subjects was not significant (P = 0.394) (Figure 4).

Figure 4.

Sagittal T1-weighted MR image (450/1) of the lumbar spine showing a manually drawn ROI positioned just within the cortical margins of the L3 vertebral body. Time-intensity data-points based on this ROI were measured from all dynamic images.

Vertebral Marrow Perfusion. When analyzed according to bone density, osteoporotic subjects had the lowest mean maximum enhancement (23.52 ± 9.9%) compared to osteopenic subjects (28.36 ± 10.8%) and subjects with normal bone density (34.49 ± 13%) (Figures 5 & 6). The observed difference in maximum enhancement between osteoporotic subjects and those with normal bone density

was significant (p < 0.001) as was the observed difference between osteopenic subjects and those with normal bone density (p = 0.023) subjects (Figure 5 & 6). When analyzed according to bone density, osteoporotic subjects had the lowest mean maximum enhancement (0.78 ± 0.3 %/sec) compared to osteopenic subjects (1.15 ± 0.6 %/sec) and those with normal bone density (1.48 ± 0.7 %/sec) (Figure 5 & 6). The observed difference in enhancement slope was significant between osteoporotic subjects and those with either osteopenia (P = 0.007) or normal bone density (p < 0.0001) (Figure 5 & 6). Osteopenic subjects also had a significantly reduced mean enhancement slope compared to those with normal bone density (p = 0.0279) (Figures 5 & 6).
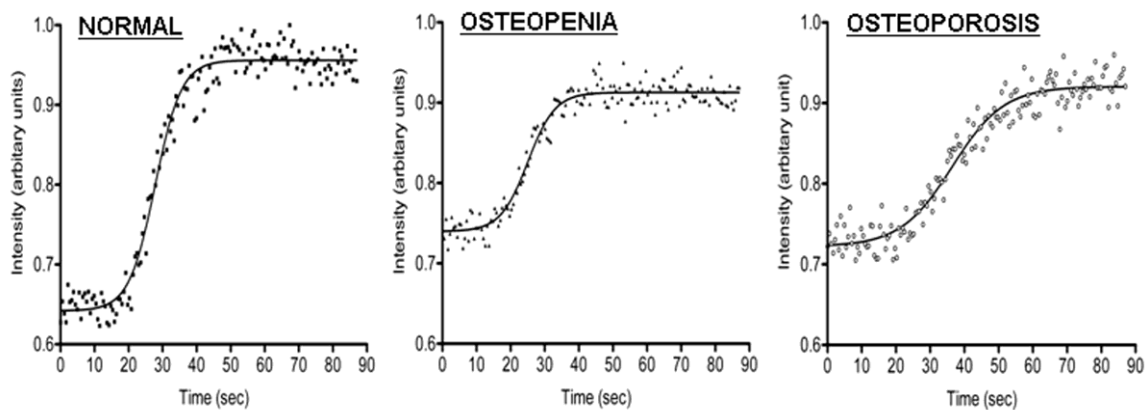
Figure 5.

Typical time-intensity curve for subjects with (a) normal bone density showing high maximum enhancement and steep enhancement slope, (b) osteopenia showing decreased maximum enhancement and a less steep enhancement slope and (c) osteoporosis showing the least maximum enhancement and the flattest enhancement slope.
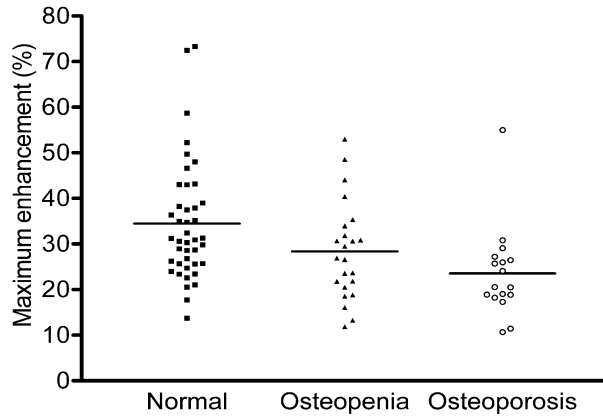
Figure 6.
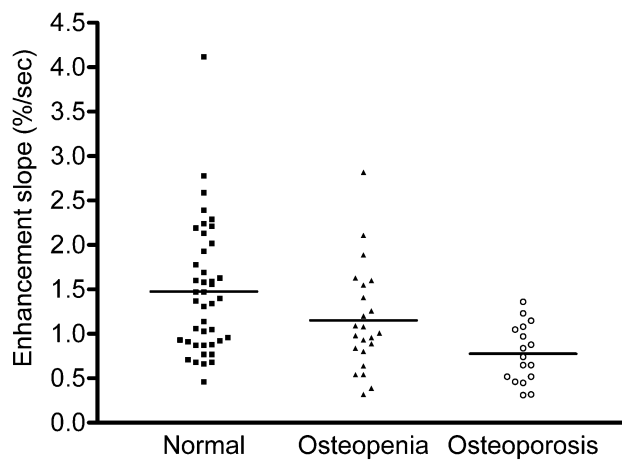
(a) Maximum enhancement and (b) enhancement slope indices for the three different groups [normal bone density (n=42), osteopenia (n=23) and osteoporosis (n=17)]. Mean value for each group is represented by the horizontal bar.

Figure 6a

Figure 6b

Correlation between Bone Density, Vertebral Marrow Perfusion and Fat Content. With reduction in bone mineral density, both maximum enhancement (r = 0.263, p = 0.0169) and enhancement slope (r = 0.419, p < 0.0001) decreased while marrow fat content increased (r = -0.32, p = 0.0034). The increase in marrow fat content correlated strongly with a decrease in both maximum enhancement (r = -0.727, p < 0.0001) (Figure 7) and enhancement slope (r = -0.545, P < 0.0001) (Figure 7).
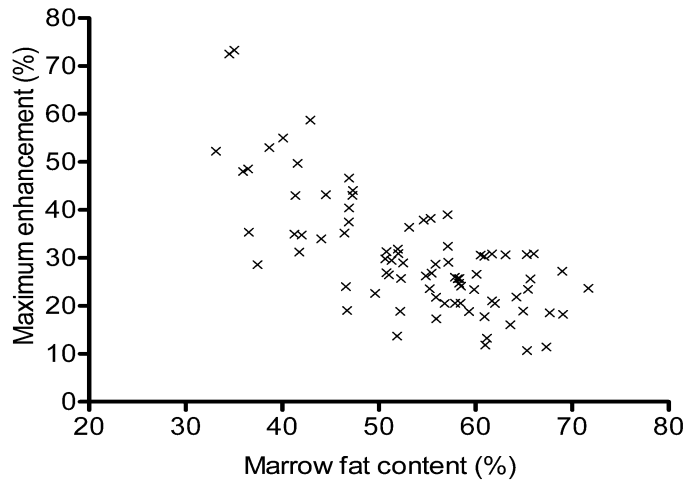
Figure 7.

Scatter plot to showing strong correlation between marrow fat content and maximum enhancement indicating that as marrow fat increased, perfusion decreased. A similar trend was observed comparing marrow fat content and enhancement slope (not shown).

SIGNIFICANCE OF THESE RESULTS

Whilst this first study was on-going, a study was published in *Radiology* which also examined the relationship between perfusion as assessed by MRI and BMD. This study by Shih et al found a significant correlation (r = 0.61, p<0.01) between peak enhancement ratio and BMD in 37 post-menopausal women patients of varying BMD who were not on hormonal replacement therapy suggesting a link between vascular disease and osteoporosis (Shih TT et al. 2004). Study 1 builds on this initial study by Shih et al in expanding the paradigm to explore the relationship between vertebral marrow perfusion, fat content and bone mineral density. Osteoporotic subjects were found to have significantly reduced vertebral marrow perfusion compared to those with osteopenia and normal bone density (Figure 2). Study 1 shows a clear trend of decreasing marrow perfusion and increasing marrow fat content in line with reducing bone density. It has not been determined in this study whether these represent independent or related variables and if a temporal relationship exists i.e. does

increase in vertebral marrow fat precede reduction in perfusion or visa versa or do these changes predate or postdate changes in bone density.

This all enhances prior epidemiological, histological and laboratory evidence that have suggested a link between osteoporosis and vascular disease. Epidemiological studies have shown how osteoporosis in the elderly is associated with an increased mortality rate, even when deaths following osteoporotic fractures are not considered (Browner WS et al. 1991). Women with osteoporosis soon after menopause have an almost two-fold increased risk of cardiovascular mortality, an association that persists after adjusting for other cardiovascular risk factors (von der Recke P et al. 1999). Histological studies have shown an increase in marrow fat and a reduction in marrow arteries and capillary sinusoids in osteoporosis (Burkhardt R et al. 1987). Using radio-labeled microspheres to assess blood flow, Bloomfield et al observed an age-related reduction in blood flow and bone density in the rat scapula, forelimb and femur (Bloomfield SA et al. 2002). Reduced perfusion possibly acting through endothelial production of nitric oxide, prostaglandin E_2 and prostaglandin I_2 can alter the balance between osteoblastic and osteoclastic activity (Bloomfield SA et al. 2002). Mice lacking the glycoprotein osteoprotegerin develop arterial calcification and early onset osteoporosis (Bucay N et al. 1998).

MR-based studies have shown vertebral marrow perfusion decreases with age, the reverse is true for marrow fat (Chen WT et al. 2001). Vertebral marrow fat content increases with age though it is unclear whether this increase is due to an increase in adipocyte size or adipocyte number (Rozman C et al. 1989, Justesen J et al. 2001). Schellinger et al reported an average vertebral marrow fat content of 20.5% in all

subjects aged 15-29 years increasing to 49.4% for all subjects aged 70-89 years (Schellinger D et al. 2001). Our results show that vertebral marrow fat content is related to bone density. Subjects with osteoporosis or osteopenia have a significantly increased marrow fat content compared to those with normal bone density. Several potential mechanisms whereby increasing marrow fat could interplay with bone strength and density have been proposed. First, an increase in marrow fat may simply represent a compensation for trabecular thinning (Schellinger D et al. 2001, Justesen J et al. 2001). Second, replacement of the more hydrostatic (and less compressible) heamopoetic marrow with the more compressible fatty marrow may potentiate vertebral weakening (Schellinger D et al, 2001). Third, as osteoblasts and adipocytes share a common pluripotent mesenchymal stem cell in the bone marrow, increased adipogenesis may be associated with decreased osteoblastogenesis (Schellinger D et al, 2001,Justesen J et al, 2001).

There are also several potential mechanisms whereby reduced bone perfusion can interrelate with increased marrow fat and osteopososis. It is conceivable for example that within the confines of the vertebral body, increasing fat could simply compress the intraosseous veins diminishing blood flow. Alternatively the metabolic activity of bone and other marrow constituents may be decreased. Marrow stem cells comprise hematopoietic stem cells, mesenchymal stem cells, and multipotent progenitor cells. These stem cells are believed to work together in neovascularisation. Differentiated hematopoietic stem cells (also known as endothelial progenitor cells) provide vascular endothelial cells while differentiated mesenchymal stem cells provide vascular smooth muscle cells (Khakoo AY et al. 2005) or provide cytokines that are central to the initiation and coordination of vascularization (Kinnaird AY et al. 2004).

These relationships will be investigated in the following Studies, particularly in Study 7.

Limitations of this study.

1. This study shows a clear trend of decreased marrow perfusion and increased marrow fat content paralleling reducing bone density. It has not been determined whether these represent independent or related variables and if a temporal relationship exists i.e. does increase in vertebral marrow fat precede reduction in perfusion or visa versa or do these changes predate or postdate changes in bone density. Longitudinal studies will help in this respect.

2. Due to simultaneous participation in another osteoporosis-related study, only males were included although osteoporosis is more common in females. Gender age-related differences in vertebral marrow perfusion and also possibly fat content do exist (Chen WT et al. 2001). On average, females less than 50 years of age demonstrate increased marrow perfusion compared to men of similar age while females over 50 years show a more marked decrease in marrow perfusion compared to men of similar age (Chen WT et al, 2001). Conversely, across age groups, males tend to have more vertebral marrow fat than females (Schellinger D et al. 2001). Therefore, the results of this study cannot necessarily be applied to females (Chen WT et al. 2001, Schellinger D et al. 2001).

3. Contrast was injected manually rather than by power injector. Variations in injection rate may have affected the enhancement slope though we believe this effect to be minimal and all participants were incurred the same potential error.

4. Sample size was small, particularly for osteopenic and osteoporotic groups, as osteoporosis is less common in men. This small sample size may have resulted

in some observed trends between groups being within the limits of statistical error.

5. We were not able to determine whether the decrease in perfusion represented an intraosseous phenomenon or was a feature of a more generalized systemic circulatory impairment.

Conclusion. This first study shows that compared to subjects with normal bone density, bone perfusion is reduced in those with osteopenia and further reduced in those with osteoporosis. In contrast, vertebral marrow fat content is increased in those with osteopenia or osteoporosis. There was a strong inverse relationship between decreasing perfusion and increasing marrow fat.

Next phase of study: Following on from this study, we wish to establish whether similar changes occur in females (as osteoporosis is more common in females) and see whether perfusion abnormalities also occur outside the bone in osteoporosis. This will be the subject of Study 2.

STUDY 2:

Vertebral marrow fat content, molecular diffusion, and perfusion indices in women with varying bone density, including osteoporosis: MR evaluation

Aim: To study whether marrow perfusion is altered in female subjects with reduced bone mineral density and how this relates to marrow fat content.

Rationale for doing this study:

Our previous study (Study 1) showed that bone perfusion was reduced in male osteoporotic subjects. In this study, we wanted to determine:

(a) Whether similar findings occurred in female subjects as osteoporosis is much more common in female subjects

(b) Whether reduced bone perfusion was a localized phenomenon confined to bone or a symptom of a more generalized circulatory impairment. We chose to do this by comparing perfusion within bone with that of paravertebral muscle which has the same blood supply.

(c) To determine whether molecular diffusion as evidenced by diffusion-weighted MRI was altered in subjects of varying BMD

<div style="border:1px solid black; text-align:center;">

STUDY 2

</div>

↓

<div style="border:1px solid black; text-align:center;">

Is marrow perfusion altered in female subjects with reduced bone mineral density and how does this relate to marrow fat content?

</div>

↓

<div style="border:1px solid black;">

110 post-menopausal female subjects

- DXA lumbar spine / right hip
- MR thoracic and lumbar spine
- MR perfusion imaging of L3 vertebral body & paravertebral muscle – axial plane
- MR diffusion L3 vertebral body
- Proton MR spectroscopy of L3 vertebral body

</div>

↓

<div style="border:1px solid black;">

MAIN FINDINGS

- As vertebral BMD ↓, there is a corresponding ↓ in perfusion indices and a corresponding ↑ in fat content i.e. trend similar to that seen in male subjects.

- The ↓ in perfusion indices only seen in vertebral body and not in the adjacent paravertebral muscle which has same arterial supply.

- Only a weak relationship between vertebral marrow ADC and BMD was found.

</div>

ABSTRACT

Purpose: To prospectively use MR imaging and spectroscopy to measure vertebral marrow fat content, marrow diffusion, marrow and erector spinae muscle perfusion in female subjects of varying bone density.

Materials and Methods: Following institutional study approval, DXA, proton MR spectroscopy, diffusion-weighted imaging, and dynamic contrast-enhanced imaging of the lumbar spine and erector spinae muscle was performed on 110 female subjects (mean age, 73 years; range, 67-84 years). Marrow fat content, marrow apparent diffusion coefficient (ADC) and perfusion parameters of marrow and spinae muscle were compared for different bone density groups (normal, osteopenia, and osteoporosis). t test comparisons and Pearson correlations were applied.

Results: Seven subjects were excluded yielding a final cohort of 103 subjects comprising 18 normal bone density subjects, 30 osteopenic subjects, and 55 osteoporotic subjects. Vertebral marrow fat content was significantly increased in osteoporotic subjects (67.8 ± 8.5%) compared to those with normal bone density (59.2 ± 10.0%) (P = 0.002). Vertebral marrow perfusion was significantly decreased in osteoporotic subjects (enhancement slope, 1.10 ± 0.51%/sec) compared to osteopenic (1.45 ± 0.51%/sec) (P = 0.01) and normal bone density subjects (1.70 ± 0.52%/sec) (P < 0.001). Erector spinae muscle perfusion did not decrease with decreasing bone density. ADC of vertebral marrow did not change with bone density.

Conclusion: Females demonstrate decreased marrow perfusion and increased marrow fat in line with decreasing bone density. Reduction in perfusion appears to occur only within the bone and does not occur in extraosseous tissues with the same arterial supply.

STUDY DETAIL:

MATERIALS AND METHODS

Subject Selection. 110 post-menopausal female subjects over the age of 65 years (mean age, 73 years; range, 67-84 years) volunteered to participate in this prospective study between March 2004 and February 2005. As part of another on-going study, recruitment notices were placed in community centers for the elderly inviting subjects to attend for dual x-ray absorptiometry (DXA) examination. Informed consent was obtained from participating subjects.. The Institutional Clinical Research Ethics Committee approved the study (Appendix). Following DXA examination, all subjects were invited to attend for MRI examination for which ethics approval and informed consent was additionally obtained. MRI examination, comprising ^{1}H MR spectroscopy, diffusion-weighted and dynamic contrast-enhanced MR imaging of the lumbar spine, was performed within a mean of 11 days (range 9-13 days) of DXA examination. Subjects were not recruited or were excluded from further analysis if there was (a) clinical or imaging evidence of metabolic bone disease or metastases; (b) a history of lumbar spinal surgery or irradiation; (c) a contraindication to MR examination; or (d) an incomplete MR examination. The results of the MRI examination were made known to the participating subjects.

DXA Examination. The average of the four levels (L1-L4) from an anteroposterior projection of the lumbar spine (Hologic QDR-4500W, Hologic, Inc., Waltham, MA) was used to obtain the bone density in g/cm^2. Based on reference values derived from a local population ((Lynn HS et al. 2005), subjects were grouped into three categories according to lumbar spinal T-score and World Health Organization criteria (WHO Study Group 1994). The in-vitro short and long term CV of DXA lumbar spine

used in this study was 0.65% while the in-vitro long term CV was 0.398. Normal bone density was defined as a T score greater than -1.0, osteopenia as a T score between -1.0 and -2.5, and osteoporosis as a T score less than -2.5.

MR Examination. MR examinations were performed on a 1.5-T whole-body MR imaging system (Intera NT, Philips, Best, Netherlands) with a maximum gradient strength of 30 mT/m. A 20-cm diameter circular surface coil, centered at L3, was used. In the event of an L3 vertebral body fracture (Genant HK et al. 1993), or other focal lesion, the L2 vertebra was analysed. Following acquisition of scout images in axial, coronal and sagittal planes, T1-weighted (repetition time [TR] msec/echo time [TE] msec, 450/1) and T2-weighted (TR/TE, 3500/120) sagittal images of the thoracic and lumbar spine were obtained to identify vertebral fracture, to help exclude metastases and to guide positioning of a volume of interest within the L3 vertebral body for spectroscopy.

MR spectroscopy technique: For spectroscopy, the width (w), depth (d) and height (h) of the L3 vertebral body were measured on MR images to define a volume of interest (VOI). A VOI with dimensions w/2 × d/2 × h/2 cm^3 was located centrally in the vertebral body (by DKWY with 10 years working experience with MRI). After local shimming and gradient adjustments, data was acquired at a spectral bandwidth of 1,000 Hz with 512 data points and 64 non-water suppressed signals were obtained using a point resolved spectroscopic sequence (TR/TE, 3000/25 msec).

MR diffusion imaging technique: Fat-suppressed diffusion-weighted images were acquired on a single axial slice through the middle of the L3 vertebral body using a

spin-echo single-shot echo-planar imaging sequence (2000/105; section thickness, 10 mm; field of view, 250 mm; matrix, 128 × 128; four signals acquired), sensitized to incoherent motion by a pair of gradient pulses. Diffusion sensitivity parameters, or b values, were altered by varying the gradient amplitude while keeping the duration and separation time constant at 30 msec and 50 msec respectively. Six diffusion-weighted images were acquired with b values of 0, 100, 200, 300, 400 and 500 sec/mm^2. Three diffusion-weighted images were acquired for each b value with the diffusion-sensitization gradient along the readout, phase-encoding and slice selection directions respectively. Isotropic diffusion-weighted image was calculated on a pixel-by-pixel basis using a similar method described elsewhere (Yeung DKW et al. 2004).

MR perfusion imaging technique: Dynamic contrast-enhanced MR images were acquired in the axial plane through the mid-L3 region. Dynamic images were obtained using a short T1-weighted gradient-echo sequence (TR/TE, 2.7/0.95; pre-pulse inversion time, 400 msec; flip angle, 15°; section thickness, 10 mm; number of slices, one; field of view, 250 mm; acquisition matrix, 256 × 256; one signal acquired). A total of 160 dynamic images were obtained from the mid-axial plane of L3 with a temporal resolution of 543 msec providing a total interrogation time of 87 sec. A bolus of gadoteric acid (Dotarem; Guerbet, Aulnay, France) at a concentration of 0.15 mmol per kilogram of body weight was injected at a rate of 2.5 mL/sec (Spectris, Medrad, Inc., Indianola, PA, USA) through a 21-gauge intravenous catheter inserted in an antecubital vein. The injection was followed by a 20-mL saline flush. Dynamic MR imaging started at the same time the contrast medium injection started (time zero).

Data Analysis

(a) Spectroscopy data. Spectra were analyzed on an off-line computer (Dell Precision 650 Workstation; Dell, Austin, Tex). Water (4.65 ppm) and lipid (1.3 ppm) peak amplitudes were measured to determine vertebral body fat content, defined as the relative fat signal amplitude in terms of a percentage of total signal amplitude (water and fat) and calculated according to the following equation:

fat content = $[I_{fat}/(I_{fat} + I_{wat})] \cdot 100$,

where I_{fat} and I_{wat} are the peak amplitudes of fat and water, respectively. No correction for relaxation losses was applied.

(b) Diffusion data. The ROI was drawn manually (by DKWY) encompassing cancellous bone on the isotropic diffusion-weighted image obtained with a b-value 0 sec/mm^2, and the same ROI was then applied to all other isotropic diffusion-weighted images obtained with different b values. Apparent diffusion coefficient (ADC) was calculated with a five-point regression method at b values of 100, 200, 300, 400 and 500 sec/mm^2 using the following equation:

$$I_b = I_0 \cdot \exp{(-b \cdot ADC)}$$

where I_b and I_0 is the mean signal intensities in the ROI at b-value b and 0 sec/mm^2, respectively.

(c) Maximum enhancement and enhancement slope. On the mid-axial T1-weighted image, ROIs separately encompassing the L3 vertebral body and the three elements of the erector spinae muscle were drawn manually (by DKWY) on a radiology workstation (Viewforum, Philips Medical System, Best, The Netherlands)

(Figure 1). The erector spinae muscle was selected rather than the psoas muscle because of its larger muscle bulk. Time-intensity curves were recorded and processed on an offline computer (Dell Precision 650 Workstation; Dell, Austin, Tex). As per study 1, two perfusion indices of the time-intensity curve were measured, namely maximum enhancement and enhancement slope.

While these indices are often predictive of perfusion they are not a direct measure of perfusion. Maximum enhancement and enhancement slope time intensity curve indices are dependent on many factors including bolus contrast concentration, blood volume, cardiovascular function, tissue perfusion, tissue permeability and available leakage space (Parker GJ et al. 1997, Cova M et al. 1991)
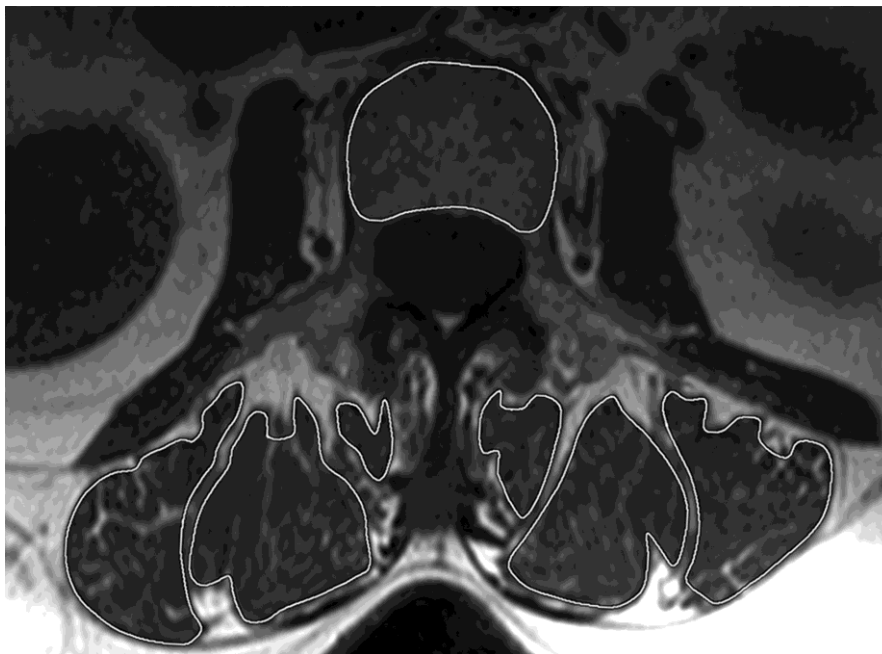
Figure 1. T1-weighted (578/12) axial image showing a manually drawn ROI positioned just within the cortical margins of the L3 vertebral body and the individual components of the erector spinae muscle for time intensity data-points measured from dynamic contrast-enhanced images. Individual components of erector spinae are spinalis, longissimus and iliocostalis from medial to lateral.

Statistical analysis. Data are presented as mean and standard deviations. Normal Q-Q and box plots were employed to examine normality and identify outliers. Logarithmic transformation was used to correct positive skewness of the variable

enhancement slope for muscle. Variables were compared amongst the three bone density groups (normal, osteopenia and osteoporosis) using the one-way ANOVA test. Post Hoc multiple comparisons were then conducted for significant variables using a Bonferroni correction. Pearson correlation coefficients were calculated to assess the linear relationship between pairs of variables. Statistical analyses were done using SPSS 11.0 (SPSS Inc., Chicago). A p-value < 0.05 was considered statistically significant.

RESULTS

Subjects. Seven subjects were excluded from the 110 female subjects initially recruited, due to failed injection in two and motion artifact in five subjects, leaving a final cohort of 103 subjects (mean age, 72 years; age range, 67-84 years) (Table 1). The L3 vertebral body was analysed in all subjects except in two subjects where the L2 vertebral body was analysed. Bone mineral density was normal in 18 subjects, osteopenic in 30 subjects and osteoporotic in 55 subjects (Table 1).

Vertebral Marrow Fat Content. Vertebral marrow fat content increased with decreasing bone density (Table 1, Figure 2). Osteoporotic subjects had, on average, a significantly higher vertebral marrow fat content than normal bone density subjects (P = 0.002) (Table 1, Figure 2). For paired data, a mild significant negative correlation was observed between T-score and vertebral marrow fat content (r = -0.36, P < 0.01) (Table 2), i.e. marrow fat increased as bone density decreased.

Figure 2. Marrow fat content for the three different bone density groups. [normal bone density (n=18), osteopenia (n=30) and osteoporosis (n=55)]. Horizontal bar represents mean value for each group.

Vertebral Marrow Maximum Enhancement and Enhancement Slope. Maximum enhancement decreased with decreasing bone density (Table 1, Figure 3). Osteoporotic subjects had significantly lower mean maximum enhancement than normal bone density subjects ($P < 0.001$) (Table 1, Figure 3). Mean enhancement slope also tended to decrease with decreasing bone density (Table 1, Figure 4). Osteoporotic subjects had a significantly lower mean enhancement slope compared to osteopenic subjects ($P = 0.01$) and normal bone density subjects ($P < 0.001$) (Table 1). Moderate positive correlation was present between T-score and both vertebral marrow maximum enhancement ($r = 0.51$, $P = < 0.001$) and enhancement slope ($r = 0.37$, $P < 0.001$) (Table 2) i.e. bone perfusion indices decreased with decreasing bone density. Of all paired variables tested, the strongest correlations found were that an increase in vertebral marrow fat content correlated with a decrease in marrow maximum enhancement ($r = -0.72$, $P < 0.001$) and enhancement slope ($r = -0.67$, $P < 0.001$) (Table 2, Figure 4).
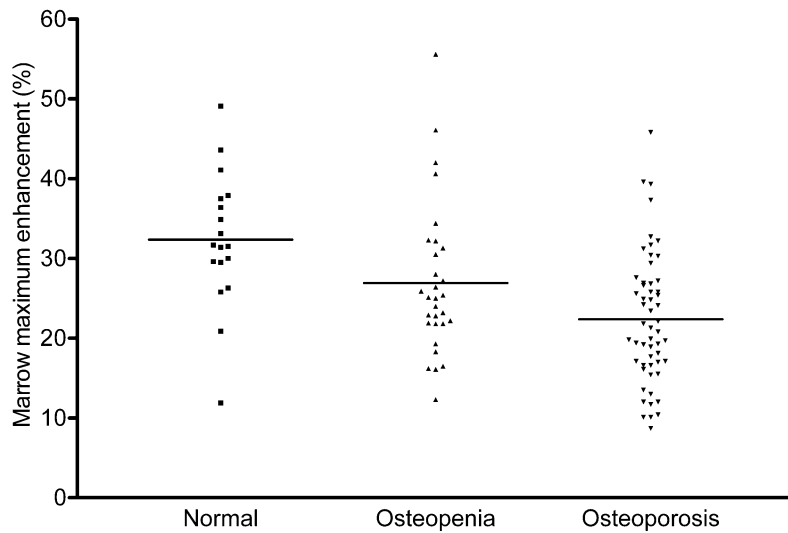
Figure 3. Vertebral marrow maximum enhancement for the three different bone density groups [normal bone density (n=18), osteopenia (n=30) and osteoporosis (n=55)]. Horizontal bar represents mean value for each group.
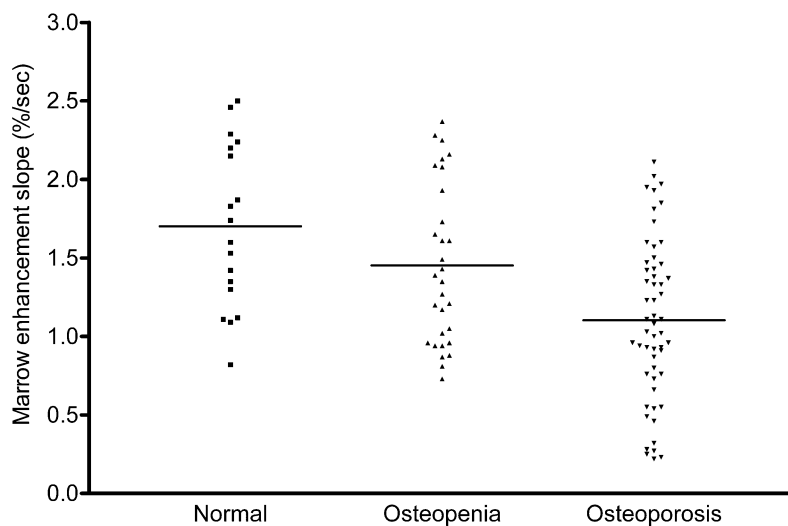
Figure 4. Vertebral marrow enhancement slope for the three different bone density groups [normal bone density (n=18), osteopenia (n=30) and osteoporosis (n=55)]. Horizontal bar represents mean value for each group.
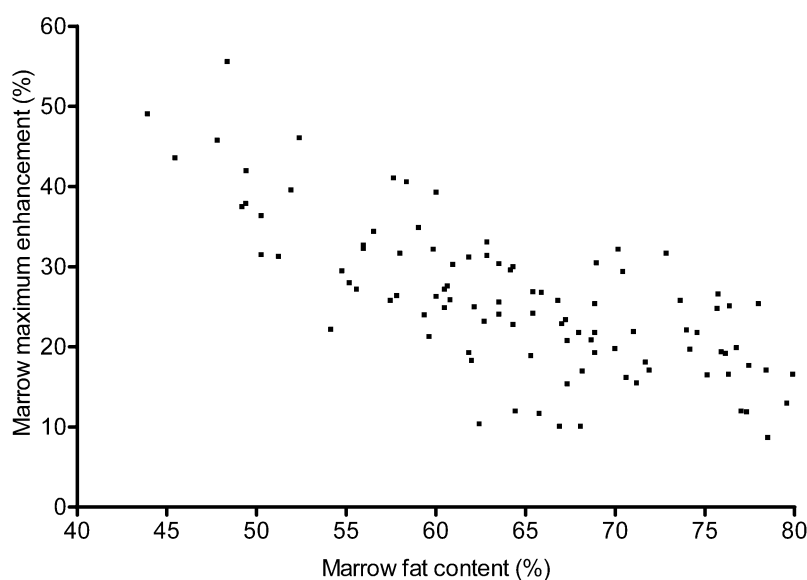
Figure 5. Scatterplot to show strong correlation between marrow fat content and maximum enhancement indicating that as marrow fat content increased perfusion decreased (r = -0.72). Similar finding was present between marrow fat content and enhancement slope (r = -0.67) (not shown).

Erector Spinae Muscle Maximum Enhancement and Enhancement Slope. Both maximum enhancement and enhancement slope in the erector spinae muscle tended to increase in osteoporotic subjects compared to osteopenic subjects and normal bone density subjects though these differences were not significant ($P = 0.08$ and $P = 0.333$, respectively) (Table 1, Figure 6). A mild significant negative correlation was observed between decreasing bone density and increasing erector spinae muscle maximum enhancement ($r = -0.24$, $P = 0.02$) (Table 2) i.e. muscle perfusion indices tended to increase as bone density decreased. No correlation was present between vertebral body marrow perfusion indices and erector spinae muscle perfusion indices ($P = 0.99$ for maximum enhancement and $P = 0.71$ for enhancement slope) (Table 2).

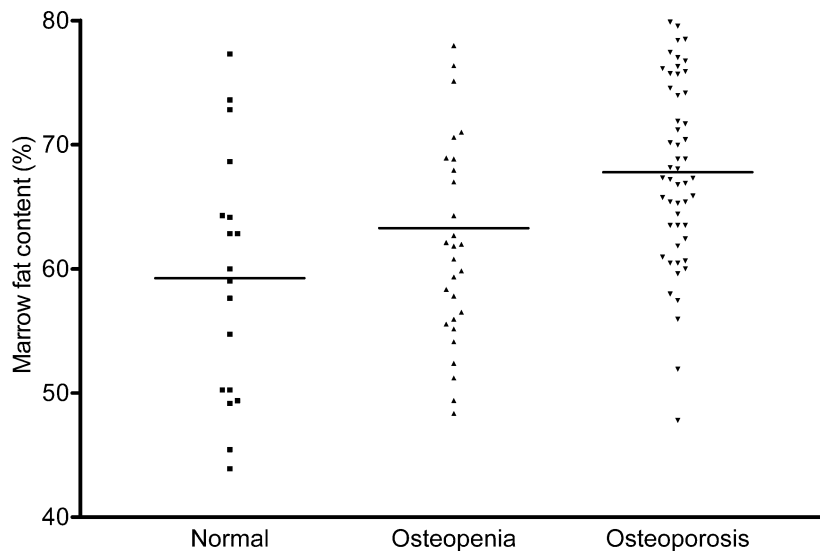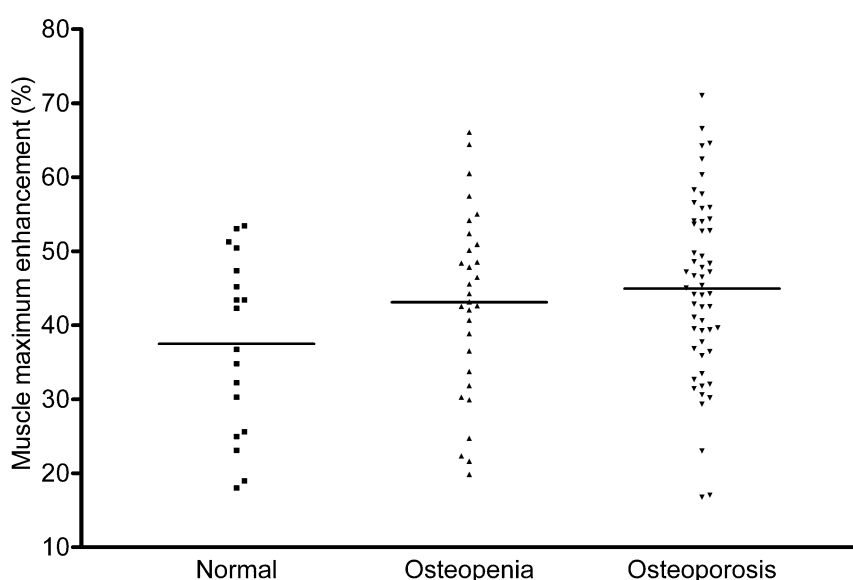Figure 6. Erector spinae muscle maximum enhancement for three different bone density groups [normal bone density (n=18), osteopenia (n=30) and osteoporosis (n=55)]. Horizontal bar represents mean value for each group. As BMD decreased, muscle perfusion, if anything, was increased. Similar results were found between erector spinae muscle enhancement slope (not shown).

Vertebral Marrow Apparent Diffusion Coefficient. No significant difference in ADC values was observed between osteoporotic subjects, osteopenic subjects and normal bone density subjects ($P = 0.51$) (Table 1). For paired data, no correlation

was present between either bone density or bone perfusion indices and marrow ADC (P > 0.05) (Table 2) though a mild positive correlation was present between vertebral marrow fat content and ADC (r = 0.24, P = 0.017) (Table 2) i.e. as marrow fat content increased, marrow diffusion decreased.

TABLE 1: MR parameters in different bone density groups

	All (n = 103)	Normal (n = 18)	Osteopenia (n = 30)	Osteoporosis (n = 55)	P Value[*]
Age (years)	72.1 ± 3.5	73.4 ± 3.5	71.4 ± 2.9	72.2 ± 3.7	0.150
T-score	-2.34 ± 1.39	-0.05 ± 0.86	-1.82 ± 0.44	-3.37 ± 0.60	<0.001[†]
Marrow fat content (%)	65.0 ± 9.6	59.2 ± 10.0	63.3 ± 9.5	67.8 ± 8.5	0.002[†]
Marrow maximum enhancement (%)	25.4 ± 9.3	32.3 ± 8.5	26.9 ± 9.5	22.4 ± 8.2	<0.001[†]
Marrow enhancement slope (%/sec)	1.31 ± 0.56	1.70 ± 0.52	1.45 ± 0.51	1.10 ± 0.51	<0.001[†]
Muscle maximum enhancement (%)	43.1 ± 12.2	37.5 ± 11.9	43.1 ± 12.4	45.0 ± 11.9	0.080
Muscle enhancement slope (%/sec)	1.50 ± 1.03	1.20 ± 0.61	1.48 ± 0.97	1.61 ± 1.15	0.333
Marrow ADC (mm^2/sec) x 10^{-3}	0.43 ± 0.12	0.46 ± 0.08	0.41 ± 0.12	0.43 ± 0.12	0.505

Table 1

Vertebral marrow fat content, maximum enhancement, enhancement slope and ADC values and muscle maximum enhancement, enhancement slope for each bone density (normal, osteopenia and osteoporosis) group. Numbers shown are mean ± 1 standard deviation (SD). [*]Calculated using one-way ANOVA test. [†]Denotes a significant difference between any of the three groups. Please refer to Results for details regarding probability significance between specific individual groups.

TABLE 2: Correlation between different MR-based parameters

Coefficient (p-value)	T-score	Marrow fat content	Marrow maximum enhancement	Marrow enhancement slope	Muscle maximum enhancement	Muscle enhancement slope	Marrow ADC
T-score	1	-0.356 (<0.001) [†]	0.510 (<0.001) [†]	0.368 (<0.001) [†]	-0.240 (0.015) [†]	-0.159 (0.110)	0.171 (0.089)
Marrow fat content		1	-0.720 (<0.001) [†]	-0.670 (<0.001) [†]	-0.044 (0.657)	-0.031 (0.755)	0.238 (0.017) [†]
Marrow maximum enhancment			1	0.834 (<0.001) [†]	-0.001 (0.990)	-0.044 (0.661)	0.021 (0.834)
Marrow enhancemernt slope				1	0.092 (0.356)	0.036 (0.716)	0.013 (0.895)
Muscle maximum enhancement					1	0.699 (<0.001) [†]	-0.072 (0.474)
Muscle enhancement slope						1	0.054 (0.590)
Marrow ADC							1

TABLE 2. Pearson's correlation coefficient test results. [†]Denotes significant correlation.

SIGNIFCANCE OF THESE RESULTS

Study 2 was undertaken to examine the relationship between vertebral bone density, vertebral marrow fat content and perfusion indices in women and shows a trend in female subjects similar to male subjects (Study 1). Reduction in bone density is associated with a corresponding increase in marrow fat (Shih TT et al. 2004, Study 1) and a reduction in marrow perfusion indices (Shih TT et al. 2004, Study 1). Comparing the results for vertebral marrow fat content of this study to those found in male subjects (Study 1), post-menopausal females appear to have a greater vertebral fat content than their male counterparts irrespective of whether they have

normal bone density (59.2 ± 9.6% versus 50.5 ± 8.7%), osteopenia (63.3 ± 9.5% versus 55.7 ± 10.2%) or osteoporosis (67.8 ± 10.2% versus 58.2 ± 7.8%). This is not in agreement with an earlier report of lumbar vertebral fat content being higher in males than females (Schellinger D et al. 2000), though this earlier report was on subjects over a wide age range whose bone density was unknown.

Maximum enhancement and enhancement slope were used as indices of perfusion. Both maximum enhancement and enhancement slope were approximately one-third less in osteoporotic subjects compared to normal bone density female subjects, a finding similar to that seen in male subjects (Study 1). Also as shown in Study 1, the overlap between marrow fat content and perfusion indices for female subjects between bone density groups indicates that fat content, maximum enhancement and enhancement slope time measurements on MR imaging cannot be used, in isolation, to reliably determine bone density (Study 1).

We also wanted to investigate in this study whether the decrease in perfusion observed with osteoporosis was a phenomenon confined to bone or also affected tissues beyond bone. The vertebral bodies and the erector spinae muscles are both supplied by the paired segmental lumbar arteries (Williams A et al. 2005, Kato H et al. 1999, Armour KE et al. 2001, Chen WT et al. 2004). If the observed reduction in perfusion indices were related to general circulatory impairment or atherosclerosis in the aorta or main lumbar arteries, one would expect a similar reduction in perfusion indices to occur in the erector spinae muscle. However, rather than decrease, perfusion indices for the erector spinae muscle tended to increase as bone density decreased. Reduction in bone density is associated with a reduction in maximum enhancement and enhancement slope within bone and this effect is not apparent in extraosseous tissues supplied by the same artery.

The MRI diffusion technique we used is mostly dependent on interstitial fluid flow, cellularity, and extracellular water volume and, to a lesser extent, on microvascular perfusion (Luypaert R et al. 2001). Increased interstitial fluid flow along bone canaliculi from repeated mechanical deformation has been proposed as an explanation for the anabolic adaptive responses occurring within bone to mechanical stress. Simulated interstitial fluid flow modulates bone growth mediators in bone cell cultures (Sterck JGH et al. 1998). Amplification of interstitial fluid flow may explain the reduced bone loss seen in post-menopausal women subjected to intermittent low magnitude vibrations (Rubin C et al. 2004). As interstitial fluid flow will contribute to MR diffusion (Luypaert R et al. 2001, Baur A et al. 2003), we examined the relationship between bone marrow diffusion and bone density. Our study was performed with the subject at rest and showed no relationship between bone marrow ADC and bone density. A weak negative association between marrow ADC and marrow fat content was found indicating a reduction in molecular diffusion as marrow fat content increased. This may in part be related to this study being performed in subjects of narrow age range. Possibly a different relationship between ADC and bone density would be found if subjects of different age range were studied.

Limitations of this study.

1. MR data were acquired from L3 while bone density scores were averaged from the four lumbar vertebrae L1-L4 as this is the accepted method of obtaining bone density 'T' scores.

2. Subjects were aware of their bone density result from DXA examination prior to enrolment for MR examination. This may have lead to a lower number of normal bone density subjects being recruited than those with osteopenia or osteoporosis.

3. Results of the MRI examination were made known to participating subjects, which may have prompted more subjects with back pain to attend for MRI examination.

Conclusion: In post-menopausal females, a decrease in bone density is associated with a corresponding increase in vertebral marrow fat content and a decrease in maximum enhancement and enhancement slope. This observed decrease in perfusion indices occurs within the vertebral body and is not seen in paravertebral tissues with the same arterial supply. Only a weak association between vertebral marrow diffusion and bone mineral density was found.

Next phase of study: A recent study has shown that as marrow fat increases, this can lead to a spurious reduction in BMD measurement by DXA. Could the results of Study 1 and Study 2 be influenced by the effect marrow fat has on DXA measurement? In other words, could osteoporosis subjects appear to have more fat because increased marrow fat is pushing down the measured BMD? This possibility will be explored in Study 3.

STUDY 3:

Could the results of Study 1 and Study 2 be spurious due to the effect of increasing marrow fat lowering BMD estimation by DXA?

Aim: Increasing marrow fat can cause an erroneous decrease in BMD measurement by DXA. In studies 1 and 2, we showed that increased marrow fat was associated with decreased BMD. In what part was this observation due to an effect of increased marrow fat falsely lowering the BMD and, in other words, making subjects with increased marrow fat appear as they have decreased BMD. The aim of this study was to investigate the degree of error introduced to DXA measurements by increasing marrow fat.

Relevance of this study:

Increase in vertebral marrow fat content may cause an erroneous reduction in BMD measurements made by dual x-ray absorptiometry (DXA) [Sorenson JA et al. 1990, Bolotin HH et al. 1998, Bolotin HH et al. 2001, Bolotin HH et al. 2007]. This is because DXA evaluates BMD by measuring the transmission of x-rays at two different photon energies [Blake GM et al. 2007]. The mathematical theory of DXA (referred to as basis set decomposition) holds that across a broad range of photon energies the X-ray transmission factor through any physical object can be decomposed into the equivalent areal densies (g/cm^2) of any two designated materials [Lehmann LA et al. 1981]. For DXA scans, the two materials chosen are

bone mineral (hydroxyapatite) and lean tissue. As a result, DXA measurements will only accurately reflect true BMD if the object being examined is composed entirely of hydroxyapatite and lean tissue. In practice, the human body is made up of not two but three main types of tissue, namely bone, lean tissue and fat. Neglecting the difference between lean and fat can lead to DXA measurement error.

DXA uses the soft tissues immediately alongside the spine as a reference to infer the soft tissue composition along the path of the spine [Sorenson JA et al. 1990]. It follows that errors will arise if the amount of fat in the bone marrow increases. As fat has a low attenuation value increasing marrow fat will reduce apparent bone mineral density [Bolotin HH et al. 1998].

There is disagreement regarding the quantitative effect of increasing vertebral bone marrow fat on spine DXA measurements. Igt has even been suggested that DXA measurements may be very seriously flawed in the estimation of bone mineral density [Bolotin HH et al. 2007]. Sorenson, in the first study to address this, estimated that an increase in the amount of fatty marrow within the lumbar vertebral bodies from 0 to 100% caused the measured BMD to decrease by a small amount from 0.03-0.04 g/cm^2 [Sorenson JA et al. 1990]. In contrast, a recent study by Bolotin found that an increase in lumbar vertebral body fatty marrow from 0 to 100% caused BMD to decrease by as much as 0.26-0.29 g/cm^2 i.e. an error about ten times greater than that predicted in the earlier study [Bolotin HH et al. 2007]. The significance of this difference can be appreciated when if you consider that, as shown from Study 1 and Study 2, the standard deviation in L3 marrow fat content is approximately ±10%. For a normal BMD measurement of 1.0 g/cm^2, this standard

deviation in marrow fat would translate into a BMD measurement error from as little as ± 0.4% or as much as ± 3.0% depending on whether the Sorenson [Sorenson JA et al. 1990] or Bolotin [Bolotin HH et al. 2007] estimate is adopted. Therefore the first question we wished to answer was how much does increasing marrow fat reduce BMD measurement by DXA?

In Study 1 and Study 2, significant increases in vertebral marrow fat content were found between subjects with normal bone density, those with osteopenia and those with osteoporosis. How much of this apparent increase in marrow fat could be accounted for by the negative effect of increased marrow fat on BMD actually leading to mis-classification of subjects as either osteopenia or osteoporosis according to T-score criteria?. In other words, subjects with osteopenia and osteoporosis are more likely to be classified as such because of the negative effect increasing marrow fat has on BMD. Would this same trend still hold true if this negative effect was taken into account? Therefore the second question we wanted to ask was whether the results of Study 1 and Study 2 would still hold true after correcting for the effect of increasing marrow fat content has BMD measurement.

STUDY OUTLINE:

```
┌─────────────────────────────────────────────────────────────────┐
│                                                                   │
│                            STUDY 3                                │
│                                                                   │
└─────────────────────────────────────────────────────────────────┘
                                ↓
┌─────────────────────────────────────────────────────────────────┐
│   Could the results of Study 1 and Study 2 be spurious due to     │
│   the effect of increasing marrow fat lowering BMD estimation     │
│                            by DXA?                                 │
└─────────────────────────────────────────────────────────────────┘
                                ↓
┌─────────────────────────────────────────────────────────────────┐
│                                                                   │
│   ●   25 males and 25 females randomly selected                   │
│   ●   Vertebral body thickness measured.                          │
│                                                                   │
│   ●   Basis set composition model used to determine extent to     │
│       which BMD is underestimated by DXA for each % ↑ in          │
│       marrow fat from 0-100%.                                     │
│   ●   Correction factors determined for males and females.        │
│   ●   Re-analysis of data from Study 1 and Study 2.               │
│                                                                   │
└─────────────────────────────────────────────────────────────────┘
                                ↓
┌─────────────────────────────────────────────────────────────────┐
│                                                                   │
│                        MAIN FINDINGS                              │
│                                                                   │
│   ●   Correction data of 0.0014 g/cm² (females) and 0.0016 g/cm²  │
│       (males) for each percentage ↑ in marrow fat fraction        │
│       should be applied to DXA (provided marrow fat fraction      │
│       known).                                                     │
│                                                                   │
│   ●   Following correction, findings of Study 1 and Study 2       │
│       still hold true.                                            │
│                                                                   │
└─────────────────────────────────────────────────────────────────┘
```

STUDY 3

↓

Could the results of Study 1 and Study 2 be spurious due to the effect of increasing marrow fat lowering BMD estimation by DXA?

↓

- 25 males and 25 females randomly selected
- Vertebral body thickness measured.

- Basis set composition model used to determine extent to which BMD is underestimated by DXA for each % ↑ in marrow fat from 0-100%.
- Correction factors determined for males and females.
- Re-analysis of data from Study 1 and Study 2.

↓

MAIN FINDINGS

- Correction data of 0.0014 g/cm^2 (females) and 0.0016 g/cm^2 (males) for each percentage ↑ in marrow fat fraction should be applied to DXA (provided marrow fat fraction known).

- Following correction, findings of Study 1 and Study 2 still hold true.

ABSTRACT

Purpose: Study 1 and 2 show that subjects with lower spine T-scores have significantly higher marrow fat content. Care is necessary in interpreting the relationship between spine T-score and marrow fat because of a selection effect in which subjects with higher marrow fat are more likely to be identified as having osteoporosis.

Methods: We studied both women (n = 103, mean age 73 y; range 67-84 y) and men (n = 82, mean age 73 y; range 67-101 y) who had spine DXA scans and 1H-MRS measurements of L3 marrow fat. The effect of varying marrow fat on BMD was modelled using vertebral body thicknesses measured in 50 men and women. Spine T-scores in each individual were adjusted for the measured marrow fat. Subjects were sorted into WHO categories based on their corrected T-scores, and the relationship between marrow fat and T-score status evaluated using regression analysis and analysis of variance. The average change in percent marrow fat per T-score unit was used to infer the fraction of the spine BMD fracture discrimination explained by marrow composition.

Findings: Mean (SD) of L1-L4 vertebral body thickness was 30.2 (2.1) mm for women and 33.4 (2.5) mm for men. When marrow fat content changed from 0 to 100% BMD was estimated to decrease by 0.14 g/cm2 (1.3 T-score units) in women and 0.16 g/cm2 (1.3 T-score units) in men. Allowing for this, there was still a trend for marrow fat to increase with decreasing T-score with a slope of -1.2 ± 0.7% per T-score unit (p = 0.078) for women and -1.4 ± 0.6% per T-score unit (p = 0.023) for men.

Conclusion: When marrow fat content is known, DXA estimation of BMD needs to be corrected by 0.0014 g/cm2 in women and 0.0016 g/cm2 in men for ever 1%

increase in marrow fat about zero. Applying this correction, the results of study 1 and study 1 regarding marrow fat and BMD still hold true.

STUDY DETAIL:

MATERIAL AND METHODS

Quantitative Effect of Vertebral Marrow Fat Content on BMD Measurement.

BMD is derived from the sum of its individual parts (Figure 1). The error produced by varying percentage marrow fat content can be calculated by applying the principle of basis set decomposition to a mathematical model designed to represent the size and composition of a lumbar vertebra (Figure 1). This method was similar to that described by Sorenson [Sorenson JA et al. 1990] and Bolotin [Bolotin HH et al. 2007], both of whom verified the mathematical model by examining a physical phantom constructed of tissue equivalent materials.
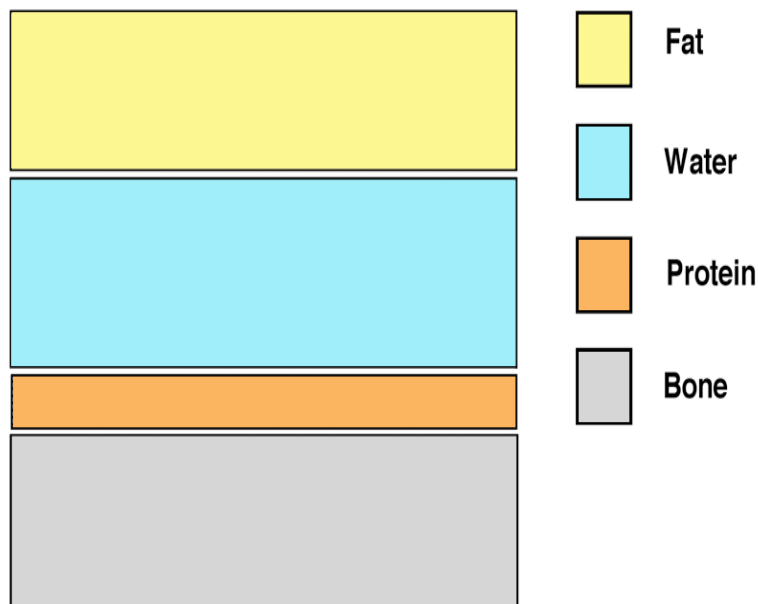
Figure 1.

The mathematical model used to calculate the effect of varying marrow fat content on DXA scan BMD measurements using basis set decomposition [Lehmann LA et al. 1981]. X-ray attenuation coefficients were those published by Hubbell & Seltzer [Hubbell JH et al.]. The base materials for basis set decomposition were hydroxyapatite and ICRU 4-component soft tissue [Hubbell JH et al.]. Bone tissue was represented by ICRU cortical bone [Hubbell JH et al.]. Marrow composition was represented by mixtures of water and fat. A protein component was included based on the marrow composition studies of Goodsitt et al. [Goodsitt MM et al. 1994]. Total marrow thickness was based on measurements of vertebral body thickness in 25 Hong Kong Chinese men and 25 women. Fat composition was based on the chemical composition adopted by Nord & Payne [Nord RH et al. 1990].

Values for mass attenuation coefficients were taken from tables published by Hubbell & Seltzer [Hubbell JH et al.], using either data for the relevant material if provided, or calculated from the chemical composition using tables of the elements. The principle of basis set decomposition was used to resolve the BMD measurement into the equivalent areal densities of hydroxyapatite ($Ca_{10}(PO_4)_6(OH)_2$) and soft tissue [Hubbell JH et al.]. Bone marrow was modelled as a mixture of water, fat and protein in the ratio 12water:1 protein [Goodsitt MM et al. 1994]. The composition of protein was represented by collagen [6]. Fat composition was based on the representative fat adopted by Nord & Payne ($C_{55.05}H_{99.26}O_3$) [Nord RH, 1990].

Vertebral body thickness measurements were made from MR images of the lumbar spine for a randomly selected group of 25 Chinese men and 25 women. Measurements were made of upper and lower vertebral depth (UVD and LVD) for each lumbar vertebra using a method similar to that described by Zhou et al. [Zhou SH et al. 2000]. The mean value of UVD and LVD for each vertebra was then averaged over L1 to L4. Calculations of the quantitative effect of marrow fat content on BMD were made for each sex for vertebral thicknesses corresponding to the mean and the 2SD upper and lower limits. Marrow thickness was obtained by multiplying the vertebral thickness figures by 0.88 to allow for a normal bone volume fraction (BV/TV) of 0.12 [ICRP 1995]. Bone volume fracture is the volume of bone per unit volume of tissue with BV/TV being an abbreviation for bone volume / total volume. Basis set decomposition was used to calculate the expected change in measured BMD in each sex when the marrow fat content measured by ^{1}H-MRS increased from 0 to 100%.

Effect of Marrow Fat Content on T-score Status. Study 1 and Study 2 showed the marrow fat content progressively increased between normal bone, osteopenic bone and osteoporotic bone. To evaluate how much this relationship was explained by a selection effect of subjects with increased marrow fat more likely to be classified as osteopenia or osteoporosis, previous analyses were repeated after correcting the measured spine BMD for the effect of marrow fat content using the correction factors calculated in the previous section. Separate corrections were performed for men and women. The measured spine BMD in each individual was corrected for the difference between the measured marrow fat content F and the mean fat content $\overline{F_s}$ for each sex using the relationship:

$$\text{BMD}_{\text{corr}} = \text{BMD}_{\text{obs}} + \square\square F - \overline{F_s})\qquad(1)$$

where $\square$ is the sex specific marrow fat correction factor previously calculated (See Appendix). Subjects were then sorted into their revised WHO categories based on T-scores calculated from their marrow fat corrected BMD values using local reference data [Lynn HS et al. 2005] and the relationship between marrow fat content and WHO T-score status re-evaluated using regression analysis and one-way analysis of variance (ANOVA). A p-value of 0.05 was required for statistical significance. The statistical significance of the difference between individual WHO categories (normal, osteopoenic or osteoporotic) was evaluated after adjusting p-values for multiple comparisons using the Bonferroni correction.

RESULTS

Quantitative Effect of Vertebral Marrow Fat Content on BMD Measurement. When basis set decomposition was used to estimate the effect of varying marrow fat content on lumbar spine BMD using the model shown in Figure 2, the change in measured BMD when the marrow fat content changed from 0 to 100% was 0.142 g/cm^2 for women and 0.157 g/cm^2 for men. The variation in estimated correction factor corresponding to ± 2SD limits for vertebral thickness was between 0.123 - 0.161 g/cm^2 for women and 0.134 - 0.181 g/cm^2 for men.

Effect of Marrow Fat Content on T-score Status. For the 103 female subjects in whom marrow fat content was known [Study 2], correlation between L3 marrow fat content and T-score changed from r = -0.279 (p = 0.004) to r = -0.175 (p = 0.078) after DXA results BMD figures were adjusted for marrow fat content using Equation (1). Although performing the fat adjustment did not alter the mean T-score for the whole study group, changes did occur in the figures for mean age, T-score and marrow fat when the subjects were subdivided into the three WHO categories based on their fat corrected T-scores (Table 1). Although there was a highly significant difference between the three WHO groups before the correction was applied (p = 0.002), this level of statistical significance was no longer present afterwards (p = 0.066). However, there was still a trend for mean marrow fat to increase as T-score decreased with the difference between the normal and osteoporotic groups changing from 8.6% before correction to 6.2% afterwards (Table 1). When the one-way ANOVA analyses were followed up to investigate the differences between the individual WHO groups, after adjusting for multiple comparisons the only statistically

120

significant difference was between the mean marrow fat figures for the normal and osteoporotic groups before the marrow fat adjustment was made (p = 0.009). After marrow fat adjustment this difference was no longer significant (p = 0.105).

TABLE1: Outline of female cohort before and after marrow fat correction

Before marrow fat correction	All (n=103)	Normal (n=18)	Osteopenia (n=30)	Osteoporosis (n=55)	p-value[1]
Age	72.1 (3.5)	73.4 (3.5)	71.4 (2.9)	72.1 (3.7)	0.150
T-score	-2.34 (1.39)	-0.05 (0.86)	-1.82 (0.44)	-3.37 (0.60)	–
% marrow fat	65.0 (9.6)	59.2 (10.0)	63.3 (9.5)	67.8 (8.5)	0.002
After marrow fat correction	All (n=103)	Normal (n=16)	Osteopenia (n=31)	Osteoporosis (n=56)	p-value[1]
Age	72.1 (3.5)	73.5 (3.6)	71.5 (2.9)	72.1 (3.7)	0.179
T-score	-2.34 (1.39)	-0.04 (0.95)	-1.70 (0.42)	-3.28 (0.59)	–
% marrow fat	65.0 (9.6)	60.4 (10.0)	64.4 (10.1)	66.6 (8.9)	0.066

[1]One way ANOVA test

Table 1 . Descriptive statistics (mean (SD)) of female subject cohort

The results of a similar analysis of 82 male subjects [Study 1] are summarised in Table 2. The correlation between L3 marrow fat content and L1-L4 T-score changed from r = -0.331 (p = 0.002) to r = -0.250 (p = 0.023) when the spine BMD figures were adjusted for marrow fat content using Equation (1). The one-way ANOVA showed that the statistically significant difference in marrow fat content between the 3 WHO groups before the marrow fat correction was applied (p = 0.006) was no longer significant afterwards (p = 0.086), and there was a similar conclusion when the normal and osteoporotic groups where compared (p = 0.006 vs. p = 0.093).

TABLE2: Outline of male cohort before and after marrow fat correction

Before marrow fat correction	All (n=82)	Normal (n=42)	Osteopenia (n=23)	Osteoporosis (n=17)	p-value[1]
Age	73.4 (5.6)	72.4 (4.3)	74.5 (7.6)	74.2 (5.3)	0.284
T-score	-0.67 (1.85)	+0.82 (1.14)	-1.56 (0.41)	-3.16 (0.50)	–
% marrow fat	53.5 (9.5)	50.5 (8.7)	55.7 (10.2)	58.2 (7.8)	0.006
After marrow fat correction	All (n=82)	Normal (n=45)	Osteopenia (n=22)	Osteoporosis (n=15)	p-value[1]
Age	73.4 (5.6)	73.1 (4.8)	73.4 (7.4)	74.2 (5.3)	0.806
T-score	-0.67 (1.85)	+0.66 (1.19)	-1.75 (0.49)	-3.33 (0.46)	–
% marrow fat	53.5 (9.5)	52.6 (9.1)	52.2 (10.2)	58.4 (8.4)	0.086

[1]One way ANOVA test

Table 2. Descriptive statistics (mean (SD)) of the male subject cohort

SIGNIFICANCE OF THESE RESULTS

BMD results obtained from DXA scanners are only correct if the human body is made up solely of bone and lean tissue. The presence of varying amounts of intra- and extra-osseous fat can cause errors in BMD measurement. Fat is largely composed of repeated methylene groups $[(CH_2)_n]$, while X-ray attenuation of lean tissue is closely approximated by water (H_2O). The difference in X-ray attenuation between fat and lean tissue is therefore equivalent to the atomic number difference between carbon and oxygen.

The relationship between bone marrow fat and DXA examination cannot be fully interpreted before first considering the effect that increasing marrow fat has on BMD measurements. In the two studies that have addresses this issue, a wide variation in the reported correction values to be used has been reported [Sorenson JA et al. 1990, Bolotin HH et al. 2007]. In the present study, the BMD change associated with a 0-100% change in marrow fat content was estimated to be 0.14 g/cm^2 for women and 0.16 g/cm^2 for men. These correction factors are substantially smaller than the figure of 0.26 g/cm^2 reported by Bolotin [Bolotin HH et al. 2007]. The reasons for this discrepancy could be different assumptions about composition of red or yellow marrow. Bolotin adopted high density polyethylene [$(CH_2)_n$] for his standard for yellow marrow, which ignores a small but significant contribution from oxygen atoms to the X-ray attenuation of fat. On the composition scale of Nord & Payne [Nord RH et al. 1990] polyethelene has a fat equivalence of 115%. The remaining factor that might explain the difference in marrow fat correction factor is the composition standard for red marrow adopted in the Bolotin study. The standard used was an epoxy resin mixed with a small percentage of calcium carbonate, making it difficult to compare with the water standard used in the present study. It is therefore possible that the difference is explained by Bolotin's standard for red marrow being too lean.

In an earlier study Sorenson reported that a change in the percentage of yellow marrow from 0 to 100% caused a BMD change of only 0.03-0.04 g/cm^2. However, when evaluated on the composition scale of Nord & Payne [Nord RH et al. 1990] the red marrow composition adopted by Sorenson had a fat equivalence of 55% while that for yellow marrow was 81%. These figures are inconsistent with direct chemical measurements of marrow composition [Goodsitt MM et al. 1994] and the small marrow fat correction factor reported in the Sorenson study is explained by the small

difference in the percentage fat values between the red and yellow marrow composites.

When the DXA spine BMD measurements were adjusted for marrow fat content using the correction factors calculated in the present study, the statistical significance of the relationship between marrow fat content and T-score was reduced in both women and men. However, there was still a trend for subjects with osteoporosis to have a higher marrow fat content with a difference between osteoporotic and normal subjects of 6.2% in women and 5.8% in men. The predicted relationship of an increase in marrow fat content of around 1.5% for each unit decrease in T-score is in good agreement with the marrow fat corrected ^{1}H-MRS data.

Limitations of this study.

1. Analysis was based on correcting total spine (L1-L4) T-scores using marrow fat content measurement in L3. However, basic conclusions were not altered when the statistical analyses were repeated for L3 T-scores.

2. By necessity ^{1}H-MRS measurements covered only approximately the central two thirds of the vertebral body. It was not possible to include the whole vertebral body since the MR spectroscopy voxel has to be cuboidal.

**Conclusion:** Increasing vertebral marrow fat content decreases measured BMD measurement by DXA. The correction factor for BMD measurement by DXA was calculated as 0.14 g/cm^2 for females and 0.16 g/cm^2 for males for a 100% change in marrow fat content. Some of the reported increase in marrow fat seen in subjects with reducing BMD is due to the negative effect that increasing marrow fat content

has on BMD estimation. Nevertheless, even after correction, previously reported trends of increasing marrow fat with decreasing BMD still hold true. Overall, with regard to everyday clinical practice, there is little benefit in adjusting DXA BMD values for marrow fat content given the known intrinsic accuracy error of DXA due to marginal osteophytosis, facet joint arthrosis etc.

Next phase of study. Following on from this study, we were satisfied that the changes seen in Study 1 and Study 2 w.r.t marrow fat and perfusion were true and not being unduly influenced by the effect of increasing marrow fat on DXA measurement. We therefore, in the next phase, wished to study whether similar changes in fat content and perfusion were apparent in the proximal femur, an anatomical area very relevant to subjects with osteoporosis. This will be studied in Study 4.

Appendix to Study 3

Predicted relationship between marrow fat content and T-score
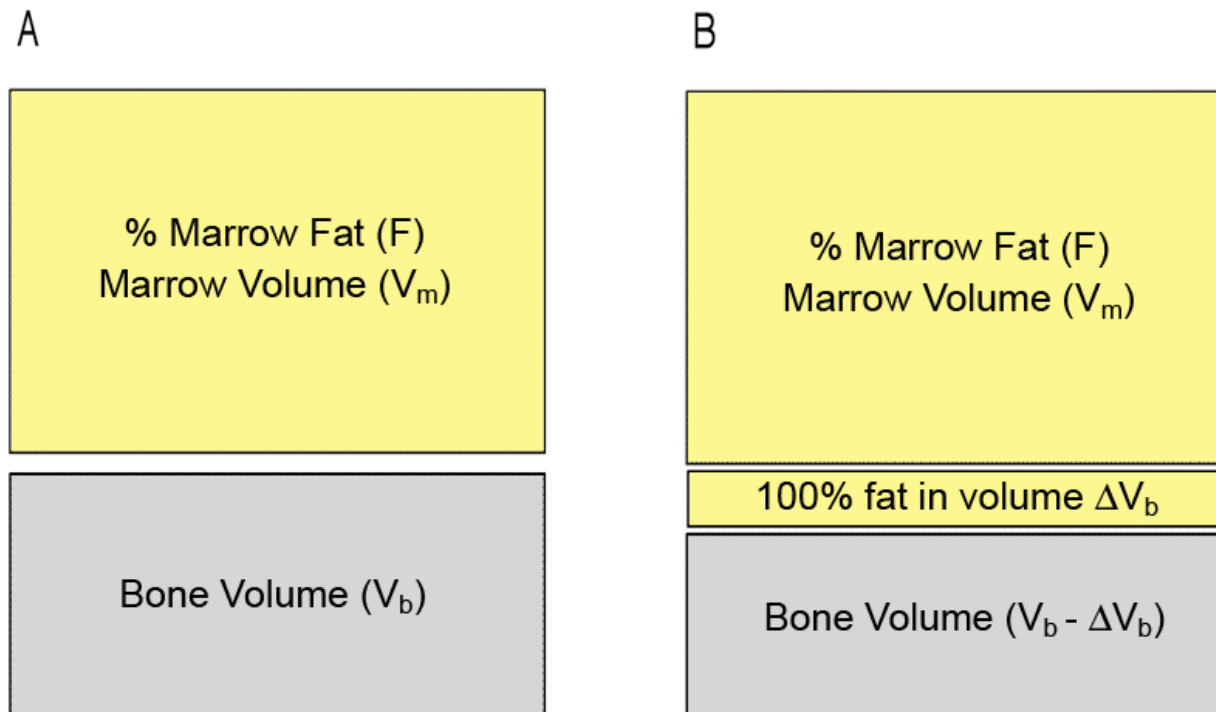
Figure 2. Calculation of predicted relationship between vertebral marrow fat content and T-score.

(A) Subjects with a T-score of zero have a mean volume of bone tissue Vb, marrow volume Vm, and average marrow fat content F.

(B) As osteoporosis develops, volume of bone tissue, Vb, decreases being replaced by fatty marrow with a fat content of 100% while the composition of original marrow tissue remains unchanged.

Let the initial volume of bone tissue be V_b, the marrow volume V_m, and the average marrow fat content F (Figure 2A). As osteoporosis develops there is a decrease in bone volume to $V_b - \Box V_b$ and a corresponding increase in marrow volume to $V_m + \Box V_b$. The new volume element of marrow is assumed to have a fat content of 100% (Figure 2B).

The new figure for the average marrow fat content is given by:

$$F + \Delta F \;=\; \frac{V_m F + \Delta V_b}{V_m + \Delta V_b} \;=\; \frac{(V_m + \Delta V_b)F + \Delta V_b(1 - F)}{V_m + \Delta V_b} \;=\; F + \frac{\Delta V_b(1 - F)}{V_m + \Delta V_b} \tag{A1.1}$$

Hence the increase in marrow fat content ΔF can be written:

$$\Delta F \;=\; \frac{\Delta V_b(1 - F)}{V_m + \Delta V_b} \;=\; (1 - F)\,\frac{\Delta V_b}{V_b}\,\frac{1}{(V_m/V_b) + (\Delta V_b/V_b)} \tag{A1.2}$$

If we assume that the initial state in Figure 2A represents a patient with a T-score of zero then the fractional change in bone volume $\Delta V_b/V_b$ can be written as $\Delta T/T_0$ where ΔT is the change in T-score corresponding to the decrease in bone volume ΔV_b and a BMD value of zero equates to a T-score of $-T_0$. Hence we can finally write:

$$\frac{\Delta F}{\Delta T} \;=\; \frac{(1 - F)}{T_0}\,\frac{1}{(V_m/V_b) + (\Delta T/T_0)} \tag{A1.3}$$

For the female population, the mean marrow fat content F was 65%, the value of T_0 was 9.3, the volume ratio of marrow to bone tissue was 2.9, and assuming a T-score change of -2.5 the ratio $\Delta T/T_0$ was 0.27 giving a $\Delta F/\Delta T$ figure of -1.2% per T-score unit. For the male population, the mean marrow fat content was 53%, the value of T_0 was 8.3, the volume ratio of marrow to bone tissue was 3.2, and assuming a T-score change of -2.5 the ratio $\Delta T/T_0$ was 0.30 giving a $\Delta F/\Delta T$ figure of -1.6% per T-score unit.

STUDY 4:

Are the same changes in perfusion and marrow fat seen in the proximal femur as were seen in the lumbar spine (Study 1 & Study 2)?

Aim: To determine whether similar changes occur in the proximal femur as previously noted in the lumbar spine (Study 1 and Study 2).

Rationale for doing this study:

Study 1 and Study 2 have shown that bone perfusion decreases as BMD decreases in the lumbar vertebrae. The decrease in perfusion seems to only affect bone and does not occur within tissues outside of bone which have the same arterial supply [Study 2]. The proximal femur is the most common site of non-vertebral osteoporotic fracture (Cummings SR et al. 2002, Sambrook P et al. 2006). Proximal femoral fractures are more strongly associated with decreased BMD, cost more to repair and cause more disability then any other type of osteoporotic fracture (Cummings SR et al. 2002). The proximal femur is also an area very prone to avascular necrosis and fracture non-union. We therefore undertook this study to further investigate the relationship between BMD, bone marrow perfusion and bone marrow fat content in the proximal femur. The relationship between marrow and muscle perfusion was also investigated.

STUDY OUTLINE:

STUDY 4

$\downarrow$

Are the same changes in perfusion and marrow fat seen in the proximal femur as were seen in the lumbar spine (Study 1 & Study 2)?

$\downarrow$

---

120 post-menopausal female subjects of varying BMD

- DXA right hip
- MR perfusion imaging of proximal femur (head, neck, shaft), acetabulum and adductor musculature.- oblique coronal plane
- Proton MR Spectroscopy of proximal femur (head, neck, shaft).

$\downarrow$

MAIN FINDINGS

- Marrow perfusion is $\downarrow\downarrow$ in the femoral head in all subjects compared to neck, shaft and acetabulum irrespective of BMD.
- Perfusion in all bone areas is $\downarrow$ with $\downarrow$ BMD. This effect is most noticeable in the femoral neck and acetabulum. Adductor muscle perfusion is unchanged with change in BMD.
- Marrow fat $\uparrow$ in femoral head compared to all other areas.
- Marrow fat $\uparrow$'s in all bone areas with $\downarrow$ BMD.
- Path analysis revealed that $\downarrow$ bone perfusion seems more related to $\uparrow$ marrow fat rather than $\downarrow$ BMD.
- Overall, similar relationship seen between BMD, marrow and muscle perfusion occurs in the proximal femur as the lumbar spine.

ABSTRACT

Purpose: Outside of the spine, the proximal femur is the most common site of osteoporotic fracture and is also an area prone to avascular necrosis and fracture non-union. This study of the proximal femur investigates the relationship between bone mineral density (BMD), bone marrow fat content, bone perfusion and muscle perfusion.

Materials and Methods: 120 healthy female subjects (mean age 74 years; age range, 67-89 underwent dual x-ray absorptiometry (DXA) examination of the hip, proton magnetic resonance (MR) spectroscopy, and dynamic contrast-enhanced MR imaging of the right proximal femur, acetabulum and adductor thigh muscle.

Results: In all bone areas examined (femoral head, femoral neck, femoral shaft, acetabulum), perfusion indices (maximum enhancement, enhancement slope) were significantly reduced in subjects with osteoporosis compared to subjects with osteopenia or normal BMD. Adductor muscle perfusion was not affected by change in BMD. As marrow perfusion decreased in the proximal femur, marrow fat increased (r = 0.827). This increase in fat content seemed to account for the decrease in marrow perfusion more than a reduction in bone mineral density. For normal bone density subjects, perfusion parameters in the femoral head were one-third of those in the femoral neck or shaft and one-fifth of those in the acetabulum.

Conclusion: Perfusion throughout the proximal femur is reduced in osteoporotic subjects compared to osteopenic and normal subjects. This reduction in perfusion only affects bone and not those tissues outside of bone with the same blood supply. As bone perfusion decreased there was a corresponding increase in marrow fat.

STUDY DETAIL:

MATERIALS AND METHODS

Subject selection. Recruitment notices were placed in community centers for the elderly inviting subjects to attend for dual x-ray absorptiometry (DXA) examination. This study cohort was a different cohort to that of earlier studies. Following DXA examination, all subjects were invited to attend for MR examination. The Institutional Clinical Research Ethics Committee approved the study (Appendix) and signed consent was obtained from all participating subjects. Details regarding subject age, hip BMD and T-score are provided in Table 1. All participating subjects were Chinese. All MR imaging examinations were performed within two weeks of DXA examination. Subjects were not recruited or excluded from further analysis if there was (a) clinical or imaging evidence of metabolic bone disease or metastases; (b) a history of hip surgery or irradiation; (c) a contraindication to MR imaging examination; or (d) an incomplete MR examination.

DXA examination. DXA examination of the right hip was performed on all subjects using a single DXA system (Hologic QDR-4500W). in-vitro short and long term CV of DXA lumbar spine used in this study was 0.65% while the in-vitro long term CV was 0.398. Based on total hip T-score and reference values derived from the local population (Lynn HS et al. 2005), subjects were grouped into three categories based on World Health Organization criteria (Kanis JA et al. 2002, WHO Study Group 1994). Normal BMD was defined as a T-score greater than -1·0, osteopenia as a T-score between -1·0 and -2·5, and osteoporosis as a T-score less than -2·5.

MR examination. MR examinations were performed on a 1·5-T whole-body MR imaging system (Intera NT, Philips) with a maximum gradient strength of 30 mT/m. A two-element circular surface coil measuring 20-cm in diameter wrapped around the right hip with the proximal tip at the level of the anterior superior iliac spine and aligned along the long axis of the thigh was used. A T1-weighted (repetition time [TR] msec/echo time [TE] msec, 540/16) oblique coronal image of the proximal femur was obtained to guide positioning of region of interests (ROIs) within the proximal femur, acetabulum and adductor musculature for spectroscopy and perfusion imaging.
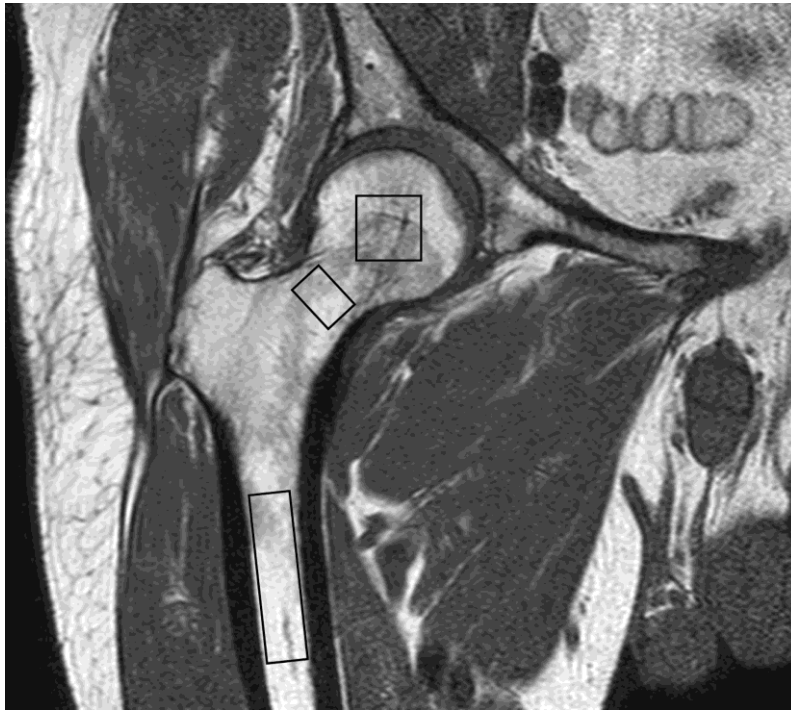

Figure 1

T1-weighted coronal MR image of proximal femur showing regions-of-interest (ROI's) used to measure perfusion in the femoral head, neck, shaft, acetabulum and adductor muscle. For the adductor muscle, a best-fit circle encompassing an area of adductor muscle proximally excluding intermuscular fat was used.

Marrow fat content was evaluated using MR spectroscopy. For spectroscopy, three separate standardized volumes of interest (VOI) were placed respectively in the femoral head ($1·5 \times 1·5 \times 1·5$ cm^3), femoral neck ($1·0 \times 1·5 \times 1·5$ cm^3), and sub-trochanteric region of the femoral shaft ($1·0 \times 1·0 \times 3·0$ cm^3). After local shimming and gradient adjustments, data was acquired at a spectral bandwidth of 1,000 Hz

with 512 data points and 64 non-water suppressed signals obtained using a point resolved spectroscopic sequence (TR/TE, 3000/25 msec).

Figure 2

T1-weighted coronal MR image of proximal femur showing regions-of-interest (ROI's) used to measure fat content in the femoral head, neck, and shaft.

Marrow perfusion and muscle perfusion was evaluated using dynamic contrast-enhanced MR imaging. For dynamic contrast-enhanced MR perfusion imaging, images were obtained in an oblique coronal plane aligned along the mid-portion of the proximal femur. Dynamic images were obtained using a short T1-weighted gradient-echo sequence (TR/TE, 2·7/0·95; pre-pulse inversion time 400 msec; flip angle 15°; section thickness 10 mm; number of slices, one; field of view 250 mm; acquisition matrix 256 $\times$ 256; one signal acquired). A total of 160 dynamic images were obtained with a temporal resolution of 540 msec over an 82 sec timeframe (i.e. 160 acquisitions x 540 msec per acquisition). A bolus of gadoteric acid (Dotarem; Guerbet) at a concentration of 0·6 mmol per kilogram body weight was injected at a rate of 2·5 mL/sec (Spectris, Medrad) through a 21-gauge intravenous catheter inserted into an antecubital vein. The injection was followed by a 20-mL saline flush.

Dynamic MR imaging started at the same time the contrast medium injection started (time zero).

Data analysis

(a) Spectroscopy data. Spectra were analyzed on an off-line computer (Dell Precision 650 Workstation) using a time-domain fitting routine. Water (4·65 ppm) and lipid (1·3 ppm) peak amplitudes were measured to determine proximal femur marrow fat content. Fat content was defined as the relative fat signal amplitude as a percentage of total signal amplitude (water and fat).

(b) Perfusion data. On the mid-coronal oblique T1-weighted image, ROIs separately encompassing the marrow cavity (excluding the cortex) of the head, neck, shaft of proximal femur, the central portion of the acetabulum and the proximal thigh musculature were drawn manually on a radiology workstation (Viewforum, Philips Medical System) (Figure 1). Time-intensity curves were recorded and processed on an offline computer. Two perfusion indices were measured. These were maximum enhancement (E_{max}), defined as the maximum percentage increase in signal intensity from baseline and enhancement slope (E_{slope}), defined as the rate of enhancement between 10% and 90% of the signal intensity difference between baseline and maximum signal intensity (Figure 2). Both parameters are derived from the first-pass phase of signal enhancement and are considered to represent arrival of contrast material into the arteries and capillaries and its diffusion into the extracellular space (Cova M et al. 1991).

Statistical analysis. Data was presented as mean and standard deviation, unless otherwise stated. Subjects were grouped as normal, osteopenia or osteoporosis according to total hip T-score. Normal Q-Q plot and box plots were employed to examine normality of parameters and identify outliers. Perfusion parameters were logarithmically transformed to correct positive skewness. As the fat content parameters were negatively skewed, they were all first subtracted by 100 and then log-transformed to correct negative skewness. The transformed parameters were compared among the three groups- normal, osteopenia and osteoporosis using linear trend test and analysis of covariance (ANCOVA) for adjusting age. Post Hoc multiple comparisons were conducted for those significant parameters using Bonferroni's correction. Pearson correlation coefficients were calculated to assess the linear relationship between different pairs of parameters. Multiple regression analysis was performed to uncover variables (age, perfusion indices, fat content) significantly associated with bone mineral density. Path analysis was used to examine the causal relationships between age, fat content, marrow perfusion and BMD. Relationships were modeled using a series of linear structural equations. All model tests were based on a covariance matrix and used maximum likelihood estimation as implemented in Lisrel 8.50. The validity of the models was evaluated and compared using Chi square statistic, goodness-of-fit index (GFI), comparative-fit index (CFI), non-normed-fit index (NNFI), root mean square error of approximation (RMSEA) and standardized root mean square residual (SRMR). Receiver operating characteristic (ROC) analysis was employed to investigate the discriminating ability of each parameter for predicting osteoporosis with area-under-ROC curve (AUC) being used as a measure of the global performance of each parameter as an effective predictor. The value corresponding to the nearest point of the ROC curve to

the top left-hand corner was chosen as the optimal threshold in that it maximizes both sensitivity and specificity (with equal weighting). Test-retest reliability of each measured parameter was assessed using intra-class correlation coefficient on absolute agreement. All statistical analyses were done using SPSS 14·0 (SPSS Inc). All statistical tests were two-sided. A p-value <0·05 was considered statistically significant.

RESULTS

Relationship between marrow fat content and bone mineral density. As BMD decreased, marrow fat content tended to increase in the femoral head (r = -0·334, p<0·01), femoral neck (r = -0·370, p<0·01) and shaft (r = -0·412, p<0·01) (Table 2). Subjects with osteoporosis had a significantly higher marrow fat content in the femoral head (p=0·001), femoral neck (p<0·001) and femoral shaft (p<0·001) than normal BMD subjects (Table 1). Similarly, subjects with osteopenia had a significantly higher marrow fat content in the femoral neck (p<0·001) and femoral shaft (p<0·001) than normal BMD subjects (Table 1).

Table 1. Characteristics, fat content and perfusion indices of subjects with osteoporosis, osteopenia and normal BMD.

	All (n=120)	Normal (n=39)	Osteopenia (n=47)	Osteoporosis (n=34)	p (trend test)	p (ANCOVA[#])
Age (years)	73·79 (4·28)	72·90 (3·75)	73·38 (4·65)	75·38 (4·00)	**0·013**	**0·032**[*]
Hip BMD(g/cm^2)	0·71 (0·12)	0·85 (0·06)	0·70 (0·04)	0·57 (0·06)	**<0·001**	**<0·001**[a,b,c]
T-score	-1·63 (1·15)	-0·33 (0·58)	-1·73 (0·41)	-2·98 (0·51)	**<0·001**	**<0·001**[a,b,c]
Fat content (%)						
Femoral head	88·47 (4·62)	86·34 (5·72)	89·14 (3·84)	89·94 (3·26)	**0·001**	**0·004**[a,c]
Femoral neck	85·06 (7·77)	80·80 (9·35)	86·19 (6·50)	88·38 (4·81)	**<0·001**	**<0·001**[a,c]
Femoral shaft	83·80 (6·36)	80·01 (5·98)	84·51 (6·32)	87·16 (4·44)	**<0·001**	**<0·001**[a,c]
Enhancement maximum (%)						
Femoral head	4·00 (2·02)	4·65 (2·46)	4·03 (1·82)	3·15 (1·21)	**0·017**	0·076
Femoral neck	11·70 (7·89)	16·09 (9·84)	10·50 (5·69)	8·06 (5·16)	**<0·001**	**<0·001** [a,c]
Femoral shaft	14·35 (10·76)	17·47 (13·67)	14·20 (8·62)	10·24 (7·89)	**0·003**	**0·010**[c]
Acetabulum	17·83 (9·64)	24·57 (9·74)	16·75 (8·42)	11·62 (5·72)	**<0·001**	**<0·001**[a,b,c]
Muscle	68·02 (21·07)	65·94 (14·46)	69·24 (27·87)	68·62 (15·84)	0·584	0·937
Enhancement slope (%/sec)						
Femoral head	0·15 (0·11)	0·20 (0·13)	0·13 (0·08)	0·11 (0·08)	**0·001**	**0·008**[c]
Femoral neck	0·47 (0·36)	0·64 (0·40)	0·42 (0·31)	0·32 (0·28)	**<0·001**	**<0·001**[a,c]
Femoral shaft	0·55 (0·43)	0·59 (0·39)	0·60 (0·46)	0·42 (0·40)	**0·010**	**0·020**[c]
Acetabulum	0·94 (0·55)	1·26 (0·49)	0·91 (0·54)	0·62 (0·42)	**<0·001**	**<0·001**[a,b,c]
Muscle	1·83 (0·89)	1·78 (0·85)	1·74 (0·76)	2·03 (1·09)	0·292	0·460

Data presented as mean (sd)

[#] ANCOVA test among the three groups adjusting for age;

[*] ANOVA test among the three groups;

[a] post hoc test with Bonferroni's correction showed significant difference between normal and osteopenia groups after adjusting for age;

[b] post hoc test with Bonferroni's correction showed significant difference between osteopenia and osteoporosis groups after adjusting for age;

[c] post hoc test with Bonferroni's correction showed significant difference between normal and osteoporosis groups after adjusting for age.

Relationship between marrow perfusion and bone mineral density. As BMD decreased, there was a corresponding decrease in bone marrow perfusion indices in the femoral head, femoral neck, femoral shaft, and acetabulum (Tables 1 and 2). This effect was most noticeable in the acetabulum, femoral neck and femoral head and least noticeable in the femoral shaft (Tables 1and 2). Except for E_{max} in the femoral head, subjects with osteoporosis had a significantly lower mean E_{max} and E_{slope} than normal BMD subjects (Table 1). This difference was most noticeable in the femoral neck and acetabulum (Table 1). While univariate analysis showed that many perfusion indices were associated with reduced BMD, multivariate regression analysis showed that, among the variables tested, E_{max} of the acetabulum and E_{slope} of the femoral head were significantly associated with BMD (Table 2).

Table 2. Correlation between perfusion indices, fat content and BMD in femoral head, neck, shaft, acetabulum and adductor thigh muscle

	Vs BMD (g/cm^2)	Vs Fat content (%) [ψ]
Enhancement max. (%)		
Femoral head	0.241*	-0.614 **, [‡]
Femoral neck	0.417 **	-0.855 **, [‡]
Femoral shaft	0.237 *	-0.653 **, [‡]
Acetabulum	0.538 **, [†]	nm
Muscle	-0.046	nm
Enhancement slope (%/sec)		
Femoral head	0.382 **, [†]	-0.549 **, [‡]
Femoral neck	0.396 **	-0.768 **, [‡]
Femoral shaft	0.168	-0.647 **, [‡]
Acetabulum	0.512 **	nm
Muscle	-0.052	nm
Fat content (%)		
Femoral head	-0.316**	
Femoral neck	-0.367 **	
Femoral shaft	-0.407 **	

nm = not measured;
**$p<0.01$ & *$p<0.05$ in univariate analysis;
[†] independently significantly ($p<0.05$) associated with BMD in multiple regression analysis;
[ψ] bivariate correlation analysis was done for corresponding fat content at these sites;
[‡] significantly correlated ($p<0.05$) with fat content at this site after Bonferroni's correction.
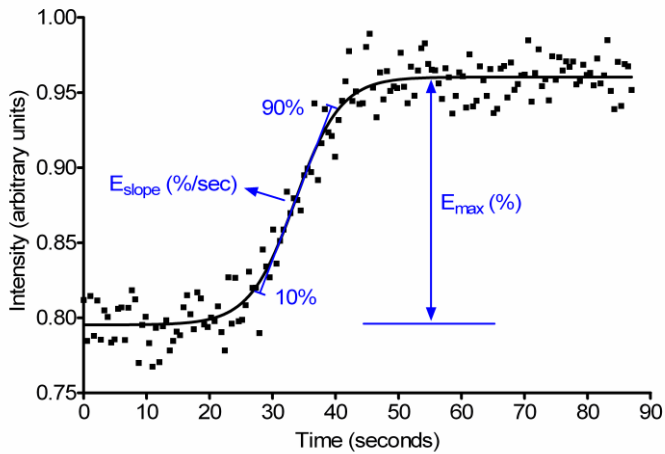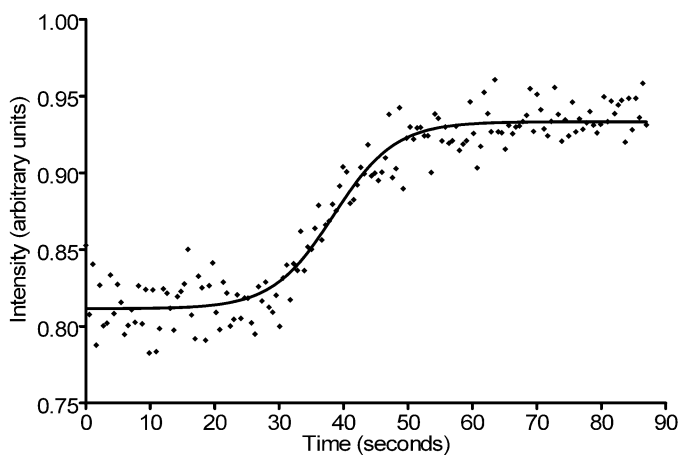
Figure 2A

Figure 2B
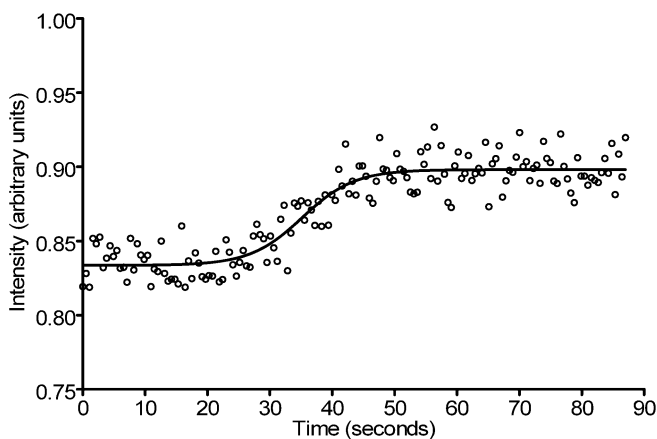
Figure 2C

Figure 2A, B,C

Time-intensity curve of femoral neck for different subjects with (A) normal bone density showing high maximum enhancement (E_{max}) and steep enhancement slope (E_{slope}), (B) osteopenia showing decreased maximum enhancement and less steep enhancement slope and (C) osteoporosis showing the least maximum enhancement and flattest enhancement slope.

Relationship between marrow perfusion and fat content. As bone marrow perfusion decreased, there was a corresponding increase in bone marrow fat content for all bone areas examined (r = -0·827). For example, as E_{max} decreased,

there was an increase in fat content in the femoral head (r = -0·614), femoral neck (r = -0·855) and shaft (r = -0·653) (Table 2). Similarly, as E_{slope} decreased, there was an increase in fat content in the femoral head (r = -0·549), femoral neck (r = -0·768) and shaft (r = -0·647) (Table 2).

Relationship between muscle perfusion and bone mineral density. Although bone perfusion indices significantly decreased, muscle perfusion indices did not change with a decrease in BMD (p>0·05) (Table 2). Both E_{max} (p=0·858) or E_{slope} (p=0·426) of the adductor thigh muscle remained unchanged in subjects with osteoporosis, osteopenia or normal BMD (Table 1).

Relationship between marrow perfusion, fat content and bone mineral density.
Since factor loadings of marrow fat content (0.90) and bone marrow perfusion (0.86) of the femoral neck were the largest, the femoral neck was chosen for path analysis. The path diagram is shown in Figure 2. All path coefficients were significant (p<0.05). The Chi square statistic, goodness-of-fit index (GFI), comparative fit index (CFI), non-normed fit index (NNFI), root mean square error of approximation (RMSEA) and standardized root mean square residual (SRMR) were respectively 3.287, 0.987, 0.998, 0.996, 0.025 and 0.051. All the fit indices indicated the model fitted the data very well. The model explained 17.8%, 73.1% and 5.5% of the variance in marrow fat content, bone marrow perfusion and bone mineral density respectively.

According to the fitted model, (i) bone mineral density and age, (ii) bone mineral density and fat content and (iii) perfusion and fat content are all inversely related as previously noted. The model indicated that there was a direct effect of marrow fat content on bone marrow perfusion and an indirect effect of age via bone mineral

density and then via fat content on bone marrow perfusion (Figure 3). There is no significant direct effect of bone mineral density on bone marrow perfusion (Figure 3). Increase in fat content seemed to be the main contributor to reduction in bone marrow perfusion (Figure 3).
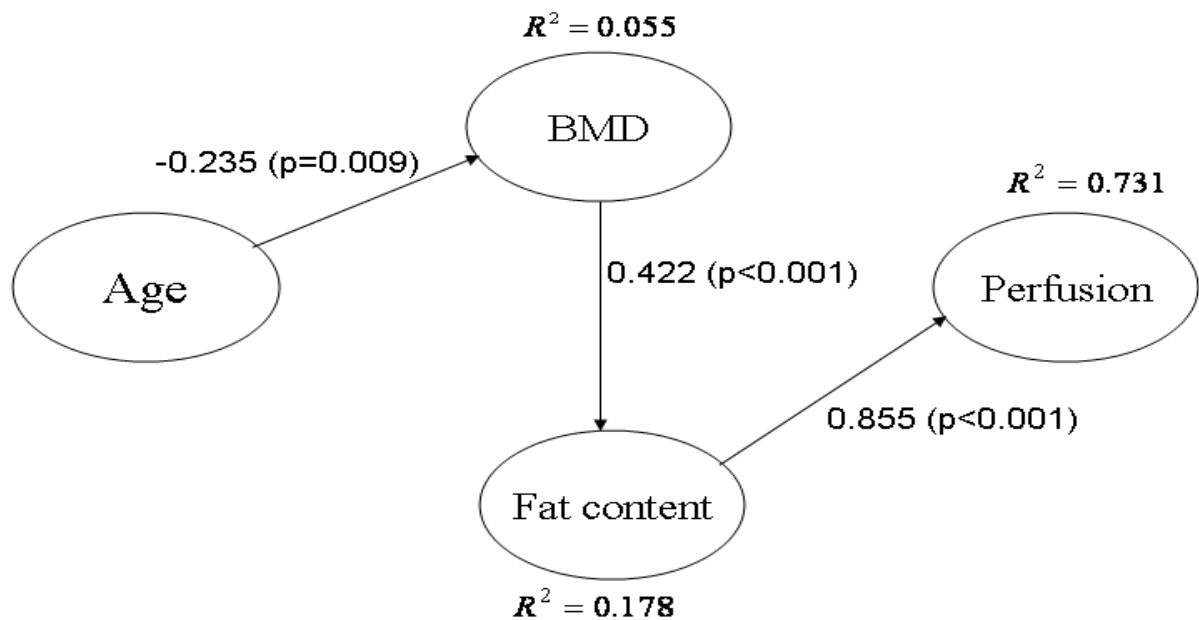
Figure 3. Path analysis of age, BMD, marrow fat content and marrow perfusion. The model indicates a direct effect of marrow fat content on perfusion and indirect effect of age via BMD and then via fat content on perfusion. There is no significant direct effect of BMD on perfusion. An increase in fat content contributes to the reduction in perfusion.

Usefulness of perfusion and fat content indices in predicting osteoporosis.

The overlap observed in perfusion and fat content indices the three subgroups (osteoporosis, osteopenia, normal bone density) indicated that these parameters in isolation are not likely to be of clinical use in predicting osteoporosis, osteopenia or normal bone density. ROC analysis of all parameters confirmed this impression. ROC analysis indicated the two best predictors of osteoporosis to be E_{max} in the acetabulum and neck of femur. An acetabulum E_{max} of <15·05 yielded a 79% (95% CI, 61–91%) sensitivity and 72% (61–81%) specificity in predicting osteoporosis

while for the femoral neck an E_{max} of <9·05 yielded a 70% (61–85%) sensitivity and 69% (57–79%) specificity.

Relative reduction in perfusion indices between different segments of proximal femur

Relative reduction in MR perfusion indices in osteopenic and osteoporotic subjects compared with normal BMD subjects is shown in Fig 2. In both male and female subjects, as BMD decreased, perfusion indices in the femoral neck decreased to a larger degree than those in the femoral head and shaft. This relative reduction in perfusion indices in the femoral neck was more apparent in osteopenic than osteoporotic subjects.
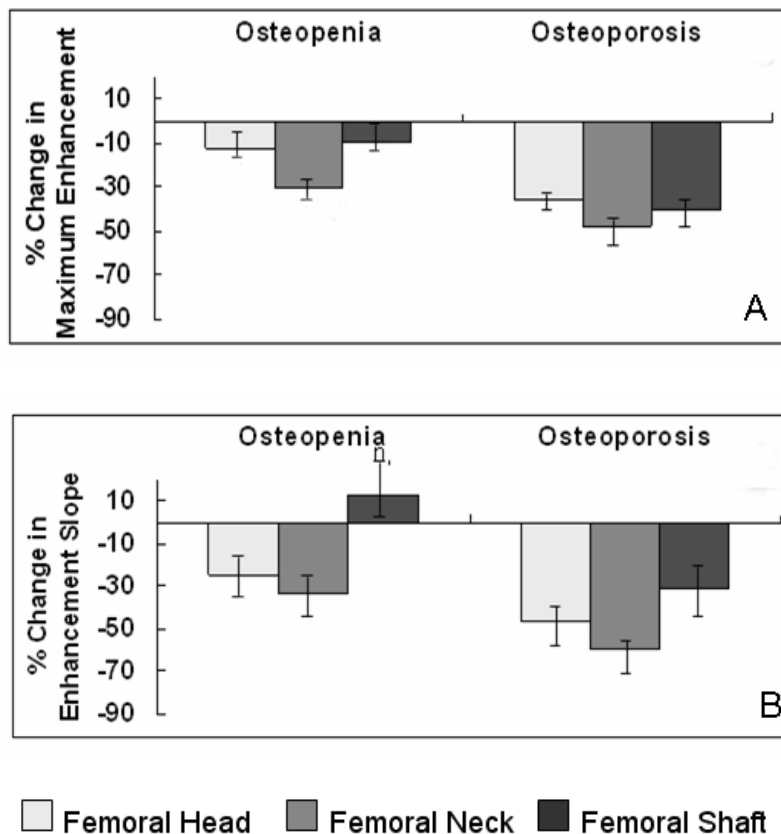

Figure 4. Relative reduction in (A) E^{max} and (B) E^{slope} in femoral head, neck and shaft in subjects with osteopenia (n=47) and osteoporosis (n=34) compared to those with normal BMD (n=39). Perfusion indices reduced most in the femoral neck region.

143

SIGNIFICANCE OF THESE FINDINGS

The main finding of Study 4 is showing for the first time that osteoporosis and osteopenia of the proximal femur and acetabulum is associated with reduced bone perfusion compared to normal bone density subjects. This concurs with our findings in Study 1 and study 2 of the lumbar spine. This study, by providing direct evidence of reduced perfusion in osteoporotic bone, strengthens the link between vascular disease and osteoporosis.

The second main observation of this study is that the reduced perfusion observed in osteoporosis of the hip region is an intraosseous occurrence rather than a reflection of a more generalized circulatory impairment. While bone perfusion decreased with reduced BMD in the proximal femur and acetabulum, no corresponding change in perfusion in the adductor thigh musculature was observed. Both the proximal femur and the adductor thigh musculature are both supplied by the profunda femoris artery. The proximal femur is supplied via the medial circumflex artery, the first branch of the profunda femoris artery (Gautier E et al. 2000), while the adductor thigh musculature is supplied by perforating muscular branches which arise from the profunda femoris just distal to the medial circumflex artery (Angrigiani C et al. 2001). The acetabulum is supplied by the internal iliac artery via the superior gluteal, inferior gluteal and obturator arteries (Beck M et al. 2003). The reduced perfusion observed within bone is of bony rather than systemic or extraosseous origin since if the latter were the case, both bone and muscle should have been affected as they have the same arterial supply. Bridgeman et al have shown, in an anatomical study, progressive occlusion of the intramedullary arteries in the proximal femur with age leading to increasing reliance on periosteal circulation for perfusion of cortical bone (Bridgeman G et al. 1996), while Laroche et al showed that intraosseous arterioles

or arterial capillaries were reduced in number in patients with proximal femoral osteoporosis with more frequent arteriosclerotic vascular lesions (rupture of internal elastic lamina, medial thickening and fibrosis) (Laroche M et al. 1995). Our study confirms that intraosseous perfusion is reduced in osteoporotic and osteopenic bone while extraosseous perfusion remains unaffected. These changes are similar to those shown in Study 2 of the lumbar vertebrae where vertebral marrow perfusion decreased in osteoporosis though paravertebral muscle with the same blood supply as the vertebrae remained unaffected. This change in emphasis between intraosseous and extraosseous perfusion in normal and osteoporotic patients may help explain some of the different patterns of bone deposition and apposition noted in osteoporosis. With aging bone resorption occurs preferentially on the trabecular and endocortical surfaces while bone apposition preferentially on the periosteal surface (Seeman E et al. 2002, Seeman E et al. 2007).

The third main finding is that as bone marrow perfusion decreased in the proximal femur, there was a reciprocal rise in marrow fat content. This reciprocal arrangement between marrow perfusion and marrow fat has not been recognized until we performed Study 1 and Study 2. Marrow fat content increases with both age and osteoporosis. The latter may simply reflect increased size or number of fat cells replacing lost bone (Rozman C et al. 1989, Justesen J et al. 2001). This current study shows that proximal femoral osteoporosis is associated with reduced marrow perfusion and reciprocal increased marrow fat content. An effect of perfusion on differentiation of marrow mesenchymal stem cells may account of this observation. The mesenchymal stem cell acts as a common precursor for osteoblasts and adipocytes in the bone marrow (Gimble JM et al. 2004). Differentiation along osteoblast or adipocyte lines is influenced by oxygen tension and oxidative stress

(D'Ippolito G et al. 2006, Fatokun AA et al. 2006, Shouhed D et al. 2005, Kha HT et al. 2004). Decreased oxygen tension or increased oxidative stress favors adiopocyte over osteoblast precursor development (D'Ippolito G et al. 2006, Fatokun AA et al. 2006, Shouhed D et al. 2005, Kha HT et al. 2004). Reduced marrow perfusion, as shown in this study, is likely to decrease oxygen tension and increase oxidative stress within the marrow. This change in microenvironment may effect mesenchymal stem cell maturation inducing adipocyte formation (i.e. increased marrow fat) over osteoblast formation (i.e. decreased BMD) (Duque G et al. 2007). Path analysis of this study indicated that an increase in marrow fat content yielded a greater contribution to decreased marrow perfusion than decreased bone mineral density. Longitudinal study, rather than cross-sectional study as performed here, should clarify this relationship more definitively. Also separate analysis of the trabecular bone (rather then cortical bone and trabecular bone as performed in this study) may help clarification.

The femoral head is an area particularly susceptible to avascular necrosis and subchondral insufficiency fracture. For normal bone density subjects, perfusion indices in the femoral head were approximately one-third of those of the femoral neck or shaft and one-fifth of those in the acetabulum. Perfusion indices in the femoral head further decreased in osteoporotic subjects thorough the effect was not as pronounced as in the femoral neck, shaft or acetabulum. This helps explain why avascular necrosis of the femoral head is not an accompaniment of osteoporosis per se though is a frequent accompaniment of osteoporotic-induced femoral neck fracture.

The femoral neck shows the most marked reduction in blood perfusion indices (Figure 4). One possible explanation of this observation is that the femoral neck

region tends to have greater portion of red marrow compared with proximal femur shaft and femoral head (Berg et al 1997), and associated reduction in red marrow volume is one of the likely causes of reduced bone perfusion seen in osteoporosis (Study 7). Osteoporosis is associated with an increased incidence of femoral neck fractures with femoral neck BMD being a strong predictor of femoral neck fracture susceptibility (Rivadeneira F et al 2007). The femoral neck is strongly dependent on trabecular bone for its strength. Trabecular bone receives all of its blood supply from the marrow cavity as opposed to cortical bone which has an additional supply from the periosteal arteries. Bone perfusion is directly associated with bone remodeling activity (Reeve J et al. 1998) which in turn is directly associated with fracture risk (Garnero P et al. 2004; Johnell O et al. 2002) Insufficiency fracture probably results from impaired bone remodeling leading to an accumulation of trabecular microdamage and microfracture progressing eventually to a clinically apparent complete fracture. As repair of any tissue requires an adequate blood supply to deliver oxygen and nutrients, impaired blood supply to the femoral neck trabecular bone may well be a contributory factor to microfracture accumulation, trabecular fracture propagation and eventual insufficiency fracture.

Delayed union and osteonecrosis due to femoral neck fracture nonunion are also relevant in the proximal femur (Matthews V et al. 2004). Nonunion occurs in 30–43% (Saito et al 1995, Jackson et al 2002, Hedstrom M et al. 2004) displaced intracapsular femoral neck fractures. One prospective multicenter study of 1503 patients with fractured neck of femur analysed the incidence of delayed union and avascular necrosis. In displaced intracapsular fractures of the proximal femur treated by reduction and fixation, the prevalence of osteonecrosis was 28% while the rate of nonunion was 33% and with only 14% of fractures being united at 6 months (Barnes

R et al. 1976).   On the other hand, in another study of patients younger than 50 years, all proximal femoral fractures healed satisfactorily even those occurring in patients with high-energy trauma. Increasing age and low bone mass clearly influence the healing of femoral neck fractures and this may be related to an underlying perfusion deficit. In other words, impaired perfusion is probably influencing both the development of and healing of proximal femoral insufficiency fractures

Limitations of this study.

1. As this was a cross-sectional study, we could not investigate whether a causal or temporal relationship existed between a decrease in bone perfusion, an increase in marrow fat and osteoporosis. This study does not explore whether these changes are primary or secondary to the development of osteoporosis nor does it explore the molecular and cellular events behind these changes as well as the effect, if any, on fracture risk.

2. As DXA was used as a measure of bone density, bone mass measurements for specific areas of interest (head, neck, shaft, and acetabulum) were not available. Bone densitometry of specific areas of the proximal femur and acetabulum would require the use of quantitative computed tomography densitometry.

3. Muscle perfusion was measured in a similar fashion to marrow perfusion but orther local factors which may influence muscle perfusion such as muscle bulk and fatty replacement were not evaluated.

Conclusion. Very similar changes are seen in the proximal femur as previously noted in the lumbar spine (Study 1 and Study 2). Reduction in perfusion only affects the bone and was not seen to effect the adductor musculature which has the same arterial supply. With decreasing BMD, reduced perfusion is most noticeable in the

femoral neck. The femoral head has increased marrow fat and decreased perfusion compared to all other areas irrespective of BMD.

Next phase of study. Following on from this study, if one wishes to perform longitudinal MR-based assessment of marrow fat fraction or perfusion, one would first need to know the reproducibility of these MR-based tests. This forms the basis of Study 5.

STUDY 5

What is the reproducibility of MR perfusion studies and ^{1}H spectroscopy of bone marrow?

Aim: This study was performed to examine the reproducibility of MR bone marrow ^{1}H MR spectroscopy and dynamic contrast-enhanced perfusion studies.

Relevance of this study

MR proton (^{1}H) spectroscopy is the most commonly used method to quantify marrow fat content while dynamic contrast-enhanced imaging is the most commonly used method to assess bone marrow perfusion. As shown in Study 1, Study 2 and Study 4, cross-sectional observational studies can be performed to study the relationship between these physiological features and bone disease. However, when one wants to investigate the longitudinal relationship between marrow fat content or perfusion and disease onset or progression or alternatively study the effect of intervention, it is critical to first know the reproducibility of the test being undertaken. This study was undertaken to measure this reproducibility in a clinical setting.

STUDY OUTLINE:

STUDY 5

↓

What is the reproducibility of MR perfusion studies and
[1]H spectroscopy of bone marrow?

↓

---

36 healthy subjects (72.9 ± 2.9 years) underwent paired MR examinations at baseline and returned for follow-up MRI assessment one week following baseline

- MR Spectroscopy of proximal femur with assessment of marrow fat in femoral head, neck and shaft.
- Dynamic-contrasted enhanced MR imaging of proximal femur with assessment of perfusion in head, neck, shaft, acetabulum and adductor muscle.

↓

MAIN FINDINGS

- Reproducibility of MRS ranged from 0.78 – 0.85, being highest in the femoral head and lowest in the femoral neck.
- Reproducibility of MR perfusion imaging ranged from 0.59 – 0.98, being highest in the acetabulum and lowest in the femoral head.
- Overall reproducibility of 1H MR spectroscopy and MR perfusion imaging is sufficiently high to warrant use in clinical trials.
- Reproducibility optimal in those areas with highest inherent fat fraction or perfusion.

ABSTRACT

Purpose: MR ^{1}H proton spectroscopy and dynamic contrast-enhanced imaging are the most common used methods of quantifying marrow fat volume fraction and marrow perfusion respectively. Before longitudinal studies investigating the influence of marrow fat content and perfusion on bone diseases are undertaken, one should first determine the test reproducibility of these techniques. This study was undertaken to measure this reproducibility.

Materials and Methods: 36 subjects (17 females, 19 males, mean age 72.9 ± 2.9 years) who underwent MR spectroscopy and /or dynamic-contrast enhanced perfusion study of the proximal femur were asked to return after one week for a repeat MR examination.

Results: Reproducibility of ^{1}H MR spectroscopy in all bone areas tested was high ranging from 0.78 to 0.85 with highest reproducibility being in the femoral head and lowest in the femoral neck. Reproducibility of paired perfusion measurements ranged from 0.59 (enhancement slope femoral head) to 0.98 (enhancement maximum acetabulum). Overall reproducibility of proton spectroscopy and dynamic contrast-enhanced imaging tended to be best in areas with highest inherent fat fraction or perfusion.

Conclusion: Reproducibility of MR proton spectroscopy or perfusion imaging is sufficiently high to warrant these techniques being applied to the longitudinal study of bone disease.

STUDY DETAIL:

MATERIAL AND METHODS

Patient Selection and Data Collection. Thirty six elderly subjects (17 females, 19 males, mean age 72.9 ± 2.9 years, range 69-78 years) who underwent ^{1}H MR spectroscopy with or without dynamic-contrast enhanced MR perfusion study of the proximal femur were asked to return again at the same time the following week for a repeat MR examination. All subjects had been recruited from local community centers as part of another on-going non-interventional osteoporosis study. The Institutional Clinical Research Ethics Committee approved the study (Appendix) with all subjects providing informed signed consent. All subjects were clinically healthy with no known systemic metastatic disease or disease in the hip region.

MR examinations were performed on a 1.5 T whole-body MR imaging system (Intera NT, Philips). The MR technique and method of analysis were identical to that described in Study 4. A detailed MR protocol was available for reference in the MR suite. To simulate clinical practice as closely as possible, the same technologist did not perform or oversee all examinations. Similarly, the supervising radiologist did not oversee patient positioning, coil positioning etc. The same person did all the data analysis for both the first and second visits. Analysis of all regions in each proximal femur (spectroscopy and perfusion) took approximately one hour to complete.

Statistical Analysis. Prior discussion with a biostatistician indicated that it would not be incorrect to include subjects of different gender and BMD in this study as large differences in the parameters to be measured (fat content and perfusion indices) between these subjects did not exist provided they were around same age group. Random selection of 20 ~ 30 subjects is a usual practice when performing a test-retest study. Test-retest reliability of each paired parameter was assessed

using intra-class correlation coefficient on absolute agreement. An inter-class correlation coefficient (ICC) of >0.8 indicates almost full agreement, 0.6–0.8 substantial agreement, 0.4–0.6 moderate agreement and <0.4 poor agreement. All statistical analyses were done using SPSS 14.0 (SPSS Inc). All statistical tests were two-sided. A p-value <0.05 was considered statistically significant.

RESULTS

All 36 subjects underwent paired MR spectroscopy studies while 29 of the 36 subjects underwent paired perfusion studies. Regarding the seven subjects who did not undergo paired perfusion studies, in four subjects, examination was limited to MR spectroscopy due to marginal impairment of renal function while the remaining three subjects declined contrast injection on the second MR visit. Results for the reproducibility of ^{1}H MR spectroscopy and perfusion indices for paired MR examinations performed at one week interval is shown in Table 1. An example of paired spectra from the same VOI in the femoral neck in a patient is shown in Figure 1. Of 36 subjects who underwent paired spectroscopy examinations, satisfactory paired spectroscopy spectra were obtained from the femoral head in all cases, from the femoral neck in 33 (92%) of 36 cases and from the femoral shaft in 34 (94%) of 36 cases. The reproducibility of ^{1}H MR spectroscopy in all of these areas was high ranging from 0.78 to 0.85 with the highest reproducibility being in the femoral head and the lowest in the femoral neck (Table 1).
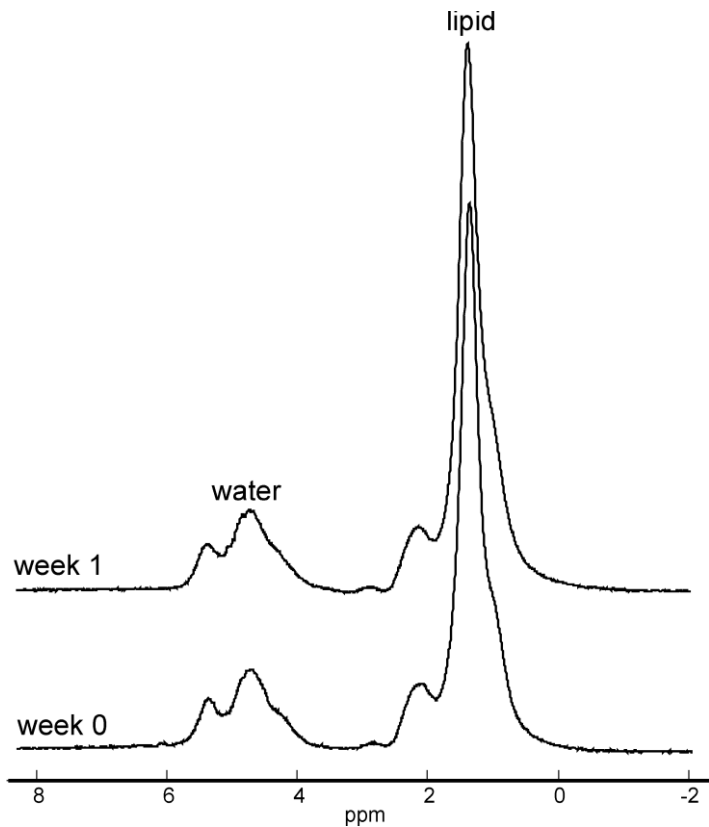
Figure 1. Spectra acquired from femoral neck from same patient at one week interval showing good reproducibility. Marrow fat content measured at week 0 was 83.1% while same measurement was 82.8% one week later.

Of 29 subjects who underwent paired MR perfusion studies, a satisfactory perfusion time-intensity curve was obtained from the acetabulum and the adductor thigh musculature in all cases. Satisfactory paired perfusion curves were obtained from the femoral head in 20 (69%) of the 29 subjects, from the femoral neck in 25 (86%) subjects and from the femoral shaft in 24 (83%) subjects. An example of paired perfusion time-series data obtained at one week interval from the same ROI drawn in the femoral neck is shown in Figure 2. The reproducibility of paired perfusion measurements was more variable than those of spectroscopy ranging from 0.59 (E_{slope} in femoral head) to 0.98 (E_{max} in acetabulum) (Table 1).
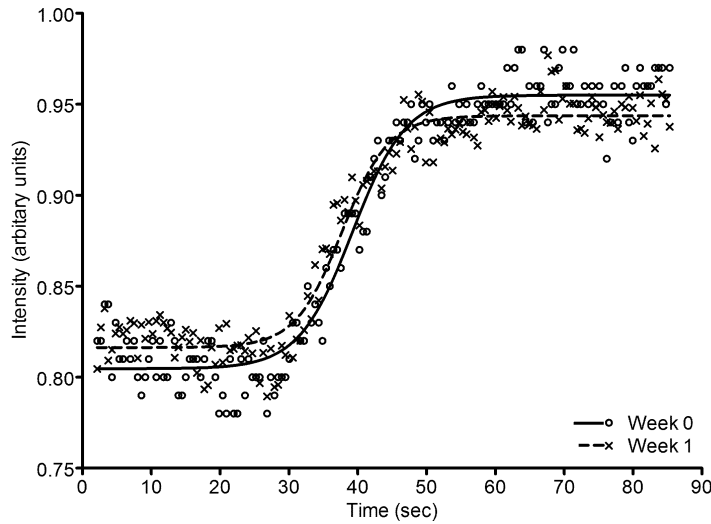
Figure 2. Time-intensity curves from femoral neck of same subject at one week interval showing fairly good reproducibility. At week 0, maximum enhancement and enhancement slope were 19.9% and 0.84 %/sec respectively; while at week 1, these same measurements were 17.3% and 0.88 %/sec respectively.

Table 1: Reproducibility of MR-based parameters at different locations

Location	N	Mean (standard deviation)		Interclass correlation (95% confidence intervals)
		1st test	2nd test	
Fat content (%)				
Femoral head	36	89.39 (3.10)	89.43 (3.71)	0.85 (0.73, 0.92)
Femoral neck	33	86.01 (5.34)	85.37 (6.33)	0.78 (0.60, 0.88)
Femoral shaft	34	83.47 (7.89)	82.64 (9.26)	0.83 (0.69, 0.91)
Enhancement max (%)				
Femoral head	20	3.09 (1.17)	2.89 (1.07)	0.77 (0.52, 0.90)
Femoral neck	25	10.12 (6.84)	9.53 (6.42)	0.94 (0.87, 0.97)
Femoral shaft	24	11.31 (7.55)	12.64 (7.40)	0.77 (0.54, 0.89)
Acetabulum	29	17.00 (10.24)	16.68 (9.73)	0.98 (0.95, 0.99)
Adductor muscle	29	54.48 (25.30)	51.46 (29.26)	0.84 (0.69, 0.93)
Enhancement slope (%/sec)				
Femoral head	20	0.10 (0.07)	0.10 (0.06)	0.59 (0.22, 0.81)
Femoral neck	25	0.39 (0.32)	0.39 (0.34)	0.90 (0.79, 0.96)
Femoral shaft	24	0.44 (0.35)	0.46 (0.31)	0.82 (0.62, 0.92)
Acetabulum	29	0.84 (0.48)	0.78 (0.47)	0.87 (0.75, 0.94)
Adductor muscle	29	1.93 (1.73)	1.86 (1.85)	0.92 (0.84, 0.96)

Table 1. Reproducibility of paired MR spectroscopy and perfusion indices of proximal femur. N = number of successful paired spectroscopy or perfusion studies who underwent repeat MR examination at one week.

SIGNIFICANCE OF THESE FINDINGS

This is the first study to examine the reproducibility of bone marrow MR spectroscopy and perfusion imaging. We choose to study the proximal femur rather than the vertebral body as inherent segmental variability in perfusion and fat content along the proximal femur (Study 4) was likely to yield a more rigorous assessment of test reproducibility.

Functional MR imaging, particularly when assessing perfusion of discrete areas, such as a bone segment, differs from standard post-contrast MR imaging in that particular care must be exercised to ensure uniformity of positioning and examination technique, contrast agent injection rate, dosage and timing of image acquisition. The protocol should be clear, precise and detailed, and the examination and analysis carried out by experienced personnel familiar with the examination protocol. Failure to obtain uniformity in examination and analysis will undermine data reproducibility. In addition, optimal shimming at different anatomical locations may be difficult to achieve. To ensure good reproducibility care must be taken to ensure that both the vertical or lateral positioning of the volume, distance to other structures such as large blood vessels and air spaces, and shim settings must be carefully controlled.

This study shows that the overall reproducibility of MR perfusion and single voxel spectroscopy of proximal femur bone marrow is high though, as expected, tends to be dependent on the fat content or perfusion of the bone area being assessed. For example, the success rate and reproducibility of MR spectroscopy was greatest in the femoral head where the fat content is higher than the femoral neck or shaft. Similarly, perfusion indices were most reproducible for the acetabulum which has the

highest perfusion indices and least reproducible in the femoral head which has the lowest perfusion indices.

Limitations of this study:

- Only two perfusion parameters were evaluated namely maximum enhancement (E^{max}) and enhancement slope (E^{slope}). These are the two most commonly applied parameters. Other more in depth two compartmental pharmokinetic models (Brix and Toft) are available though these have not been commonly used and have not been evaluated for the bone marrow perfusion.

- Study was performed at 1.5T. The results are likely to be improved at 3T.

Conclusion. The test reproducibility of MR spectroscopic and perfusion studies of bone is high though is dependent on the fat content or perfusion of the area being measured. Overall the reproducibility of these techniques is sufficiently high to indicate that MR proton spectroscopy or perfusion imaging can be applied longitudinally to evaluate either the longitudinal relationship or effect of therapeutic intervention between bone disease and marrow fat content or perfusion.

Next phase of study. Study 1, 2 and 4 showed that marrow fat fraction is increased in osteoporosis. Does marrow fat composition also change? This is relevant since certain long-chain polyunsaturated fats in the diet have been shown to be associated with reduced BMD while in culture long-chain polyunsaturated fatty acids have been shown to affect bone formation. This forms the basis of Study 6.

Marrow fat content increases but does the composition of marrow fat change in osteoporosis?

Aim: To investigate (a) whether bone marrow fat composition is altered in subjects of varying BMD; (b) whether regional differences in marrow fat composition exist and (c) whether differences in composition exist between marrow and subcutaneous fat.

Relevance of this study:

We have shown in Study 1, Study 2 and Study 4 how marrow fat is increased in subjects with low bone mass and osteoporosis. This accumulation of marrow fat may simply represent a passive process with fat occupying space vacated by trabecular bone or it may be indicative of a more active process with marrow fat actively accumulating at the expense of bone centered on a change in stromal cell differentiation from an osteoblastic to an adipocytic pathway (Duque G et al. 2008). This has lead to the suggestion that osteoporosis may be a type of lypotoxic disease with osteoporosis being the 'obesity of bone' (Duque G et al. 2008, Rosen CJ et al. 2006).

Marrow fat content increases as BMD decreases but does the composition of marrow fat remain the same or does marrow fatty acid composition also change? This question is relevant given that fatty acids have been shown to influence bone metabolism in vitro (Coetzee M et al. 2007, Poulsen RC et al. 2008, Maurin AC et al. 2002, Musacchio E et al. 2007, Coetzee M et al. 2007) while animal studies (Poulsen RC et al. 2006, Poulsen RC et al. 2007, Watkins BA et al. 2000, Reinwald

S et al. 2004) and data in humans from NHANES (Corwin RL et al. 2006) indicate that dietary fatty acid composition may affect BMD. Marrow fat is a major component of trabecular bone microenvironment. It is conceivable that changes in marrow fat composition over and above increases in the amount of marrow fat could affect bone metabolism and contribute to the development of osteoporosis. No previous studies have investigated the relationship between marrow fatty acid composition and BMD. To address this issue, we analyzed the fatty acid composition of bone marrow and subcutaneous tissue samples from subjects undergoing orthopedic surgery and related fatty acid composition to BMD.

STUDY 6

↓

Does the composition of marrow fat change in osteoporosis?

↓

126 healthy subjects (98 females 34 males, 69.7 ± 10.5 years)

- Marrow and subcutaneous fat samples obtained from each patient at time of orthopedic surgery.
- DXA examination lumbar spine and right hip within one week of sample collection.
- Composition of marrow and subcutaneous fat samples analyzed by gas chromatography.

↓

MAIN FINDINGS

- 22 fatty acids identified in marrow and subcutaneous fat.
- Significant differences in marrow fat composition found between marrow and subcutaneous fat as well as between marrow fat obtained from proximal femur and proximal tibia.
- Other than minor differences likely to be inconsequential, no difference in marrow fatty acid composition was evident between subject groups of varying BMD (normal, low bone mass, and osteoporosis).

ABSTRACT:

Purpose: To investigate the fatty acid composition in subjects of varying bone mineral density (BMD).

Methods: Samples of marrow fat and subcutaneous fat from 126 subjects (98 females, 34 males, mean age 69.7 ± 10.5 years) undergoing orthopedic surgery were analyzed for fatty acid composition using gas chromatography. These results were correlated with BMD assessed by DXA.

Findings: A total of 22 fatty acids were identified in marrow and subcutaneous fat. Significant differences in fatty acid composition existed between marrow and subcutaneous fat as well as between marrow fat samples obtained from the proximal femur and proximal tibia. Other than cis-7-hexadecenoic acid [C16:1 (n=9)] and docosanoic acid [C22:0], no difference in marrow fatty acid composition was evident between subject groups of varying BMD (normal, low bone mass, and osteoporosis).

Conclusion: There exists a wide range of individual fatty acids in marrow fat. Marrow fatty acid composition differs from that of subcutaneous fat and varies between predominantly erythropoetic and fatty marrow sites. Other than cis-7-hexadecenoic acid [C16:1 (n=9)] and docosanoic acid [C22:0], no difference in marrow fatty acid composition was evident between subjects of varying BMD

STUDY DETAIL:

MATERIALS AND METHODS

Subjects. Bone marrow and subcutaneous fat of 126 subjects (94 females, 32 males, mean age 69.7 ± 10.5 years) of Chinese descent were extracted while undergoing elective orthopedic surgery (comprising Austin-Moore hemiarthroplasty n= 32; total hip arthroplasty n=6; total knee arthroplasty n=80; transforaminal lumbar interbody fusion n=5 and posterior spinal fusion n=3). Subject demographics including age, BMD and T-score are shown in Table 1. Informed signed consent was obtained from each patient to participate in this study prior to surgery. The study protocol and patient consent forms were approved by the Ethics Committee, Chinese University of Hong Kong.

**TABLE 1: Demographic and descriptive statistics for male and female subjects**

Demographic data			Overall	Male	Female
Number of subject			126	32	94
Average age (years)			69.7±10.5	68.4±11.1	70.2±10.3
Spine	BMD (g/cm^2)		0.89±0.20	1.00±0.19	0.85±0.19
	T-score		-0.82±1.54	0.05±1.19	-1.15±1.53
	Cohorts	Normal	48	20	28
		Low bone mass	29	5	24
		Osteoporosis	14	0	14
Femoral Neck	BMD (g/cm^2)		0.65±0.15	0.71±0.17	0.63±0.14
	T-score		-2.09±1.42	-1.64±1.04	-2.25±1.50
	Cohorts	Normal	25	9	16
		Low bone mass	46	15	31
		Osteoporosis	49	7	42

Table 1. Subject age, BMD and T-score data of all subjects (overall, male and female subjects) as well as different bone density cohorts (normal, low bone mass and osteoporosis)

Collection of bone marrow and subcutaneous fat samples. Marrow fat samples were obtained immediately after the bone was transected and prior to cleansing or instrumentation. A small quantity of marrow fat (3-5 ml) was extracted from the transected bone and transferred to a sterile glass bottle containing no saline, preservatives or other solution. For operations around the hip or knee, the marrow fat sample was obtained from the diaphyseal end of the transected femur or tibia respectively (Figure 1). During the same operation, a small quantity (approximately 2cm^3) of subcutaneous fat was removed from the site of surgical incision prior to cleansing and transferred to a separate sterile dry glass bottle (Figure 2). The marrow fat sample was stored in a freezer at -80°C while the subcutaneous fat was stored at -20°C until both samples were sent to the Chemistry Department for gas chromatography analysis within one week of collection.
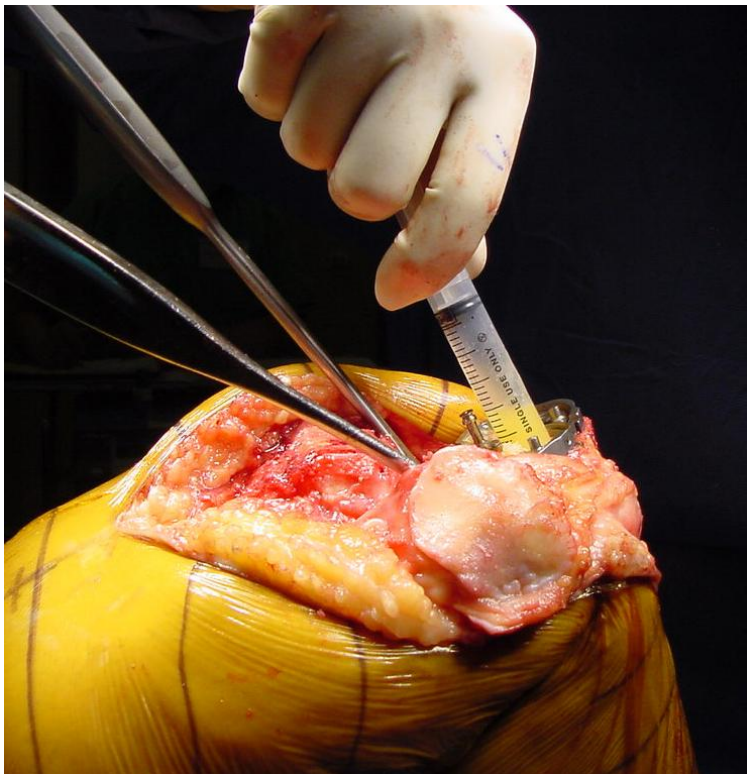

Figure 1. Aspiration of marrow fat from proximal tibia during knee replacement.
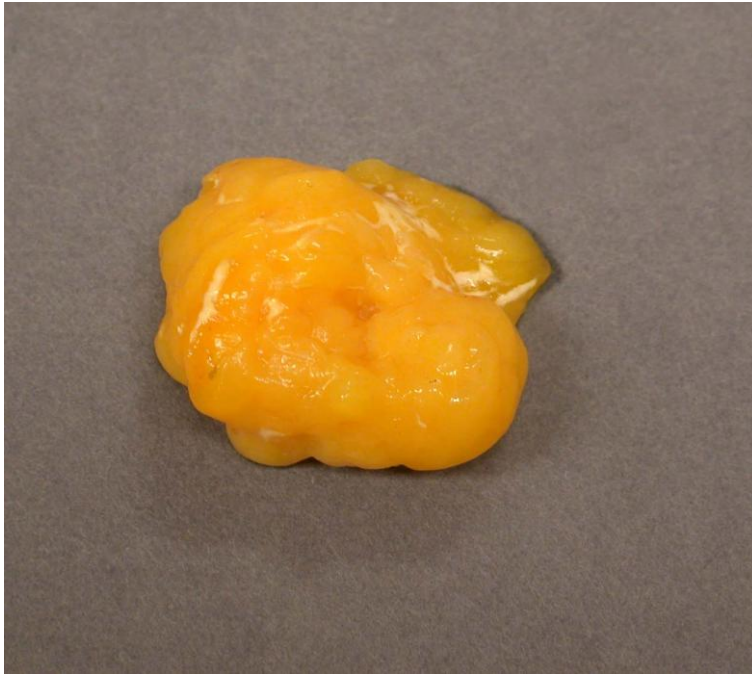
Figure 2. Sample of subcutaneous fat removed from hip region during total hip replacement.

Gas chromatography analysis of fatty acids. Total lipids derived from human bone marrow and subcutaneous fat were first extracted in chloroform-methanol (2:1 vol/vol) containing heptadecanoic acid (C17:0) as an internal standard for fatty acid quantification. The fatty acids in extracted lipids were then converted to the corresponding methyl esters with 14% boron trifluoride in methanol and toluene (2:1 vol/vol) under nitrogen gas at 90°C for 60 min. The fatty acid methyl esters were analyzed on a flexible silica capillary column (Innowax 19091N-213, 30m × 0.32mm internal diameter; J&W Scientific, Folsom, CA, USA) in a Shimadzu gas–liquid chromatograph equipped with a flame-ionization detector (GC 2010, Shimadzu, Kyoto, Japan). Column temperature was programmed from 150°C to 200°C at a rate of 15°C/min, then from 200°C to 250°C at a rate of 2°C/min and then held for 5 min. Injector and detector temperatures were set at 220°C and 270°C, respectively. The carrier gas used was helium at a head pressure of 15 psi. Each fatty acid methyl ester was quantitatively calculated on the basis of the proportion in each chromatogram of the internal standard added to each sample (Figure 3). Fatty acid

composition was defined as the relative fraction of each type of fatty acid as a percentage of the total fatty acid composition.
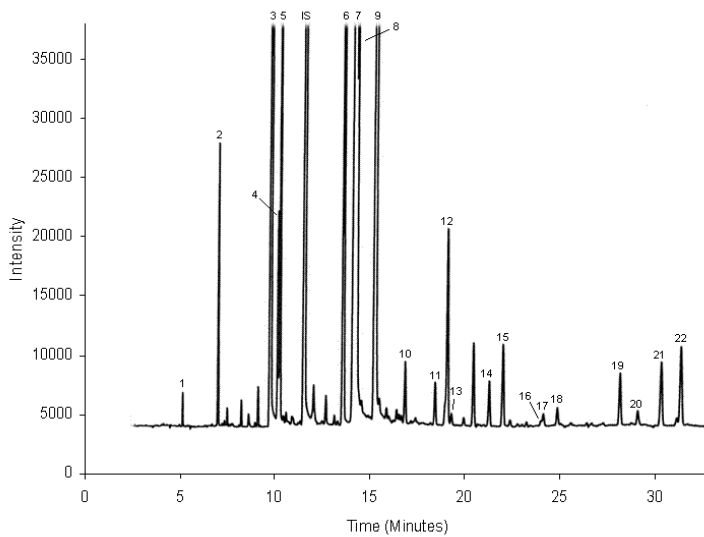
Figure 3. Gas chromatography spectrum of marrow fat. Each fatty acid methyl ester is quantified based on peak high relative to internal standard.

DXA examination. Dual energy x-ray absorpiometry (DXA) of the lumbar spine (L2-L4) and right hip (or left hip if patients had operation in right hip/knee) was performed on all subjects using the same DXA system (Norland XR-46). Left hip was examined if operation had been performed on the right side. DXA was performed 4-5 days post-operation in subjects following hip or knee arthroplasty and 6-7 days post-operation for all other patients. For spinal surgery patients or those with a recognizable fracture on DXA, only femoral neck BMD was analyzed. Based on the lowest score either from the lumbar spine or the femoral neck, and using local reference data, each patient was assigned a T-score (Lynn HS et al. 2005). Subjects were grouped into three categories with normal bone mineral density defined as a T-score greater than -1.0, low bone mass as a T-score between -1.0 and -2.5, and osteoporosis as a T-score less than -2.5.

Figure 4. DXA examination of right hip being performed. If right hip had been operated upon, contralateral hip was examined as well as lumbar spine.

Statistical analysis. Paired T-test was used to test for differences in fatty acid composition between subcutaneous and marrow fat. Independent T-test was used to test for gender and regional differences in marrow fatty acid composition. Analysis of variance (ANOVA) was used to compare values in fatty acid composition across different bone density groups (normal, low bone mass, and osteoporosis). Pearson correlation was used to determine correlation between marrow fatty acid composition, individual fatty acid composition and bone mineral density. All statistical analysis was performed using the statistical package for social sciences (Version 13) (SPSS Inc., Chicago, Illinois 60606, USA), and the level of statistical significance was set at $p < 0.05$.

RESULTS

Marrow fatty acid composition. Bone marrow fatty acid composition for the whole cohort is shown in Table 2. Marrow fat was composed of 29% saturated fat, 51% monounsaturated fats and 20% polyunsaturated fats. A total of 22 individual fatty acids were identified in marrow fat (Table 2 and Appendix). The three most abundant fatty acids in human bone marrow were oleic acid [C18:1 (n-9)], palmitic acid [C16:0]

and linoleic acid [C18:2 (n-6)], which accounted for 44%, 23% and 18% of the total marrow fatty acids respectively. When gender differences were analyzed, marrow fat in males contained significantly higher eicosanoic acid [C20:0] (0.16±0.06% vs 0.12±0.07%, p=0.011) and significantly higher cis-11-eicosenoic acid [C20:1(n-9)] (0.79±0.19% vs. 0.67±0.20%, p=0.004) content compared to females. For the remaining fatty acids, no significant gender difference in marrow fat content was apparent.

No correlation was found between age and marrow fatty acid composition (p>0.05). Similarly the relative amount of n-3, n-6, monounsaturated fatty acids, or saturated fatty acids present in marrow fat remained unchanged with age (p>0.05).

Subcutaneous fatty acid composition. Subcutaneous fatty acid composition for the whole cohort is shown in Table 2. Subcutaneous fat was comprised of 23% saturated fats, 58% monounsaturated fats and 19% polyunsaturated fats. Similar to marrow fat, a total of 22 individual fatty acids were identified in subcutaneous fat (Table 2 and Appendix). Also similar to marrow fat, the most abundant fatty acids in human subcutaneous fat were oleic acid [C18:1 (n-9)], palmitic acid [C16:0] and linoleic acid [C18:2 (n-6)] which accounted for 47%, 19% and 17% of the total subcutaneous fatty acid respectively (Table 2 and Appendix). When gender differences were analyzed, subcutaneous fat in males contained a significantly higher amount of tetradecanoic acid [C14:0] (1.40±0.48% vs. 1.20±0.34%, p=0.037), significantly lower amount of cis-7-hexadecenoic acid [C16:1(n-9)] (0.74±0.16% vs. 0.84±0.16%, p=0.004), significantly higher amount of cis-11-eicosenoic acid [C20:1(n-9)] (0.76±0.13% vs. 0.67±0.16%, p=0.006), significantly lower amount of

all-cis-5,8,11-eicosatrienoic acid [C20:3(n-9)] (0.17±0.08% vs. 0.24±0.11%, p=0.000) compared to females. For the remaining fatty acids, no significant gender difference in subcutaneous fat content was apparent.

No correlation was found between age and subcutaneous fatty acid composition (p>0.05). Similarly the relative amount of n-3, n-6, monounsaturated fatty acids, or saturated fatty acids present in subcutaneous fat remained unchanged with age (p>0.05).

Differences between marrow and subcutaneous fatty acid composition. No difference in either the polyunsaturated fat content or the n-6/n-3 ratio between marrow fat and subcutaneous fat was apparent (Table 2). However, the amount of monounsaturated fat content was significantly (p<0.01) lower and saturated fat content significantly higher (p<0.01) in marrow fat than subcutaneous fat (Table 2). This difference was reflected by a significant difference in the amount of many fatty acids between marrow and subcutaneous fat (Table 2).

Differences in marrow fatty acid composition from proximal femur and proximal tibia. Marrow fat obtained from the proximal femur had a higher saturated fat content (p<0.01) than marrow obtained from the proximal tibia (Table 3). The polyunsaturated fat content and the n-6/n-3 ratio were similar in specimens obtained from the proximal femur and proximal tibia (Table 3). Significant differences in ten of the 22 fatty acids were apparent in samples taken from the proximal femur and proximal tibia (Table 3).

Marrow fatty acid composition in relation to BMD. The relative content of saturated fats, monounsaturated fats and polyunsaturated fats as well as n-6/n-3 ratio was comparable across all three bone density subgroups (normal, low bone mass, and osteoporosis) (Table 4). Neither n-3 or n-6 fatty acid group content or n-6/n-3 ratio showed significant variation across the three bone density groups. No significant correlation was found between marrow fatty acid composition and BMD ($p > 0.05$). Regarding the relationship between individual fatty acids content and BMD, the content of all fatty acids, except for cis-7-hexadecenoic acid [C16:1 (n-9)] and docosanoic acid [C22:0], was similar in subjects with normal bone density, low bone mass and osteoporosis (Table 4). The marrow fat content of cis-7-hexadecenoic acid [C16:1 (n-9)] was significantly less in osteoporotic subjects compared to low bone mass subjects ($p<0.01$) and normal subjects ($p<0.05$), while docosanoic acid [C22:0] was significantly lower ($p<0.05$) in osteopenic subjects compared to osteoporotic subjects (Table 4). There was a weak correlation between decreasing cis-7-hexadecenoic acid [C16:1 (n-9)] and decreasing BMD ($r = 0.24$, $p= 0.01$). However, no correlation between marrow fatty acid composition and BMD was present for all the other fatty acids ($p > 0.05$). These results were unchanged when separate analysis were performed on samples obtained solely from the proximal femur (n=38) and the proximal tibia (n = 80) or when separate analysis were performed for male and female gender. Similarly, when BMD of the proximal femur was compared with marrow obtained only from the proximal femur (n=38), no difference in marrow fatty acid composition between normal (n=4), low bone mass (n=7) or osteoporotic (n=28) subjects was apparent. Mean subject age for the three BMD groups was significantly different (normal: 61.6 years; low bone mass: 67.6 years; osteoporosis: 75.9 years; $p<0.05$).

Table 2. Total fatty acid composition (mean ± SD) of marrow fat and subcutaneous fat for 123 subjects [†]

Major fatty acid groups	Fatty acid composition (%)	
	Marrow	Subcutaneous
n-3	1.33 ± 0.47	1.36 ± 0.60
n-6	18.69 ± 3.83	18.06 ± 4.41
Monounsaturated fatty acid	50.82 ± 3.23 **	57.74 ± 4.25 **
Saturated fatty acid	29.02 ± 4.19 **	22.62 ± 4.01 **
n-3/n-6 (ratio)	15.58 ± 5.68	15.42 ± 6.18
Individual fatty acids		
C12:0	0.14 ± 0.11	0.13 ± 0.10
C14:0	1.09 ± 0.31 **	1.22 ± 0.35 **
C16:0	22.53 ± 2.70 **	18.62 ± 2.96 **
C16:1(n-9)	0.85 ± 0.15	0.83 ± 0.15
C16:1(n-7)	2.62 ± 0.80 **	6.36 ± 2.07 **
C18:0	5.10 ± 1.85 **	2.54 ± 1.08 **
C18:1(n-9)	44.33 ± 3.04 **	46.98 ± 2.79 **
C18:1(n-7)	2.18 ± 0.39 **	2.75 ± 0.56 **
C18:2(n-6)	18.18 ± 3.81*	17.38 ± 4.33*
C18:3(n-3)	0.74 ± 0.27 **	0.80 ± 0.31 **
C20:0	0.12 ± 0.05 **	0.09 ± 0.06 **
C20:1(n-9)	0.70 ± 0.19	0.69 ± 0.15
C20:1(n-7)	0.08 ± 0.05	0.09 ± 0.04
C20:3(n-9)	0.15 ± 0.08 **	0.23 ± 0.11 **
C20:4(n-6)	0.25 ± 0.27 *	0.37 ± 0.19 *
C20:5(n-3)	0.04 ± 0.04 **	0.07 ± 0.05 **
C22:0	0.04 ± 0.05 **	0.02 ± 0.02 **
C22:1(n-9)	0.07 ± 0.04 **	0.04 ± 0.03 **
C22:4(n-6)	0.15 ± 0.06	0.15 ± 0.08
C22:5(n-6)	0.11 ± 0.09 **	0.16 ± 0.12 **
C22:5(n-3)	0.27 ± 0.12 **	0.22 ± 0.13 **
C22:6(n-3)	0.29 ± 0.19	0.28 ± 0.23

. * $p<0.05$ and ** $p<0.01$ represent significant differences in fatty acid composition between marrow fat and subcutaneous fat. [†]Data from 123 subjects rather than 126 subjects included as three subjects did not have subcutaneous fat samples removed at the time of surgery.

Table 3. Comparison of the fatty acid composition (mean ± SD) between marrow fat obtained from proximal femur and proximal tibia

	Fatty acid composition (%)	
	Proximal femur (n=38)	Proximal tibia (n=80)
Major fatty acid groups		
n-3	1.33 ± 0.77	1.41 ± 0.41
n-6	18.45 ± 5.16	19.36 ± 2.95
Monounsaturated fatty acid	49.49 ± 5.53	51.24 ± 2.55
Saturated fatty acid	30.55 ± 5.55 **	27.85 ± 2.28 **
n-6/n-3 (ratio)	16.36 ± 6.94	15.01 ± 5.04
Individual fatty acids (%)		
C12:0	0.16 ± 0.12	0.12 ± 0.10
C14:0	1.06 ± 0.35	1.09 ± 0.28
C16:0	22.87 ± 3.49	22.11 ± 1.82
C16:1(n-9)	0.71 ± 0.12 **	0.92 ± 0.14 **
C16:1(n-7)	2.62 ± 0.98	2.55 ± 0.68
C18:0	6.23 ± 2.54 **	4.41 ± 0.64 **
C18:1(n-9)	42.91 ± 4.93 *	44.93 ± 2.36 *
C18:1(n-7)	2.33 ± 0.35 **	2.06 ± 0.34 **
C18:2(n-6)	17.66 ± 4.61	18.93 ± 2.95
C18:3(n-3)	0.63 ± 0.32 **	0.81 ± 0.21 **
C20:0	0.16 ± 0.05 **	0.10 ± 0.04 **
C20:1(n-9)	0.76 ± 0.21 **	0.65 ± 0.17 **
C20:1(n-7)	0.08 ± 0.04	0.07 ± 0.06
C20:3(n-9)	0.18 ± 0.15	0.14 ± 0.05
C20:4(n-6)	0.48 ± 1.01	0.20 ± 0.07
C20:5(n-3)	0.05 ± 0.10	0.04 ± 0.03
C22:0	0.07 ± 0.08 **	0.02 ± 0.01 **
C22:1(n-9)	0.09 ± 0.05 **	0.05 ± 0.02 **
C22:4(n-6)	0.16 ± 0.10	0.16 ± 0.04
C22:5(n-6)	0.14 ± 0.10 **	0.08 ± 0.06 **
C22:5(n-3)	0.26 ± 0.14	0.27 ± 0.10
C22:6(n-3)	0.39 ± 0.50	0.29 ± 0.16

* $p < 0.05$ and ** $p < 0.01$ represent significant differences in fatty acid composition proximal tibia and proximal femur.

Table 4. Fatty acid composition (mean ± SD) and individual fatty acid content of marrow fat in 126 subjects segregated according to BMD group

	Fatty acid composition (%)		
	Normal (n=28)	Low bone mass (n=46)	Osteoporosis (n= 52)
Major fatty acid groups			
n-3	1.36 ± 0.50	1.32 ± 0.50	1.37 ± 0.64
n-6	18.36 ± 3.64	18.79 ± 3.93	18.84 ± 4.59
Monounsaturated fatty acid	51.03 ± 2.63	50.92 ± 2.77	50.30 ± 4.97
Saturated fatty acid	29.09 ± 3.24	28.83 ± 3.28	29.32 ± 5.21
n-6/n-3 (ratio)	14.68 ± 3.95	16.06 ± 5.83	15.46 ± 6.24
Individual fatty acids (%)			
C12:0	0.14 ± 0.10	0.13 ± 0.11	0.14 ± 0.10
C14:0	1.07 ± 0.33	1.11 ± 0.33	1.06 ± 0.29
C16:0	22.58 ± 2.11	22.63 ± 2.45	22.44 ± 3.11
C16:1(n-9)	0.87 ± 0.16 ^	0.90 ± 0.16 **	0.78 ± 0.15 ^ **
C16:1(n-7)	2.72 ± 0.92	2.37 ± 0.56	2.72 ± 0.88
C18:0	5.13 ± 1.57	4.82 ± 0.97	5.49 ± 2.50
C18:1(n-9)	44.35 ± 2.53	44.74 ± 2.64	43.71 ± 4.48
C18:1(n-7)	2.22 ± 0.43	2.09 ± 0.37	2.22 ± 0.37
C18:2(n-6)	17.77 ± 3.54	18.37 ± 3.92	18.20 ± 4.23
C18:3(n-3)	0.72 ± 0.23	0.75 ± 0.26	0.71 ± 0.31
C20:0	0.14 ± 0.06	0.11 ± 0.04	0.13 ± 0.06
C20:1(n-9)	0.72 ± 0.21	0.68 ± 0.18	0.71 ± 0.22
C20:1(n-7)	0.08 ± 0.04	0.07 ± 0.04	0.08 ± 0.07
C20:3(n-9)	0.16 ± 0.11	0.13 ± 0.05	0.17 ± 0.11
C20:4(n-6)	0.32 ± 0.47	0.19 ± 0.10	0.37 ± 0.82
C20:5(n-3)	0.05 ± 0.06	0.04 ± 0.03	0.05 ± 0.07
C22:0	0.05 ± 0.04	0.03 ± 0.02 *	0.06 ± 0.08 *
C22:1(n-9)	0.08 ± 0.05	0.06 ± 0.02	0.07 ± 0.05
C22:4(n-6)	0.17 ± 0.06	0.14 ± 0.05	0.16 ± 0.08
C22:5(n-6)	0.11 ± 0.10	0.10 ± 0.09	0.12 ± 0.10
C22:5(n-3)	0.26 ± 0.11	0.26 ± 0.13	0.27 ± 0.12
C22:6(n-3)	0.32 ± 0.24	0.28 ± 0.18	0.35 ± 0.41

* $p < 0.05$ represent significant difference between low bone mass and osteoporosis group (22:0 Behenic acid); ** $p < 0.01$ represent significant difference between low bone mass and osteoporosis group (age, 16:1(n-9) (cis-7-hexadecenoic acid)); ^ $p < 0.05$ represent significant difference between normal and osteoporosis group (16:1(n-9) cis-7-hexadecenoic acid).

SIGNIFICANCE OF THESE RESULTS

This is the first study to investigate the relationship between marrow fatty acid composition and bone mineral density. Previous studies have shown how an increase in certain fats, in particular long chain polyunsaturated fatty acids, or a change in the n-6/n-3 ratio, can affect bone formation or resorption influencing bone density and strength. For example, long chain n-6 fatty acids such as arachidonic acid and its metabolite prostaglandin PGE2 are pro-inflammatory with PGE_2 being a potent stimulator of RANKL expression. This can reduce the OPG/ RANKL ratio and may increase osteoclastogenesis (Coetzee M et al. 2007). On the other hand, long chain n-3 fatty acids such as eicosapentaenoic acid, docosahexaenoic acid and γ-linolenic have anti-inflammatory activity and may inhibit this PGE2-stimulated increase in RANKL expression [Poulsen RC et al. 2008]. Animal studies have shown how a diet enriched with γ-linolenic acid and high-dose eicosapentaenoic acid can exacerbate the effects of ovariectomy on BMD and how these effects can be attenuated by docosahexaenoic acid fatty acid [Poulsen RC et al. 2006, Poulsen RC et al 2007]. Rats fed a low n-6/n-3 ratio diet for 42 days showed a reduced level of bone PGE2 and increased bone formation markers (Watkins BA et al. 2000) while rats fed a diet high in n-3 fatty acids for 28 days reversed prior defects in bone remodeling (Reinwald S et al. 2004).

In humans, cross-sectional studies have shown that diets high in polyunsaturated fats have a positive effect on bone (Corwin RL et al. 2006, Weiss LA et al. 2005). Kruger et al showed how women eating a diet rich in n-3 maintained or increased BMD as opposed to women on normal diet who lost BMD (Kruger MC et al, 1998). On the other hand, Bassey et al failed to show any effect on BMD in post-

menopausal women randomized to either an n-3 rich diet or placebo (Bassey EJ et al. 2000).

Trabecular bone is the most metabolically responsive component of bone. As marrow fat constitutes the main microenvironment of trabecular bone, changes in marrow fat may well influence trabecular bone metabolism. Only a few studies have analyzed the fatty acid composition of human bone marrow. Lund et al identified seven fatty acids in marrow from the femora of 12 patients post-mortem (Lund PK et al.). Yeung et al has reported on the fatty acid composition of twelve cadaver bone samples analyzed by both high resolution proton magnetic resonance spectroscopy and gas chromatography (Yeung DK et al. 2008). Whilst the current study provides a more detailed analysis of human marrow fat, the spectrum of marrow fatty acid composition is comparable with these two previous studies.

Marrow and subcutaneous fat was obtained from subjects undergoing orthopedic surgery. A total of 22 fatty acids were identified in marrow and subcutaneous fat. No consistent differences in marrow fatty acid composition for varying BMD were apparent. In particular, the overall polyunsaturated fatty acid content, the n-6/n-3 ratio and the percentage composition of those fatty acids most frequently implicated in bone remodeling, namely docosahexaenoic acid, arachidonic acid, γ-linolenic acid and eicosapentaenoic acid, were unchanged in subjects with normal BMD, low bone mass or osteoporosis.

The failure of this study to find a significant relationship between marrow fatty acid composition and BMD would tend to suggest that marrow fat composition is not likely

to be having a direct effect on bone metabolism. The two associations found between fatty acid composition and BMD are likely to be inconsequential given that they account for <1% (for C16:1(n-9)) and <0.1% (for C22:0) of the total marrow fatty acid composition. Our results do not, however, refute the possibility of an active switch in mesenchymal stem cell differentiation between adiopocytosis and osteoblastogenesis (Duque G et al. 2008, Rosen CJ et al. 2006) since such a switch would only be expected to affect the amount but not the composition of marrow fat.

Several significant differences were apparent in fatty acid composition between marrow fat and subcutaneous fat indicating that subcutaneous fat cannot be reliably used as an indicator of marrow fatty acid composition. Considerable differences were also present in fatty acid composition in samples obtained from the proximal femur and proximal tibia. This is to be expected since proximal femur marrow is likely to contain more erythropoetic i.e. red marrow than the proximal tibial marrow which is predominantly fatty. Whilst marrow fat is derived mainly from fatty marrow, erythropoetic marrow also contains some fat. In rabbits, Tavassoli et al. found that predominantly erythropoetic marrow (from the spine) contained more saturated fatty acids than fat from predominantly fatty marrow (from the calcanei) (Tavassoli M et al. 1977). This is similar to the spectrum of change we have shown in specimens obtained from the proximal femur and proximal tibiae. Nevertheless, separate analyses of samples obtained from the proximal femur or tibia showed no difference in marrow fatty acid composition across the different BMD groups.

The significance of this study for future clinical studies can be appreciated by a recent study which examined subcutaneous and marrow fat at 7T. Ten separate spectra (representing ten separate fatty acids) were identified indicating that, in the

near future, one should be able to obtain reliable data on both the composition as well as the amount of marrow fat.
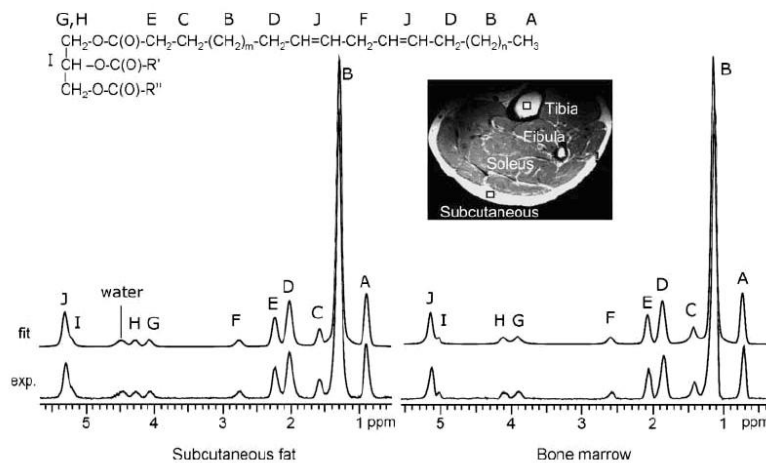
Figure 5: Spectra of subcutaneous fat and marrow fat obtained in vivo at 7T. Water signal is suppressed [from Ren J et al. 2008]. It is increasingly likely that in future more revealing spectra will be obtainable from musculoskeletal tissues in vivo using clinical Mr scanners.

Limitations of this study.

1. BMD was obtained at the lumbar spine or proximal femur, while marrow fat samples were obtained from different regions and we have shown that marrow fatty acid composition can vary from one site to another possibly related to the relative red:fatty marrow content. Nevertheless, the results still held true with no difference in marrow fat content between normal, low bone mass and osteoporotic subjects being apparent when a separate sub-analysis of the proximal femur (BMD and marrow fatty acid composition) was performed.

2. We studied fatty acid composition but did not study the active constituents of these fatty acids. Therefore, in this cohort, it is not known whether fatty acid metabolism changed with BMD or whether there is a change in the fatty acid metabolites with BMD (Watkins BA et al. 2001, Poulsen RC et al. 2007).

3. Due to the small number of spine samples, no reliable comparison between spinal and appendicular marrow could be undertaken. This small number of spine

samples reflects the difficultly in obtaining marrow samples at the time of spine surgery.

Conclusion. Significant differences in fatty acid composition were evident between marrow fat and subcutaneous fat. Significant differences were also evident in marrow fat samples obtained from the proximal femur and proximal tibia. However, no change in marrow fatty acid composition was evident in samples obtained from groups of subjects with different BMD (normal, low bone mass, and osteoporosis).

Next phase of study: We now wished to explore possible reasons behind the reduced perfusion seen in osteoporotic bone. This is the basis of Study 7.

Appendix to study 6.

List of individual fatty acids with common name or abbreviation and systematic name

Fatty acid	Common name	Systematic name
Saturated		
C12:0	Lauric acid	dodecanoic acid
C14:0	Myristic acid	tetradecanoic acid
C16:0	Palmitic acid	hexadecanoic acid
C18:0	Stearic acid	octadecanoic acid
C20:0	Arachidic acid	eicosanoic acid
C22:0	Behenic acid	docosanoic acid
Monounsaturated		
C16:1 (n-9)		*cis*-7-hexadecenoic acid
C16:1 (n-7)	Palmitoleic acid	*cis*-9-hexadecenoic acid
C18:1 (n-9)	Oleic acid	*cis*-9-octadecenoic acid
C18:1 (n-7)	Vaccenic acid	*cis* 11-octadecenoic acid
C20:1 (n-9)	Eicosenoic Acid	*cis*-11-eicosenoic acid
C20:1 (n-7)	Paullinic acid	*cis*-13-eicosenoic acid
C22:1 (n-9)	Erucic acid	*cis*-13-docosenoic acid
Polyunsaturated		
C18:2 (n-6)	Linoleic acid	*cis*, *cis*-9,12-octadecadienoic acid
C18:3 (n-3)	α -Linolenic acid	all-*cis*-9,12,15-octadecatrienoic acid
C20:3 (n-9)	Mead acid	all-cis-5,8,11-eicosatrienoic acid
C20:4 (n-6)	Arachidonic acid	all-*cis*-5,8,11,14-eicosatetraenoic acid
C20:5 (n-3)	EPA	all-*cis*-5,8,11,14,17-eicosapentaenoic acid
C22:4 (n-6)	Adrenic acid	all-cis-7,10,13,16-docosatetraenoic acid
C22:5 (n-6)	Osbond acid	all-*cis*-4,7,10,13,16-docosapentaenoic acid
C22:5 (n-3)	DPA	all-*cis*-7,10,13,16,19-docosapentaenoic acid
C22:6 (n-3)	DHA	all-*cis*-4,7,10,13,16,19-docosahexaenoic acid

Likely causes of reduced bone perfusion in osteoporosis: novel findings in an ovariectomy rat model

Aim: To investigate the cause of reduced vertebral perfusion in a rat ovariectomy (OVX) model.

Rationale for doing this study: Studies 1, 2 & 4 showed how bone perfusion indices are reduced in osteoporotic bone though the cause of this reduction in perfusion indices is not clear. Several potential reasons for decreased bone perfusion in osteoporosis have been proposed such as a reduced requirement due to decreased bone turnover or an effect of increased marrow fat content impeding venous return within the confined marrow cavity. Endothelial function represents another potential link between bone perfusion and reduced bone mineral density (Sanada M et al. 2004) as does a change in marrow content over and above an increase in fat content. The temporal relationship between reduced BMD and reduced perfusion is also unknown i.e. do reduced perfusion indices predate a reduction in bone mineral density or visa versa.

We undertook this longitudinal animal-based study to investigate the cause of reduced bone perfusion in osteoporosis. In particular, we wanted to investigate the temporal relationship between bone perfusion and BMD as well as the relationship with vascular reactivity and marrow content. Bilateral ovariectomy (OVX) in the adult

female rat is a commonly used model for studying the effects of bone loss (Jee WS et al. 2001, Liu XQ et al. 2008, Lelovas PP et al. 2008).

STUDY 7

↓

What causes the reduced vertebral perfusion seen with reduced BMD?

↓

22 Sprague-Dawley rats

↙   ↘

ovariectomy   sham-surgery

(11 rats)   (11 rats)

- Lumbar spine BMD measured by quantitative CT densitometry
- Lumbar spine perfusion measured by dynamic contrast-enhanced MRI
- Endothelial function assessed pharmacologically
- Marrow content assessed histologically

↓

MAIN FINDINGS

- BMD and marrow perfusion ↓ occur in synchrony rather than one predating the other.
Post-OVX state also associated with:

- ↑ endothelial dysfunction (in both aorta and femoral artery)
- ↑ fatty marrow (due to ↑ in marrow fat cell number rather than size)
- ↓ erythropoetic marrow

Overall, ↓ perfusion found with ↓ BMD most likely associated with ↓ in the amount of erythropoetic marrow ± impaired endothelial function rather than any observed effect in marrow fat or bone turnover.

ABSTRACT

Purpose: To investigate the cause of reduced vertebral perfusion in a rat ovariectomy (OVX) model.

Materials and Methods: Twenty two Sprague-Dawley rats were studied. CT bone densitometry and MR perfusion imaging was performed at baseline, two, four and eight weeks post-OVX (n=11) or sham surgery (n=11). Perfusion parameters analyzed were maximum enhancement (E^{max}) and enhancement slope (ES). After euthanasia, the aorta and femoral artery were analyzed for vessel reactivity while the lumbar vertebrae were analyzed for marrow content.

Results: For control rats, BMD, E^{max} and E^{slope} remained constant while in OVX rats, a comparable reduction in both BMD and perfusion parameters at two weeks post-OVX (BMD 9.3%, E^{max} 11.6%, E^{slope} 9%) was seen with a further reduction in these parameters at 4 weeks (BMD 17.5%; E^{max} 15.6%; E^{slope} 33%) and again at 8 weeks (BMD 18.8%; E^{max} 14.2%; E^{slope} 33%) compared to control group. Endothelial dysfunction was observed in both the aorta and femoral artery of OVX group but not control group. Increased marrow fat area occurred in the OVX group (52.9% vs 21.6%, $p<0.01$) due to increase in fat cell number. Decreased erythropoetic marrow (32.5% vs 48.6%, $p <0.05$) was also observed in the OVX group.

Conclusion: Reduced bone perfusion occurs in synchrony with reduced BMD. The most likely causes of reduced bone perfusion are reduction in the amount of erythropoetic marrow and endothelial dysfunction rather than a change in bone turnover or an increase in marrow fat (due to an increase in fat cell number) post-OVX.

STUDY DETAILS:

METHODS

The experimental protocol was approved by the local Animal Experiment Ethics Committee. Twenty-two 6-month-old female Sprague-Dawley rats were used in this study. The animals were housed 2-3 animals per stainless steel cage at 22°C temperature under a 12-hour light, 12-hour dark cycle while receiving a standard rat chow diet and water *ad libitum.* For MRI examination and surgery, rats were anesthetized using a combination of xylazine (10mg/kg) and ketamine (90mg/kg).

CT assessment of vertebral bone mineral density. Rat lumbar vertebral BMD was measured using a clinical multidetector CT scanner (LightSpeed VCT 64, General Electric, USA) employing continuous axial 0.625 mm slice thickness acquisitions. A more detailed description of the methodology we used to obtain small animal BMD from a clinical CT scanner has been reported (Wang et al. 2009) (Figure 1 & 2). The coefficient of variance for BMD assessment was 1.4±0.6%. Lumbar vertebral BMD for each rat was defined as the mean BMD of vertebrae L2-L5. To eliminate any potential effect of retained gadolinium on bone densitometry, CT was performed prior to MR perfusion studies in all cases.
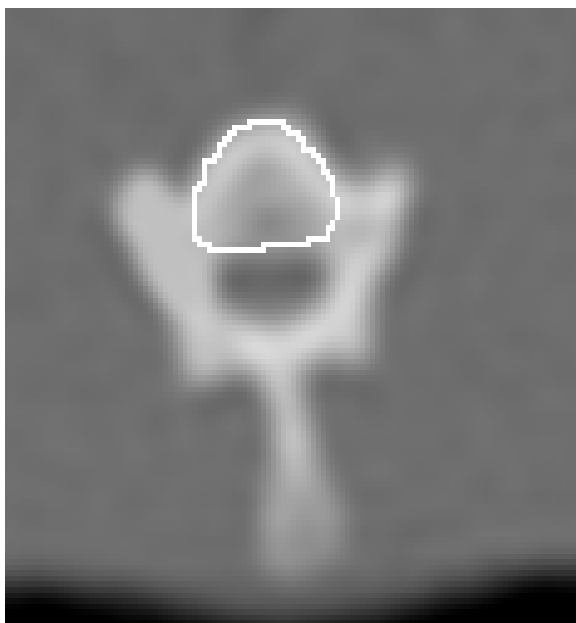
Figure 1. Axial MDCT of L3 vertebral body with 0.625mm thick acquisitions. Quantitative CT of each lumbar vertebral body from L2-L5 was performed and the lumbar spine BMD for that rat defined as the mean BMD of the four vertebral bodies measured.
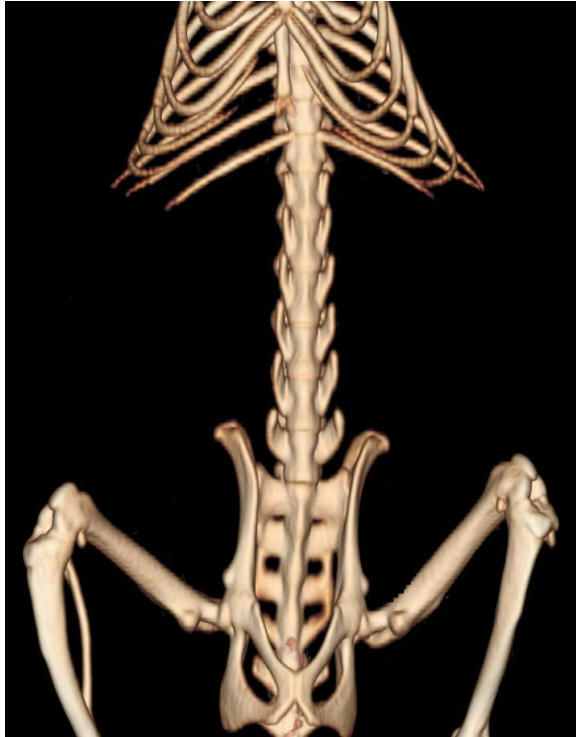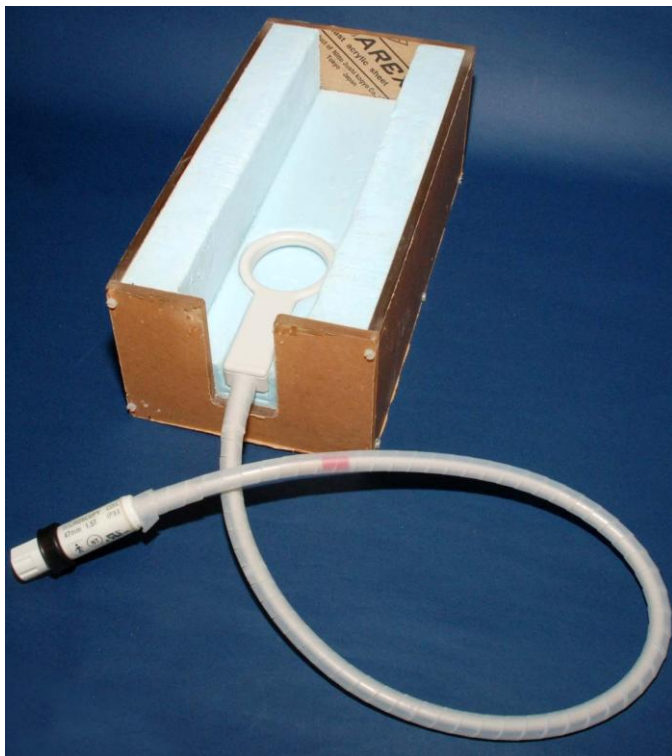
Figure 2. Surface rendering three dimensional reconstruction of rat lower thorax, lumbar spine and pelvis. The rat has got six lumbar vertebrae. Lumbar vertebrae L2-L5 were used to determine lumbar BMD.

MR assessment of vertebral bone perfusion. MRI was performed on a 1.5 Tesla clinical MR imaging system (Intera NT, Philips Medical Systems, Best, The Netherlands) with a maximum gradient strength of 30 mT/m. Rats were anaesthetized, and the tail vein cannulated with a 24G heparinised catheter (Figure 3). The rat was then placed placed in a specially designed cradle (Figure 4). A surface coil with a diameter of 4.7 centimeters (Micro 4.7, Philips Medical Systems, Best, The Netherlands) was placed within this cradle under the rat lumbar spine region as the radiofrequency receiver coil while a body volume coil was used as the radiofrequency transmitter.

**Figure 3**. Cannulation of rat tail vein with 24G heperanised catheter.

Figure 4 Cradle used to hold rat and receiver coil during MR scanning.

Following a coronal scout scan, a mid-sagittal T1-weighted image of the lumbar spine was obtained. A dynamic short T1-weighted gradient echo sequence MR series was obtained in the sagittal plane using the following parameters: TR=4 msec, TE=1.4 msec, flip angle=15, slice thickness=5 mm, matrix = 128×51, in-plane resolution=0.625×0.625 mm, NEX=1. Temporal resolution was approximately 0.6 second/ acquisition. After 60 baseline image acquisitions, a gadolinium-based

contrast agent (Gd-DOTA, Guerbet Group, Roissy CDG cedex, France at a dose of 0.3mmol/kg i.e. 0.15ml for a 250-gram rat) was injected into the tail vein followed by a bolus flush of 0.5ml normal saline. Bolus injection was completed in less than one second. Tail vein cannulation, bolus injection and normal saline flush were carried out by the same operator skilled in small animal procedures. Dynamic MRI took approximately 8 minutes to complete with 800 images being acquired.

Dynamic MRI images were processed on a radiologic workstation (Viewforum, Philips Medical System, Best, The Netherlands). Regions-of-interest (ROIs) was drawn over the cancellous part of the lumbar vertebrae from L2-L5 excluding the vertebral cortex (Figure 5).
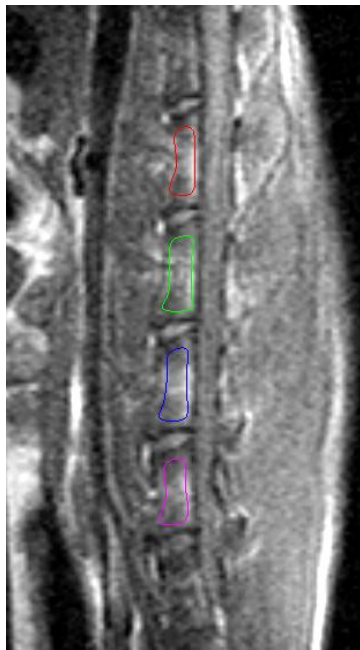
Figure 5. Mid-sagittal T1-weighted image of a rat lumbar spine. Regions-of-interest outlining the meduallary canal and excluding the cortex of the lumbar vertebrae from L2-L5. The rat lumbar spine has six rather than five vertebral bodies.

Signal enhancement over time was recorded, and plotted as a time-signal intensity curve. From this time-signal intensity curve, two MR perfusion indices were analyzed, namely, maximum enhancement (E^{max}) and enhancement slope (E^{slope}), both of them relating to the first rapidly rising part of the curve. Maximum enhancement was defined as the maximum percentage increase of signal intensity from baseline.

Enhancement slope was defined as the rate of enhancement between 10% and 90% of the maximum signal intensity difference between maximum signal intensity (I_{max}) and baseline signal intensity (I_{base}). Thus, these perfusion indexes were calculated as follows (6):

$$E^{max} = [\frac{(I_{max} - I_{base})}{I_{base}}] \cdot 100,$$

$$E^{slope} = [\frac{(I_{max} - I_{base}) \cdot 0.8}{I_{base} \cdot (t_{90\%} - t_{10\%})}] \cdot 100$$

Where I_{base} was defined as the mean signal intensity of the first 50 images, I_{max} was defined as the maximum value of the first rapidly rising part of the time-signal intensity curve, $t_{10\%}$ and $t_{90\%}$ were the time when signal intensity reaches 10% and 90% of the signal intensity difference between I_{base} and I_{max}, respectively. Data from four lumbar vertebrae L1-L4 were measured, and the mean value of these four vertebrae taken as the results for that animal.

Ovariectomy and sham surgery. After baseline CT densitometry and MR examination, 11 rats underwent bilateral ovariectomy (OVX) with surgery being performed through a subcostal incision. Ovaries together with surrounding fat tissue were removed. Successful ovariectomy was confirmed at necropsy through absence of ovarian tissue and atrophy of uterine horns. The remaining 11 rats underwent similar sham surgery with exposure of the ovaries though no excision.
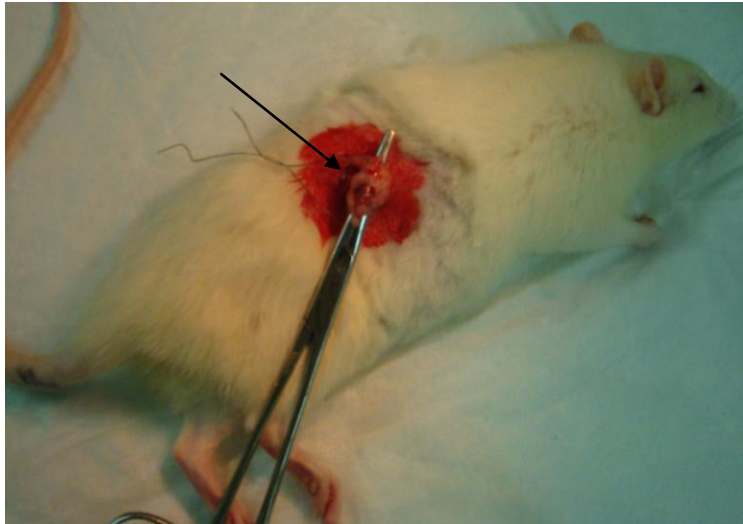
Figure 6. Right ovariectomy performed through subcostal incision. A separate incision was made on the left side for left ovariectomy.

Longitudinal CT and MR assessments of vertebral BMD and perfusion. Repeat CT bone densitometry and measurement of lumbar vertebral perfusion with MRI were performed at two, four and eight weeks following OVX surgery. After CT and MRI examinations at week eight, the animals were sacrificed with cervical dislocation. The abdominal aorta and right femoral artery were harvested fresh to assess vascular reactivity and the lumbar spine vertebrae were harvested for assessment of vertebral marrow content.

Vascular reactivity assessment. For vascular reactivity assessment, the aorta and right femoral artery of each rat were dissected and transferred to ice-cold oxygenated Krebs solution while being stored. Arteries were dissected free of surrounding connective tissues. Two 3 mm wide ring segments were cut from each aorta or femoral artery. The endothelium was removed from one ring by gently rubbing the luminal surface with stainless steel wire. The endothelium was left intact on the other one ring. Each aortic ring was mounted between two stainless steel wire hooks submerged in an organ bath while each femoral ring was mounted in a myograph chamber held between two tungsten wires (40 µm diameter) in a multi-

myograph system. Each arterial ring was kept in Krebs solution (pH 7.2-7.4) at 37 °C with 95% O_2 and 5% CO_2. A resting tension of 2.5g was applied to the aorta and 0.5g to the femoral artery (as determined by length-maximum tension relationship measurements) and one hour allowed for both rings to assume a stable resting tension. To investigate endothelium-dependent relaxation, which is mediated by nitric oxide (NO) from the endothelium, endothelium-intact rings were first contracted using 1μM phenylephrine to establish a stable constricted tone and then acetylcholine was added cumulatively to the bathing solution to induce relaxation. Relaxation was expressed as percentage reduction in arterial contraction. To investigate endothelium-independent relaxation or vascular smooth muscle sensitivity to nitric oxide, endothelium-denuded phenylephrine-constricted rings were relaxed by sodium nitroprusside, a nitric oxide (NO) donor. Phenylephrine-induced contraction was also assessed in both the OVX and control groups, as was the degree to which this was abolished by L-NAME (N(G)-nitro-L- arginine methyl ester) at 100μmol/L. L-NAME, a nitric oxide synthase inhibitor, inhibits the synthesis of NO from L-arginine.
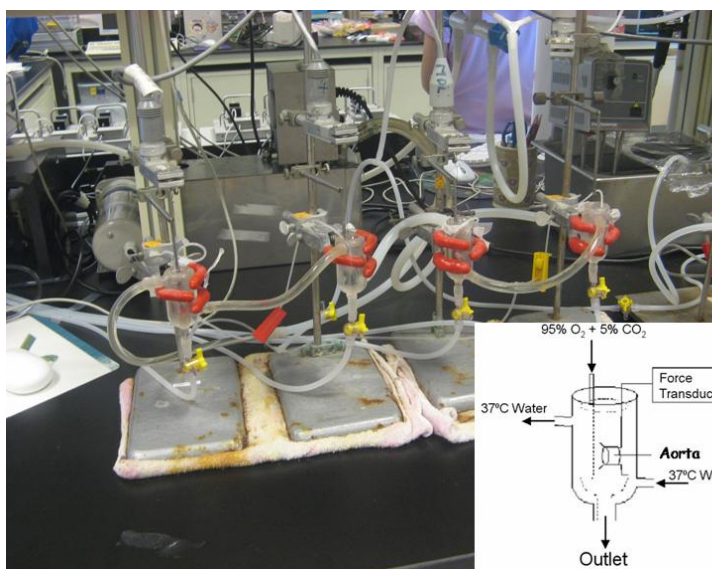
Figure 7. Organ bath setup for measuring isometric forces generated by large arteries such as the rat aorta.

Figure 8. Myograph setup for measuring isometric forces generated by smaller arteries such as the rat femoral artery.

Histological assessment of vertebral marrow cavity. For histology, the excised lumbar spine was fixed with 10% buffered formalin for three days and then decalcified with 10% formic acid for four weeks. All the decalcified samples were embedded in paraffin, and cut into 6mm thick axial sections. Sections were stained with hematoxylin and eosin (H&E). For vertebral marrow fat, trabecular bone and erythropoetic marrow analysis, four vertebral sections from each of the four vertebrae (L2-L5) under a magnification of 200× were randomly selected for evaluation. In other words, a total of 16 sections were analyzed from each rat. Percentage area of marrow fat, trabecular bone and erythropoetic marrow was measured in each histological section using imaging processing software (Image-Pro Plus 5.1, Media Cybernetics Inc., Bethesda, MD, USA). The mean values of all fields measured from each animal were used for statistical analysis.

Statistical analysis. CT, MRI, and histological data was expressed as mean ± standard deviation (SD) while vascular reactivity data was expressed as mean ±

standard error of mean (SEM). All statistical analyses were performed using SPSS 14.0 (SPSS Inc., Chicago, IL, USA). Mann-Whitney U test was used for paired comparison and Wilcoxon Signed Ranks Test was used for non- paired comparison. All statistical tests were two-sided. A p-value of <0.05 was considered statistically significant.

RESULTS

One rat died during OVX surgery while four rats died during the course of the study due to anesthesia or infection. The total number of control and OVX rats available for analysis at various time points is shown in Table 1.

Table 1: Animals Available for Analysis

	Experiment Time Course*			
	baseline	week 2	week 4	week 8
Control group for BMD measurement	11	6	11	10
OVX group for BMD measurement	11	5	8	7
Control group for MRI measurement	11	6	10	10
OVX group for MRI measurement	11	5	8	7
Control group for myograph & histology assessment	n/a	n/a	n/a	10
OVX group for myograph & histology assessment	n/a	n/a	n/a	7

*Number of rats available for analysis during the course of the study. Five of the 22 rats died due to surgery, anesthesia or infection.

Vertebral bone mineral density.
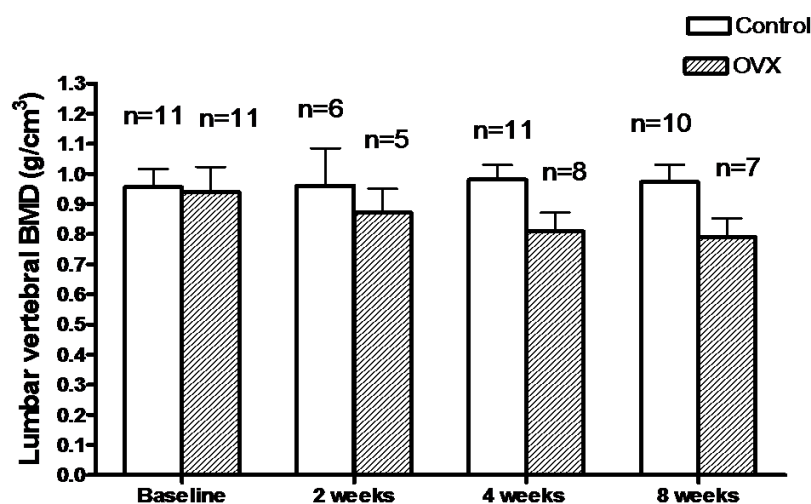
Figure 9. Rat lumbar vertebral BMD during the course of the study. BMD values remained constant for control rats while BMD in the OVX rats started to decrease by week 2, and further decreased by week 4 and week 8.

BMD values remained consistent in the control rats with no significant difference seen over the four time points (p>0.05). On the other hand, in the OVX rats, BMD decreased significantly from baseline by 9.3% at week 2 post OVX (p=0.043), by 17.5% at week 4 post OVX (p<0.001), and by 18.8% at week 8 post OVX (p<0.001). The difference between week 4 and week 8 was not significant (p=0.536) (Figure 9).

Vertebral perfusion. At baseline there was no difference in maximum enhancement (E^{max}) (p=0.71) or enhancement slope (E^{slope}) (p=0.8) between control and OVX rats. For control rats, both E^{max} and E^{slope} remained stable during the course of the study (p>0.05) (Figure 10 and 11). At week 2, E^{max} of OVX group was 11.6% less than that of control group, and E^{slope} was 9% less that of control group though these differences did not reach statistical significance (p=0.31 and 0.54, respectively) (Figure 10 and 11). At week 4, E^{max} of OVX group was 15.6% less than that of control group (p=0.027), and E^{slope} was 33.6% less that of control group (p=0.03) (Figures 10 -12). At week 8, E^{max} of OVX group was 14.2% less than that of control

group (p=0.02), and E^{slope} slope was 32.9% less that of control group (p=0.01) (Figures 10 – 12). No significant difference between week 4 and week 8 was present for both E^{max} and E^{slope} in the OVX group.
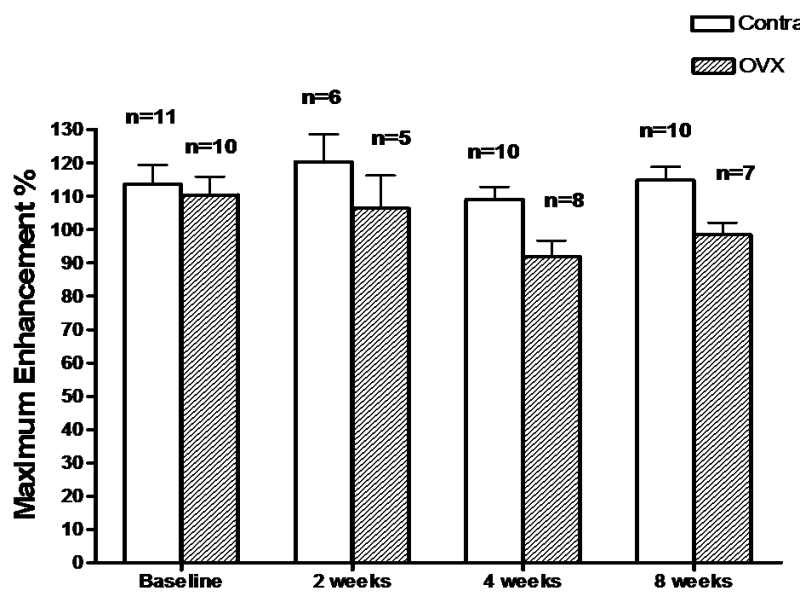
Figure 10. MRI perfusion indices of maximum enhancement (E^{max}) during the course of the study. For control rats, E^{max} remained constant, while in OVX rats, E^{max} started to decrease by week 2 and further decreased by week 4.
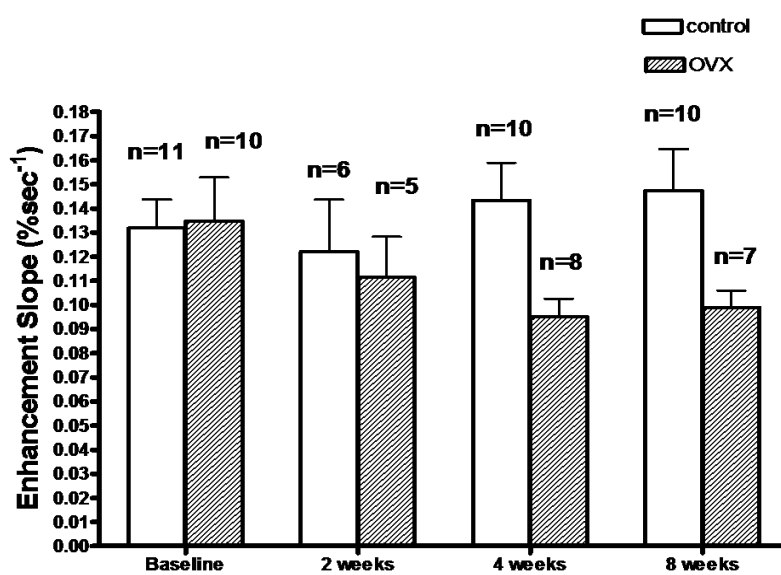
Figure 11. MRI perfusion indices of enhancement slope (E^{slope}) during the course of the study. For control rats, E^{slope} remained constant, while in OVX rats, E^{slope} started to decrease by week 2 and further decreased by week 4.
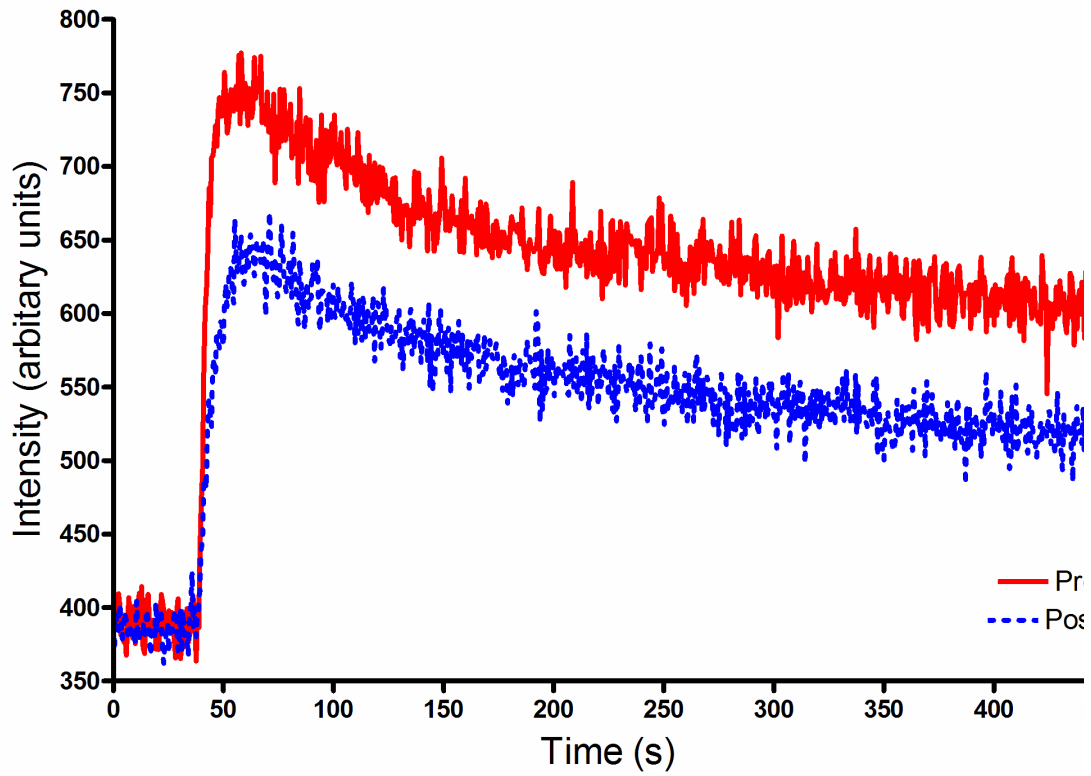
Figure 12. Typical time-intensity enhancement curve from rat lumbar vertebra (L3) at baseline (top trace) and 4 weeks post-OVX (bottom trace). Time-intensity curve in OVX rat shows reduced E^{max} and a less steep E^{slope}. X-axis: time in seconds, Y-axis: signal intensity in arbitrary unit.

Vascular reactivity. Acetylcholine-mediated endothelium-dependent relaxation in phenylephrine constricted aortic and femoral arterial rings was impaired in OVX group when compared to the sham-operated control group; while endothelium-independent relaxation by sodium nitroprusside (SNP), a NO donor, was comparable between the two groups (Figure 13). Phenylephrine-induced contraction was greater in OVX group than in control group; while this discrepancy was abolished in the presence of L-NAME, a nitric oxide synthase inhibitor (Figure 13).
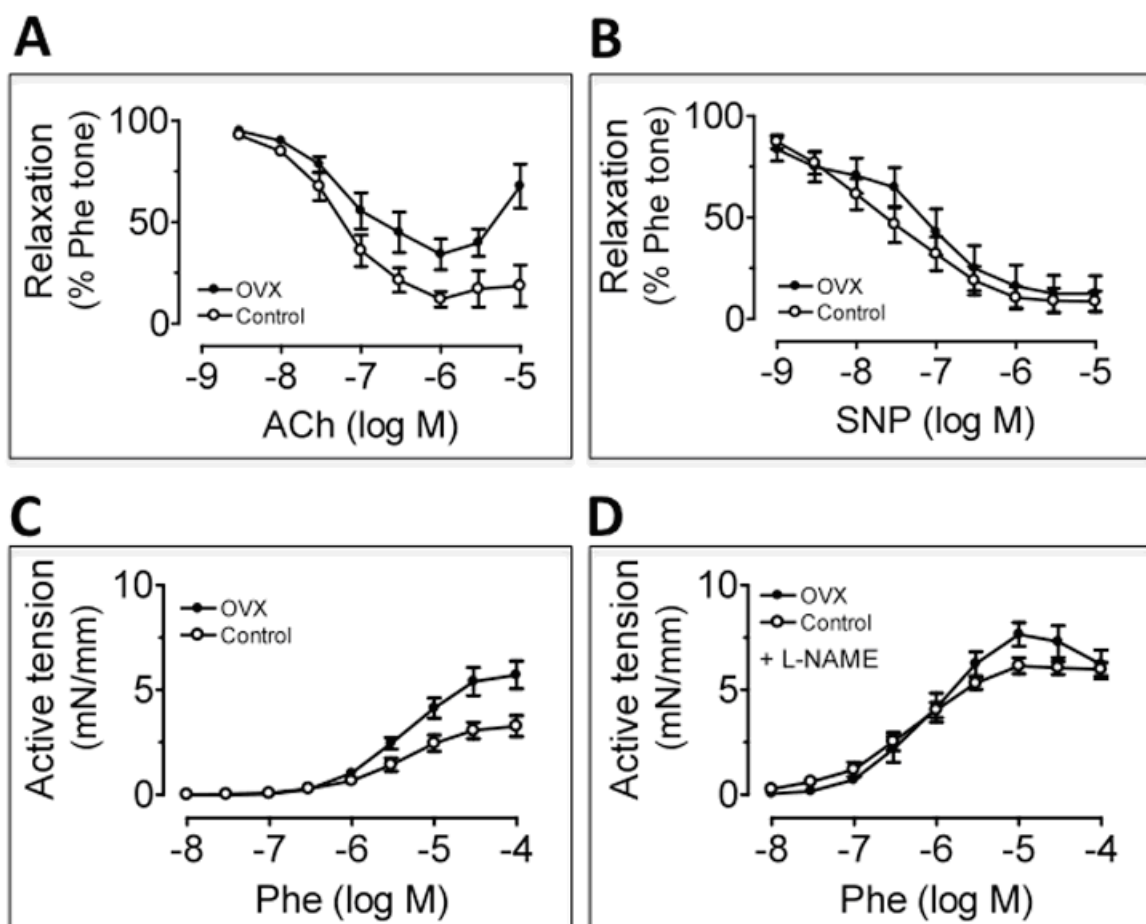
Figure 13: (A) Acetylcholine-mediated endothelium-dependent relaxation in phenylephrine constricted aortic rings was significantly impaired in OVX group compared to controls (p<0.05). (B) Endothelium-independent vasodilatation by sodium nitroprusside was comparable between two groups. (C) Phenylephrine-induced contraction was significantly greater in OVX group than controls (p<0.05). (D) This effect was abolished by L-NAME. Only results for aortic ring are shown since very similar results were observed in femoral rings.

Histological assessment of vertebral marrow cavity. The vertebrae of OVX rats contained significantly less trabecular bone, more marrow fat and less erythropoetic marrow than control rats (Figure 14). In the control group, marrow fat cell area was 21.6% ± 4.2% (p<0.01), bone trabecular area was 29.8% ± 3.9% (p<0.01) and erythropoetic marrow was 48.6% ± 4.5% (p<0.05). In the OVX group, marrow fat cell area was 52.9% ± 4.6%, bone trabecular area was 14.6% ± 3.7% and erythropoetic marrow was 32.5% ± 4.8% (Figure 14). In other words, the increase in fat cell area in the OVX groups was accompanied not just by a reduction in the amount of trabecular bone but also be a decrease in the amount of erythropoetic marrow.

The fat cell (adipocyte) number in the control group was 39 ± 5 per (200✗) field while the fat cell number in the OVX group was 92 ± 6 per (200✗) field. Therefore the increase in fat cell area by a factor of 2.45 (52.9% vs. 21.6%) in the OVX group was accompanied by a corresponding increase in fat cell number by a factor of 2.35 (92 vs. 39). This indicates that the increase in fat in the marrow space that accompanies OVX is essentially all due to increase of fat cell number rather than an increase in individual fat cell size (Figure 14).
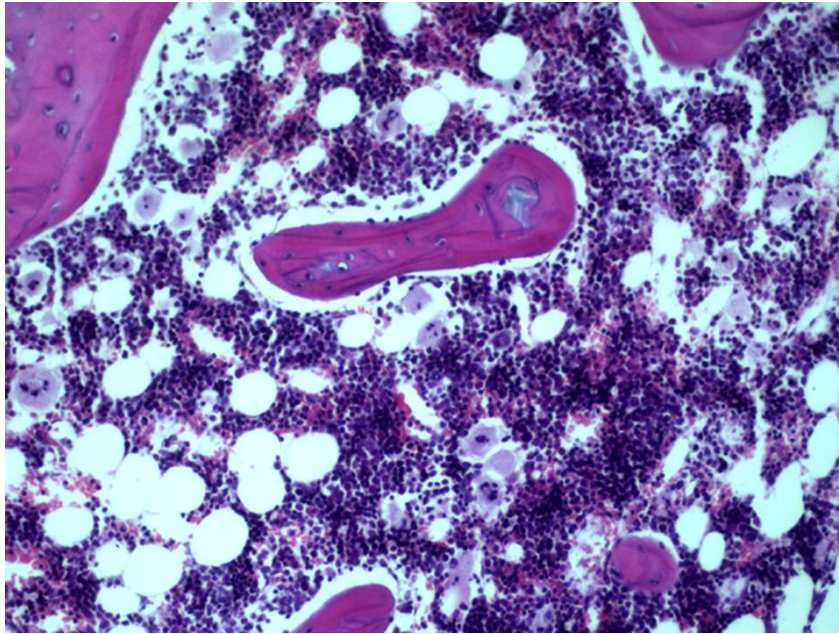
A
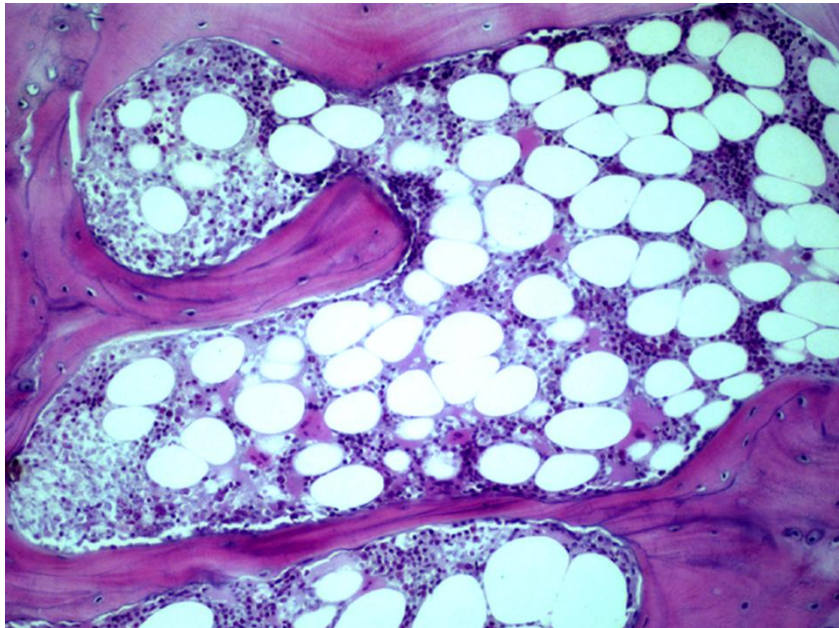
B

Figure 14:
Representative histopathological sections (H&E stain; magnification 200×) of lumbar vertebral body medullary canal in (A) control and (B) OVX rat. More fat cells were in the inter-trabecular space in the OVX rat than the control rat. This is also a notable reduction in the amount of erythropoetic marrow of the OVX rat compared to the control rat.

SIGNIFICANCE OF THESE RESULTS

In this study, we used a 1.5T clinical MR scanner and a small surface radiofrequency coil, both available in most clinical institutions, to study vertebral perfusion in a rat ovariectomy model. The relationship between bone perfusion, bone mineral density, arterial reactivity and marrow content was studied.

As expected, sex hormone deficiency led to a reduction in vertebral bone mineral density. At the first assessment with CT and MR two weeks post-OVX, a comparable reduction in both vertebral BMD and perfusion parameters was observed with a further reduction in both parameters being seen at 4 weeks post-OVX and again at 8 weeks post-OVX. At two week post-OVX, a reduction in BMD as well as both perfusion parameters by a factor of about 10% was observed. There was no indication that reduced bone perfusion either pre- or post-dated reduced BMD. It would seem most likely reduced bone perfusion occurs concurrently with a reduction in BMD rather than one particular parameter predating the other.

We also investigated the relationship bone perfusion and vascular reactivity. OVX-induced endothelial dysfunction is known to occur in the aorta but this effect has not been previously shown in the femoral arteries (Wong CM et al, 2008, Taddei S et al. 1996). Endothelial dysfunction resulting from decreased nitric oxide (NO) bioavailability was observed in the aorta and femoral arteries of OVX rats though not in the control rats. This endothelial dysfunction could through impaired vasodilatation or enhanced vascular tone lead to reduced blood flow and is therefore a likely cause of the reduced perfusion seen with reduced BMD post-OVX. These results are supportive of those described by Prisby et al who, using radiolabelled microspheres,

demonstrated a reduction of 21% in metaphyseal blood flow in old rats compared to young rats (Prisby RD et al. 2007). This reduction in blood flow was associated with impaired endothelium-dependent vasodilatation and decreased nitric oxide bioavailability (Prisby RD et al. 2007). Decreased release of endothelium-derived substances such a nitric oxide (NO) or PGI_2 is of particular interest in osteoporosis as both NO and PGI_2 have a potential downstream effect of promoting bone formation and limiting resorption (Samuels A et al, 2001). Endothelial dysfunction is not likely however to be the sole cause of reduced bone perfusion in the presence of reduced BMD since the effects of endothelial dysfunction are more likely to be systemic with the aorta and femoral artery seen to be equally affected in this study.

Another possible cause of reduced bone post-OVX as shown in this study is an alteration in marrow content. The medullary cavity is composed mainly of marrow fat, trabecular bone, erythropoetic marrow with a small component occupied by vascular channels (arterioles, venules and capillary sinusoids). Within the confined space of the vertebral body, an increase in one component can only occur at the expense of another component. Clinical MR spectroscopic studies have shown that as BMD decreases, there is a reciprocal increase in marrow fat content. The rat vertebral body is too small to allow proton MR spectroscopy at 1.5T though we were able to study the effect of OVX on marrow content histologically. Following ovariectomy, increased marrow fat area of 31.3% (from 21.6% to 52.9%) was observed secondary an increase in fat cell number rather than fat cell size. This increased fat cell number may be the result of mesenchymal stem cell differentiation switching more towards adipocytosis rather than osteoblastogenesis (Duque G 2008, Rosen CJ et al 2006).

The relative increase in marrow fat area was coincident, not just with a reduction in the amount of trabecular bone which decreased by 15% (from 29% to 14%), but also with a reduction in the amount of erythropoetic marrow which decreased by 16% (from 48% to 32%). This reduction is erythropoetic marrow may be akin to the 'senile anaemia' which has not to our knowledge previously being assessed or quantified in an experimental animal model (Takasaki M et al. 1999, Justesen J et al. 2001, Verma S et al. 2002, Steiniche T et al. 1995). Both the increase in marrow fat and decrease in erythropoetic marrow may be related to estrogen depletion given that the post-menopausal state is recognized to be associated with both increase in body mass and anemia (Hartsock RJ et al. 1965). It appears, therefore, that the increase in fat content post-OVX is not simply due to fat occupying the space vacated by not just reduced amount of trabecular bone but also a reduced amount of erythropoetic marrow. A preliminary PET imaging study has indicated that the metabolic activity of erythropoetic marrow is up to six times greater than that of fatty marrow (Chahal HJ et al. 2007). Overall, it seems most likely that this erythropoetic marrow may be accounting for the reduced bone perfusion seen accompanying reduction in BMD. To our knowledge, this is the first study to show that there is a decrease in the amount of red marrow post-OVX.

Limitations of this study.

1. The study cohort is small and the findings need to be validated in larger pre-clinical as well as clinical studies.

2. We studied the cause of reduced perfusion in a rat-OVX model. This equated to an abrupt withdrawl of estrogen. Although frequently used a model for post-menopausal and senile osteoporosis in humans, the pathophysiological processes behind both entities may not be strictly comparable. Further study in human is indicated. This study provides a good indication as to the direction this further study should take.

3. More in-depth MR-based perfusion models such as those used by Brix and Tofts (Basu S et al. 2007, Tofts PS et al. 1997) would help to provide information on specific elements of perfusion such as arterial input, available extracellar space, capillary exchange and contrast elimination permeability.

Conclusion. This pre-clinical study is the first post-OVX osteoporosis model to consider bone loss in unison with changes in perfusion, endothelial function, red and fatty marrow. As bone loss clearly does not occur in isolation, this more encompassing paradigm may well be the model that best serves future osteoporotic research. Rather than pre- or post-dating change in BMD, reduced bone perfusion seems to occur in synchrony with reduced BMD. Likely causes of reduced bone perfusion that occurs in association with reduced BMD include endothelial dysfunction and, more particularly, a hitherto non-quantified reduction in the amount of erythropoetic marrow. This decrease in erythropoetic marrow post- OVX

accompanies an increase in marrow fat, the latter occurring as a result of increase in fat cell number rather than fat cell size.

Next phase of study: At this stage sufficient time has elapsed since Studies 1,2 and Study 4 were undertaken to study whether if increased marrow fat or decreased perfusion at baseline could predict future accelerated bone loss. This forms the basis of Study 8.

Subjects from Study 4 rather than Study 1 or 2 were chosen for longitudinal follow up as in this age group (> 65 years), serial DXA examination of the lumbar spine (as per Study 1 and 2) is not that reliable and often increases rather the decreases on serial examination due to loss of vertebral height, facet joint arthrosis etc..

STUDY 8

Do perfusion indices or marrow fat content predict rate of bone loss?

Aim: To determine if marrow fat content or perfusion indices at baseline are related to subsequent rate of bone loss.

Rationale for doing this study: In Study 1, 2 and 4, we showed that osteoporosis was associated with increased marrow fat content and decreased marrow perfusion indices both for the lumbar spine and the proximal femur. Within each bone density group (normal bone mineral density, osteopenia and osteoporosis), a wide range of fat content and perfusion indices were observed (Figure 1 and 2) although the overall trend was for subjects with osteoporosis to have increased marrow fat and decreased perfusion indices (E^{max} and E^{slope}) compared to normal subjects. No difference in muscle perfusion indices across bone mineral density groups (normal, osteopenia, osteoporosis) was apparent (Figure 2).

To help determine whether increased marrow fat content or decreased perfusion predict bone loss, we undertook this longitudinal study of subjects who had undergone marrow fat content assessment and perfusion imaging of the proximal femur at baseline (i.e. subjects from Study 4)
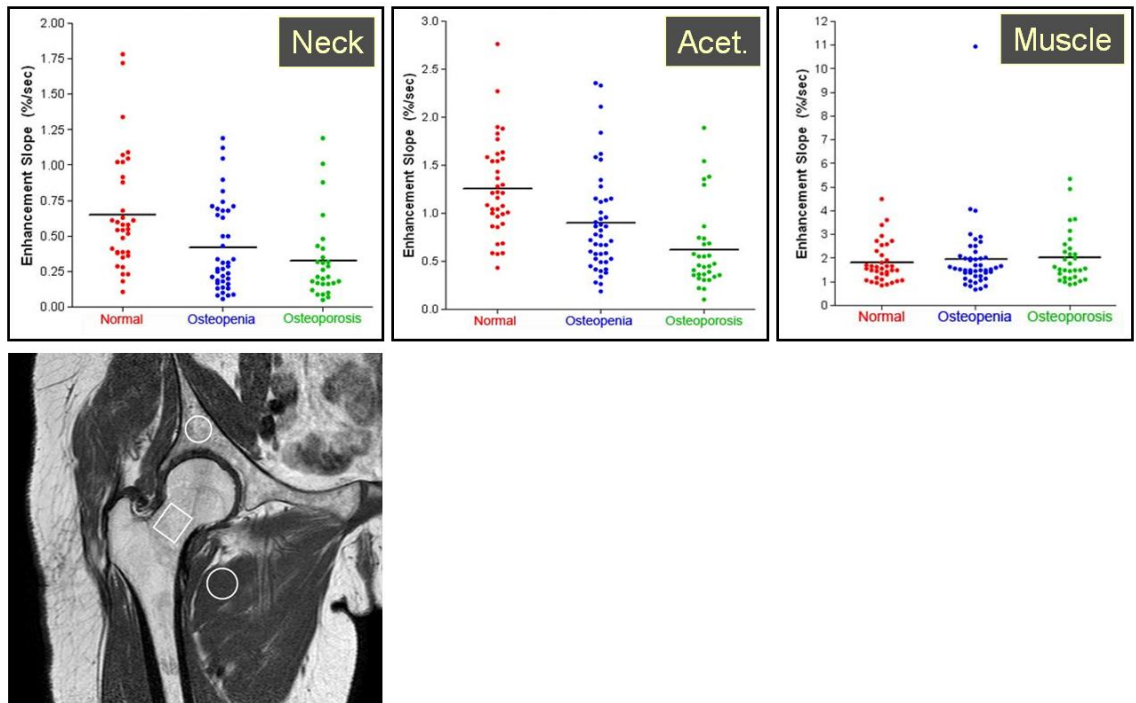
Figure 1. Enhancement slope (E^{slope}) of femoral neck, acetabulum and adductor muscle in 120 subjects with normal BMD, osteopenia and osteoporosis at baseline (from Study 4). Enhancement maximum (E^{max}) showed a similar trend (not shown). Note how a range of perfusion indices were present for each group.
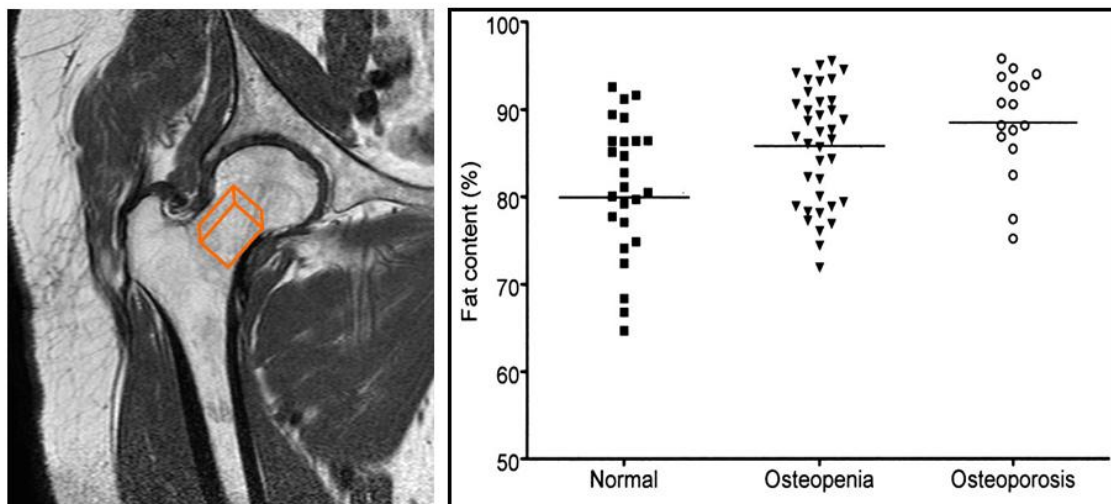
Figure 2. MR spectroscopy of femoral neck in 120 subjects with normal BMD, osteopenia and osteoporosis at baseline (from Study 4). MR spectroscopy was not performed in the acetabulum or adductor muscle at baseline. Note how range of values present in each group.

STUDY OUTLINE:

STUDY 8

↓

To determine whether increased marrow fat or decreased perfusion at baseline could predict future accelerated bone loss?

↓

- 120 post-menopausal female subjects (Study 4 cohort)
  MRS and DCE MRI plus DXA of hip region at baseline
- Subjects separated into two groups according to marrow fat content and perfusion indices i.e. whether:
  < or > median marrow fat content
  < or > median marrow or muscle perfusion indices (E^{max} and E^{slope})
- DXA examination of hip repeated in 52 subjects at two and four years to determine longitudinal bone loss.

↓

MAIN FINDINGS

- Subjects < median marrow or muscle perfusion indices had significantly ↑ bone loss in ensuring four years.
- Subjects > marrow fat content also tended to have ↑ bone loss though this did not reach statistical significance.
- Perfusion and marrow fat parameters were comparable to known risk factors at predicting bone loss
- Acetabulum E^{max} > median had a sensitivity of 89% in distinguishing between slow losers (<1% annum) and fast losers (> 1% annum).

ABSTRACT

PURPOSE: To determine if marrow fat content or perfusion indices at baseline can predict bone loss.

MATERIALS AND METHODS: 120 post-menopausal female subjects underwent hip BMD at baseline following by marrow fat content assessment of femoral neck by MR spectroscopy and MR perfusion imaging of femoral neck, acetabulum and muscle. Of these 120 subjects, 52 subjects were followed-up with repeat BMD at two and four years.

RESULTS: Percentage decline in femoral neck BMD at two and four post-baseline was greater in subjects with increased marrow fat or decreased perfusion indices after adjusting for baseline BMD, age, weight and weight change. Most MR parameters correlated better with 4 year decrease in BMD than currently applied risk factors. Acetabulum E^{slope}, femoral neck E^{max}, E^{slope} and marrow fat content had a sensitivities of 89%, 81%, 75% and 72% respectively for distinguishing between fast and slow bone losers.

CONCLUSION: Perfusion indices and to a lesser degree marrow fat content were comparable to known risk factors at predicting bone loss. Selected perfusion indices have a moderate to high sensitivity in discriminating between fast and slow bone losers.

MATERIALS AND METHODS

The initial cohort consisted of 120 post-menopausal female subjects the details of which are outlined in Table 1. These subjects were recruited by placing notices in community centers for the elderly inviting subjects to attend for DXA examination. Following DXA examination of the right hip, subjects were invited to attend for MR spectroscopy and perfusion imaging of the right hip. These results are presented in Study 4 and outlined in Figure 1 and 2.

Table 1. Cohort characteristics

Baseline	All (n=120)	Normal (n=39)	Osteopenia (n=47)	Osteoporosis (n=34)
Age (years)	73·79 (4·28)	72·90 (3·75)	73·38 (4·65)	75·38 (4·00)
Hip BMD(g/cm^2)	0·71 (0·12)	0·85 (0·06)	0·70 (0·04)	0·57 (0·06)
T-score	-1·63 (1·15)	-0·33 (0·58)	-1·73 (0·41)	-2·98 (0·51)

Followed-up at 2 & 4 years	All (n=52)	Normal (n=20)	Osteopenia (n=24)	Osteoporosis (n=8)
Age (years)	72.37 (4.16)	71.80 (3.98)	72.04 (4.26)	74.75 (3.99)
Hip BMD(g/cm^2)	0.74 (0.10)	0.84 (0.04)	0.71 (0.05)	0.58 (0.03)
T-score	-1.38 (0.95)	-0.43 (0.39)	-1.67 (0.43)	-2.89 (0.29)

Table 1. Details of cohort at baseline and cohort follow-up at 2 & 4 years. Follow-up cohort contained less osteoporotic subjects but was otherwise unchanged from baseline cohort.

From the cohort of 120 subjects examined at baseline, 52 subjects were suitable and available to return for repeat DXA at both two and fours years post-baseline. This DXA examination of the right hip at two and four years was performed on the same DXA machine (Hologic QDR-4500W) as baseline by the same experienced DXA technologists. Characteristics of the 52 subjects followed up at two and four years are shown in Table 1. No repeat MR examination was performed. The remaining 64 subjects were not followed up or were not included in the current analysis as they

had either started osteoporotic medication (n=24), were non-contactable (n=2), had died (n=1), did not wish to return for further DXA study (n=15) or are not scheduled to return for four year follow up until two years later (n=26).

The median level for marrow fat content in the femoral head and perfusion indices (E^{max} and E^{slope}) in the femoral neck, acetabulum and muscle across all bone mineral density groups at baseline was determined. For each particular area and parameter, follow-up subjects were divided into two cohorts according to whether their original marrow fat content or perfusion index (E^{max} and E^{slope}) was greater than or less than the overall median value.

Statistical analysis. Data was presented as mean and standard deviation, unless otherwise stated. All statistical analyses were done using the statistical package SAS, version 9.1 (SAS Institute, Inc., Cary, North Carolina). Spearman partial correlation coefficient was used to determine association between MR-based parameters and femoral neck percentage BMD change at two and four years. Analysis of covariance (ANCOVA) was performed to examine the mean femoral neck BMD change between the above and below median of the MR-based parameters. Pearson correlation coefficient was used to assess the relationship between traditional risk factors and percentage femoral neck BMD change. Linear regression was applied to examine how MR-based parameters and other potential risk factors predict femoral neck bone loss. Parital R^2 was shown for comparing effects contributed from different factors. Fisher exact test was used to test the sensitivity of MR parameters in distinguishing slow from fat bone losers. Slow bone losers were defined as subjects with on average <1% decline in femoral neck BMD per annum. Fast bone losers were defined as subjects with on average >1% decline in femoral neck BMD per annum. All statistical tests were two-sided. A p-value <0·05 was considered statistically significant.

Results

(a) BMD reduction at femoral neck between different cohorts. Percentage decline in femoral neck BMD from baseline at two and four years was greater in subjects with increased marrow fat at the femoral neck and in subjects with decreased perfusion indices at the femoral neck, acetabulum and adductor muscle after adjusting for baseline BMD, age, weight and weight change. The same trend was observed in all areas with a greater reduction in BMD between cohorts at four years than two years (Table 2 and Figures 1-4). The difference between cohorts was significant for acetabulum E^{slope} and muscle E^{max} at four years (Table 2 and Figures 3B and 4A).

Table 2 Bone loss in MR-based cohorts with above and below median value at baseline

Parameter [median value]	Time period	Estimated mean (SE) of femoral neck BMD% change		p-value
		< median	≥ median	
Femoral neck fat content (%) [median= 85.5]	year 0 → year 2 [n=51]	-0.342 (0.768)	-1.560 (0.807)	0.2985
	year 0 → year 4 [n=44]	-1.310 (1.270)	-4.722 (1.334)	0.0603
Femoral neck E^{max} (%) [median =10.9]	year 0 → year 2 [n=47]	-0.945 (0.864)	-0.752 (0.800)	0.7212
	year 0 → year 4 [n=41]	-4.870 (1.378)	-0.971 (1.276)	0.0780
Femoral neck E^{slope} (%/sec) [median=0.36]	year 0 → year 2 [n=47]	-1.053 (0.877)	-0.659 (0.810)	0.8685
	year 2 → year 4 [n=41]	-4.191 (1.446)	-1.558 (1.336)	0.4868
Acetabulum E^{max} (%), [median=16.8]	year 0 → year 2 [n=52]	-1.011 (0.830)	-0.855 (0.771)	0.6536
	year 2 → year 4 [n=45]	-4.010 (1.387)	-1.970 (1.287)	0.4987
Acetabulum E^{slope} (%/sec) [median=0.87]	year 0 → year 2 [n=52]	-2.017 (0.748)	0.210 (0.767)	0.2248
	year 2 → year 4 [n=45]	-5.624 (1.192)	-0.097 (1.221)	0.0141
Muscle E^{max} (%) [median=68.8]	year 0 → year 2 [n=52]	-1.961 (0.750)	0.060 (0.732)	0.0721
	year 2 → year 4 [n=45]	-5.741 (1.174)	-0.226 (1.147)	0.0091
Muscle E^{slope} (%/sec) [median=1.57]	year 0 → year 2 [n=52]	-1.161 (0.769)	-0.705 (0.752)	0.6654
	year 2 → year 4 [n=45]	-4.413 (1.262)	-1.496 (1.234)	0.1354

Table 2: Estimated mean (SE) of BMD% change from year 0 to year 4.

ANCOVA adjusted for covariates including age, weight, weight change
and baseline BMD. Bold: p-value<0.05

(b) Correlation between perfusion indices and marrow fat at baseline and percentage reduction in femoral neck BMD at two and four years. A mild to moderate significant correlation (ranging from 0.23 to 0.52) was present between perfusion indices in the femoral neck, acetabulum and muscle and percentage reduction in femoral neck BMD at four years (Table 3). This correlation (r= 0.52) was greatest for acetabulum E^{slope}. The correlation between marrow fat content and percentage reduction in femoral neck BMD at four years did not reach statistical significance (Table 3).

Table 3: Relationship between MR based parameters at basleine and subsequent bone loss

Parameter		Femoral neck BMD % change			
		year 0 → year 2		year 0→ year 4	
		Coefficient[1]	p-value	Coefficient[1]	p-value
Femoral neck	fat content (%)	-0.1155	0.4244	-0.2293	0.1391
	E^{max}(%)	0.0039	0.9795	0.3924	**0.0123**
	E^{slope}(%/sec)	0.0014	0.9926	0.3628	**0.0214**
Acetabulum	E^{max}(%)	0.1908	0.1800	0.2356	0.1237
	E^{slope}(%/sec)	0.2628	0.0625	0.5173	**0.0003**
Muscle	E^{max}(%)	0.1900	0.1817	0.3065	**0.0430**
	E^{slope}(%/sec)	0.1205	0.3995	0.2794	0.0662

Table 3: Relationship between marrow fat, bone and muscle perfusion and
femoral neck bone loss adjusted for baseline BMD from 0 → 2 years and
from 0 → 4 years. Bold: p-value<0.05. [1]Spearman partial correlation coefficient

(c) Correlation between selected known risk factors and percentage BMD change of femoral neck. Analysis of the present cohort using risk factors known to be associated with more rapid reduction in femoral neck BMD (Lau EMC et al

2006) showed that this association was strongest with age, weight, weight

change for past two years and baseline femoral neck BMD (Table 4).

Table 4. Relationship between bone los and clinical risk factors

Parameter	Femoral neck BMD % change	
	year 0→ year 4	
	Coefficient[1]	p-value
Age	-0.0575	0.7110
Weight	0.4259	**0.0039**
Weight change for past 2 years	-0.2586	0.0901
Height	-0.0254	0.8702
Baseline femoral neck BMD	0.2118	0.1676
Grip strength	-0.1410	0.3613
Physical activity (PASE)	-0.1045	0.4995
Calcium/ Calories	-0.0801	0.6054
Diabetes	0.2345	0.1254
Fracture after 50 years	-0.1242	0.4218
Height change from 25 years old	-0.0645	0.7443
Smoker	0.1529	0.3218
Daily alcohol intake	0.0097	0.9504

Table 4: Relationship between femoral neck bone loss for 4 years and
clinical risk factors. Bold: p-value<0.05. [1]Pearson correlation coefficient.

(d) Comparison of known risk factors with perfusion indices in predicting

regarding correlation with percentage reduction in femoral neck BMD.

Analyzing the effect of these variables and the two perfusion indices most

strongly associated with percentage reduction in femoral neck BMD, showed that

perfusion indices had a comparable association with percentage reduction in

femoral neck BMD than all of the previously identified variables such as subject

age, weight, weight change over two years and baseline femoral neck BMD

(Table 5).

Table 5; Multivariate regression analysis of MR-based paramenters and clinical risk factors

Parameter	Femoral neck BMD % change year 0→ year 4		
	Coefficient	p-value	Partial R^2
Muscle Fat content (%) > median	-2.2482	0.1292	0.0628
Age	-0.0419	0.8119	0.0016
Weight	0.3150	**0.0020**	0.2348
Weight change for past 2 years	-0.5686	**0.0238**	0.1341
Baseline femoral neck BMD	-0.1073	0.4471	0.0162
			R^2=0.3715
Muscle E^{max} (%) > median	3.2933	**0.0184**	0.1412
Age	-0.1562	0.3595	0.0227
Weight	0.2893	**0.0027**	0.2181
Weight change for past 2 years	-0.6597	**0.0066**	0.1828
Baseline femoral neck BMD	-0.0991	0.4498	0.0155
			R^2=0.4226
Acetabulum E^{slope} (%/sec) > median	3.0006	**0.0392**	0.1100
Age	-0.1013	0.5492	0.0098
Weight	0.2486	**0.0158**	0.1476
Weight change for past 2 years	-0.5544	**0.0210**	0.1357
Baseline femoral neck BMD	-0.1518	0.2481	0.0359
			R^2=0.4017

Table 5: Multivariate linear regression analysis showing predictive ability of three selected MR parameters (muscle E^{max} (%/sec) < median, acetabulum E^{slope} (%/sec) < median and marrow fat content (%) >median) compared with traditional risk factors in determining femoral neck bone loss over 4 years. Partial R^2 depicts relative effect of each variable individually while summation reflects total effect. Bold: p value <0.05.

(e) Sensitivity of marrow fat and perfusion induces in identifying subjects as slow or rapid bone losers.

Of the various MR parameters analyzed, acetabulum E^{slope} proved the most sensitive indicator for differentiating subjects as fast or slow bone losers with a sensitivity of 89% (Table 6). Next most sensitive were the various femoral neck E^{max}, E^{slope} and marrow fat content with sensitivities of 81%, 75% and 72% respectively. Muscle enhancement did not prove to be sensitive in distinguishing between fast and slow bone losers.

Table 6: Sensitivity of MR-based parameters in distinguishing fast from slow bone losers

Parameter (median value)	Rapid loser		Sensitivity (95% CI)	p-value
	No (number/percentage)	**Yes** (number/percentage)		
Femoral neck fat content (%)				
<median (= 85.5%)	18 (69.2%)	5 (27.8%)	0.722 (0.46, 0.89)*	**0.0132**
≥median	8 (30.8%)	13 (72.2%)		
Femoral neck E^{max} (%)				
<median (= 10.9%)	6 (24.0%)	13 (81.3%)	0.813 (0.54, 0.95)	**0.0005**
≥median	19 (76.0%)	3 (18.8%)		
Femoral neck E^{slope} (%/sec)				
<median (= 0.36 %/sec)	7 (28.0%)	12 (75.0%)	0.750 (0.47, 0.92)	**0.0046**
≥median	18 (72.0%)	4 (25.0%)		
Acetabulum E^{max} (%)				
<median (= 16.8%)	10 (37.0%)	11 (61.1%)	0.611 (0.36, 0.82)	0.1376
≥median	17 (63.0%)	7 (38.9%)		
Acetabulum E^{slope} (%/sec)				
<median (= 0.87 %/sec)	7 (25.9%)	16 (88.9%)	0.889 (0.64, 0.98)	**<0.0001**
≥median	20 (74.1%)	2 (11.1%)		
Muscle E^{max} (%)				
<median (= 68.8%)	11 (40.7%)	11 (61.1%)	0.611 (0.36, 0.82)	0.2307
≥median	16 (59.3%)	7 (38.9%)		
Muscle E^{slope} (%/sec)				
<median (= 1.57 %/sec)	11 (40.7%)	11 (61.1%)	0.611 (0.36, 0.82)	0.2307
≥median	16 (59.3%)	7 (38.9%)		

Table 6. Sensitivity of marrow fat content and perfusion indices in predicting rapid decline in femoral neck BMD. Rapid loser defined as femoral neck BMD decline of > 1% per annum. *Sensitivity refers to marrow fat content > median and perfusion indices < median. Bold: p-value<0.05, Fisher exact test.

Median Femoral Neck Fat Content (%)
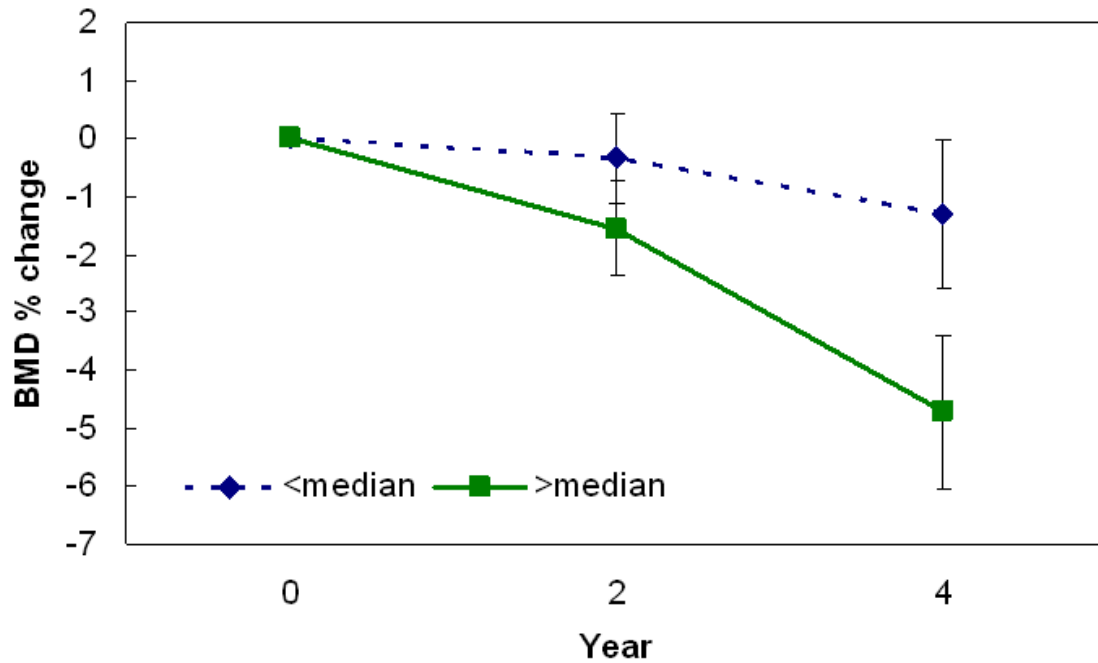
Figure 1. Mean % reduction in femoral neck BMD over four year period in subjects with < or >
the median fat content (=85.5%). BMD in subjects with <median fat content declined 1.3% while
BMD subjects with >median fat content declined 4.7%.
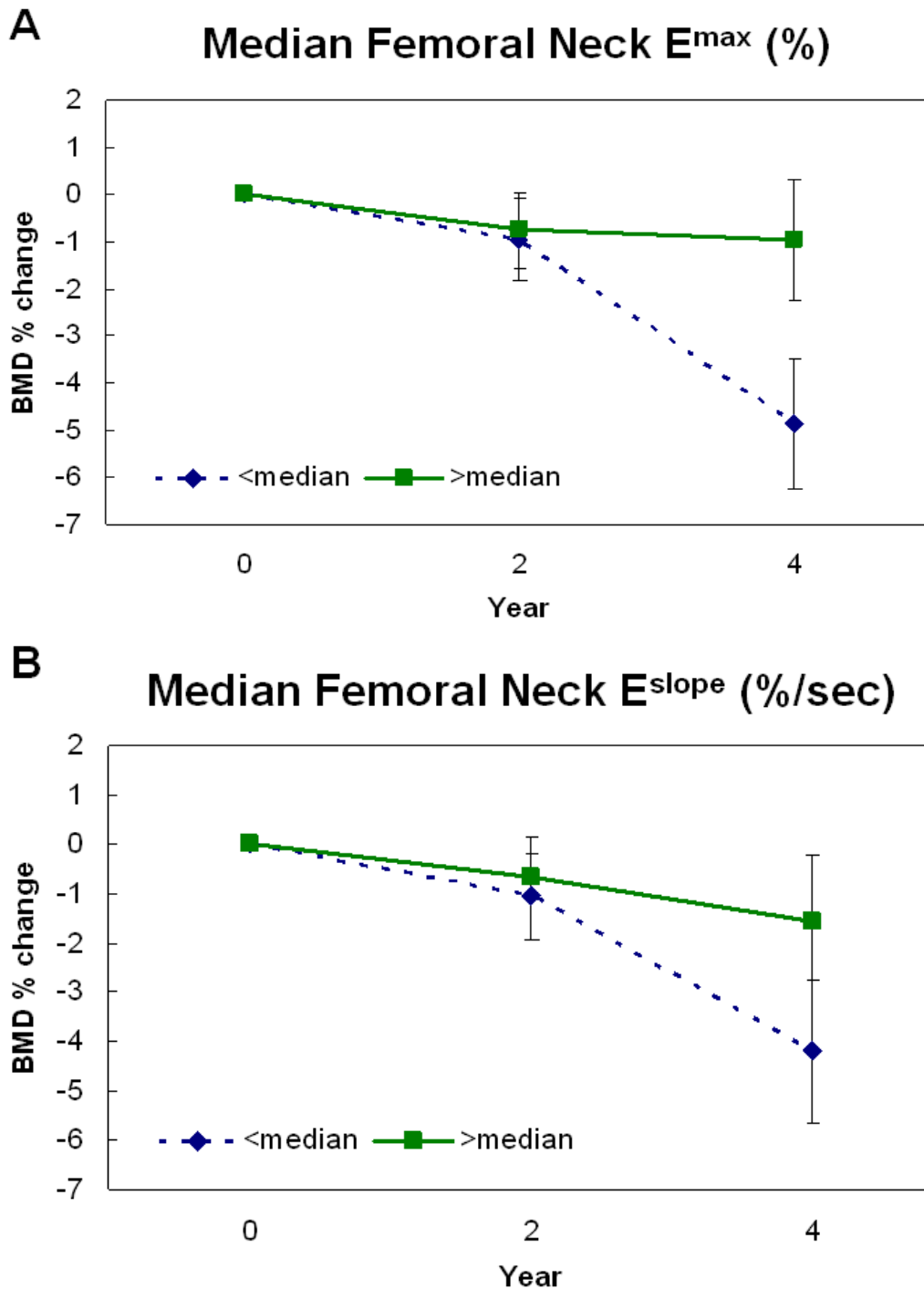
Figure 2. Mean % reduction in femoral neck BMD over four year period in subjects with < or > the median E^{max} (= 10.9%) or E^{slope} (= 0.36 %/sec) at the femoral neck. (A) BMD in subjects with <median E^{max} declined 4.9% while while BMD in subjects with >median E^{max} declined 1.0%. (B) BMD in subjects with <median E^{slope} declined 4.2% while while BMD in subjects with >median E^{slope} declined 1.6%.
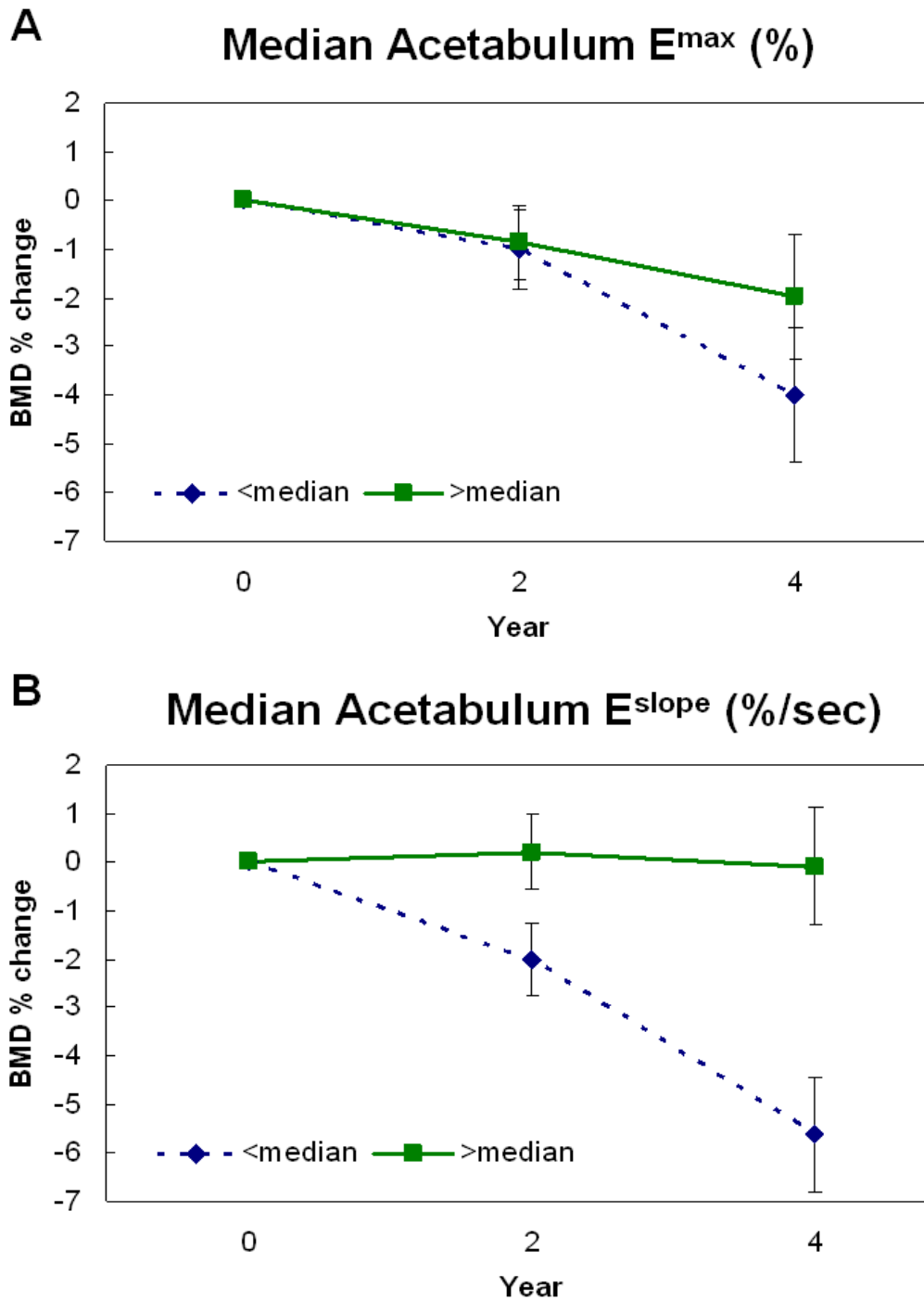
Figure 3. Mean % reduction in femoral neck BMD over four year period in subjects with < or > the median E^{max} (= 16.8%) or E^{slope} (= 0.87 %/sec) at the acetabulum. (A) BMD in subjects with <median E^{max} declined 4.0% while while BMD in subjects with >median E^{max} declined 1.9%. (B) BMD in subjects with <median E^{slope} declined 5.6% while while BMD in subjects with >median E^{slope} declined 0.1%

A

Median Muscle E^{max} (%)

B

Median Muscle E^{slope} (%/sec)
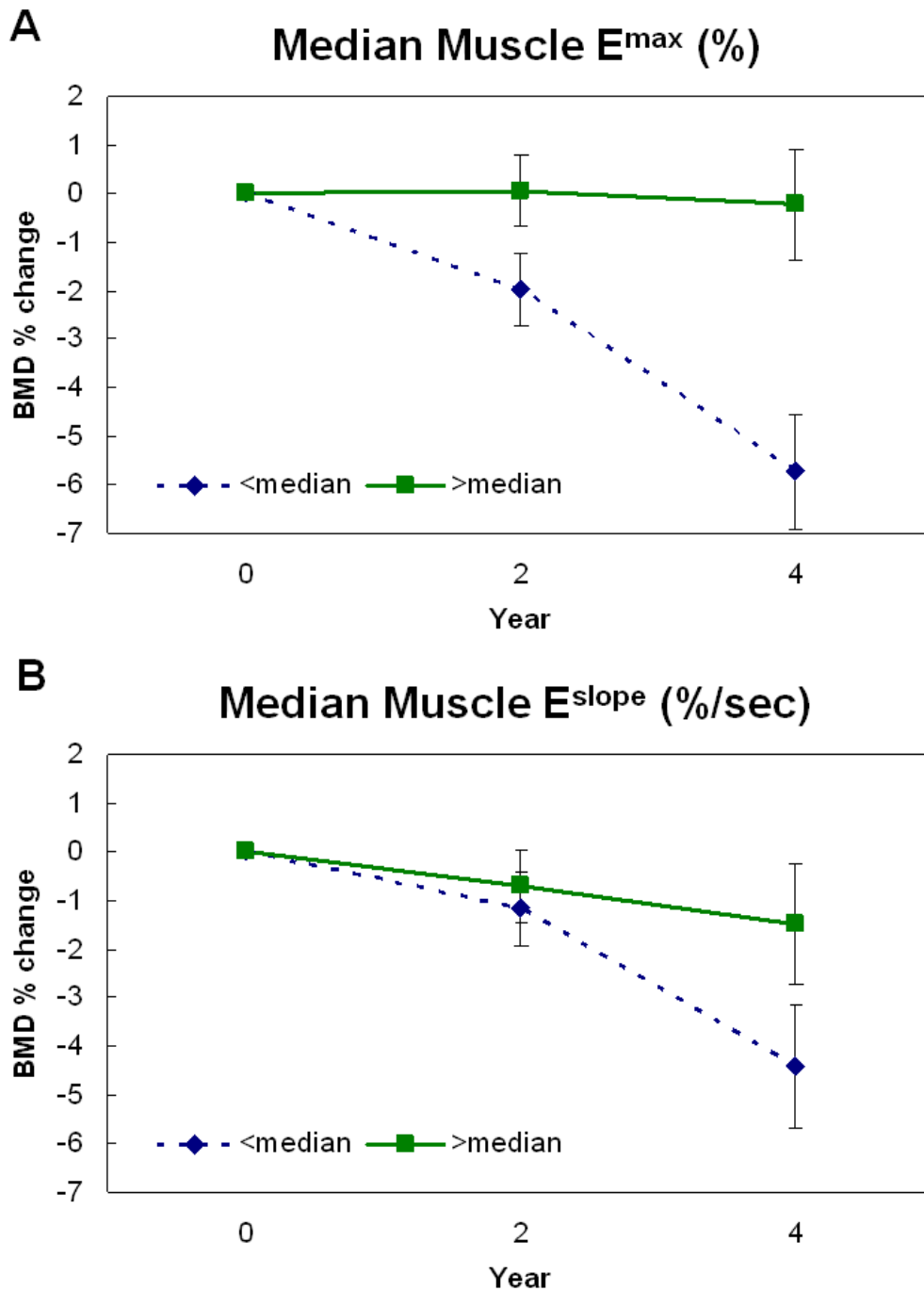
Figure 4. Mean % reduction in femoral neck BMD over four year period in subjects with < or > the median E^{max} (= 68.8%) or E^{slope} (= 1.57 %/sec) at the acetabulum. (A) BMD in subjects with <median E^{max} declined 5.7% while while BMD in subjects with >median E^{max} declined 2.2%. (B) BMD in subjects with <median E^{slope} declined 4.4% while while BMD in subjects with >median E^{slope} declined 1.5%.

SIGNIFICANCE OF THESE RESULTS

Rather than all subjects of the same age and gender losing bone at the same rate, some subjects loose bone at a faster rate. A means of identifying subjects more likely to loose bone at a faster rate would be helpful in allowing such individuals to be targeted for specific anti-osteoporotic medication. Ideally one would hope to recognize these subjects at the outset before bone loss occurs. At the moment, clinical and densitometry measures at baseline provide the best predictors of further bone loss. Recognized useful parameters are age and weight at baseline, weight loss over two years and baseline BMD. The predictive value of urinary and serum bone turnover markers is limited by wide inherent variability [Garnero et al 1999].

The aim of this study was to see if the presence of increased marrow fat or decreased perfusion at baseline could predict future bone loss. For the purpose of this study, we defined slow losers as <1% decline in femoral neck BMD per annum and fast losers as >1% decline in femoral neck BMD per annum. Higher marrow fat content and lower perfusion indices (both in bone and muscle) at baseline was associated with more severe bone loss over a four year period. Several of the MR parameters assessed were comparable wirth currently applied clinical risk factors in predicting bone loss at the femoral neck. The parameter with the highest correlation was acetabulum E^{slope}. This higher correlation with acetabular and not femoral neck perfusion may reflect the relatively better bone perfusion and possible truer assessment of bone in the acetabulum compared to the proximal femur (Study 4, Study 5). For all bone areas examined in Study 4 (femoral head, neck, shaft and acetabulum) perfusion indices were highest in the acetabulum (with E^{max} and E^{slope} being about 50-100% higher than those in the femoral neck, Study 4).

We also found a moderate correlation found between muscle Emax and subsequent bone loss. This was unexpected since previous cross-sectional studies (Study 2 and Study 4) had shown no relationship between decreasing BMD and muscle perfusion. It emphasizes that we cannot ignore the potential role of a generalized vascular problem such as endothelial function being involved in bone loss.

MR perfusion parameters also proved to be useful at distinguishing between fast and slow bone losers. Acetabulum E^{slope} values larger than 0.87%/sec (median value) had a sensitivity of 89% for distinguishing between slow and fast losers at baseline while the sensitivity of femoral neck perfusion median parameters was 75-81% and that of femoral neck marrow fat content was 72%. The predictive ability of muscle perfusion indices were less than those of bone.

It was also surprising how some perfusion parameters such as Acetabulum E^{slope} showed good correlation and predictive power, whilst very closely related parameters such as Acetabulum E^{max} did not show as good correlation or predictive ability. E^{max} is considered to be more related to total uptake of gadolinium contrast agent into the interstitial space, and is dependent on blood flow, micro-vessel density, and interstitial fluid movement (Reddick WE et al. 1999, Taylor JS et al. 2000, Choyke PL et al. 2003) while E^{slope} tends to be more dependent on blood flow and vessel permeability (Reddick WE et al. 1999, Taylor JS et al. 2000, Choyke PL et al. 2003). More research into the factors influencing these parameters and more detailed analysis of marrow perfusion imaging using pharmokinetic compartmental modeling needs to be undertaken.

This is the first study to assess the predicative value of marrow fat and perfusion indices. We are certainly not advocating that MR be applied at this stage as a means to predict bone loss. The predictive ability of MR is only compable to but no better

than clinical risk factors. MR would been to be substantially better than clinical evlation for it to be a clinically useful measure. In addition, many epidemiological as well as cost-effectiveness issues have not been addressed in this study. The findings, nevertheless, are sufficiently encouraging to say that bone perfusion and also probably marrow fat are integrally related to bone loss and do show potential in the prediction of bone loss.

Limitations of this study.

1. The main limitation of this study is the relatively small sample size of 52 subjects being followed up over a four year period out of an initial cohort of 120 subjects. Nevertheless, statistical significance was achieved with many perfusion parameters and close to statistical significance for other perfusion parameters and marrow fat content.

2. This study was performed solely on female subjects. Perfusion indices in the proximal femur tend to be higher in female post-menopausal subjects than male subjects of comparable age (Study 4). Whether a similar predictive potential is seen in male subjects is not known.

3. Due to the small cohort size, we did not determine fracture prevalence in this study. Although low femoral neck BMD is a strong predictor of proximal femoral fracture (Cummings et al. 1994), predicting BMD loss is not the same as predicting fracture risk.

Conclusion. Perfusion parameters, and to a lesser degree, marrow fat content, are predictive of the severity of bone loss. These MR indices correlated with subsequent bone loss similar to currently applied risk factors. Selected perfusion parameters had a moderate to high sensitivity in distinguishing fast and slow bone losers.

SUMMARY

A finely tuned equilibrium that exists between bone deposition by osteoblasts and resorption by osteoclasts helps maintain skeletal bone mass. After peak bone mass is attained in the third to four decade of life, progressive bone loss occurs throughout the skeleton preferentially affecting the trabecular rather than the cortical component of bone. As a result, those bone parts with relatively more trabecular bone (vertebral bodies, neck of femur and distal radius) sustain the greatest loss in bone strength and become particularly susceptible to fracture often with minimal or no trauma. This state of increased bone fragility is known as osteoporosis which is defined as a skeletal disorder characterized by compromised bone strength predisposing to an increased risk of fracture.

Currently, we rely on either bone density or the occurrence of a low energy fracture to diagnose osteoporosis. This approach is inherently flawed since bone needs to be lost or a fracture needs to occur before we can identify a patient with osteoporosis. And once bone is lost it does not necessarily recover with treatment. Treatment can improve bone density and improve bone strength but bone quality will probably never return to normal and treatment effect is not necessarily sustained. It would be much better if a means existed of recognizing the early stage of the osteoporotic process before bone loss occurs. Another limitation with current osteoporosis management is

the delay involved in evaluating new treatments. Currently used end-points to test

treatment efficiency are bone loss or fracture as no reliable predictors of future bone

loss have been identified. The result is that many years relapse before the effect of

treatment can be evaluated. Finally, many risk factors for osteoporosis and

osteoporotic fracture have been identified though no unifying etiology regarding the

pathophysiology of this disorder exists.

Recent research utilizing high resolution imaging techniques such as CT and MR

have gone a very long way to improving our understanding of bone architecture, bone

quality and fracture risk prediction. Recent developments in MR imaging technology

have also allowed non-invasive evaluation of bone marrow. While, to date, most

osteoporotic research has concentrated on the mineralized component of bone, it

may well be that study of the bone marrow could provide answers to some of the

on-going questions about osteoporosis pathophysiology and management. After all,

metabolically active trabecular bone is bathed in bone marrow and is likely to react to

changes in this bone microenvironment. We undertook the studies presented in this

thesis with a view of bettering our understanding of the physiological processes

occurring within the bone marrow in osteoporotic subjects with the ultimate aim of

being able to indentify features which would point to the initiation of the osteoporotic

process before bone loss occurs. A simple analogy would be the recognition and

treatment of early coronary artery disease before heart failure or myocardial infarction ensues.

In these studies we have shown that perfusion seems to be reduced in osteoporotic bone, that this effect is seen in both males and females (Study 1, 2 & 4) and affects the proximal femur in a similar fashion to the vertebral body (Study 1,2 & 4). The apparent reduced perfusion seen in osteoporotic bone occurs within the bone and is not a reflection of a more generalized circulatory disturbance (Study 2 & 4). In line with this decreased perfusion is an increase in marrow fat which can be quantified by MR spectroscopy (Study 1,2, 4 and 7). We have been able to quantify the error of increasing marrow fat on BMD estimation by DXA (Study 3). This effect is not large and does not affect the findings of our studies. We have shown that the perfusion of the femoral head is inherently poor in normal subjects while in osteoporosis perfusion in the femoral neck region tends to diminish relatively more than in the femoral head and shaft (Study 4). Bone perfusion decreases soon after estrogen depletion and occurs in line with rather than pre-or post-dating bone loss (Study 7). The most likely causes of decreased perfusion are, primarily, a previously unrecognized concomitant reduction in the red cell mass accompanying estrogen depletion and secondarily endothelial dysfunction (Study 7). Increase in marrow fat seems to occur as a result of increase in fat cell number rather than fat cell size (Study 7) and is most likely due to a

switch in mesenchymal stem cell differentiation from osteoblastogenesis to adipocytosis. Although long chain polyunsaturated fatty acids in diet or co-culture have been shown to affect bone metabolism, the fatty acid composition of marrow fat is not altered between subjects with normal bone mineral density, low bone mass (osteopenia) or osteoporosis (Study 6). Hence, it is unlikely that fatty acids in the marrow have a direct effect on bone formation. Clear differences do exist between subcutaneous and marrow fat so that the former cannot be used a mirror of the latter in future studies (Study 6). Longitudinal study using either serial MRS or perfusion imaging of the bone marrow is feasible as the reproducibility of these techniques is high (Study 4), particularly in areas with either high fat content or relatively good perfusion (Study 4). Independent of baseline BMD level, the presence of high marrow fat content or reduced perfusion either in bone or muscle at baseline does predict accelerated bone loss over the ensuing 4 years (Study 8). Elderly subjects with increased marrow fat content or decreased perfusion tend to loose bone at an average rate of 1.25% per annum compared to those with decreased marrow fat content or increased perfusion who loose bone at an average rate of 0.25% per annum (Study 8).

Bone loss clearly does not occur in isolation. Instead in occurs in conjunction with changes in fat, other marrow constituents and perfusion. A more encompassing

paradigm which looks at bone as well as its microenvironment is likely to be the

model that best serves future osteoporotic research. We are continuing with this line

of research, studying in greater detail the type of perfusion abnormalities occurring in

bone; the reasons behind these changes; the change in marrow composition with

osteoporosis, and the feasibility of using MR to evaluate these changes in vivo.

References

Alagiakrishnan K, Juby A, Hanley D, Tymchak W, Sclater A. Role of vascular factors in osteoporosis. J Gerontol A Biol Sci Med Sci 2003;58:362-366.

Armour KE, Armour KJ, Gallagher ME, Godecke A, Helfrich MH, Reid DM, Ralston SH. Defective bone formation and anabolic response to exogenous estrogen in mice with targeted disruption of endothelial nitric oxide synthase. Endocrinology 2001;142:760-766.

Anetzberger H, Thein E, Becker M, Zwissler B, Messmer K. Microspheres accurately predict regional bone blood flow. Clin Orthop Relat Res 2004;424:253-265.

Angrigiani C, Grilli D, Thorne CH. The adductor flap: a new method for transferring posterior and medial thigh skin. Plast Reconstr Surg 2001;107:1725–1731.

Bagger YZ, Tankó LB, Alexandersen P, Qin G, Christiansen C; Prospective Epidemiological Risk Factors Study Group. Radiographic measure of aorta calcification is a site-specific predictor of bone loss and fracture risk at the hip. J Intern Med. 2006;259:598-605.

Barnes R, Brown JT, Garden RS, Nicoll EA. Subcapital fractures of the femur: A prospective review. J Bone Joint Surg Br 1976;58:2–24.

Bassey EJ, Littlewood JJ, Rothwell MC, Pye DW. Lack of effect of supplementation with essential fatty acids on bone mineral density in healthy pre- and postmenopausal women: two randomized controlled trials of Efacal v. calcium alone. Br J Nutr 2000;83:629-635.

Basu S, Houseni M, Bural G, Chamroonat W, Udupa J, Mishra S, Alavi A. Magnetic resonance imaging based bone marrow segmentation for quantitative calculation of pure red marrow metabolism using 2-deoxy-2-[F-18] fluoro-D-glucose-positron emission tomography: a novel application with significant implications for combined structure-function approach. Mol Imaging Biol 2007;9:361-365.

Baur A, Dietrich O, Reiser M. Diffusion-weighted imaging of bone marrow: current status. Eur Radiol 2003;13:1699-1708.

Baur A, Stabler A, Bartl R, Lamerz R, Scheidler J, Reiser M. MRI gadolinium enhancement of bone marrow: age-related changes in normals and in diffuse neoplastic infiltration. Skeletal Radiol 1997; 26:414-418.

Beck M, Leunig M, Ellis T, Sledge JB, Ganz R. The acetabular blood supply: implications for periacetabular osteotomies. Surg Radiol Anat 2003; 25:361–367.

Bernard C, Liney G, Manton D, Turnbull L, Langton C. Comparison of fat quantification methods: a phantom study at 3.0T. J Magn Reson Imaging 2008;27:192-197.

Blake GM, Fogelman I. The role of DXA bone density scans in the diagnosis and treatment of osteoporosis. Postgrad Med J 2007;83:509-517.

Blake GM, Park-Holohan SJ, Cook GJ, Fogelman I. Quantitative studies of bone with the use of 18F-fluoride and 99mTc-methylene diphosphonate. Semin Nucl Med 2001;31:28-49.

Bloomfield SA, Hogan HA, Delp MD. Decreases in bone blood flow and bone material properties in aging Fischer-344 rats. Clin Orthop 2002; 396:248-257.

Bridgeman G, Brookes M. Blood supply to the human femoral diaphysis in youth and senescence. J Anat. 1996;188:611-621.

Browner WS, Seeley DG, Vogt TM, Cummings SR. Non-trauma mortality in elderly women with low bone mineral density. Study of Osteoporotic Fractures Research Group. Lancet 1991; 338:355-358.

Bolotin HH. DXA *in vivo* BMD methodology: an erroneous and misleading research and clinical gauge of bone mineral status, bone fragility and bone remodelling. Bone 2007;41:138-154.

Bolotin H, Sievanen H, Grashuis J. Patient-specific DXA bone mineral density inaccuracies: quantitative effects of nonuniform extraosseous fat distributions. J Bone Miner Res 2003;18:1020-1027.

Bolotin HH, Sievansen H, Grashuis JL, Kuiper JW, Jarvinen TL. Inaccuracies inherent in patient-specific dual-energy x-ray absorptiometry bone mineral density measurements: comprehensive phantom-based evaluation. J Bone Miner Res 2001;16:417-426.

Bolotin HH. Analytic and quantitative exposition of patient-specific systematic inaccuracies inherent in planar DXA-derived in-vivo BMD measurements. Med Phys 1998;25:139-151.

Bucay N, Sarosi I, Dunstan CR, et al. Osteoprotegerin-deficient mice develop early onset osteoporosis and arterial calcification. Genes Dev 1998;12:1260-1268.

Burkhardt R, Kettner G, Bohm W et al. Changes in trabecular bone, hematopoiesis and bone marrow vessels in aplastic anemia, primary

osteoporosis, and old age: a comparative histomorphometric study. Bone 1987; 8:157-164.

Chahal HS, Drake WM. The endocrine system and ageing. J Pathol 2007;211:173-180.

Chen WT, Ting-Fang Shih T, Hu CJ, Chen RC, Tu HY. Relationship between vertebral bone marrow blood perfusion and common carotid intima-media thickness in aging adults. J Magn Reson Imaging 2004;20:811-816.

Chen WT, Shih T, Chen RC et al. Vertebral bone marrow perfusion evaluated with dynamic contrast-enhanced MR imaging: significance of aging and sex. Radiology 2001; 220:213-218.

Chen LT, Chen MF, Porter VL. Increased bone marrow blood flow in rabbits with acute hemolytic anemia. Am J Hematol 1986;22:35-41.

Choyke PL, Dwyer AJ, Knopp MV. Functional tumor imaging with dynamic contrast-enhanced magnetic resonance imaging. J Magn Reson Imaging 2003;17:509-520.

Coetzee M, Haag M, Kruger MC. Effects of arachidonic acid, docosahexaenoic acid, prostaglandin E(2) and parathyroid hormone on osteoprotegerin and RANKL secretion by MC3T3-E1 osteoblast-like cells. J Nutr Biochem 2007;18:54-63.

Coetzee M, Haag M, Joubert AM, Kruger MC. Effects of arachidonic acid, docosahexaenoic acid and prostaglandin E(2) on cell proliferation and morphology of MG-63 and MC3T3-E1 osteoblast-like cells. Prostaglandins Leukot Essent Fatty Acids 2007;76:35-45.

Compston JE, Croucher PI. Histomorphometric assessment of trabecular bone remodelling in osteoporosis. Bone and Mineral 1991;14:91-102.

Cook GJR, Blake GM, Marsden PK, Cronin B, Fogelman I. Quantification of skeletal kinetic indices in Paget's disease using dynamic ^{18}F-fluoride positron emission tomography. J Bone Miner Res 2002;17:854-859.

Cooper C. Epidemiology of osteoporosis. Osteoporos Int 1999;9:S2-8.

Cooper C, Atkinson EJ, Kotowicz M, O'Fallon WM, Melton LJ 3rd. Secular trends in the incidence of postmenopausal vertebral fractures. Calcif Tissue Int. 1992;51(2):100-104.

Copp DH, Shim SS. Extraction ratio and bone clearance of Sr^{85} as a measure of effective bone blood flow. Circ. Res 1965;16: 461-467.

Corwin RL, Hartman TJ, Maczuga SA, Graubard BI. Dietary saturated fat intake is inversely associated with bone density in humans: analysis of NHANES III. J. Nutr 2006;136:159-165.

Cova M, Kang YS, Tsukamoto H et al. Bone marrow perfusion evaluated with gadolinium-enhanced dynamic fast MR imaging in a dog model. Radiology 1991;179:535-539.

Crock HV, Yoshizawa H. The blood supply of the lumbar vertebral column. Clin Orthop Relat Res 1976;115:6-21.

Cummings, SR, Melton LJ. Epidemiology and outcomes of osteoporotic fractures. Lancet 2002;359:1761–1767.

Cummings SR, Nevitt MC, Browner WS, Stone K, Fox KM, Ensrud KE, Cauley J, Black D, Vogt TM. Risk factors for hip fracture in white women. Study of Osteoporotic Fractures Research Group. N Engl J Med. 1995;23:767-773.

Cumming JD. A Method for studying the rate of blood flow through the bone marrow of a rabbit's femur. J. Physiol 1960;152: 39P-40P.

Damilakis J, Maris TG, Karantanas AH. An update on the assessment of osteoporosis using radiologic techniques. Eur Radiol 2007;17:1591-1602.

D'Ippolito G, Diabira S, Howard GA, Roos BA, Schiller PC. Low oxygen tension inhibits osteogenic differentiation and enhances stemness of human MIAMI cells. Bone 2006;39:513-22.

Donahue MJ, Lu H, Jones CK, Pekar JJ, van Zijl PC. An account of the discrepancy between MRI and PET cerebral blood flow measures. A high-field MRI investigation. NMR Biomed 2006;19:1043-1054.

Duque G. As a matter of fat: New perspectives on the understanding of age-related bone loss. BoneKEy-Osteovision 2007;4; 129-140.

Duque G. Bone and fat connection in aging bone. Curr Opin Rheumatol 2008;20:429-34.

Edholm DG, Howarth S, McMichael J. Heart Failure and bone blood flow in osteitis deformans. Clin. Sci 1945;5:249-260.

Eriksen EF, Eghbali-Fatourechi GZ, Khosla S. Remodeling and vascular spaces in bone. J Bone Miner Res 2007;22:1-6.

Fatokun AA, Stone TW, Smith RA. Hydrogen peroxide-induced oxidative stress in MC3T3-E1 cells: The effects of glutamate and protection by purines. Bone 2006;39:542-51.

Faulkner K. The tale of the T-score: review and perspective. Osteoporos Int 2005;16:347-352.

Frederickson JM. Honour AJ. Copp DH. Measurement of Initial bone clearance of Ca^{45} from blood in the rat. Fed. Proc 1955;14: 49.

Frost ML, Fogelman I, Blake GM, Marsden PK, Fogelman I. Dissociation between global markers of bone formation and direct measurement of spinal bone formation in osteoporosis. J Bone Miner Res 2004;19:1797-1804.

Galbraith SM, Lodge MA, Taylor NJ, Rustin GJ, Bentzen S, Stirling JJ, Padhani AR. Reproducibility of dynamic contrast-enhanced MRI in human muscle and tumours: comparison of quantitative and semi-quantitative analysis. NMR Biomed 2002;15:132-42.

Garnero P, Delmas PD. Contribution of bone mineral density and bone turnover markers to the estimation of risk of osteoporotic fracture in postmenopausal women. J Musculoskelet Neuronal Interact. 2004;4:50-63.

Garnero P, Sornay-Rendu E, Duboef F, Delmas PD. Markers of bone turnover for the prediction of fracture risk. Osteoporos Int 1999;11(Suppl 6):55-65.

Gautier E, Ganz K, Krugel N, Gill T, Ganz R. Anatomy of the medial femoral circumflex artery and its surgical implications. J Bone Joint Surg Br 2000;82:679–683.

Genant HK, Wu CY, van Kuijk C, Nevitt MC. Vertebral fracture assessment using a semiquantitative technique. J Bone Miner Res 1993;8:1137-1148.

Gimble JM, Nuttall ME. Bone and fat: old questions, new insights. Endocrine 2004;23:183-8.

Griffith JF, Yeung DK, Tsang PH, et al. Compromised bone marrow perfusion in osteoporosis. J Bone Miner Res 2008;23:1068-1075.

Griffith JF, Yeung DK, Antonio GE, Wong SY, Kwok TC, Woo J, Leung PC. Vertebral marrow fat content and diffusion and perfusion indexes in women with varying bone density: MR evaluation. Radiology 2006;241:831-838.

Griffith JF, Yeung DK, Antonio GE, Lee FK Hong, AW, Wong, SY, Lau E.M, Leung PC. Vertebral bone mineral density, marrow perfusion, and fat content in healthy men and men with osteoporosis: dynamic contrast-enhanced MR imaging and MR spectroscopy. Radiology 2005;236:945–951.

Gross PM, Heistad DD, Marcus ML. Neurohumoral regulation of blood flow to bones and marrow. Am J Physiol 1979;237:H440-448.

Goodsitt MM, Hoover P, Veldee MS, Hsueh SL. The composition of bone marrow for a dual-energy quantitative computed tomography technique. A cadaver and computer simulation study. Invest Radiol 1994;29:695-704.

Gurkan UA, Akkus O. The mechanical environment of bone marrow: a review. Ann Biomed Eng. 2008;36:1978-1991.

Hadjidakis DJ, Androulakis II. Bone remodeling. Ann N Y Acad Sci 2006;1092:385-396.

Hauge EM, Qvesel D, Eriksen EF, Mosekilde L, Melsen F. Cancellous bone remodeling occurs in specialized compartments lined by cells expressing osteoblastic markers. J Bone Miner Res. 2001;16:1575-1582.

Hartsock RJ, Smith EB, Petty CS. Normal variations with aging of the amount of hematopoetic tissue in bone marrow from the anterior iliac crest. A study made from 177 cases of sudden death examined by necropsy. Am J Clin Pathol 1965;43:326-331.

Hedstrom. M. Are patients with a nonunion after a femoral neck fracture more osteoporotic than others? BMD measurement before the choice of treatment? A pilot study of hip BMD and biochemical bone markers in patients with femoral neck fractures. Acta Orthop Scan 2004;75:50–52.

Holling E, Oey RS, Boland HC. Pulmonary Hypertrophic Osteoartropathy. Lancet 1961;2:1269-1274.

Hubbell JH, Seltzer SM. Tables of x-ray mass attenuation coefficients and mass energy absorption coefficients. (accessed 2009)
http://physics.nist.gov/PhysRefData/XrayMassCoef/cover.html

Hwang S, Panicek DM. Magnetic resonance imaging of bone marrow in oncology, Part 1. Skeletal Radiol 2007;36:913-920.

ICRP. Basic anatomical and physiological data for use in radiological protection: the skeleton. ICRP Publication 70. Oxford, UK: International Commission on Radiological Protection. 1995.

Iversen PO, Nicolaysen G, Benestad HB. Blood flow to bone marrow during development of anemia or polycythemia in the rat. Blood 1992;79:594-601.

Jackson M, Learmonth ID. The treatment of nonunion after intracapsular fracture of the proximal femur. Clin Orthop Relat Res. 2002 ;399:119-128.

Jee WS, Yao W. Overview: animal models of osteopenia and osteoporosis. J Musculoskelet Neuronal Interact 2001;1:193-207.

Johnell O, Oden A, De Laet C, Garnero P, Delmas PD, Kanis JA. Biochemical indices of bone turnover and the assessment of fracture probability. Osteoporos Int 2002;13:523-526.

Johnell O, Kanis JA, Oden A, Johansson H, De Laet C, Delmas P, Eisman JA, Fujiwara S, Kroger H, Mellstrom D, Meunier PJ, Melton LJ 3rd, O'Neill T, Pols H, Reeve J, Silman A, Tenenhouse A. Predictive value of BMD for hip and other fractures. J Bone Miner Res 2005;20:1185-1194.

Justesen J, Stenderup K, Ebbesen EN, Mosekilde L, Steiniche T, Kassem M. Adipocyte tissue volume in bone marrow is increased with aging and in patients with osteoporosis. Biogerontology 2001;2:165–171.

Kanis, JA. Diagnosis of osteoporosis and assessment of fracture risk. Lancet 2002;359:1929–1936.

Kato H, Hasegawa M, Takada T, Torii S. The lumbar artery perforator based island flap: anatomical study and case reports. Br J Plast Surg 1999;52:541-546.

Kha HT, Basseri B, Shouhed D, Richardson J, Tetradis S, Hahn TJ, Parhami F. Oxysterols regulate differentiation of mesenchymal stem cells: pro-bone and anti-fat. J Bone Miner Res 2004;19:830-40.

Knopp EA, Cowper SE. Nephrogenic systemic fibrosis: early recognition and treatment. Semin Dial 2008;21:123-128.

Knopp MV, Giesel FL, Marcos H, von Tengg-Kobligk H, Choyke P. Dynamic contrast-enhanced magnetic resonance imaging in oncology. Top Magn Reson Imaging 2001;12:301-308.

Knothe Tate ML, Niederer P, Knothe U. In vivo tracer transport through the lacunocanalicular system of rat bone in an environment devoid of mechanical loading. Bone 1998;22:107-117.

Kruger MC, Coetzer H, de Winter R, Gericke G, van Papendorp DH. Calcium, gamma-linolenic acid and eicosapentaenoic acid supplementation in senile osteoporosis. Aging (Milano) 1998;10:385-394.

Kugel H, Jung C, Schulte O, Heindel W. Age- and sex-specific differences in the 1H-spectrum of vertebral bone marrow. J Magn Reson Imaging 2001; 13:263-268.

Lahtinen T, Alhava EM, Karjalainen P, Romppanen T. The effect of age on blood flow in the proximal femur in man. J Nucl Med 1981;22:966-972.

Lang P, Honda G, Roberts T, Vahlensieck M, Johnston JO, Rosenau W, Mathur A, Peterfy C, Gooding CA, Genant HK. Musculoskeletal neoplasm: perineoplastic edema versus tumor on dynamic postcontrast MR images with spatial mapping of instantaneous enhancement rates. Radiology 1995;197:831-839.

Laroche M, Ludot I, Thiechart M, Arlet J, Pieraggi M, Chiron P, Moulinier L, Cantagrel A, Puget J, Utheza G, et al. Study of the intraosseous vessels of the femoral head in patients with fractures of the femoral neck or osteoarthritis of the hip. Osteoporos Int 1995;5:213–217.

Lehmann LA, Alvarez RE, Macovski A, Brody WR, Pelc NJ, Riederer SJ, Hall AL. Generalized image combinations in dual KVP digital radiography. Med Phys 1981;8: 659-667.

Lelovas PP, Xanthos TT, Thoma SE, Lyritis GP, Dontas IA. The laboratory rat as an animal model for osteoporosis research. Comp Med 2008;58:424-30.

Leonard AE, Pereira SL, Sprecher H, Huang YS. Elongation of long-chain fatty acids. Prog Lipid Res 2004;43:36-54.

Lichtman MA. The ultrastructure of the hemopoietic environment of the marrow: a review. Exp Hematol 1981;9:391-410.

Liu XQ, Chen HY, Tian XY, Setterberg RB, Li M, Jee WS. Alfacalcidol treatment increases bone mass from anticatabolic and anabolic effects on cancellous and cortical bone in intact female rats. J Bone Miner Metab 2008;26:425-35.

Luypaert R, Boujraf S, Sourbron S, Osteaux M. Diffusion and perfusion MRI: basic physics. Eur J Radiol 2001;38:19-27.

Lund PK, Abadi DM, Mathies JC. Lipid composition of normal human bone marrow as determined by gas chromatography. J Lipid Res 1962;3:95.

Lynn HS, Lau EM, Au B, Leung PC. Bone mineral density reference norms for Hong Kong Chinese. Osteoporos Int 2005;16:1663-1668.

Marcovitz PA, Tran HH, Franklin BA, O'Neill WW, Yerkey M, Boura J, Kleerekoper M, Dickinson CZ. Usefulness of bone mineral density to predict significant coronary artery disease. Am J Cardiol. 2005;96:1059-1063.

Marks SC, Odgren PR. Structure and development of the skeleton. In J.P. Bilezikian, L.G. Raisz, Rodan G.A (Eds.) Principles of bone biology. New York Academic 2002;1:3-15.

Marshall D, Johnell O, Wedel H. Meta-analysis of how well measures of bone mineral density predict occurrence of osteoporotic fractures. BMJ. 1996;312:1254-1259.

Martin TJ, Seeman E. Bone remodelling: its local regulation and the emergence of bone fragility. Best Pract Res Clin Endocrinol Metab. 2008;22(5):701-722.

Martiat P, Ferrant A, Cogneau M, Bol A, Michel C, Rodhain J, Michaux JL, Sokal G. Assessment of bone marrow blood flow using positron emission tomography: no relationship with bone marrow cellularity. Br J Haematol 1987;66:307-310.

Matthews V, Cabanela ME. Femoral neck nonunion treatment. Clin Orthop Relat Res 2004; 419:57-64.

Maurin AC, Chavassieux PM, Vericel E, Meunier PJ. Role of polyunsaturated fatty acids in the inhibitory effect of human adipocytes on osteoblastic proliferation. Bone 2002;31:260-266.

McCarthy I. The physiology of bone blood flow: a review. J Bone Joint Surg Am. 2006;88 Suppl 3:4-9.

McCarthy ID. Fluid shifts due to microgravity and their effects on bone: a review of current knowledge. Ann Biomed Eng 2005;33:95-103.

McLean RR. Proinflammatory cytokines and osteoporosis. Curr Osteoporos Rep. 2009;7:134-139.

Messa C, Goodman WG, Hoh CK, Choi Y, Nissenson AR, Salusky IB, Phelps ME, Hawkins RA. Bone metabolic activity measured with positron emission tomography and ^{18}F-fluoride ion in renal osteodystophy: correlation with bone histomorphometry. J Clin Endo Metab 1993;77:949-955.

Montazel JL, Divine M, Lepage E, Kobeiter H, Breil S, Rahmouni A. Normal spinal bone marrow in adults: dynamic gadolinium-enhanced MR imaging. Radiology 2003;229:703-709.

Moore SG, Dawson KL. Red and yellow marrow in the femur: age-related changes in appearance at MR imaging. Radiology. 1990;175(1):219-223.

Musacchio E, Priante G, Budakovic A, Baggio B. Effects of unsaturated free fatty acids on adhesion and on gene expression of extracellular matrix macromolecules in human osteoblast-like cell cultures. Connect Tissue Res 2007;48:34-38.

Nakashima K, de Crombrugghe B. Transcriptional mechanisms in osteoblast differentiation and bone formation. Trends Genet 2003;19:458-466.

Ness J, Aronow WS. Comparison of prevalence of atherosclerotic vascular disease in postmenopausal women with osteoporosis or osteopenia versus without osteoporosis or osteopenia. Am J Cardiol. 2006;97:1427-1428.

Nevitt MC, Cummings SR, Stone KL, Palermo L, Black DM, Bauer DC, Genant HK, Hochberg MC, Ensrud KE, Hillier TA, Cauley JA. Risk factors for a first-incident radiographic vertebral fracture in women > or = 65 years of age: the study of osteoporotic fractures. J Bone Miner Res. 2005;20:131-140.

Nguyen N, Pongchaiyakul C, Center J, Eisman J, Nguyen T. Identification of high-risk individuals for hip fracture: a 14-year prospective study. J Bone Miner Res 2005;20:1921-1928.

Nord RH, Payne RK. Standards for body composition calibration in DEXA. Current Research in Osteoporosis and Bone Mineral Measurement. London, UK: British Institute of Radiology.1990; 27-28.

Parfitt AM. The mechanism of coupling: a role for the vasculature.
Bone 2000;26:319-23.

Parker GJ, Suckling J, Tanner SF, Padhani AR, Revell PB, Husband JE, Leach MO. Probing tumor microvascularity by measurement, analysis and display of contrast agent uptake kinetics.   Magn Reson Imaging 1997;7:564-574.

Piert M, Machulla H-J, Jahn M, Stahlschmidt A, Becker GA, Zittel TT.   Coupling of porcine bone blood flow and metabolism in high-turnover bone disease measured by ^{15}OH20 and ^{18}F-fluoride ion positron emission tomography. Eur J Nucl Med 2002;29:907-914.

Piert M, Zittel TT, Becker GA, Jahn M, Stahlschmidt A, Maier G, Machulla H-J, Bares R. Assessment of porcine bone metabolism by dynamic ^{18}F-fluoride PET: correlation with bone histomorphometry. J Nucl Med 2001;42:1091-1100.

Piert M, Zittel TT, Machulla HJ, Becker GA, Jahn M, Maier G, Bares R, Becker HD. Blood flow measurements with [(15)O]H2O and [18F]fluoride ion PET in porcine vertebrae. J Bone Miner Res. 1998;13:1328-1336.

Prisby RD, Ramsey MW, Behnke BJ, et al. Aging Reduces Skeletal Blood Flow, Endothelium-Dependent Vasodilation and Nitric Oxide Bioavailability in Rats. J Bone Miner Res 2007;22:1280-1288.

Port M, Idée JM, Medina C, Robic C, Sabatou M, Corot C. Efficiency, thermodynamic and kinetic stability of marketed gadolinium chelates and their possible clinical consequences: a critical review. Biometals 2008;21:469-490.

Poulton TB, Murphy WD, Duerk JL, Chapek CC, Feiglin DH. Bone marrow reconversion in adults who are smokers: MR Imaging findings. Am J Roentgenol 1993;161:1217-1221.

Poulsen RC, Wolber FM, Moughan PJ, Kruger MC. Long chain polyunsaturated fatty acids alter membrane-bound RANK-L expression and osteoprotegerin secretion by MC3T3-E1 osteoblast-like cells. Prostaglandins Other Lipid Mediat 2008;85:42-48.

Poulsen RC, Moughan PJ, Kruger MC. Long-chain polyunsaturated fatty acids and the regulation of bone metabolism. Exp Biol Med (Maywood) 2007;232:1275-1288.

Poulsen RC, Firth EC, Rogers CW, Moughan PJ, Kruger MC. Specific effects of gamma-linolenic, eicosapentaenoic, and docosahexaenoic ethyl esters on bone post-ovariectomy in rats. Calcif Tissue Int 2007;81:459-471.

Poulsen RC, Kruger MC. Detrimental effect of eicosapentaenoic acid supplementation on bone following ovariectomy in rats. Prostaglandins Leukot Essent Fatty Acids 2006;75:419-27.

Ratcliffe JF. The arterial anatomy of the adult human lumbar vertebral body: a microarteriographic study. J Anat 1980;131:57-79.

Rawlinson SC, el-Haj AJ, Minter SL, Tavares IA, Bennett A, Lanyon LE. Loading-related increases in prostaglandin production in cores of adult canine

cancellous bone in vitro: a role for prostacyclin in adaptive bone remodeling? J Bone Miner Res 1991;6:1345-1351.

Reddick WE, Taylor JS, Fletcher BD. Dynamic MR imaging (DEMRI) of microcirculation in bone sarcoma. J Magn Reson Imaging 1999;10:277-285.

Reece RJ, Kraan MC, Radjenovic A, Veale DJ, O'Connor PJ, Ridgway JP, Gibbon WW, Breedveld FC, Tak PP, Emery P. Comparative assessment of leflunomide and methotrexate for the treatment of rheumatoid arthritis, by dynamic enhanced magnetic resonance imaging. Arthritis Rheum 2002;46:366-372.

Reeve J, Arlot M, Wootton R, Edouard C, Tellez M, Hesp R, Green JR, Meunier PJ. Skeletal blood flow, iliac histomorphometry, and strontium kinetics in osteoporosis: a relationship between blood flow and corrected apposition rate. J Clin Endocrinol Metab 1988;66:1124-1131.

Reinwald S, Li Y, Moriguchi T, Salem N Jr, Watkins BA. Repletion with (n-3) fatty acids reverses bone structural deficits in (n-3)-deficient rats. J Nutr 2004;134:388-394.

Ren J, Dimitrov I, Sherry AD, Malloy CR. Composition of adipose tissue and marrow fat in humans by 1H NMR at 7 Tesla. J Lipid Res 2008 49:2055-2062.

Rivadeneira F, Zillikens MC, De Laet CE, Hofman A, Uitterlinden AG, Beck TJ, Pols HA. Femoral neck BMD is a strong predictor of hip fracture susceptibility in elderly men and women because it detects cortical bone instability: the Rotterdam Study. J Bone Miner Res 2007;22:1781-1790.

Rodan GA. Introduction to bone biology. Bone 1992;13:S3-6.

Rosen CJ, Bouxsein ML. Mechanisms of disease: is osteoporosis the obesity of bone? Nat Clin Pract Rheumatol 2006;2:35-43.

Rozman C, Feliu E, Berga L, Reverter JC, Climent C, Ferran MJ. Age-related variations of fat tissue fraction in normal human bone marrow depend both on size and number of adipocytes: a stereological study. Exp Hematol 1989; 17:34-37.

Rubin C, Recker R, Cullen D, Ryaby J, Mccabe J, McLeod K. Prevention of post-menopausal bone loss by a low magnitude, high frequency mechanical stimuli: a clinical trial assessing compliance, efficacy and safety. J Bone Miner Res 2004;19:343-351.

Sahota O, Pearson D, Cawte SW, San P, Hosking DJ. Site-specific variation in the classification of osteoporosis, and the diagnostic reclassification using the lowest individual lumbar vertebra T-score compared with the L1-L4 mean, in early postmenopausal women. Osteoporos Int. 2000;11:852-857.

Saito N, Miyasaka T, Toriumi H. Radiographic factors predicting non-union of displaced intracapsular femoral neck fractures. Archives of Orthopaedic and Trauma Surgery 1995;14: 183-187.

Sambrook P, Cooper C. Osteoporosis. Lancet 2006;367:2010–2018.

Samuels A, Perry MJ, Gibson RL, Colley S, Tobias JH. Role of endothelial nitric oxide synthase in estrogen-induced osteogenesis. Bone 2001;29:24–29.

Sanada M, Taguchi A, Higashi Y, Tsuda M, Kodama I, Yoshizumi M, Ohama K. Forearm endothelial function and bone mineral loss in postmenopausal women. Atherosclerosis. 2004;176:387-92.

Schellinger D, Lin CS, Hatipoglu HG, Fertikh D. Potential value of vertebral proton MR spectroscopy in determining bone weakness. Am J Neuroradiol 2001;22:1620-1627.

Schellinger D, Lin SC, Fertikh D, Lee JS, Lauerman WC, Henderson F, Davis Normal Lumbar Vertebrae: Anatomic, Age, and Sex Variance in Subjects at Proton MR Spectroscopy-Initial Experience. Radiology 2000;215:910-916.

Schuit SC, Klift Mvd, Weel AE, et al. Fracture incidence and association with bone mineral density in elderly men and women: the Rotterdam Study. Bone. 2004;34:195-202.

Schoutens A, Verhas M, Dourov N, Verschaeren A, Mone M, Heilporn A. Anaemia and marrow blood flow in the rat. Br J Haematol 1990;74:514-518.

Seeman E. The periosteum--a surface for all seasons. Osteoporos Int. 2007;18:123–128.

Seeman E. Pathogenesis of bone fragility in women and men. Lancet 2002;359:1841–1850.

Shaw Ne. Observations on the intramedullary blood-flow and marrow-pressure in bone. Clin Sci. 1963;24:311-318.

Shih TT, Liu HW, Chang CJ, Wei SY, Shen LC, Yang PC. Correlation of MR lumbar bone marrow perfusion with bone mineral density in female subjects. Radiology 2004;233:121-128.

Shih TT, Chang CJ, Tseng WY et al. Effect of calcium channel blockers on vertebral bone marrow perfusion of the lumbar spine. Radiology 2004; 231:24-30.

Shim SS, Copp DH, Patterson FP. An Indirect method of bone blood-flow measurement based on the bone clearance of a circulating bone-seeking radioisotope. J. Bone and Joint Surg, 1967; 49A: 693-702.

Shouhed D, Kha HT, Richardson JA, Amantea CM, Hahn TJ, Parhami F. Osteogenic oxysterols inhibit the adverse effects of oxidative stress on osteogenic differentiation of marrow stromal cells. J Cell Biochem 2005;95:1276-1283.

Smalt R, Mitchell FT, Howard RL, Chambers TJ. Induction of NO and prostaglandin E2 in osteoblasts by wall-shear stress but not mechanical strain. Am J Physiol 1997;273:E751-758.

Steiniche T. Bone histomorphometry in the pathophysiological evaluation of primary and secondary osteoporosis and various treatment modalities. APMIS Suppl 1995;51:1-44.

Sterck JGH, Klein-Nulend J, Lips P, Burger EH. Response of normal and osteoporotic human bone cells to mechanical stress in vitro. Am J Physiol Endocrinol Metab 1998;274:E1113-E1120.

Sorenson JA. Effects of nonmineral tissues on measurement of bone mineral content by dual-photon absorptiometry. Med Phys 1990;17:905-912.

Sornay-Rendu E, Munoz F, Duboeuf F, Delmas P. Rate of forearm bone loss is associated with an increased risk of fracture independently of bone mass in postmenopausal women: the OFELY study. J Bone Miner Res 2005;20:1929-1935.

Soppela P, Nieminen M. The effect of wintertime undernutrition on the fatty acid composition of leg bone marrow fats in reindeer (Rangifer tarandus tarandus L.). Comp Biochem Physiol B Biochem Mol Biol 2001;128:63-72.

Steiner RM, Mitchell DG, Rao VM, Schweitzer ME. Magnetic resonance imaging of diffuse bone marrow disease. Radiol Clin North Am 1993;31:383-409.

Swiontkowski MF, Winquist RA, Hansen ST Jr. Fractures of the femoral neck in patients between the age of twelve and forty nine years. J Bone Joint Surg Am 1984;66:837–846.

Taddei S, Virdis A, Ghiadoni L, Mattei P, Sudano I, Bernini G, Pinto S, Salvetti A. Menopause is associated with endothelial dysfunction in women. Hypertension 1996;28:576-582.

Takasaki M, Tsurumi N, Harada M, Rokugo N, Ebihara Y, Wakasugi K. Changes of bone marrow arteries with aging. Japanese Nippon Ronen Igakkai Zasshi 1999;36:638-643.

Tavassoli M, Houchin DN, Jacobs P. Fatty acid composition of adipose cells in red and yellow marrow. A possible determinant of haematopoietic potential. Scand J Haematol 1977,8:47-53.

Tenenhouse A, Joseph L, Kreiger N, Poliquin S, Murray TM, Blondeau L, Berger C, Hanley DA, Prior JC; CaMos Research Group.Canadian Multicentre Osteoporosis Study. Estimation of the prevalence of low bone density in Canadian women and men using a population-specific DXA reference standard: the Canadian Multicentre Osteoporosis Study (CaMos). Osteoporos Int 2000;11:897-904.

Theill LE, Boyle WJ, Penninger JM. RANK-L and RANK: T cells, bone loss, and mammalian evolution. Annu Rev Immunol 2002;20:795-823.

Travlos GS. Normal structure, function, and histology of the bone marrow. Toxicol Pathol. 2006;34:548-565.

Tofts PS. Modeling tracer kinetics in dynamic Gd-DTPA MR imaging. J Magn Reson Imaging 1997;7:91-101.

Vande Berg BC, Lecouvet FE, Moysan P, Maldague B, Jamart J, Malghem J. MR assessment of red marrow distribution and composition in the proximal femur: correlation with clinical and laboratory parameters. Skeletal Radiol. 1997; 26:589–596.

VanDyke D, Anger H O, Yano Y, Bozzini C. Bone blood flow shown with F^{18} and positron camera. Am. J. Physiol 1965;209:65-70.

Verma S, Rajaratnam JH, Denton J, Hoyland JA, Byers RJ. Adipocytic proportion of bone marrow is inversely related to bone formation in osteoporosis. J Clin Pathol 2002;55:693-8.

Von der Recke P, Hansen MA, Hassager C. The association between low bone mass at the menopause and cardiovascular mortality. Am J Med. 1999; 106:273-278.

Yeung DK, Lam SL, Griffith JF, Chan AB, Chen Z, Tsang PH, Leung PC. Analysis of bone marrow fatty acid composition using high-resolution proton NMR spectroscopy. Chem Phys Lipids 2008;151:103-109.

Yeung DKW, Wong SYS, Griffith JF, Lau EMC. Bone marrow diffusion in osteoporosis: evaluation with quantitative MR diffusion imaging. JMRI reference. J Magn Reson Imaging 2004;19:222-228.

Wang YX, Griffith JF, Zhou H, Choi KC, Hung VW, Yeung DK, Qin L, Ahuja AT. Rat lumbar vertebrae bone densitometry using multidetector CT. Eur Radiol. 2009;19:882-90.

Watkins BA, Li Y, Lippman HE, Seifert MF. Omega-3 polyunsaturated fatty acids and skeletal health. Exp Biol Med (Maywood) 2001;226:485-497.

Watkins BA, Li Y, Allen KG, Hoffmann WE, Seifert MF. Dietary ratio of (n-6)/(n-3) polyunsaturated fatty acids alters the fatty acid composition of bone compartments and biomarkers of bone formation in rats. J Nutr 2000;130: 2274-2284.

Weathersby HT. The origin of the artery of the ligamentum teres femoris. J Bone Joint Surg Am 1959;41A:261-263.

Weinman DT, Kelly PJ, Owen CA Jr, Orvis A L. Skeletal clearance of Ca47 and Sr^{85} and skeletal blood flow in dogs. Proc. staff meet. Mayo clin 1963;38: 559-570.

Weiss LA, Barrett-Connor E, von Muhlen D. Ratio of n-6 to n-3 fatty acids and bone mineral density in older adults: the Rancho Bernardo Study. Am J Clin Nutr 2005;81:934-938.

Weiss LP, Wislocki GB. Seasonal variations in hematopoiesis in the dermal bones of the nine-banded armadillo. Anat Rec 1956;126:143-163.

WHO Study Group. Assessment of risk fracture and its implications to screening for post-menopausal osteoporosis. WHO, Geneva. WHO technical report series 1994;843.

Williams A, Newell RLM, Collins P. Back and macroscopic anatomy of the spinal cord. In: Standring S, ed. Gray's anatomy. The anatomical basis of clinical practice. 39th ed. Edinburgh. Elsevier, 2005;734-776.

Wong CM, Yung LM, Leung FP, Tsang SY, Au CL, Chen ZY, Yao X, Cheng CH, Lau CW, Gollasch M, Huang Y. Raloxifene protects endothelial cell function against oxidative stress. Br J Pharmacol 2008;155:326-34.

Zhou SH, McCarthy ID, McGregor AH, Coombs RRH, Hughes SPF. Geometrical dimensions of the lower lumbar vertebrae – analysis of data from digitized CT images. Eur Spine J 2000;9:242-248.

ABBREVIATION LIST (in alphabetical order)

AIF: Arterial input function
ANCOVA: Analysis of covariance
AUC: Area under the curve
BOLD: Blood oxygen level dependent
BMC:Bone mineral content
BMD: Bone mineral density
C: carbon
Ca: calcium
CFA: Comparative fit index
CT: Computed tomography
DCE: Dynamic contrast enhanced
DXA dual x-ray absorbiometry
Emax: Enhancement maximum
Eslope: Enhancement slope
F: Fluroride
FDG: Flurodeoxyglucose
G: Glomerular filtration rate
Ge: Germanium
Ga: Gallium
GFI: Goodness of fit index
H: Hydrogen
IDEAL: Iterative Decomposition of water with Echo Asymmetry and Least-squares
estimation.
Imax: Intensity maxium
Ibase: Intensity baseline
K: Potassium
L: Lower vertebral depth
Mg: Magnesium
MR : magnetic resonance
MRI: magnetic resonance imaging
MUFA: Monounsaturated fatty acids
MVP: Metabolic volumetric product
N: Nitrogen
Na: Sodium
NHANES: *National Health and Nutrition Examination Survey*
NNFI: Non-normed fit-index
NSF: Neprogenic sclerosing fibrosis
O: Oxygen
OPG: Osteoprotegerin
QCT: Quantitative CT
PET: Positron Emission Tomography
PPM: parts per million
PRESS: point-resolved spectroscopy

PQCT: Peripheral quantitative CT
PUFA: Polyunsaturated fatty acids
RANK: receptor-activated nuclear-kappa
RANKL: receptor-activated nuclear-kappa ligand
RMSEA: Root mean square error of approximation
ROC: Receiver operating characteristic
ROI: Region of interest
P:Phosphorus
SNR: Signal to noise ratio
STEAM: Stimulated echo acquisition mode
SRMR: Standardized root mean square rsidual
S: Sulphur
SD: standard deviation
SUV: standardized uptake value
TE: Time to echo
TR: Time to repetition
U:Upper vertebral depth
VOI: Volume of interest
WHO : World Health Organization

APPENDIX

<u>Ethics approval and Consent forms</u>

On the following pages, the forms for Ethics Approval on human studies granted by The Chinese University of Hong Kong – New Territories East Cluster Clinical Research Ethics Committee are presented

The Ethics Approval for animal studies granted by The Chinese University of Hong Kong, Animal Experimentation Ethics Committee are also presented.

Samples of consent forms used for the clinical studies in this Thesis are also presented. A similar consent was used for several of the clinical studies.

THE CHINESE UNIVERSITY OF HONG KONG

FACULTY OF MEDICINE

SHATIN. NT. HONG KONG

香 港 中 文 大 學
醫 學 院

香 港 新 界 沙 田

GENERAL OFFICE FAX. NO. 醫學院辦事處傳真： (852) 2603 6958

院長
鍾尚志教授
Dean
Professor S.C. Sydney Chung

Tel (電話): (852) 2609 6870
Fax (傳真): (852) 2603 6958
E-mail (電郵): sydneychung@cuhk.edu.hk

副院長（行政）
霍泰輝教授
Associate Dean (Administration)
Professor T.F. Fok

Tel (電話): (852) 2632 2850
Fax (傳真): (852) 2648 9134
E-mail (電郵): taifaifok@cuhk.edu.hk

副院長（臨床期科學）
張明仁教授
Associate Dean (Clinical)
Professor Allan M.Z. Chang

Tel (電話): (852) 2632 3489
Fax (傳真): (852) 2636 0008
E-mail (電郵): mangzchang@cuhk.edu.hk

副院長（醫學教育）
鄭振耀教授
Associate Dean (Medical Education)
Professor Jack C.Y. Cheng

Tel (電話): (852) 2632 2727
Fax (傳真): (852) 2637 7889
E-mail (電郵): jackcheng@cuhk.edu.hk

副院長（臨床前期科學）
李卓予教授
Associate Dean (Pre-Clinical)
Professor C.Y. Lee

Tel (電話): (852) 2609 6876
Fax (傳真): (852) 2603 5382
E-mail (電郵): cheukyulee@cuhk.edu.hk

副院長（研究）
盧煜明教授
Associate Dean (Research)
Professor Y.M. Dennis Lo

Tel (電話): (852) 2632 2563
Fax (傳真): (852) 2636 5090
E-mail (電郵): loym@cuhk.edu.hk

策劃處處長
陳燿墉先生
Planning Officer
Mr. Andrew Y.Y. Chan

Tel (電話): (852) 2609 6788
Fax (傳真): (852) 2603 6958
E-mail (電郵): yungchan@cuhk.edu.hk

Your Ref:

Our Ref: FM/C/13 – CRE-2002.282

5 September 2002

Dr. James Francis Griffith
Dept. of Diagnostic Radiology and
    Organ Imaging
CUHK

Dear Dr. Griffith,

      I write to inform you that ethical approval has been given for you to engage in the project named below:

Project Title   :   **"Evaluation of Water Diffusion in Normal Vertebral Bone Marrow with Quantitative Magnetic Resonance Diffusion – Weighted Imaging"**
[Ref. No. CRE-2002.282]

Investigator(s)   :   **Dr. James Francis GRIFFITH, Dept. of Diagnostic Radiology and Organ Imaging, CUHK**

               Dr. David KW YEUNG, Physicist, Dept. of Clinical Oncology, PWH

               Dr. Samuel Yeung Shan WONG, Physician, Jockey Club for Osteoporosis Care and Control, School of Public Health, CUHK

Duration   :   **6 Months**

Location of Study   :   **Prince of Wales Hospital**

Conditions by Clinical Research Ethics Committee (if any):   **Nil**

      It will be much appreciated if the completion of the project will be reported to the Committee in due course.

Yours sincerely,

Andrew Chan
Secretary
Clinical Research Ethics Committee

AC/bn

Serving the Community Through Quality Education, Caring Practice and Advancement of Health Sciences

254

THE CHINESE UNIVERSITY
OF HONG KONG

FACULTY OF MEDICINE
SHATIN. NT. HONG KONG

香 港 中 文 大 學
醫 學 院
香 港 新 界 沙 田

GENERAL OFFICE FAX. NO. 醫學院辦事處傳真： (852) 2603 6958

院長
鍾尚志教授
Dean
Professor S.C. Sydney Chung

Tel (電話): (852) 2609 6870
Fax (傳真): (852) 2603 6958
E-mail (電郵): sydneychung@cuhk.edu.hk

副院長 (行政)
霍泰輝教授
Associate Dean (Administration)
Professor T.F. Fok

Tel (電話): (852) 2632 2850
Fax (傳真): (852) 2648 9134
E-mail (電郵): taifaifok@cuhk.edu.hk

副院長 (臨床期科學)
張明仁教授
Associate Dean (Clinical)
Professor Allan M.Z. Chang

Tel (電話): (852) 2632 3489
Fax (傳真): (852) 2636 0008
E-mail (電郵): mangzchang@cuhk.edu.hk

副院長 (醫學教育)
鄭振耀教授
Associate Dean (Medical Education)
Professor Jack C.Y. Cheng

Tel (電話): (852) 2632 2727
Fax (傳真): (852) 2637 7889
E-mail (電郵): jackcheng@cuhk.edu.hk

副院長 (臨床前期科學)
李卓予教授
Associate Dean (Pre-Clinical)
Professor C.Y. Lee

Tel (電話): (852) 2609 6876
Fax (傳真): (852) 2603 5382
E-mail (電郵): cheukyulee@cuhk.edu.hk

副院長 (研究)
盧煜明教授
Associate Dean (Research)
Professor Y.M. Dennis Lo

Tel (電話): (852) 2632 2563
Fax (傳真): (852) 2636 5090
E-mail (電郵): loym@cuhk.edu.hk

策劃處處長
陳燿墉先生
Planning Officer
Mr. Andrew Y.Y. Chan

Tel (電話): (852) 2609 6788
Fax (傳真): (852) 2603 6958
E-mail (電郵): yungchan@cuhk.edu.hk

Your Ref:

Our Ref: FM/C/13 – CRE-2002.286

5 September 2002

Dr. James Francis Griffith
Dept. of Diagnostic Radiology and
 Organ Imaging
CUHK

Dear Dr. Griffith,

 I write to inform you that ethical approval has been given for you to engage in the project named below:

Project Title : **"Evaluation of Osteoporosis Using Proton and Phosphorous Magnetic Resonance Spectroscopy: Comparison with DEXA Findings"**
[Ref. No. CRE-2002.286]

Investigator(s) : **Dr. James Francis GRIFFITH, Dept. of Diagnostic Radiology and Organ Imaging, CUHK**

Dr. David KW YEUNG, Physicist, Dept. of Clinical Oncology, PWH

Dr. Samuel Yeung Shan WONG, Physician, Jockey Club for Osteoporosis Care and Control, School of Public Health, CUHK

Duration : **6 Months**

Location of Study : **Prince of Wales Hospital**

Conditions by Clinical Research Ethics Committee (if any): **Nil**

 It will be much appreciated if the completion of the project will be reported to the Committee in due course.

Yours sincerely,

Andrew Chan
Secretary
Clinical Research Ethics Committee

AC/bn

Serving the Community Through Quality Education, Caring Practice and Advancement of Health Sciences

香港中文大學醫學院
Faculty Of Medicine
The Chinese University Of Hong Kong

醫 院 管 理 局
新 界 東 醫 院 聯 網
Hospital Authority
New Territories East Cluster

Joint CUHK – New Territories East Cluster Clinical Research Ethics Committee
香港中文大學--新界東醫院聯網 臨床研究倫理 聯席委員會

Secretary of the Clinical Research Ethics Committee   c/o
Centre for Clinical Trials and Epidemiological Research, Faculty of Medicine, The
Chinese University of Hong Kong, 5th Floor, School of Public Health, Prince of Wales Hospital.
Tel : (852) 2252 8717   Fax : (852) 2645 3098

To: Prof. James F. Griffith   29 April 2003
        Dept. of Diagnostic Radiology and Organ Imaging
        Prince of Wales Hospital

Ethics Approval of Research Protocol

CREC Ref:	**CRE-2003.121**
Date of Approval:	**29 April 2003**
Protocol Title:	**Evaluation of Osteoporosis with Diffusion Magnetic Resonance Imaging and Spectroscopy**
Investigator(s):	**James F. GRIFFITH, David Ka Wai YEUNG, Samuel WONG, Edith LAU and P.C. LEUNG**
Proposed Start Date:	**01 October 2003**
Proposed End Date:	**30 September 2005**

I write to inform you that ethics approval has been given to you to conduct the captioned study in accordance with the following document(s) submitted:

- Protocol

- Patient Information and Consent form in English and Chinese version

This ethics approval will be valid for 12 months.   Application for further renewal can be made by submitting the Renewal and Research Progress Report Form to the CREC.   It will be much appreciated if the completion of the project will be reported to the Committee in due course.

(Prof. Joseph Lau)
Secretary, Joint CUHK-NTEC
Clinical Research Ethics Committee

c.c. Mrs. Alice Yip – RTAO (Ref. Earmarked Grant 2003/2004)

Encl. CREC/CT0001 – w.e.f. 4/2003 (for HA employee concerned ONLY)

256

Joint The Chinese University of Hong Kong – New Territories East Cluster Clinical Research Ethics Committee

香港中文大學–新界東醫院聯網 臨床研究倫理 聯席委員會

Secretary of the Clinical Research Ethics Committee c/o Centre for Epidemiology and Biostatistics,
Faculty of Medicine, The Chinese University of Hong Kong, 5th Floor, Postgraduate Education Centre, Prince of Wales Hospital.
Tel : (852) 2252 8717   ~~Fax : (852) 2645 3098~~ Fax No.: 2646 6653

To: Prof. James F. Griffith (Principal Investigator)   3 June 2004
     Dept. of Diagnostic Radiology and Organ Imaging
     Prince of Wales Hospital

Ethics Approval of Research Protocol

CREC Ref. No.:   **CRE-2004.166**

Date of Approval: **03 June 2004***

Protocol Title: **Functional Magnetic Resonance Imaging Study of Osteoporosis**

Investigator(s):   **PWH - James F. GRIFFITH, Gregory Ernest ANTONIO, David Ka Wai YEUNG, Edith Ming Chu LAU, Samuel Yeung Shan WONG and Ping Chung LEUNG**

I write to inform you that ethics approval has been given to you to conduct the captioned study in accordance with the following document(s) submitted:

- Protocol

- Information Sheet in English and Chinese version

- Informed Consent Form in English and Chinese version

This ethics approval* will be valid for 12 months.   Application for further renewal can be made by submitting the Renewal and Research Progress Report Form to the CREC.   It will be much appreciated if the completion of the project will be reported to the Committee in due course.

The Joint CUHK-NTEC Clinical Research Ethics Committee serves to ensure that research complies with the Declaration of Helsinki, ICH GCP Guidelines, local regulations, HA and University policies.

(Prof. Joseph Lau)
Secretary, Joint CUHK-NTEC
Clinical Research Ethics Committee

c.c. Mrs. Alice Yip – RTAO (Ref. Earmarked Grant)
JL/ci

Joint The Chinese University of Hong Kong – New Territories East Cluster
Clinical Research Ethics Committee
香港中文大學–新界東醫院聯網 臨床研究倫理 聯席委員會

Flat 3C, Block B, Staff Quarters, Prince of Wales Hospital, Shatin, HK
Tel : (852) 2632 3935   Fax : (852) 2646 6653   Website : http://www.crec.cuhk.edu.hk

To: Prof. James Francis Griffith (Principal Investigator)   10 April 2007
      Dept. of Diagnostic Radiology & Organ Imaging
      Prince of Wales Hospital

Ethics Approval of Research Protocol

CREC Ref. No.:	**CRE-2007.154**
Date of Approval:	**10 April 2007***
Protocol Title:	**Is There Relationship Between Bone Mineral Density and Marrow Fat Composition in Human Subjects?**
Investigator(s):	**James Francis Griffith, David K. YEUNG, Kai Chow CHOI, Ping Chung LEUNG and Kwok Sui LEUNG**

I write to inform you that ethics approval has been given to you to conduct the captioned study in accordance with the following document(s) submitted:

- Study Protocol
- Patient Information Sheet and Consent Form in Chinese Version
- Lifestyle Questionnaire in Chinese Version
- Food Frequency Questionnaire in Chinese Version

This ethics approval* will be valid for 12 months.   Application for further renewal can be made by submitting the Ethics Renewal and Research Progress Report Form to the CREC (Download the electronic form template from the http://www.crec.cuhk.edu.hk or http://ntec.home/Research%20Ethics/main.asp). It will be much appreciated if the completion of the project will be reported to the Committee in due course.

The Joint CUHK-NTEC Clinical Research Ethics Committee serves to confirm that research complies with the Declaration of Helsinki, ICH GCP Guidelines, local regulations, HA and University policies.

(Prof. Joseph Lau)
Secretary, Joint CUHK-NTEC
Clinical Research Ethics Committee

c.c. Ms. Alice Ngan – RTAO (Ref. Earmarked Grant 2006/2007)
Encl. CREC/CT0001 – w.e.f. 4/2003 for HA(NTEC) employee concerned ONLY
JL/ci

Joint The Chinese University of Hong Kong – New Territories East Cluster
Clinical Research Ethics Committee
香港中文大學–新界東醫院聯網 臨床研究倫理 聯席委員會

Flat 3C, Block B, Staff Quarters, Prince of Wales Hospital, Shatin, HK
Tel : (852) 2632 3935   Fax : (852) 2646 6653   Website : http://www.crec.cuhk.edu.hk

To: Prof. James F. GRIFFITH (Principal Investigator)   4 October 2007
      Dept. of Diagnostic Radiology & Organ Imaging
      Prince of Wales Hospital

Ethics Approval of Research Protocol

CREC Ref. No.:	**CRE-2007.359**
Date of Approval:	**04 October 2007***
Protocol Title:	**Reproducibility of Functional MR Imaging Techniques in Bone and Relationship to Endothelial Function Studies**
Investigator(s):	**James F. GRIFFITH, David Kai Wai YEUNG and Timothy KWOK**

I write to inform you that ethics approval has been given to you to conduct the captioned study in accordance with the following document(s) submitted:

- Protocol
- Patient Information Sheet and Consent Form in English Version
- Patient Information Sheet and Consent Form in Chinese Version

This ethics approval* will be valid for 12 months.   Application for further renewal can be made by submitting the Ethics Renewal and Research Progress Report Form to the CREC (Download the electronic form template from the http://www.crec.cuhk.edu.hk or http://ntec.home/Research%20Ethics/main.asp). It will be much appreciated if the completion of the project will be reported to the Committee in due course.

The Joint CUHK-NTEC Clinical Research Ethics Committee serves to confirm that research complies with the Declaration of Helsinki, ICH GCP Guidelines, local regulations, HA and University policies.

(Prof. Joseph Lau)
Secretary, Joint CUHK-NTEC
Clinical Research Ethics Committee

Encl. CREC/CT0001 – w.e.f. 4/2003 for HA(NTEC) employee concerned ONLY
JL/ci

Joint The Chinese University of Hong Kong – New Territories East Cluster Clinical Research Ethics Committee

香港中文大學–新界東醫院聯網 臨床研究倫理 聯席委員會

Flat 3C, Block B, Staff Quarters, Prince of Wales Hospital, Shatin, HK
Tel : (852) 2632 3935   Fax : (852) 2646 6653   Website : http://www.crec.cuhk.edu.hk

To: Prof. James GRIFFITH (Principal Investigator)   8 April 2008
     Dept. of Diagnostic Radiology & Organ Imaging
     Prince of Wales Hospital

Ethics Approval of Research Protocol

CREC Ref. No.:   **CRE-2008.133**

Date of Approval: **08 April 2008***

Protocol Title: **Relationship between Estrogen Depletion, Bone Perfusion, Bone Marrow Fat Content, Endothelial Function and Bone Mineral Density: A Pilot Clinical Study**

Investigator(s):   **James GRIFFITH and Christopher HAINES**

I write to inform you that ethics approval has been given to you to conduct the captioned study in accordance with the following document(s) submitted:

- Research Protocol
- Patient Informed Consent Form in English Version
- Patient Informed Consent Form in Chinese Version

This ethics approval* will be valid for 12 months.   Application for further renewal can be made by submitting the Ethics Renewal and Research Progress Report Form to the CREC (Download the electronic form template from the http://www.crec.cuhk.edu.hk or http://ntec.home/Research%20Ethics/main.asp). It will be much appreciated if the completion of the project will be reported to the Committee in due course.

The Joint CUHK-NTEC Clinical Research Ethics Committee is organized and operates according to ICH-GCP and the applicable laws and regulations.

(Ms. Eva Kong)
Hospital Administrator
Joint CUHK-NTEC
Clinical Research Ethics Committee

Encl. CREC/CT0001 – w.e.f. 4/2003 for HA(NTEC) employee concerned ONLY
EK/ci

June 25, 2009

Professor WANG Yixiang
Department of Diagnostic Radiology and Organ Imaging
Faculty of Medicine

Dear Professor Wang,

<u>Animal Experimentation Ethics Approval</u>

I am pleased to confirm that the Animal Experimentation Ethics Committee agrees to grant ethical approval for your research project entitled "Relationship between estrogen deficiency, intervertebral disc nutrient supply, and intervertebral disc degeneration: an experimental study in ovariectomized female rats" (Ref No. 09/062/GRF and 476509).

Thank you for your attention.

Yours sincerely,

Professor Christopher Haines
Chairman
Animal Experimentation Ethics Committee

cc   Dr Anthony James, Laboratory Animal Services Centre
     Mrs Cecilia Lam, Research Administration Office

THE CHINESE UNIVERSITY OF HONG KONG

MEMO

From	Professor Christopher J Haines Chairman Animal Experimentation Ethics Committee	To	Professor James GRIFFITH Dept of Diagnostic Radiology & Organ Imaging Faculty of Medicine
Ref.			
Tel. No.	2632 2800	Your Ref.	
Date	June 12, 2008	dated	

Animal Experimentation Ethics Approval

I am pleased to confirm that the Animal Experimentation Ethics Committee agrees to grant ethical approval for your research project entitled "Relationship between bone perfusion, marrow fat content and bone mineral density: an experimental study with ovariectomy-induced osteoporosis in a rat model" (Ref No. 08/058/ERG and 464508).

Thank you for your attention.

Professor Christopher J Haines

cc   Mrs Cecilia Lam, Research Administration Office
     Dr Anthony James, Laboratory Animal Services Centre

CJH/JC/cp

Patient consent form for
Functional Magnetic Resonance Imaging of Osteoporosis

Perfusion, diffusion and spectroscopy are new magnetic resonance imaging (MRI) techniques that are believed to be useful in obtaining physiological information from bones.   The information obtained could be valuable in understanding bone diseases, in particular, osteoporosis and could lead to better prevention of this disease as well as new treatments.

Perfusion measures the blood flow in the bones. Diffusion measures how easily small particles (molecules) can move around inside your bone. Spectroscopy measures the content of fat and other substances inside your bones. We will be looking only at the bones in the lumbar spine (i.e. the lower back) during this examination.

We would like to obtain your consent to perform this MRI examination to examine the bones in your spine.   An injection will be given during the examination. The substance injected is a very standard, safe agent to show up blood flow better. It is used every day in clinical practice. Otherwise, there will be no pain or discomfort involved and you will not notice anything unusual during the examination. There will be no side effects or late effects from the examination. Magnetic resonance imaging is a very safe imaging test that has been used in routine clinical practice for over 10 years. It does not involve any X-ray irradiation.

We will write a report on our findings regarding any changes in your lumbar spine and send this report to your clinicians at the osteoporosis centre.

The information gathered will be kept confidential and will be used solely for research. We would like to obtain your consent for us to use the information for that purpose.   Whether you decide to join the study or not is entirely your decision and is not going to affect your treatment.   You can decide to withdraw from the study at any time and your treatment or management will not be affected in any way.

<u>Consent form</u>

I have read the explanatory statement and agree to participate in the above study.   The nature and the purpose of the study has been explained to me. I understand that the examination results may be used for research purposes.

_____   _____
Patient's signature   Doctor's signature

_____   _____
Patient's name and ID no.   Doctor's name

_____   _____
Date   Date

<u>Patient consent form:</u>

Reproducibility of functional MR imaging techniques in bone and relationship to endothelial function studies

Magnetic resonance imaging (MRI) is a safe investigation that can provide information about bones. This MRI examination would look at your lumbar spine ('lower back') and right hip. It would look at the fat within your bones and well as the blood flow. This would involve you having an injection into a vein on the back of your hand or forearm. This injection is safe provided your kidneys are working properly so we will check that before you have the examination. The MRI examination will take approximately about 35 minutes. It does not involve any X-ray irradiation. We will examine your lumbar spine and hip. We will let you and your clinician know the results of the examination.

We will also look at how healthy your arteries are by checking your endothelial function and intimal thickness. Both of these tests look at whether there is any atherosclerosis (hardening) of your arteries. It is an ultrasound test which does not involve any infections. You will have to take a tablet under your tongue before one part of the examination to dilate your arteries temporarily. This effect will only last a short time. We will let you and your clinician know the results of the examination.

The information obtained could be valuable in better understanding osteoporosis and could lead to better treatment of this disease as well as better prevention. The information gathered will be kept confidential and will be used solely for research. We would like to obtain your consent for us to use the information for this purpose. Whether or not you decide to join the study is entirely your decision and is not going to affect your treatment. You can decide to withdraw from the study at any time and your treatment or management will not be affected in any way.

If you have any questions regarding these issues, please feel free to contact Prof James Griffith, Dept of Diagnostic Radiology and Organ Imaging, Prince of Wales Hospital.

<u>Consent Agreement</u>

I have read the explanatory statement and agree to participate in the above study. The nature and the purpose of the study have been explained to me by Dr.＿＿＿＿＿＿ . I understand that the examination results may be used for research purposes.

＿＿＿＿＿＿＿＿＿　　＿＿＿＿＿＿＿＿
Patient's signature　　　　Doctor's signature

＿＿＿＿＿＿＿＿＿　　＿＿＿＿＿＿＿＿
Patient's name and ID no.　Doctor's name

＿＿＿＿＿＿＿＿＿＿　　＿＿＿＿＿＿＿＿
Date　　　　　　　　　Date

磁力共振灌注成像彌散成像及波譜分析應用於脊椎檢查
病人同意書

磁力共振的灌注成像彌散成像及波譜分析是一種嶄新的技術，它能在創傷的情況下提供人體的生理狀態，相信這在臨床上對瞭解骨質疏鬆等骨骼疾病是極有價值的。故我們希望徵求你的同意，使用這些磁力共振技術去檢查你的脊椎，並同意在是次檢查中為你注射檢查專用的造影劑。

磁共振用於常規臨床實踐已超二十年。它是一種安全的檢查技術，並不涉及 X 光輻射。檢查共需約三十分鐘，檢查中需靜脈注射一種釓磁共振造影劑。釓磁共振造影劑在全世界每天用於常規磁共振檢查，迄今的临床经验提示釓磁共振造影劑非常安全。虽然有报道注射釓磁共振造影劑后，如果病人原有中重度肾功能伤害，那么发式一种叫肾原性系统性纤维化的严重病变的可能性会提高。但肾原性系统性纤维化的发生率很低，而且，醫生只选肾功能较好的病人参加本研究。

你在是次磁力共振檢查的資料將被保密，並純粹應用於學術用途分析應用於學術用途，故在此希望徵得你的同意。同意與否，純為自願性質，絕不影響你的治療。再者，你可以隨時退出是項學術研究。

同意書

　　　　我已閱讀以上解釋說明，並同意參加上述之研究。該研究的性質和目的已由醫生為我解釋，我理解該項檢查的結果會應用于學術用途。

病人簽名:　　　　　　　　醫生簽名:

病人姓名及身份證號碼:　　　　醫生姓名:

日期:　　　　　　　　　日期:

磁力共振灌注成像彌散成像及波譜分析應用於脊椎檢查

病人同意書

　　磁力共振的灌注成像彌散成像及波譜分析是一種嶄新的技術，它能在創傷的情況下提供人體的生理狀態，相信這在臨床上對暸解骨質疏鬆等骨骼疾病是極有價值的。故我們希望徵求你的同意， 使用這些磁力共振技術去檢查你的脊椎， 並同意在是次檢查中為你注射檢查專用的造影劑。

　　磁力共振掃描應用於臨床診斷上已超過 10 年，雖然未確知其潛在長遠影響，但肯定不含 X-光輻射。

　　你在是次磁力共振檢查的資料將被保密，並純粹應用於學術用途 分析應用於學術用途，故在此希望徵得你的同意。同意與否，純為自願性質，絕不影響你的治療。再者，你可以隨時退出是項學術研究。

同意書

　　我已閱讀以上解釋說明，並同意參加上述之研究。該研究的性質和目的已由醫生為我解釋，我理解該項檢查的結果會應用于學術用途。

病人簽名:　　　　　　　　　　醫生簽名:

病人姓名及身份證號碼:　　　　醫生姓名:

日期:　　　　　　　　　　　　日期:

香港中文大學放射診斷學系

參加骨髓脂肪與骨質密度關係之臨床研究計劃<u>同意書</u>

下述簽名者:

姓名: _____ 身份証號碼: _____ 組別: _____

本人在此聲明自願參加骨髓脂肪與骨質密度關係之臨床研究計劃:

1. 本人已經完全明白是次參予此臨床研究計劃的類型、目的、意義及所使用的方法(包括個人資料及病歷查詢、於手術時由醫生抽取骨髓脂肪組織)。
2. 本人明白抽取骨髓脂肪樣本並不會對健康構成任何副作用。
3. 本人願意接受骨質密度檢查,及有關生活狀況及飲食習慣之問卷調查。
4. 本人確定現在沒有懷孕/有懷孕的可能性。
5. 本人有權提出有關研究計劃的各種問題,而且提問將會得到完滿的解答。
6. 本人明白有權利退出是次研究計劃。
7. 研究人員已向本人詳細解釋計劃及同意書內容。本人已經完全瞭解此研究計劃及同意書的所有內容細節。

病人姓名 _____ 病人簽名 _____ 日期 _____

****

下述簽名者
茲證明上述自願參加者已清楚了解所參與的研究計劃,並對以上同意書沒有任何疑問。

見証人姓名_____ 見証人簽名 _____ 日期 _____